

Dipyrazolylphosphanes in Condensation and P–N/P–P Bond
Metathesis Reactions

DISSERTATION

zur Erlangung des akademischen Grades

Doctor rerum naturalium

(Dr. rer. nat.)

vorgelegt

dem Bereich Mathematik und Naturwissenschaften
der Technischen Universität Dresden

von

M.Sc. Robin Schoemaker

geboren am 05.07.1991 in Nordhorn

Eingereicht am 09.06.2020

Verteidigt am 04.09.2020

Gutachter:

Prof. Dr. Jan J. Weigand

Prof. Dr. Christian Müller

Die Dissertation wurde in der Zeit von 11/2015 bis 06/2020 in der Professur für
Anorganische Molekülchemie der Technischen Universität Dresden angefertigt.

I am very much indebted to Prof. Dr. Jan J. Weigand for his generous support, help and advice.

Content

1. Introduction	3
1.1. Pyrazolyl-substituted Phosphanes – Synthesis and Application in Condensation Reactions	4
1.2. Pyrazolyl-substituted Phosphorus Compounds in Scrambling Reactions.....	7
1.3. Polyphosphanes in Methylation Reactions.....	12
1.4. Classification of Pyrazolyphosphanes	14
2. Objectives	16
3. Synthesis of Pyrazolyphosphanes	18
3.1. Synthesis of Type II Phosphanes.....	18
3.2. Synthesis of Pyrazolyl-substituted Phosphorus Chlorides	21
4. Reactivity of Type II Phosphanes towards Secondary Phosphanes	24
4.1. P–P Bond Formation <i>via</i> Condensation Reactions.....	24
4.2. Coinage Metal Complexes of Triphosphane 48	26
4.3. P–P Bond Formation <i>via</i> P–N/P–P Bond Metathesis Reactions	31
4.4. Methylation Reactions of Triphosphane 48 and P–P/P–P Bond Metathesis Reaction	35
5. 1,4,2-Diazaphospholium Triflates – Synthesis and Reactivity	41
5.1. One-Pot Synthesis of 1,4,2-Diazaphospholium Triflate Salts.....	43
5.2. Halogenation Reactions of 61 [OTf]	49
5.3. Substitution Reactions of 61 ^{Cl2} [OTf].....	53
6. Dipyrazolylphosphanes in Condensation Reactions with Primary Phosphanes.....	57
6.1. Synthesis of Mixed-substituted Tetraphosphetanes	58
6.2. Coinage Metal Complexes of Tetraphosphetane 72	60
6.3. Methylation Reactions of Tetraphosphetanes 71 and 72	64
7. Gold Chloride induced Cleavage of P–P Bonds.....	71
8. Reactivity studies of Pyridyl-substituted Polyphosphanes towards PdCl ₂ and PtCl ₂ ..	79
9. Oxidation of 48 and Subsequent Deprotonation Studies.....	86
10. Summary.....	91
11. Prospect	96
12. Experimental Details	99
12.1. Materials and Methods	99
12.2. Syntheses and Characterization Data regarding Compounds in Chapter 3	101
12.3. Syntheses and Characterization Data regarding Compounds in Chapter 4.....	113
12.4. Syntheses and Characterization Data regarding Compounds in Chapter 5	126

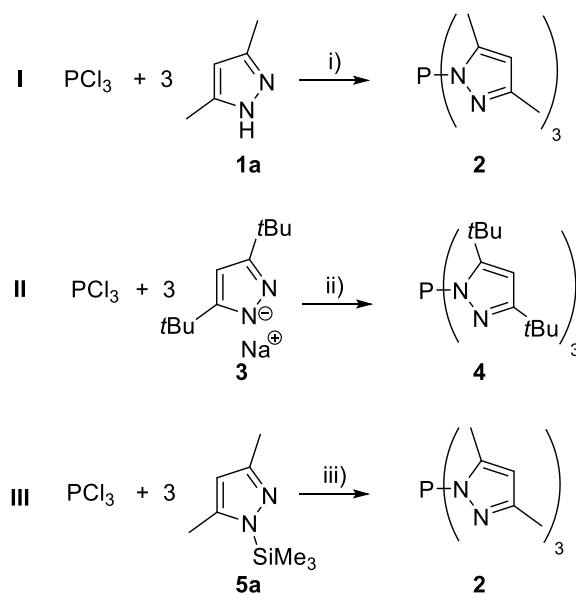
12.5. Syntheses and Characterization Data regarding Compounds in Chapter 6.....	139
12.6. Syntheses and Characterization Data regarding Compounds in Chapter 7.....	149
12.7. Syntheses and Characterization Data regarding Compounds in Chapter 8.....	151
12.8. Syntheses and Characterization Data regarding Compounds in Chapter 9.....	154
13. Crystallographic Details.....	156
17. Abbreviations.....	179
18. References.....	180
19. Acknowledgement.....	193
20. Publications and Conference Contributions.....	194
20.1. Peer Reviewed Publications.....	194
20.2. Oral presentations.....	194
20.3. Poster presentations.....	194

1. Introduction

Phosphorus plays a crucial role in modern p-block chemistry.¹ One reason for that is the diagonal relationship between phosphorus and carbon.² Comparable to carbon and its chemistry, phosphorus tends to form homoatomic bonds, which is explainable by the relatively high P–P single bond energy (ca. 200 kJ/mol).³ Thus, a plethora of polyphosphorus compounds are reported in the last decades comprising of fascinating bonding motifs⁴ and interesting applications in coordination⁵⁻⁷ and synthetic⁸⁻¹¹ chemistry, as well as in ligand design.^{12,13} A crucial point in the chemistry of polyphosphanes is of course the formation of P–P bonds. Numerous synthetic procedures are established and reviewed including salt metathesis,^{4a,14} dehalosilylation¹⁵ and dehalostannylation¹⁶ reactions, base promoted dehydrohalogenation reactions¹⁷ and dehydrogenative coupling reactions mediated by main group compounds¹⁸ or catalysis by transition metals.^{5,19} Moreover, dialkylamino-substituted phosphanes are used in condensation reactions to form P–P bonds since the early 1960's. Yet these reactions need elevated temperatures, somewhat limiting the formation of polyphosphorus compounds as stated by the few examples reported.^{17d,20} The application of pyrazolyl-substituted phosphanes in P–P bond formation reactions is a relatively young field of research.²¹ Their synthesis and general chemical behavior as well as advantages in comparison to dialkylamino-substituted phosphanes is discussed in the following chapter.

1.1. Pyrazolyl-substituted Phosphanes – Synthesis and Application in Condensation Reactions

Following the pioneering work by the group of Peterson,²² mainly three synthetic pathways are established for the synthesis of pyrazolyl-substituted phosphanes.²³ Reacting 3,5-dimethylpyrazole (**1**) with phosphorus trichloride in the presence of triethylamine in THF gives the desired tris(3,5-dimethylpyrazolyl)phosphane (**2**) in 96% yield next to triethylammonium chloride (Scheme 1; **I**).^{23a}



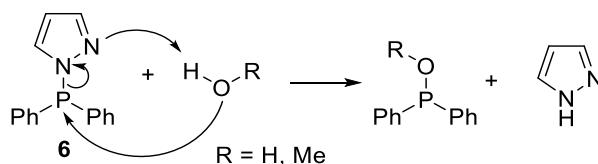
Scheme 1. Synthetic procedures towards pyrazolyl-substituted phosphanes; i) 3 NEt₃, -3 [HNEt₃]Cl, THF, r.t., 96%; ii) -3 NaCl, THF, 66 °C, 90%; iii) -3 Me₃SiCl, neat, r.t., 98%.

Sterically encumbered pyrazolyl-substituted phosphanes are accessible *via* the reaction of phosphorus trichloride with sodium pyrazolide **3** as shown by the synthesis of tris(3,5-di-*tert*-butylpyrazolyl)phosphane (**4**) (Scheme 1, **II**).^{23b} Another convenient way for the formation of **2** is the reaction of PCl₃ with 3,5-dimethyl-1-(trimethylsilyl)pyrazole (**5a**) (Scheme 1, **III**).^{22,23b} The solvent free reaction gives **2** in essentially quantitative yields after stirring at ambient temperature and subsequent evaporation of the co-produced trimethylsilylchloride *in vacuo*.

All reported tripyrazolyl-substituted phosphanes are colorless solids that are prone to hydrolysis, but are stable when stored under dry, inert gas, such as N₂ or Ar.²³ The necessary exclusion of moisture when working with pyrazolyl-substituted phosphanes indicates their higher reactivity compared to dialkylamino-substituted phosphanes. The latter hydrolyze in

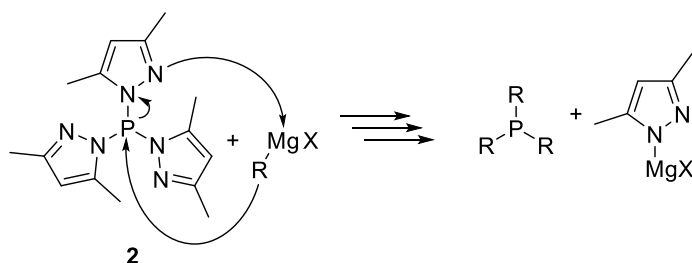
the presence of water only slowly,²⁴ and even dialkylamino-substituted phosphanes which are stable towards water, methanol and ethanol are reported.²⁵

Peterson and co-workers further investigated the protolysis of **6** with water or methanol and could prove that it readily gives 1*H*-pyrazole and diphenyl phosphinous acid or methyl diphenylphosphinite, respectively (Scheme 2).^{22b}



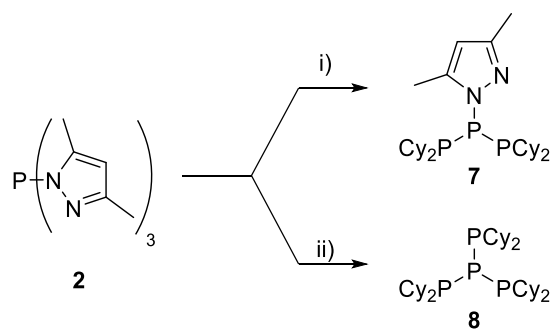
Scheme 2. Protolysis of **6** with either water or methanol.

Accordingly, the reaction of **6** with sodium methoxide yields methyl diphenylphosphinite and sodium pyrazol-1-ide. In a similar fashion, reacting **6** with phenyllithium yields Ph_3P and lithium pyrazol-1-ide.^{22b} Such exchange reactions are also observed for **2** with Grignard reagents (RMgX , $\text{R} = \text{Me, Ph}$; $\text{X} = \text{Cl, Br}$) yielding the corresponding tertiary phosphanes PR_3 (Scheme 3).²⁶ The salt metathesis reactions are feasible due to interaction of the free lone pair of the pyrazolyl moiety and the Lewis acidic metal atom in lithium organyles or Grignard reagents (Scheme 3).



Scheme 3. Reaction of **2** with a Grignard reagent; $\text{R} = \text{Me, Ph}$; $\text{X} = \text{Cl, Br}$.

Even though this remarkable synthetic potential is known since the mid 1970's,²² pyrazolyl-substituted phosphanes were mainly used for coordination chemistry,²⁷ due to their structural resemblance with the famous pyrazolylborate ligands.²⁸ Yet, in 2012 our group reported on the facile synthesis of a triphosphane and an *iso*-tetraphosphane from tripyrazolylphosphane **2**.^{21b} Reacting **2** with Cy_2PH yields either triphosphane **7** or *iso*-tetraphosphane **8**, depending on the stoichiometry applied (Scheme 4).

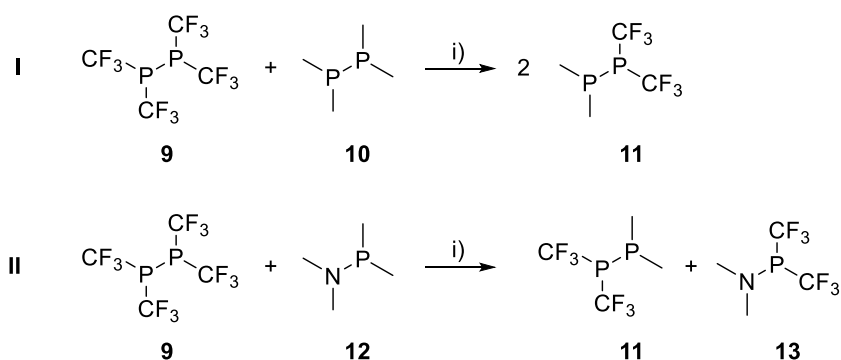


Scheme 4. Synthesis of triphosphane **7** and *iso*-tetraphosphane **8**; i) 2 Cy₂PH, -2 **1a**, MeCN, r.t., 91%; ii) 3 Cy₂PH, -3 **1a**, MeCN, r.t., 95%.^{21b}

This condensation reaction gives only dimethylpyrazole **1a** as the side product. Since both polyphosphanes **7** and **8** precipitate from the reaction mixture, they are conveniently isolated by filtration in yields above 90%. It is important to note that *iso*-tetraphosphane **8** was previously synthesized by metathesis of K[P(SiMe₃)₂] with 3 equivalents Cy₂PCl in yields of only 10%,²⁹ which furthermore points out the practicability of P–P bond formation using pyrazolyl-substituted phosphanes as [P₁]-precursors.

1.2. Pyrazolyl-substituted Phosphorus Compounds in Scrambling Reactions

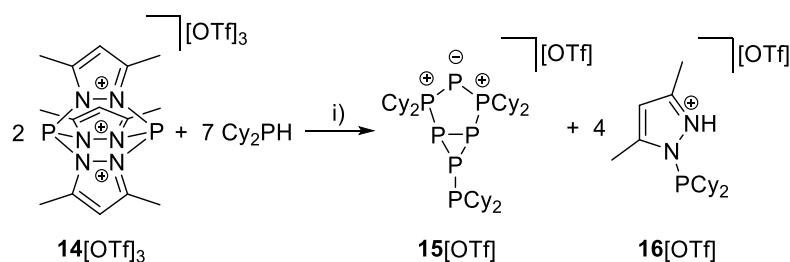
Scrambling reactions are fairly well known in polyphosphorus chemistry.^{4a} Mixtures of cyclic polyphosphanes (RP)_n (R = alkyl, aryl; n = 3-5), obtained e.g. from the reduction of dichlorophosphanes R₂PCl₂, often form the thermodynamically favored ring size *via* a so called *scrambling*.³⁰ Such reactions are also observed for unsymmetrically substituted diphosphanes and triphosphanes, which are often in a state of equilibrium.³¹ These equilibria are controllable as shown by Mills and co-workers.^{31f} Mixing tetrakis(trifluoromethyl)-diphosphane (**9**) and tetramethyldiphosphane (**10**) yields the asymmetric diphosphane **11** (Scheme 5; I). This exchange reaction is best understood as a P–P/P–P bond metathesis reaction, with an exchange of the different R₂P moieties driven by their unequal Lewis basicity.



Scheme 5. Formation of **11** *via* P–P/P–P (**I**) and P–N/P–P (**II**) bond metathesis; i) C₆D₆, r.t..

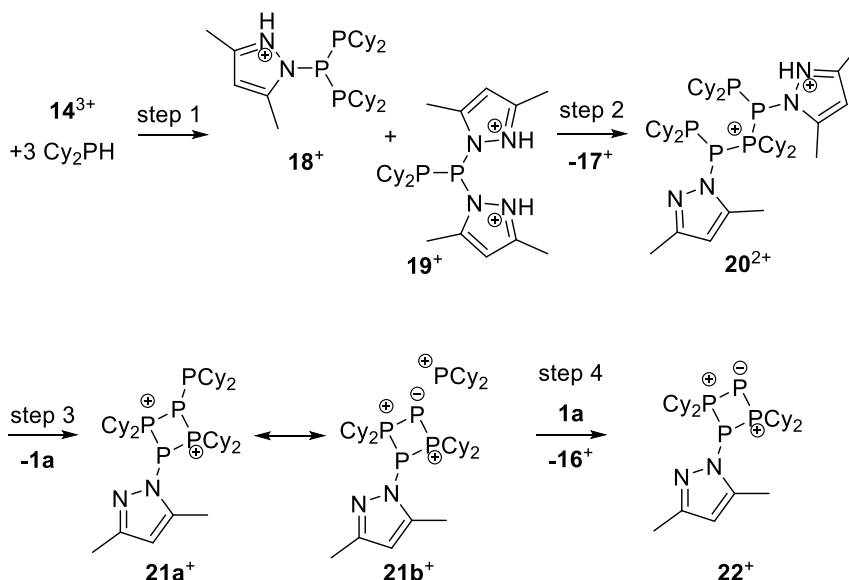
In the same contribution Mills et al. reported the formation of **11** which can be understood as a P–N/P–P bond metathesis from **9** and dimethylamino-substituted phosphane **12** (Scheme 5; II). A similar exchange is observed in the reaction of **9** and Me₂As–AsMe₂.^{31f} This motivates to further research on controlled scrambling reactions within polypnictogen based derivatives and especially encourages the research on nitrogen-substituted phosphanes in that matter.

During the last years, pyrazolyl-substituted phosphorus compounds were shown to be very interesting starting materials for the synthesis of polyphosphorus compounds.^{32,33} Reacting the pyrazolyl-based diphosphorus trication **14**[OTf]₃ with a secondary phosphane such as Cy₂PH, gives bicyclic polyphosphorus compound **15**[OTf] and **16**[OTf] (Scheme 6).³²



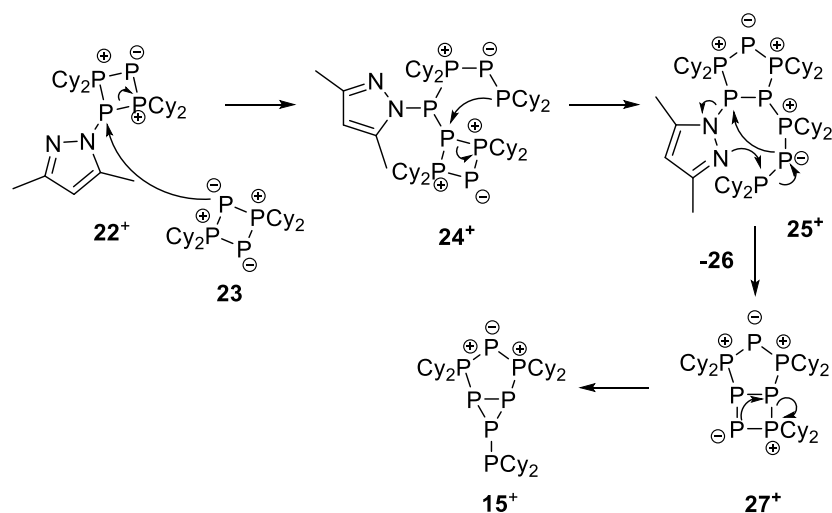
Scheme 6. Reaction of **14[OTf]₃** with Cy_2PH ; i) CH_2Cl_2 , **-17[OTf]** (3,5-dimethylpyrazolium triflate), **-1a**, r.t., 45% **15[OTf]**, 54% **16[OTf]**.³²

The formation of **15[OTf]** was investigated by reacting **14[OTf]₃** with various amounts of Cy_2PH and subsequent multinuclear NMR spectroscopic studies. This revealed the formation of tetraphosphorus cation **22⁺**, which was isolated and fully characterized as its triflate salt. The formation of **22⁺** can be understood as a series of subsequent substitution steps, followed by a base-induced reduction (Scheme 7).



Scheme 7. Proposed mechanism for the stepwise formation of **22⁺**.³²

In step one the intermediates **18⁺** and **19²⁺** are formed *via* a protolysis reaction of **14³⁺** and Cy_2PH . **18⁺** reacts then with **19²⁺** by substituting one pyrazoliumyl moiety forming intermediate **20⁺** and **17⁺** after deprotonation (step 2). In a similar intramolecular substitution cation **20²⁺** rearranges to **21⁺** (step 3), displayed by two resonance structures **21a⁺** and **21b⁺**. Presence of **1a** enables a base-induced redox reaction, rationalising formation of **22⁺** under release of **16⁺** (step 4). Cation **22⁺** is proven to be an intermediate in the formation of **15[OTf]** *via* a test reaction of **22[OTf]** with 0.5 equivalents of Cy_2PH . Formation of **23** is proposed by protolysis reaction of **22⁺** with a secondary phosphane. By a nucleophilic attack of **23** on **22⁺**, formation of cation **15⁺** is initiated according to Scheme 8.

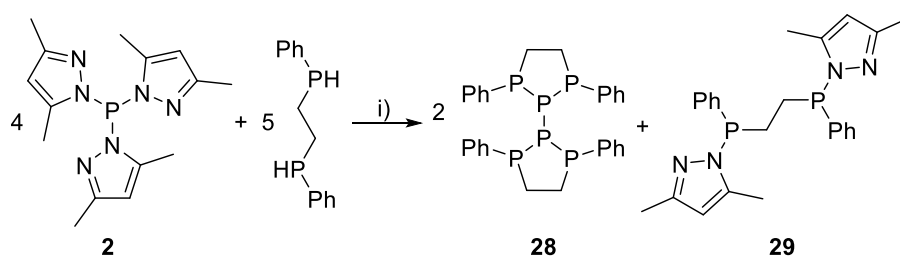


Scheme 8. Plausible mechanism for the formation of 15^+ .³²

Due to the nucleophilic attack of 23 on 22^+ , intermediate 24^+ is formed, which rearranges to 25^+ via an intramolecular nucleophilic substitution. 25^+ undergoes a P–N/P–P metathesis to form 27^+ under concomitant liberation of 1-(dicyclohexylphosphanyl)-3,5-dimethyl-1*H*-pyrazole (26). Cation 27^+ finally rearranges to 15^+ , thus, the whole process is considered a P–P/P–P bond metathesis.

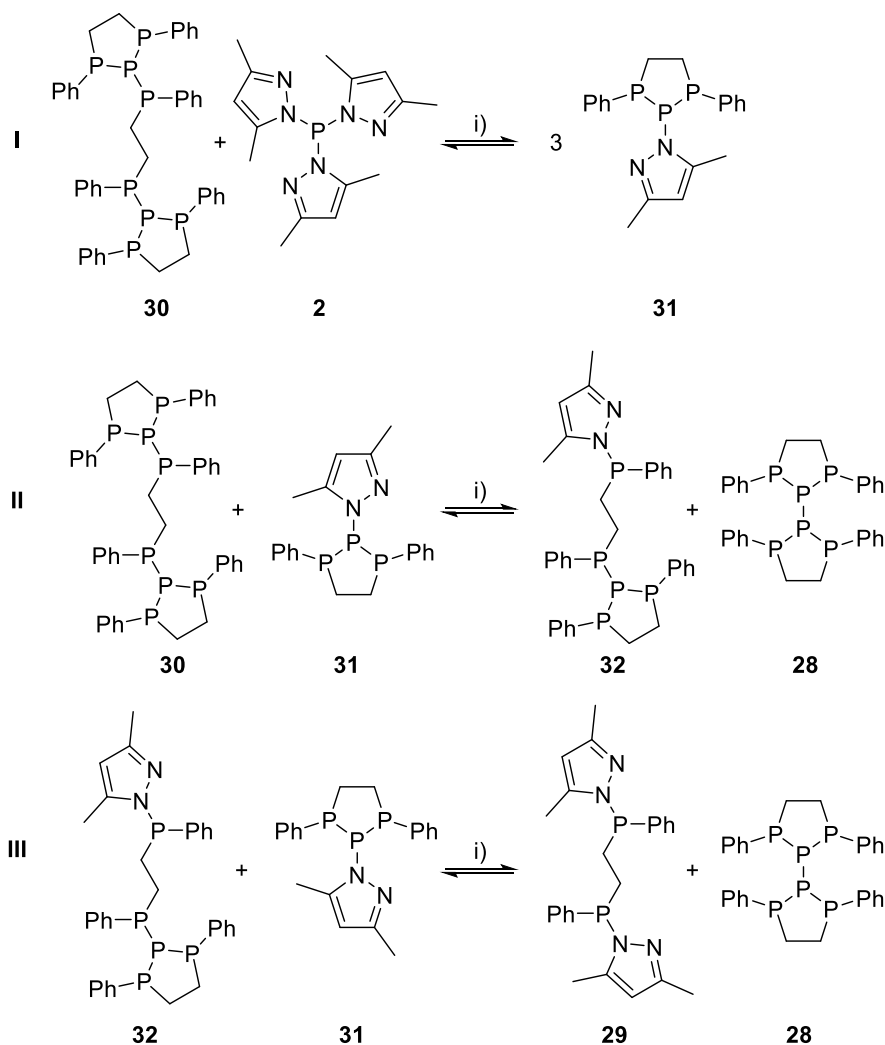
In total, eight P–P bonds are formed from pyrazolyl-substituted phosphorus trication 14^{3+} via a series of protolysis and base induced P–P coupling reactions. The synthesis of 15 [OTf] is an example of the reactivity of pyrazolyl-stabilized phosphorus cations. Moreover, also neutral pyrazolyl-substituted phosphorus species were reported in the synthesis of polyphosphorus compounds.³³

While tripyrazolylphosphane 2 reacts with secondary phosphane Cy_2PH by means of a condensation reaction and release of $1a$ (*vide supra*), the reaction with the phosphane bis(phenylphosphanyl)ethane yields hexaphosphane 28 and pyrazolylphosphane 29 (Scheme 9).³³



Scheme 9. Synthesis of 28 ; i) -10 $1a$, MeCN, r.t., 58%.³³

The formation of **1a** indicates a protolysis reaction, while formation of the P–N bonds in **29** and the central P–P bond in **28** is a result of a P–N/P–P bond metathesis. Thus, stepwise protolysis of **2** with bis(phenylphosphaneyl)ethane and subsequent P–N/P–P bond metathesis were assumed. This was verified by multinuclear NMR spectroscopic investigations.



Scheme 10. Formation of hexaphosphane **28** via three P–N/P–P bond metathesis steps; i) CH₂Cl₂, r.t..

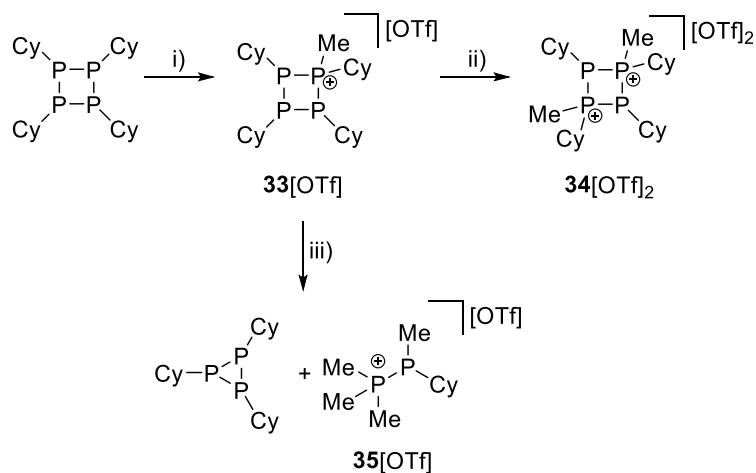
Octaphosphane **30** is formed via condensation reaction of **2** and bis(phenylphosphaneyl)ethane in a 2 : 3 ratio under concomitant release of six equivalents **1a**. **30** is then reacting with another equivalent of **2** forming three equivalents of triphospholane **31** via P–N/P–P bond metathesis reaction (Scheme 10; **I**).

Triphospholane **31** reacts then with another equivalent of **30** yielding hexaphosphane **28** next to pyrazolyl-substituted pentaphosphane **32** (Scheme 10; **II**). The latter was observed by ³¹P NMR spectroscopy as a pair of diastereomers by two AMXYZ spin systems. **32** reacts with

another equivalent of triphospholane **31**, exchanging another triphospholaneyl moiety for a pyrazolyl moiety. This final step yields another equivalent hexaphosphane **28** next to the side product **29** (Scheme 10, **III**). The synthesis of **28** starting from the [P₁]-building block **2** constitutes a novel synthetic approach towards P–P bond formation from conveniently accessible pyrazolyl-substituted phosphanes.

1.3. Polyphosphanes in Methylation Reactions

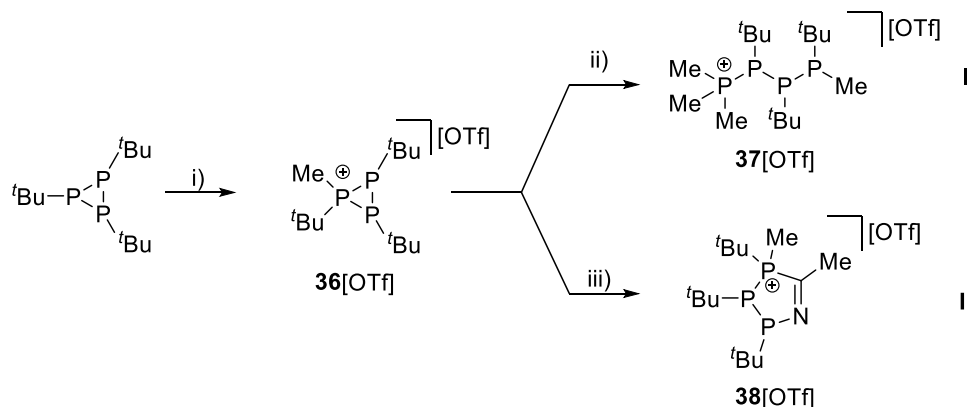
Interesting methylation reactions of polyphosphorus compounds with MeOTf were reported by Schmutzler and co-workers. They methylated dimethylurea bridged P₂ compounds and characterized the products crystallographically.³⁴ With a special interest in catenated polyphosphorus cations, Burford and co-workers investigated the methylation of diphosphanes and *cyclo*-polyphosphanes ((RP)_n R = alky, aryl; n = 3-5), thus, a plethora of cationic polyphosphorus salts with intriguing structural motifs resulted.³⁵ This led to examples intriguingly illustrating the diagonal relationship of phosphorus and carbon, like the hexamethyldiphosphanediium dication, resembling the phosphorus analogue of ethane.^{35e} Moreover, methylation of polyphosphanes has a tremendous impact on the reactivity of these compounds. Methylation of diphosphanes, for example, cause lower energies for the heterolytic cleavage of the λ³P–λ⁴P⁺ bond compared to neutral diphosphanes, as theoretical studies performed on diphosphane-1-ium cations indicate.³⁶ These theoretical studies help to understand the reactivity of λ³P–λ⁴P⁺ bonds, which are conveniently obtained *via* methylation of polyphosphanes. Burford and co-workers further studied methylation reactions of *cyclo*-polyphosphanes and their reactivity.³⁵



Scheme 11. Methylation of (CyP)₄ and phosphonium abstraction of 33[OTf]; i) 1.5 eq. MeOTf, CH₂Cl₂, r.t., 43%; ii) excess MeOTf, neat, r.t.; iii) 1.2 eq. PMe₃, CH₂Cl₂, r.t., 43% (CyP)₃.

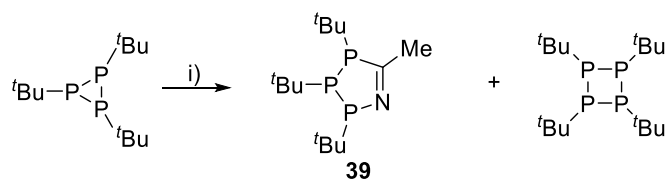
Treatment of (CyP)₄ with an excess MeOTf initially yields tetraphosphetanium triflate 33[OTf], while further stirring for 17 h yields tetraphosphetandium 34[OTf]₂ (Scheme 11).^{35c} Further treatment of tetraphosphetanium triflate 33[OTf] with PMe₃ yields tricyclohexyltriphosphirane and diphosphane-1-ium cation 35⁺ by an phosphonium abstraction reaction.^{35a,d} As (CyP)₄ and PMe₃ do not react with each other, the phosphonium abstraction becomes only feasible after methylation of (CyP)₄ and, thus, causing a higher Lewis acidity

of the so generated λ^4 -phosphorus atom. The same applies for the reactivity of $(t\text{BuP})_3$ and PMe_3 . Only the methylated triphosphiranium triflate salt **36**[OTf] reacts with PMe_3 (Scheme 12; **I**), yielding acyclic tetraphosphanium triflate salt **37**[OTf].³⁷ This nucleophilic ring opening reaction is discussed to resemble structurally and mechanistically the ring opening of an epoxide.³⁷



Scheme 12. Synthesis of triphosphiranium triflate **36**[OTf] and subsequent reaction to tetraphosphonium triflate **37**[OTf] (top) or **38**[OTf] (bottom); i) 2 eq. MeOTf, PhF, r.t., 87%; ii) 1.2 eq. PMe_3 , CH_2Cl_2 , r.t., 75%; iii) excess MeCN, 80 °C, 88%.

Refluxing **36**[OTf] in MeCN yields azatriphospholium triflate salt **38**[OTf] (Scheme 12; **II**). The formation of **38**[OTf] is proposed *via* a sequential ring-opening/ring-closing mechanism with MeCN as the nucleophile.³⁸ While $(t\text{BuP})_3$ is stable in refluxing MeCN for 24 h,³⁹ a solution of $(t\text{BuP})_3$ in PhF undergoes conversion to $(t\text{BuP})_4$ in the presence of one equivalent of Me_3SiOTf at ambient temperature over the course of 72 h.⁴⁰



Scheme 13. Lewis acid induced ring-opening/ring-closing reaction of $(t\text{BuP})_3$; i) 15 mol% Lewis acid, MeCN/PhMe (1 : 1), 90 °C.

Furthermore, reacting $(t\text{BuP})_3$ in a 1 : 1 mixture of MeCN and PhMe with catalytic amounts of a Lewis acid yields mixtures of azatriphospholane **39** and $(t\text{BuP})_4$ with a ratio dependent on the Lewis acid used (Scheme 13).³⁹ This P–P bond association and dissociation behaviour of polyphosphorus compounds assisted by Lewis acids is of special interest with a regard to P–P/P–P bond metathesis (*vide infra*).

1.4. Classification of Pyrazolylphosphanes

In our effort to further control the aforementioned metathesis (*vide supra*) and driven by our general interest in azole- and azine-substituted phosphanes, our research group envisioned the synthesis of pyrazolyl-substituted phosphanes with additional substituents bound to phosphorus *via* the carbon atom. This limits the number of P–N bound pyrazolyl-substituents and, therefore, the possible reaction pathways by P–N/P–P bond metathesis. For a better overview and in thought of a systematic approach, Chart 1 organizes the general types of phosphanes with respect to their number of P–N bound substituents as *SynPhos*^a type I to type IV phosphanes.

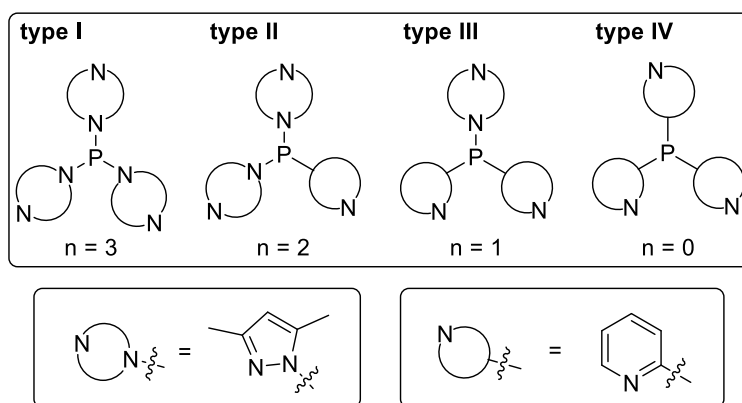
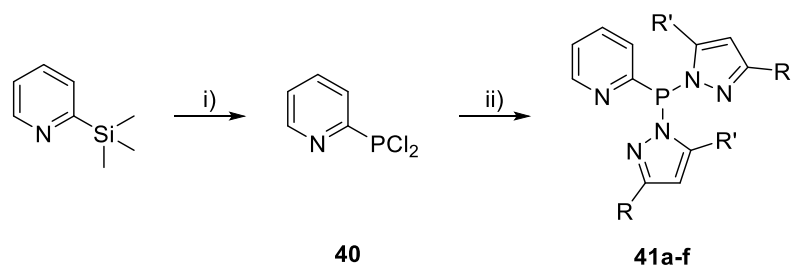


Chart 1. Classification of *N*-heterocyclic-substituted phosphanes in type I to IV phosphanes (*n* is the number of P–N bonds) and one example each for a P–N bound substituent and a P–C bound substituent.

Whereas in type I phosphanes all three substituents are bound *via* P–N bonds, type II phosphanes are defined by two P–N bonds and one P–C bond. This order is maintained in type III phosphanes with one P–N and two P–C bonds and is finalized in type IV phosphanes featuring only P–C bonds. Importantly, all substituents at the phosphorus atom exhibit an additional sp^2 hybridized donor atom such as nitrogen, being essential as further reaction or coordination site and for the possible formation of resonance stabilized reaction intermediates. First results in the synthesis of type II phosphanes are reported in my master thesis.⁴¹ Starting with a new, salt-free synthesis of 2-pyridyl-dichlorophosphate **40** on a multi-gram scale, type II phosphanes **41a-f** are conveniently prepared by the reaction of **40** with trimethylsilyl-substituted phosphanes **5a-f** as mentioned before (Scheme 14).^{22,41,42}

^a *SynPhos* ist the acronym of the ERC funded project „Highly-Reactive (Regenerative) Phosphorus Building Blocks – New Concepts in Synthesis“ (Grant No 307616) and stands for reagents which can be applied in efficient, selective and high-yielding molecular transformation reactions.



Scheme 14. Synthesis of type II phosphanes **41a-f** starting from 2-(trimethylsilyl)pyridine; i) 3 eq. PCl_3 , - Me_3SiCl , 76 °C, 48 h, 81%; ii) 2.1 eq. **5a-f**, -2 Me_3SiCl , r.t., 16 h, 97% (**5a/41a** $\text{R} = \text{R}' = \text{Me}$), 64 % (**5b/41b** $\text{R} = \text{R}' = \text{'Pr}$), 67 % (**5c/41c** $\text{R} = \text{R}' = \text{'Bu}$), 91% (**5d/41d** $\text{R} = \text{R}' = \text{Ph}$; CH_2Cl_2 used as solvent), 71% (**5e/41e** $\text{R} = \text{CF}_3$, $\text{R}' = \text{H}$), 89% (**5f/41f** $\text{R} = \text{CF}_3$, $\text{R}' = \text{Me}$).

Refluxing 2-(trimethylsilyl)-pyridine in a threefold excess of PCl_3 gives **40** in good yields on a multi-gram scale. Further reaction with two equivalents of **5a-f** yields type II phosphanes **41a-f** (Scheme 14).

The thus synthesized phosphanes **41a-f** have neither been characterized by X-ray analysis nor have they been studied in P–P bond formation reactions. This is one objective of this work.

2. Objectives

The objective of this work is to explore new synthetic routes towards polyphosphanes *via* condensation and P–N/P–P bond metathesis of the aforementioned **SynPhos** type II phosphanes. In the master thesis, the synthesis of **41a-f** is described by reacting 2-(pyridyl)-dichlorophosphane (**40**) with the corresponding 1-(trimethylsilyl)-pyrazoles **5a-f** (*vide supra*). Next to synthesizing type II phosphanes with different P–C bound heterocycles, especially the reactivity of type II phosphanes towards primary and secondary phosphanes is targeted, establishing the **SynPhos** type II phosphanes as suitable [R–P] building blocks in polyphosphorus chemistry (Chart 2).

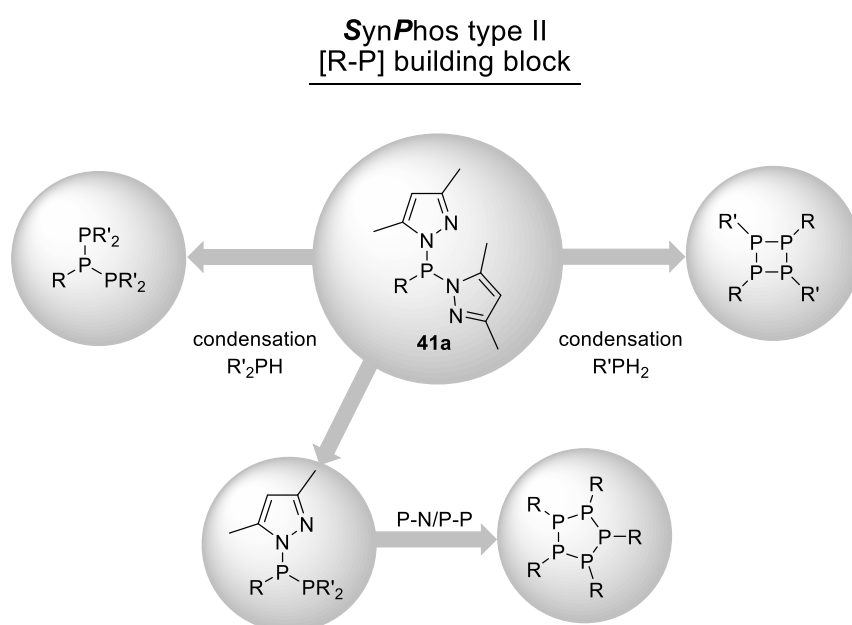


Chart 2. **SynPhos** type II phosphanes as [R–P] building blocks in condensation and P–N/P–P bond metathesis reactions; R = pyridyl; R' = alkyl, aryl.

Similar to the synthesis of **7** and **8**, **SynPhos** type II phosphanes should allow for the stepwise substitution of the pyrazolyl moieties by dialkyl- or diarylphosphaneyl groups yielding di- and triphosphanes. Furthermore, the type II phosphanes should serve as excellent educts in the synthesis of *cyclo*-phosphanes. Either in condensation reactions with primary phosphanes or in P–N/P–P bond metathesis reactions. Thus, the already known **SynPhos** type II phosphanes **41a-f** should conveniently enable the introduction of pyridyl-substituents into polyphosphorus chemistry. Therefore, not only their synthesis is envisioned, but also the exploration of their chemistry.

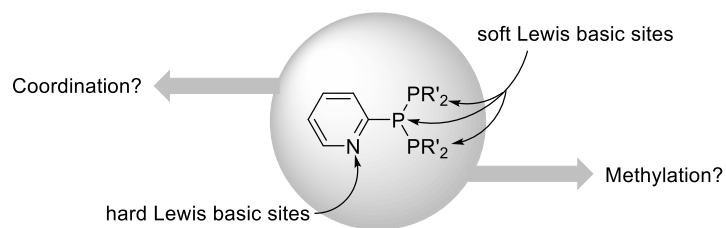


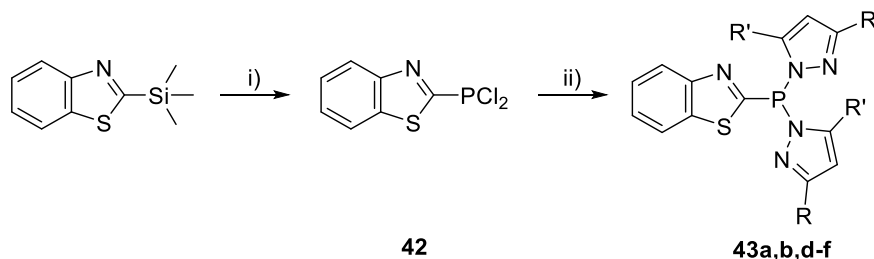
Chart 3. Envisioned pyridyl-substituted triphosphane, bearing hard and soft Lewis basic sites.

Chart 3 exemplarily shows a pyridyl-substituted triphosphane, which should be accessible in analogy to triphosphane **7** (*vide supra*). Bearing multiple different Lewis basic sites, reactions with various electrophiles are a promising way to understand the chemical behavior of pyridyl-substituted polyphosphanes. This may be achieved by the reaction with the strong alkylation reagent MeOTf, envisioning a convenient way towards multiply-charged, highly reactive polyphosphorus cations. Next to methylation reactions, the coordination chemistry of pyridyl-substituted polyphosphanes is of interest. While phosphaneyl moieties for example are rather soft donors according to the HSAB concept, the pyridyl-substituent bears a harder donor site. This is best studied by coordination with selected coinage metal salts.

3. Synthesis of Pyrazolylphosphanes

3.1. Synthesis of Type II Phosphanes

To further extend the library of type II phosphanes 2-benzo[*d*]thiazolyl-dichlorophosphate **42** was synthesized and reacted with trimethylsilyl-substituted pyrazoles **5** in the same manner as mentioned before yielding type II phosphanes **43** (Scheme 15).⁴³



Scheme 15. Synthesis of type II phosphanes **43a,b,d-f** starting from 2-(trimethylsilyl)benzo[*d*]thiazole; i) 3 eq. PCl_3 , $-\text{Me}_3\text{SiCl}$, 76 °C, 48 h, 67%; ii) 2.1 eq. **5**, $-2 \text{ Me}_3\text{SiCl}$, 96% (**5a/43a** R = R' = Me), 85 % (**5b/41b** R = R' = *i*Pr), 73% (**5d/43d** R = R' = Ph), 51% (**5e/43e** R = CF_3 , R' = H), 58% (**5f/43f** R = CF_3 , R' = Me).

Refluxing 2-(trimethylsilyl)-benzo[*d*]thiazole in a threefold excess of PCl_3 gives an orange residue after evaporation off all volatiles *in vacuo*. From this residue **42** is obtained *via* sublimation as a colorless, crystalline solid in good yields of 67%. As **42** is a solid it is dissolved in Et_2O before addition of **5** yielding phosphanes **43** in yields up to 96%. Each type II phosphane **43** shows a singlet resonance in the ^{31}P NMR spectrum in the range of $\delta(^{31}\text{P}) = 38.0\text{-}54.1$ ppm. Together with pyridyl-substituted phosphanes **41** a small library of eleven type II phosphanes is available which are fully characterized. The structural connectivity is confirmed for all eleven type II phosphanes by X-ray analysis. Suitable crystals can be obtained either by addition of *n*-pentane to saturated CH_2Cl_2 solutions of the phosphane (**41a**, **41d**, **41f**, **43a**, **43b**, **43d**) or by cooling a saturated solution of the phosphane in Et_2O (**43e**, **43f**) or *n*-hexane (**41b**, **41c**, **41e**) from room temperature to -30 °C. The molecular structures are depicted in Figure 1, with the geometrical parameters given in Table 1. All depicted phosphanes **41** and **43** show the typical pyramidal geometry of the phosphorus atom, known for P(III) compounds. The P–C bond lengths of **41** (see Table 1) are comparable to the P–C bond lengths reported for tris(2-pyridyl)phosphane (1.824(3)-1.834(3) Å)⁴⁴ and the P–C bonds in **43** (see Table 1) are comparable to those in tris(2-benzothiazolyl)phosphane (P–C 1.820(2) Å).⁴⁵ The P–N bonds in **41** and **43** are slightly elongated compared to the P–N bonds reported for tri(1*H*-pyrazol-1-yl)phosphane (P–N

1.714(4) Å).⁴⁶ This might be caused by the P–C bound aromatic substituent and its positive inductive effect.

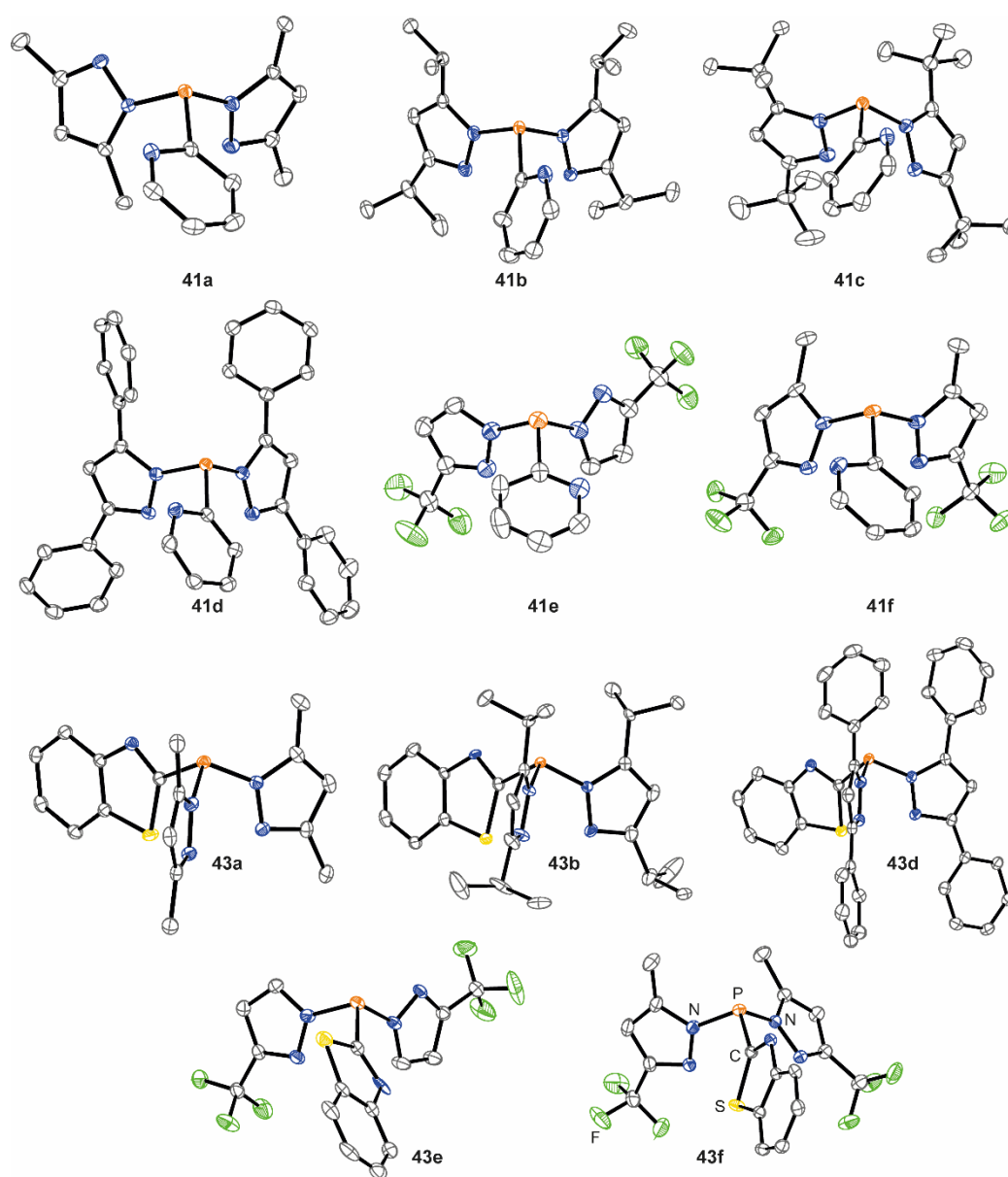


Figure 1. Molecular structures of type II phosphanes **41** and **43** (hydrogen atoms and solvate CH_2Cl_2 in **43b** $\cdot\text{CH}_2\text{Cl}_2$ are omitted for clarity and thermal ellipsoids are displayed at 50% probability). Selected geometrical parameters are given in Table 1.

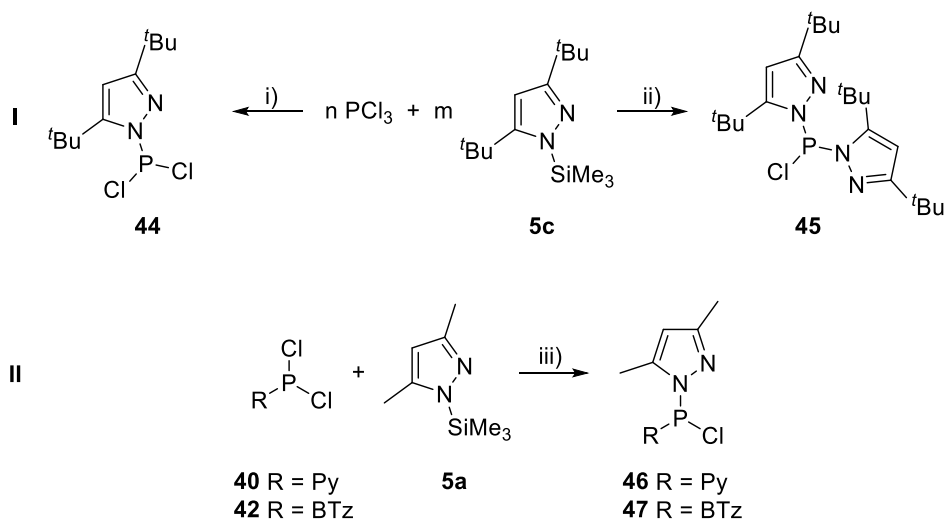
Table 1. Selected geometrical parameters of crystallographically characterized type II phosphanes **41** and **43**.

	P–C in Å	P–N in Å ^a	C–P–N in ° ^a	N–P–N
41a	1.827(1)	1.72	100.7	103.26(5)
41b	1.829(1)	1.73	101.4	104.14(5)
41c	1.841(4)	1.74	98.2	100.29(6)
41d	1.830(1)	1.74	101.2	100.88(5)
41e	1.838(3)	1.73	99.5	100.7(1)
41f	1.824(1)	1.73	101.3	100.90(5)
43a	1.829(2)	1.719(1) ^b	101.26(5) ^b	103.84(7)
43b	1.822(9)	1.717(5) ^b	101.9(3) ^b	105.0(4)
43d	1.823(1)	1.73	100.1	101.85(6)
43e	1.832(2)	1.73	98.8	100.76(10)
43f	1.824(2)	1.73	101.5	100.26(6)

a) Average bond lengths and angles are given; b) exact values due to symmetry.

3.2. Synthesis of Pyrazolyl-substituted Phosphorus Chlorides

Peterson and co-workers not only investigated on tripyrazolylphosphanes like **2** but also reported the synthesis of 1-(dichlorophosphaneyl)-3,5-dimethylpyrazole in 98% yield from **5a** and PCl_3 .²² The product was solely characterized by mass spectrometry and the synthesis is not reproducible in our laboratories. Yet, changing the substituents on the pyrazole in 3,5-position allows the synthesis of pyrazolyl-substituted chlorophosphanes. Reacting **5c** and PCl_3 yields pyrazolyldichlorophosphate **44** or dipyrazolylchlorophosphate **45** depending on the stoichiometry applied (Scheme 16; I).



Scheme 16. Synthesis of pyrazolylchlorophosphanes **44-47**; i) $n = 2$, $m = 1$, $-\text{Me}_3\text{SiCl}$; ii) $n = 1$, $m = 2$, $-\text{Me}_3\text{SiCl}$; iii) $-\text{Me}_3\text{SiCl}$, n -pentane.

Both phosphanes **44** and **45** are isolated as colorless solids after evaporation of all volatiles *in vacuo* in essentially quantitative yields on a multi-gram scale and show a singlet resonance each in the ^{31}P NMR spectrum **44**: $\delta(^{31}\text{P}) = 148.5$ ppm, **45**: $\delta(^{31}\text{P}) = 106.4$ ppm. Moreover, one chloro-substituent of dichlorophosphanes **40** and **42** can be selectively exchanged with a pyrazolyl moiety by the reaction with **5a** (Scheme 16; II). Reacting either **40** or **42** with one equivalent **5a** in n -pentane gives a colorless precipitate of pyrazolyl-chlorophosphate **46** or **47** in very good yields of 84% and 95%, respectively. These phosphanes also show a singlet resonance each in the ^{31}P NMR spectrum **46**: $\delta(\text{P}) = 80.1$ ppm and **47**: $\delta(\text{P}) = 76.1$ ppm. Crystals of **44-47** suitable for X-ray analysis are obtained by slow vapor diffusion of n -pentane into saturated CH_2Cl_2 solutions of each phosphane. The molecular structures are depicted in Figure 2.

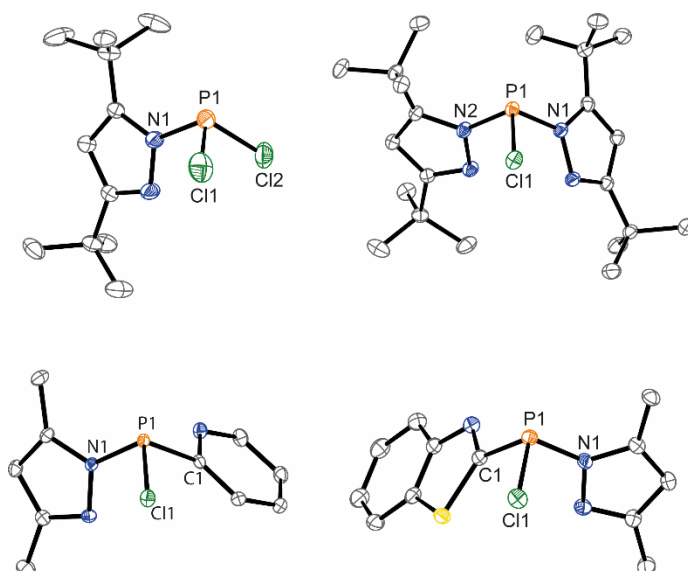


Figure 2. Molecular structures of **44** (top left), **45** (top right), **46** (bottom left) and **47** (bottom right; hydrogen atoms are omitted for clarity and thermal ellipsoids are displayed at 50% probability). Selected bond lengths (Å) and angles (°) for **44**: P1–Cl1 2.0577(11), P–Cl2 2.0435(10), P1–N2 1.703(2), N1–P1–Cl1 100.50(9), Cl1–P1–Cl2 99.43(4), Cl2–P1–N1 99.75(8); **45**: P1–Cl1 2.0633(4), P1–N1 1.7175(9), P1–N2 1.7183(10), Cl1–P1–N1 98.67(3), N1–P1–N2 101.22(4), N2–P1–Cl1 101.40(4); **46**: P1–Cl1 2.0728(5), P1–Cl1 1.8352(14), P1–N1 1.7155(12), Cl1–P1–Cl1 99.80(5), C1–P1–N1 99.62(6), N1–P1–Cl1 101.06(4); **47**: P1–Cl1 2.0839(6), P1–Cl1 1.8227(17), P1–N1 1.7179(14), Cl1–P1–Cl1 98.37(7), C1–P1–N1 97.93(7), N1–P1–Cl1 100.51(5).

All four phosphanes show the pyramidal geometry expected for a P(III) compound. Due to a positive mesomeric effect of the pyrazole moieties on the phosphorus, the P–Cl bonds in phosphanes **44** (2.0577(11) Å) and **45** (2.0633(4) Å) are slightly elongated compared to the P–Cl bond length in PCl₃ (2.043(3) Å).⁴⁷ An additional inductive effect of the P–C bound aromatic substituents leads to a further elongation of the P–Cl bonds in **46** (2.0728(5) Å) and **47** (2.0839(6) Å). The P–N bond in **44** (1.703(2) Å) is shortened compared to the P–N bonds in **45** (1.7175(9) and 1.7183(10) Å), **46** (1.7155(12) Å), **47** (1.7179(14) Å) and tri(1*H*-pyrazol-1-yl)phosphane (P–N 1.714(4) Å).⁴⁶ This is best explained due to the presence of two instead of one electron withdrawing chloride-substituent in **44**. The P–C bonds in **46** (1.8352(14) Å) and **47** (1.8227(17) Å) are comparable to **41a** (1.827(1) Å) and **43a** (1.829(2) Å).

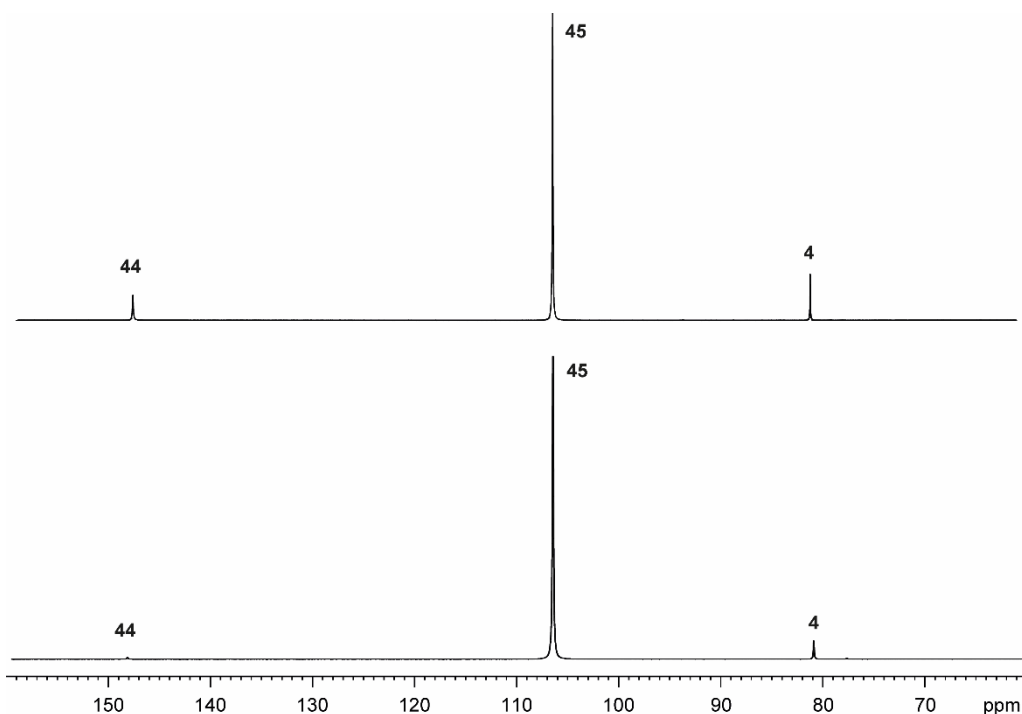
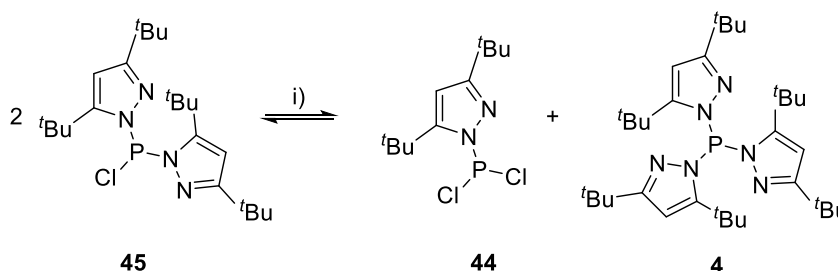


Figure 3. ^{31}P NMR spectra of **45** in CD_2Cl_2 for 1 h (bottom) and after 6 h (top) (CD_2Cl_2 , 300 K).

All phosphanes **44-47** are colorless solids that are stable when kept under inert conditions. Yet, in solution an exchange of the pyrazolyl- and chlorido-substituents is observed. Figure 3 shows the ^{31}P NMR spectra of **45** after 1 h and after 6 h in CD_2Cl_2 solution. A scrambling reaction is observed, forming dichlorophosphane **44** and tripyrazolylphosphane **4** (Scheme 17).



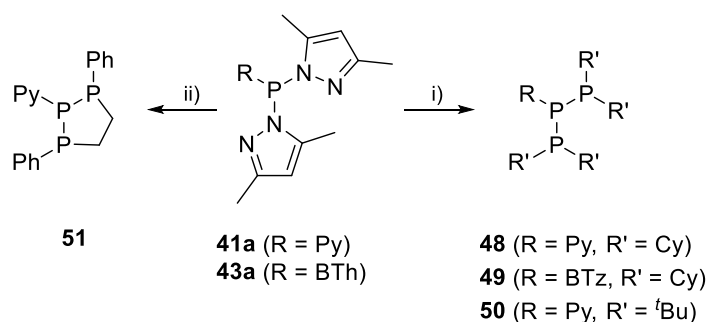
Scheme 17. Scrambling reaction of **45**, **44** and **4**; i) CD_2Cl_2 , r.t.

Similar P–N/P–Cl exchange reactions are known from dialkylamino-substituted phosphanes and widely used in the synthesis of chlorophosphanes.⁴⁸ Yet, further investigations on pyrazolyl-substituted chlorophosphanes was abstained as a main focus of this thesis lies on the *SynPhos* type II phosphanes and their use in P–P bond formation reactions.

4. Reactivity of Type II Phosphanes towards Secondary Phosphanes

4.1. P–P Bond Formation *via* Condensation Reactions

In analogy to the synthesis of **7** and **8** starting from *SynPhos* type I phosphane **2** (*vide supra*) the reaction of type II phosphanes **41a** and **43a** towards secondary phosphanes was investigated. Reacting **41a** and **43a** with secondary phosphanes R'_2PH ($R' = \text{Cy}$, $t\text{Bu}$ or $R'_2PH = \text{PhP(H)C}_2\text{H}_4\text{P(H)Ph}$) yields triphosphanes **48-50** and 1,2,3-triphosholane **51** under concomitant release of 3,5-dimethylpyrazole (Scheme 18).



Scheme 18. Synthesis of triphosphanes **48-50**: i) 2 eq. R'_2PH , -2 **1a**, MeCN; and triphosholane **51**: 1 eq. $\text{PhPH}(\text{CH}_2)_2\text{PPh}$, -2 **1a**, MeCN.

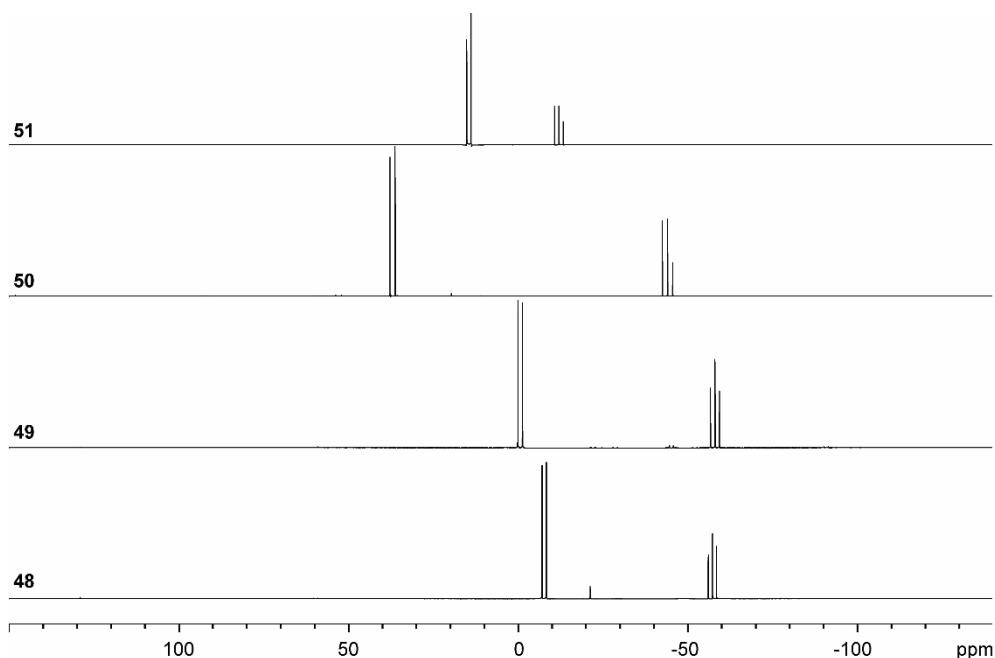


Figure 4. ^{31}P NMR spectra of compounds **48-51**. (all in CD_2Cl_2 , 300 K) **48**: AX_2 spin system: $\delta(\text{P}_A) = -57.3$ (1P), $\delta(\text{P}_X) = -7.7$ (2P) ppm; $^1J(\text{P}_A\text{P}_X) = -251$ Hz; **49**: AX_2 spin system: $\delta(\text{P}_A) = -58.1$ (1P), $\delta(\text{P}_X) = -0.7$ (2P) ppm; $^1J(\text{P}_A\text{P}_X) = -269$ Hz; **50**: AX_2 spin system: $\delta(\text{P}_A) = -44.1$ (1P), $\delta(\text{P}_X) = 37.0$ (2P) ppm; $^1J(\text{P}_A\text{P}_X) = -307$ Hz; **51**: AX_2 spin system: $\delta(\text{P}_A) = -12.1$ (1P), $\delta(\text{P}_X) = 14.5$ (2P) ppm; $^1J(\text{P}_A\text{P}_X) = -261$ Hz.

Compounds **48-51** readily precipitate from the reaction mixture and are isolated by filtration. Subsequent washing with MeCN and drying *in vacuo* gives **48-51** as colorless solids in good to excellent yield (96% (**48**); 93% (**49**); 77% (**50**); 69% (**51**)). The ^{31}P NMR spectra of all compounds give rise to AX_2 spin systems which are characteristic for triphosphanes and 1,2,3-triphospholanes (Figure 4). Single crystals for X-ray analysis are obtained by slow vapor diffusion of *n*-pentane into saturated CH_2Cl_2 solutions of **48-51**. The molecular structures of **48-51** are depicted in Figure 5. The structural parameters compare very well with similar triphosphanes⁴⁹ and are thus not discussed in detail. Only the bond angle of the P-P-P moiety in compound **51** is approximately 10° wider which can be explained by the sterically demanding *tert*-butyl substituents.

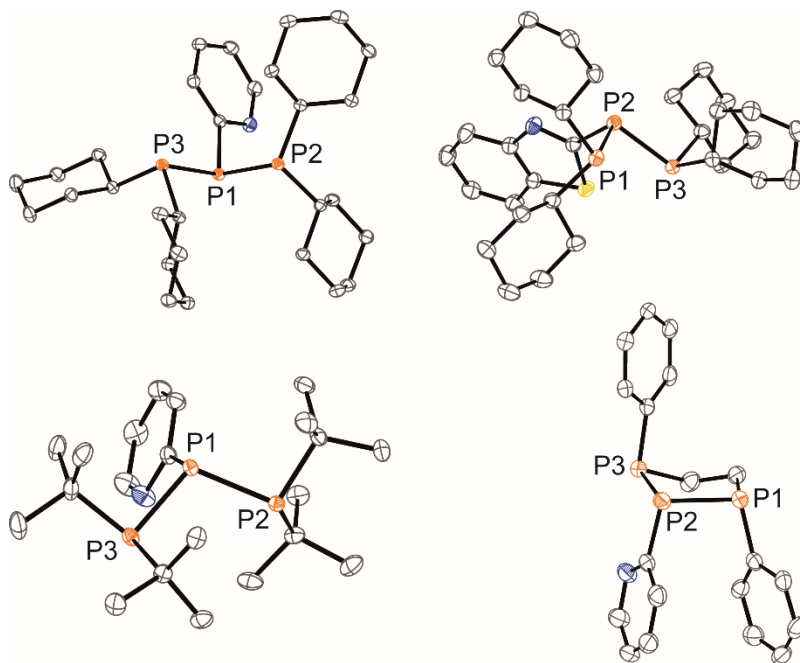
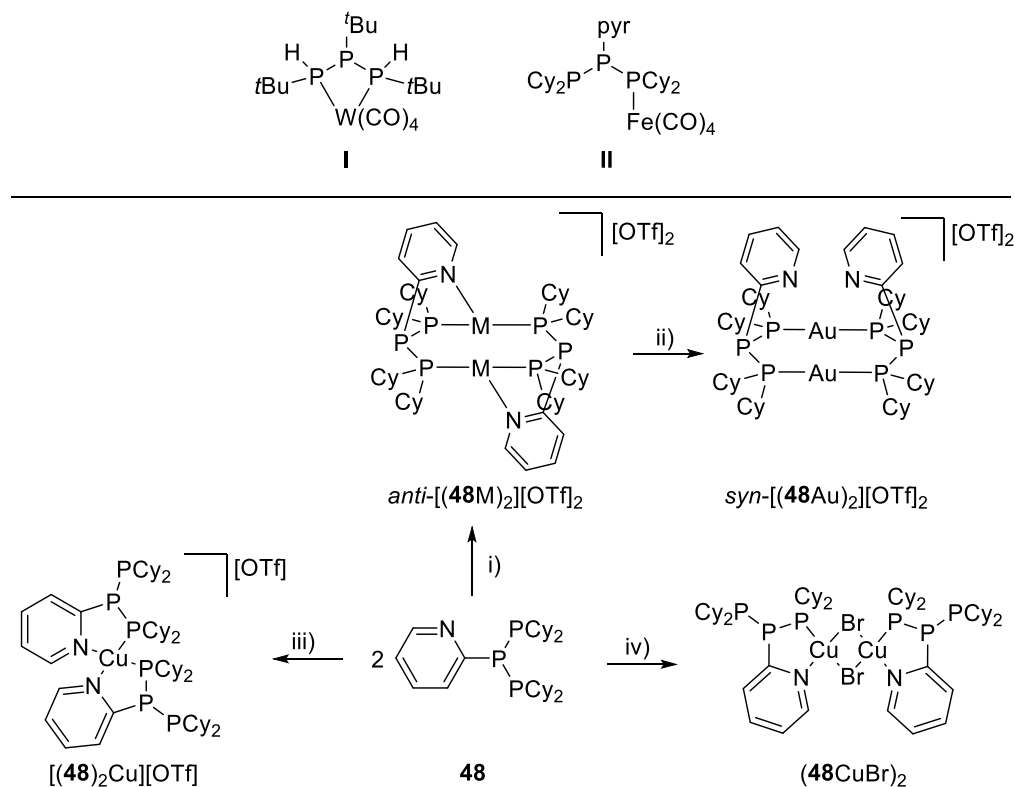


Figure 5. Molecular structures of the triphosphanes **48** (top left), **49** (top right), **50** (bottom left) and triphospholane **51** (bottom right) (hydrogen atoms are omitted for clarity, thermal ellipsoids are displayed at 50% probability). Selected bond lengths (Å) and angles ($^\circ$) for **48**: P1–P2 2.2301(3), P1–P3 2.2371(3), P3–P1–P2 97.389(12); **49**: P1–P2 2.2377(5), P2–P3 2.2234(5), P1–P2–P3 98.112(19); **50**: P1–P2 2.2181(3), P1–P3 2.2485(3), P2–P1–P3 107.642(14); **51**: P1–P2 2.2703(16), P2–P3 2.1971(18), P1–P2–P3 97.16(6).

4.2. Coinage Metal Complexes of Triphosphane **48**

In recent years numerous examples on the coordination chemistry of anionic⁵⁰ and zwitterionic⁵¹ oligophosphorus compounds towards transition metals have been reported. Also few examples of neutral triphosphanes coordinated to transition metals are known, however, the triphosphane moiety was assembled while coordinated to at least one metal center.⁵² Yet, to the best of knowledge only two complexes of free triphosphanes coordinating to metal carbonyls have been structurally characterized (Scheme 19, top),^{11,53} while another example is described in solution.⁵⁴ In complex **I** the triphosphane ligand chelates the $W(CO)_4$ moiety while in complex **II** the coordination of the $Fe(CO)_4$ moiety proceeds only *via* the free electron pair of one of the dicyclohexylphosphane groups. Featuring an additional nitrogen-based donor site in **48-51** the formation of multi-dentate coinage metal complexes is of interest. Triphosphane **48** yielded the first triphosphane coordination complexes of Cu(I), Ag(I) and Au(I) (Scheme 19).

Known triphosphanes coordinating to metal carbonyls



Scheme 19. Known transition metal complexes featuring a neutral triphosphane ligand (top); Synthesis of coinage metal coordination complexes starting from triphosphane **48** (bottom); i) 2 eq. $Ag[OTf]$, PhF (M = Ag); 2 eq. $[(MeCN)_4Cu][OTf]$, -8 MeCN, CH_2Cl_2 (M = Cu); ii) 2 eq. $(tht)AuCl$, -2 tht, -2 $AgCl$, MeCN; iii) 1 eq. $[(MeCN)_4Cu][OTf]$, -4 MeCN, CH_2Cl_2 ; iv) 2 eq. $(tht)CuBr$, -2 tht, THF.

Reacting **48** with an equimolar amount of Ag[OTf] in fluorobenzene at ambient temperature leads to the formation of a colorless precipitate, which is isolated by filtration to yield the dinuclear complex $[(\mathbf{48Ag})_2][\text{OTf}]_2$ in essentially quantitative yield. The corresponding reaction of **48** with $[(\text{MeCN})_4\text{Cu}][\text{OTf}]$ in CH_2Cl_2 gives colorless plates upon slow vapor diffusion of *n*-pentane at $-30\text{ }^\circ\text{C}$ which can be isolated as $[(\mathbf{48Cu})_2][\text{OTf}]_2$ up to a yield of 94%. Further transmetallation reaction of $[(\mathbf{48Ag})_2][\text{OTf}]_2$ with (tht)AuCl in MeCN yields $[(\mathbf{48Au})_2][\text{OTf}]_2$ in 64% yield by the concomitant precipitation of AgCl. Slow diffusion of *n*-pentane into a CH_2Cl_2 solution of **48** and $[(\text{MeCN})_4\text{Cu}][\text{OTf}]$ in a 2 : 1 ratio yields 93% of crystalline $[(\mathbf{48})_2\text{Cu}][\text{OTf}]$. Formation of $(\mathbf{48CuBr})_2$ is achieved by slow diffusion of *n*-pentane into a THF solution of equimolar amounts of **48** and (tht)CuBr. The molecular structures of the aforementioned coinage metal complexes are shown in Figure 6 and the structural parameters are summarized in Table 2. Different from the known coordination motifs for **I** and **II**, the molecular structures of $[(\mathbf{48Cu})_2][\text{OTf}]_2$, $[(\mathbf{48Ag})_2][\text{OTf}]_2$ and $[(\mathbf{48Au})_2][\text{OTf}]_2$ reveal dinuclear metal complexes featuring two triphosphane ligands. In addition to the terminal coordinating phosphorus atoms, the nitrogen atoms of the pyridyl-substituents are involved in the coordination resulting in an approximately tetrahedral coordination environment of the respective metal center.

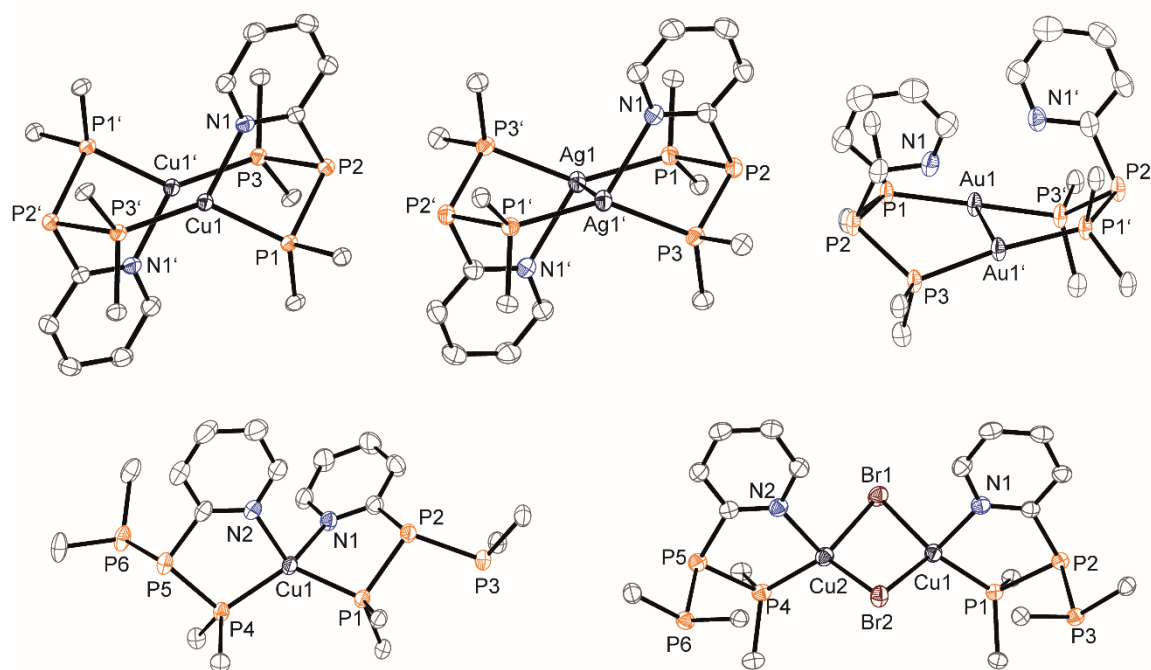


Figure 6. Molecular structures of the coinage metal complexes $[(\mathbf{48Cu})_2]^{2+}$ in $[(\mathbf{48Cu})_2][\text{OTf}]_2 \cdot 4 \text{CH}_2\text{Cl}_2$, $[(\mathbf{48Ag})_2]^{2+}$ in $[(\mathbf{48Ag})_2][\text{OTf}]_2 \cdot \text{MeCN}$, $[(\mathbf{48Au})_2]^{2+}$ in $[(\mathbf{48Au})_2][\text{OTf}]_2$, $[(\mathbf{48})_2\text{Cu}]^+$ in $[(\mathbf{48})_2\text{Cu}][\text{OTf}] \cdot n\text{-C}_5\text{H}_{12}$ and $(\mathbf{48CuBr})_2$ in $(\mathbf{48CuBr})_2 \cdot n\text{-C}_5\text{H}_{12} \cdot \text{THF}$ (hydrogen atoms, anions and solvate molecules are omitted for clarity, cyclohexyl groups are represented only by their phosphorus bound carbon atoms, thermal ellipsoids are displayed at 50% probability). Selected geometrical parameters are given in Table 2.

Table 2: Selected geometrical parameters of crystallographically characterized coinage metal complexes depicted in Figure 6.

	$[(\mathbf{48Cu})_2]^{2+}$	$[(\mathbf{48Ag})_2]^{2+}$	$[(\mathbf{48Au})_2]^{2+}$	$[(\mathbf{48})_2\text{Cu}]^+$ (a)	$(\mathbf{48CuBr})_2$ (a)
M1–M1' in Å	2.8225(5)	2.9013(4)	2.880(3)	-	2.942
M1–P1 in Å	2.2755(4)	2.3818(8)	2.3033(8)	2.243	2.191
M1–P3' in Å	2.2176(5)	2.4468(7)	2.3198(8)		
M–N in Å	2.0485(14)	2.404(3)	2.948(3)	2.106	2.116
P–P ^a in Å	2.225	2.176	2.226	2.212	2.214
P1–M1–P3 in °	136.520(18)	143.96(3)	171.52(3)	-	-
P–P–P ^a in °	98.26(2)	100.16(4)	98.29(5)	104.43	102.43

(a) average bond lengths and angles are given.

While the molecular structures of the dinuclear complexes $[(\mathbf{48Cu})_2][\text{OTf}]_2$ and $[(\mathbf{48Ag})_2][\text{OTf}]_2$ reveal an *anti*-arrangement with inversion symmetry, the gold complex $[(\mathbf{48Au})_2][\text{OTf}]_2$ crystallizes as centro-symmetrical *syn*-isomer. The inversion process within the complexes has been investigated by variable temperature NMR experiments and quantum mechanical calculations (*vide infra*). The difference in the arrangement in the solid state causes a widening of the P–M–P angles from the copper complex $[(\mathbf{48Cu})_2][\text{OTf}]_2$ (P3'–Cu1–P1 136.520(18)°) over the silver complex $[(\mathbf{48Ag})_2][\text{OTf}]_2$ (P1–Ag1–P3' 143.96(3)°) to an almost linear geometry around the gold atoms in $[(\mathbf{48Au})_2][\text{OTf}]_2$ (P1–Au1–P3' 171.52(3)°). The distances between the silver atoms in $[(\mathbf{48Ag})_2][\text{OTf}]_2$ and the gold atoms in $[(\mathbf{48Au})_2][\text{OTf}]_2$ indicate the presence of argentophilic and aurophilic interactions, respectively.⁵⁵ As the distance between the copper atoms in $[(\mathbf{48Cu})_2][\text{OTf}]_2$ is slightly larger than the sum of the van der Waals radii of two copper atoms (2.80 Å)⁵⁶, intermetallic interactions can be excluded. The observed P–M bond lengths in $[(\mathbf{48M})_2][\text{OTf}]_2$ as well as those in $[(\mathbf{48})_2\text{Cu}][\text{OTf}]$ and $(\mathbf{48CuBr})_2$ are in good agreement with bond lengths reported for the structurally similar $[\text{M}_2(\text{dcpm})_2]^{2+}$ cations (M = Cu(I), Ag(I) or Au(I); dcpm = bis(dicyclohexylphosphanyl)methane).⁵⁷ For $(\mathbf{48CuBr})_2$ the formation of the typical Cu_2X_2 (X = halogenide) geometry is found, only marginally differing from the typical planar arrangement reported for many Cu_2X_2 -type structures.⁵⁸ Compared to the free ligand **48** the P–P bond lengths and the P–P–P angles in the coinage metal complexes are only marginally altered.

The room temperature NMR spectra of the dinuclear complexes $[(\mathbf{48Au})_2][\text{OTf}]_2$ and $[(\mathbf{48Ag})_2][\text{OTf}]_2$ give rise to broadened resonances due to dynamic processes in solution.⁵⁹ The low temperature ³¹P NMR spectrum of $[(\mathbf{48Au})_2][\text{OTf}]_2$ shows two separate AA'XX'X''X''' spin systems at $\delta(\text{P}_A) = -34.2$ ppm, $\delta(\text{P}_X) = 52.6$ ppm and $\delta(\text{P}_A) = -37.8$ ppm, $\delta(\text{P}_X) = 50.3$ ppm corresponding to the respective *syn*- and *anti*-isomers

(Figure 7). Details on the coupling constants are included in the experimental details (*vide infra*). For $[(48\text{Ag})_2][\text{OTf}]_2$ also two isomers are observed by two separate AA'XX'X''X''' spin systems at $\delta(\text{P}_\text{A}) = -48.5$ ppm, $\delta(\text{P}_\text{X}) = 36.1$ ppm and $\delta(\text{P}_\text{A}) = -51.5$ ppm, $\delta(\text{P}_\text{X}) = 36.1$ ppm (Figure 7).

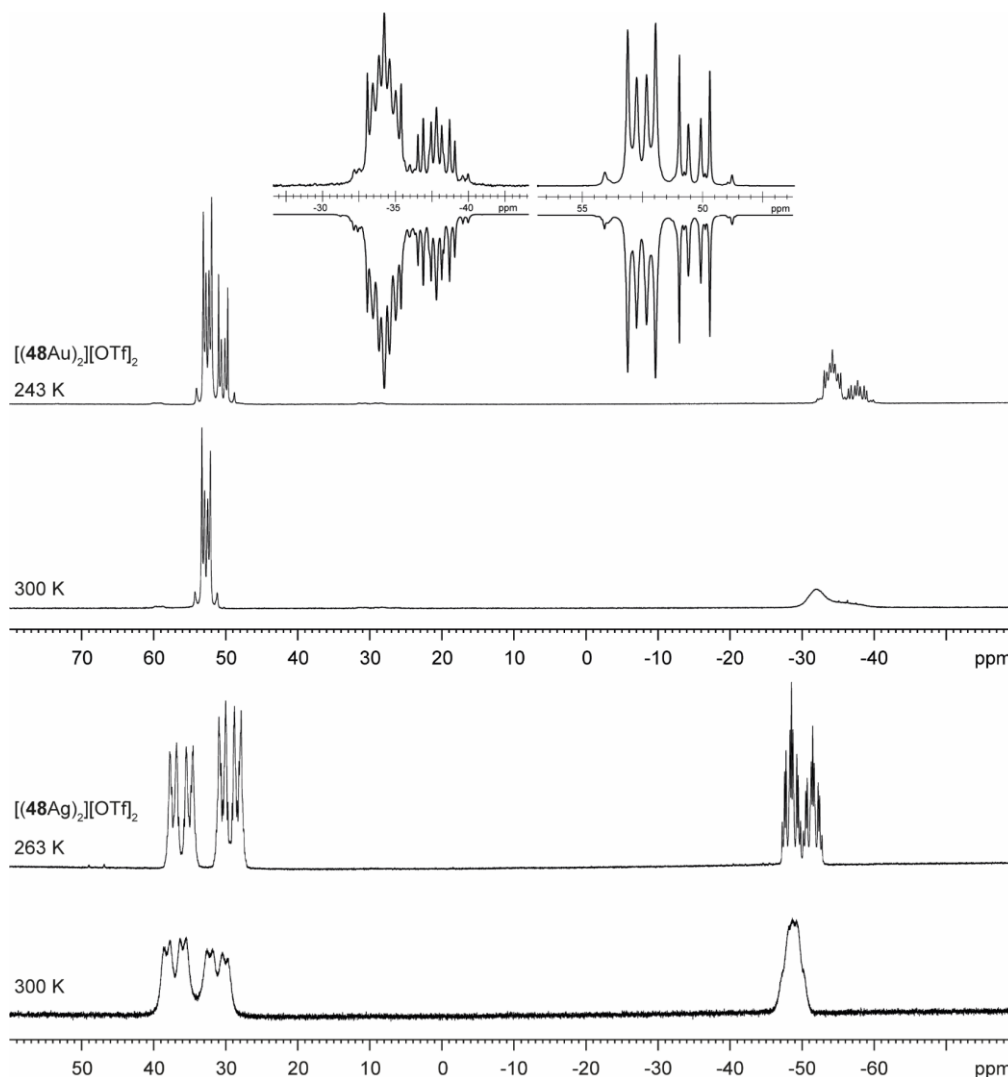


Figure 7. ^{31}P NMR spectra of compound $[(48\text{Ag})_2][\text{OTf}]_2$ in CD_3CN at 300 K and 263 K and of $[(48\text{Au})_2][\text{OTf}]_2$ in CD_2Cl_2 at 300 K and 243 K; insets show the two AA'XX'X''X''' spin systems of the experimental (upwards) and fitted spectra (downwards) for $[(48\text{Au})_2][\text{OTf}]_2$ at 243 K.

Due to the existence of three isotopologues for $[(48\text{Ag})_2][\text{OTf}]_2$, as a result of the complexation to the $^{107}\text{Ag}/^{109}\text{Ag}$ nuclei, iteratively fitting the corresponding ^{31}P NMR spectrum was refrained from. The ^{31}P NMR spectrum of the dinuclear copper complex $[(48\text{Cu})_2][\text{OTf}]_2$ shows only the resonances of one AA'XX'X''X''' spin system at $\delta(\text{P}_\text{A}) = -39.1$ ppm and $\delta(\text{P}_\text{X}) = 15.4$ ppm. An additional broadened AX₂ spin system ($\delta(\text{P}_\text{A}) = -37.5$ ppm, $\delta(\text{P}_\text{X}) = 15.3$ ppm ($^1J(\text{P}_\text{A}\text{P}_\text{X}) = -168$ Hz) gives rise to the formation of a monomeric

species in solution which was not further investigated. A comparable AX_2 spin system is observed for $[(\mathbf{48})_2\text{Cu}][\text{OTf}]$ ($\delta(\text{P}_A) = -44.8$ ppm, $\delta(\text{P}_X) = -8.9$ ppm ($^1J(\text{P}_A\text{P}_X) = -275$ Hz) as well as for $(\mathbf{48}\text{CuBr})_2$ ($\delta(\text{P}_A) = -46.6$ ppm, $\delta(\text{P}_X) = -6.2$ ppm ($^1J(\text{P}_A\text{P}_X) = -253$ Hz). For both mononuclear copper complexes, the resonances in the ^{31}P NMR spectrum are noticeably broadened due to the fast quadrupole relaxation of the ^{63}Cu nucleus.⁵⁹

Theoretical calculations performed at the BP86-D3/def2-TZVP level of theory support the isomerization in the dinuclear metal complexes $[(\mathbf{48M})_2]^{2+}$. For $[(\mathbf{48Cu})_2]^{2+}$ a relative energy difference between the *syn*- and the *anti*-isomer of 5.0 kcal/mol was found which explains that only one isomer is observed in the ^{31}P NMR spectrum. While the two isomers of $[(\mathbf{48Ag})_2]^{2+}$ are isoenergetic with a difference of 0.1 kcal/mol, the *syn*-isomer of $[(\mathbf{48Au})_2]^{2+}$ is favored by 1.7 kcal/mol compared to its *anti*-isomer. The optimized geometries also show the different coordination behavior of the pyridyl-moieties in the three metal complexes $[(\mathbf{48M})_2]^{2+}$. While the free electron pair of the pyridyl nitrogen atom is pointing towards the metal center in $[(\mathbf{48Cu})_2]^{2+}$ and $[(\mathbf{48Ag})_2]^{2+}$ it is pointing towards the middle of the Au–Au bond in $[(\mathbf{48Au})_2]^{2+}$ (Figure 8, top). The calculations furthermore indicate that the isomerization is not driven by rotation but proceeds *via* dissociation of the M(I)–N coordination bond or *pseudo*-coordination in case of $[(\mathbf{48Au})_2]^{2+}$ and subsequent association of the ligand on the opposite side (Figure 8). This interconversion is highest in energy for $[(\mathbf{48Cu})_2]^{2+}$ (14.7 kcal/mol), followed by $[(\mathbf{48Ag})_2]^{2+}$ (13.2 kcal/mol) and finally $[(\mathbf{48Au})_2]^{2+}$ (9.6 kcal/mol).

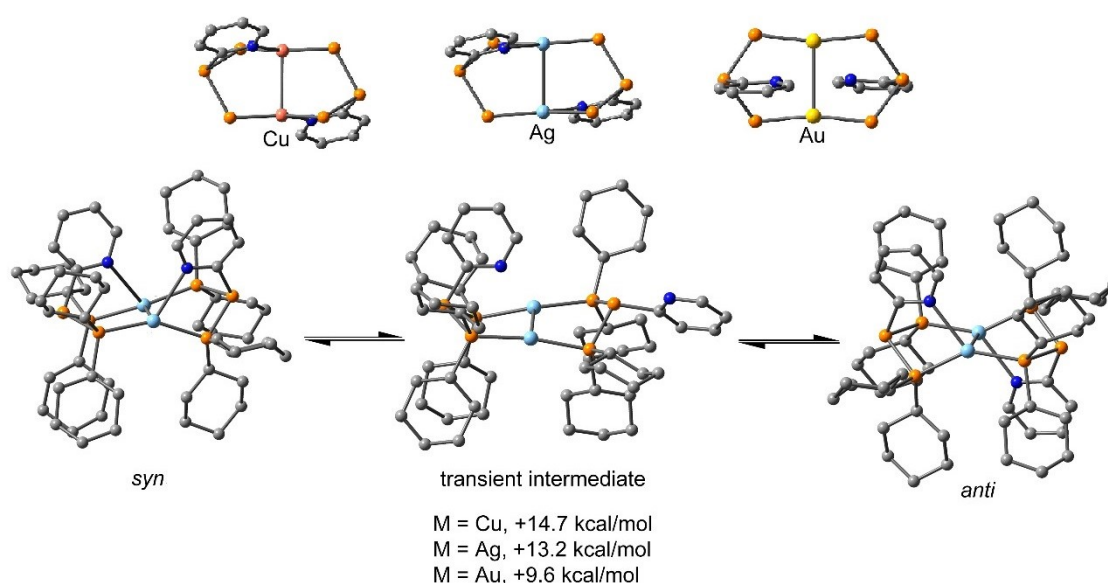


Figure 8. Optimized geometries of $[(\mathbf{48M})_2][\text{OTf}]_2$ using the BP86-D3/def2-TZVP functional, showing the different coordination arrangement of the pyridyl-moieties towards the metal atoms ($M = \text{Cu}, \text{Ag}, \text{Au}$; top) and interconversion mechanism of the *syn*- and *anti*-isomers of $[(\mathbf{48M})_2]^{2+}$; ($M = \text{Cu}, \text{Ag}, \text{Au}$; bottom).

4.3. P–P Bond Formation *via* P–N/P–P Bond Metathesis Reactions

Further reactivity studies on triphosphane **48** revealed that this compound readily rearranges in solution by means of a P–P/P–P bond metathesis reaction. After 24 h the CD₂Cl₂ solution of **48** shows an additional singlet resonance at $\delta(\text{P}) = 21.0$ ppm, which is assigned to tetracyclohexyldiphosphane^{18e} and an AA'BB'C spin system at $\delta(\text{P}) = 14.0\text{--}25.2$ ppm being characteristic for pentaphospholanes of type (RP)₅,^{18e,60} which is assigned to (PyP)₅ **52** (Figure 9).

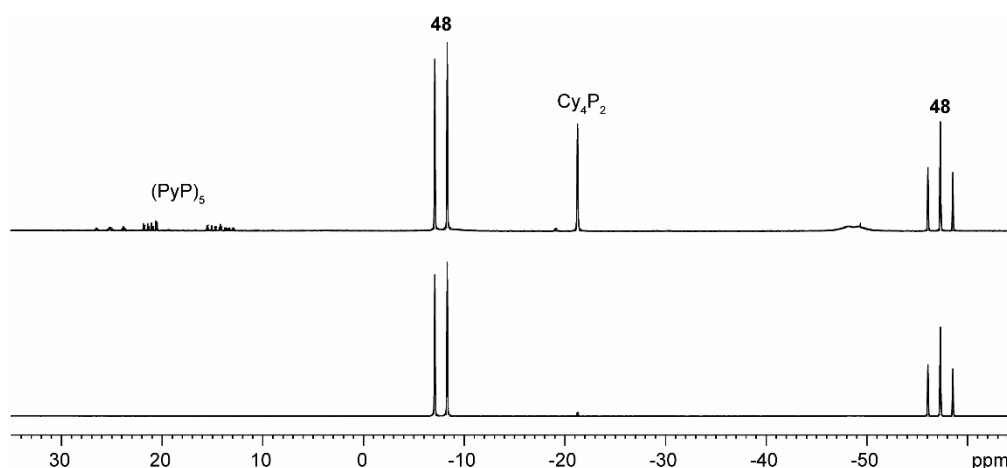


Figure 9. ³¹P NMR spectra of **48** in CD₂Cl₂ after 30 min (bottom) and 24 h (top) at ambient temperature (CD₂Cl₂, 300 K).

Moreover, the ³¹P NMR spectroscopic investigation on the reaction of **52** with Cy₄P₂ yielding **48** illustrates that pentaphospholane **52** might be used as PyP-synthon as it inserts into the P–P bond of Cy₄P₂ (Figure 10).

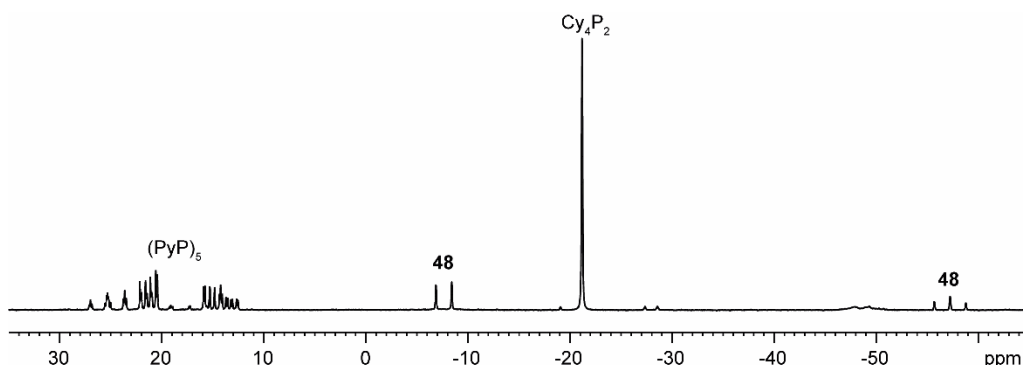
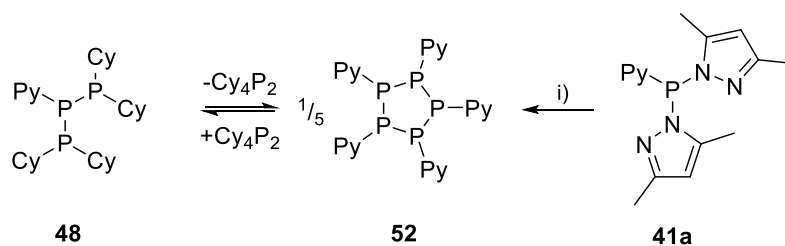


Figure 10. ³¹P NMR spectra of a mixture of (PyP)₅ and Cy₄P₂ in a 1 : 5 ratio after 3 d at ambient temperature in CD₂Cl₂ (CD₂Cl₂, 300 K).

As the scrambling reaction of **48** in CD₂Cl₂ is in a state of equilibrium, the isolation of **52** is hampered. The selective synthesis of pentaphospholane **52** is achieved by the equimolar reaction of **41a** with Cy₂PH in Et₂O as non-polar solvent (Scheme 20).



Scheme 20. Chemical equilibrium of **48**, Cy₄P₂ and **52** (left) and selective synthesis of **52** from **41a** (right); i) 1 eq. Cy₂PH, -**1a**, -**26**, Et₂O.

The formed precipitate is filtered off and dried *in vacuo* giving **52** in 98% yield as a colorless powder which shows an AA'BB'C spin system in the ³¹P NMR spectrum (Figure 12). **26** (Cy₂Ppyr) is identified as a side product in the supernatant by its singlet resonance in the ³¹P NMR spectrum (δ(P) = 58.4 ppm),⁶¹ indicating a P–N/P–P bond metathesis reaction.^{21d} To further understand the formation of **52**, the reaction in CD₂Cl₂ is studied by means of two dimensional ³¹P NMR spectroscopic experiments (Figure 11). After 3 h compound **41a** is still present in solution while Cy₂PH is fully consumed by the condensation reaction with **41a** to form the triphosphane **48** (*vide supra*) and the diphosphane **53** which is identified by an AX spin system (δ(P_A) = 10.2 ppm, δ(P_X) = 33.4 ppm; ¹J(P_AP_X) = -281 Hz; cross peaks highlighted in green circles (Figure 11)). The AMX spin system at δ(P_A) = -35.6 ppm, δ(P_M) = -7.2 ppm and δ(P)_X = 29.9 ppm (cross peaks highlighted in red circles) is assigned to triphosphane **54** which is formed *via* a P–N/P–P bond metathesis reaction of two equivalents of **53** and *via* a P–N/P–P bond metathesis reaction of **41a** and **48** (Scheme 21). In both cases **26** is liberated. A further chain growth is proposed in which triphosphane **54** reacts with **53** under the release of **26** in a P–N/P–P oligomerization reaction which ultimately yields pentaphospholane **52**. Furthermore, the formation of tetraphosphetane **55** (δ(P) = -49.4 ppm) is assumed, which can be formed *via* the reaction of two equivalents **54** under concomitant release of **26** (Scheme 21). Similar to the known ring expansion reactions of certain cyclophosphanes,³⁰ **55** might react to form pentaphospholane **52**, being the thermodynamically favored product. In analogy to the synthesis of **52**, isolation of the corresponding benzothiazolyl-substituted pentaphospholane **56** is achieved in yields of 72%. Crystals suitable for X-ray analysis are obtained for both compounds by the slow diffusion of *n*-pentane into saturated CH₂Cl₂ solutions at -30 °C (Figure 12).

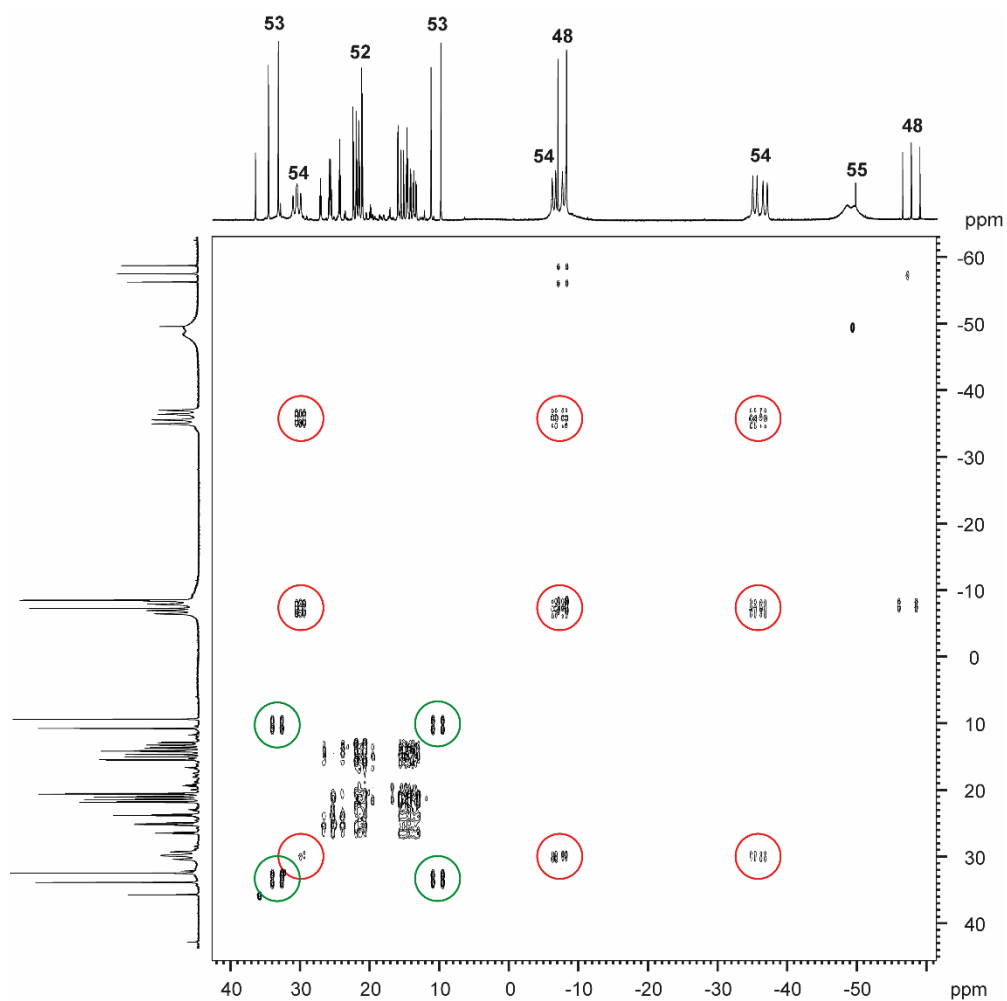
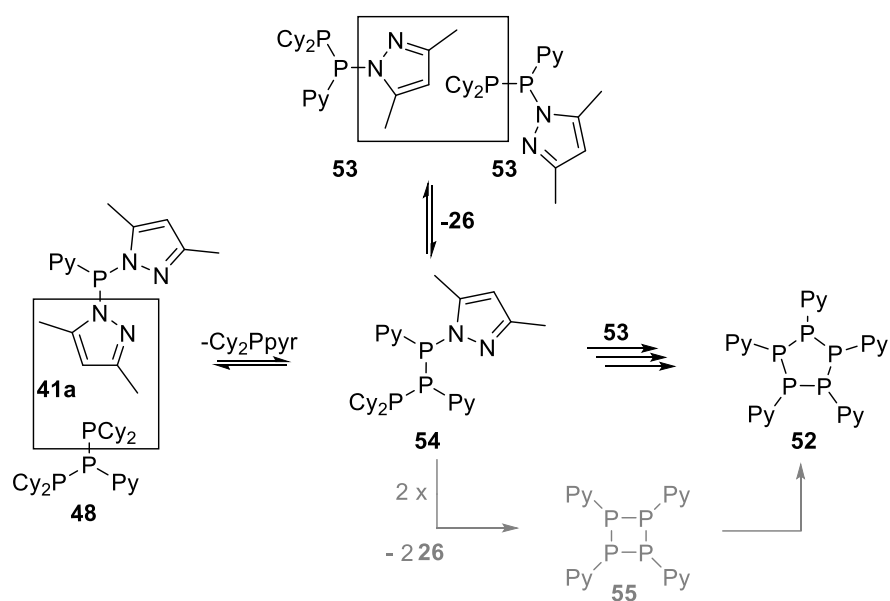


Figure 11. ^{31}P - ^{31}P COSY NMR spectra of a mixture of **41a** and Cy_2PH in a 1 : 1 ratio after 3 h in CD_2Cl_2 (CD_2Cl_2 , 300 K, 2D cross peaks of **53** are highlighted in green circles, cross peaks of **54** are highlighted in red circles).



Scheme 21. Possible formation of **52** via P-N/P-P bond metathesis reactions.

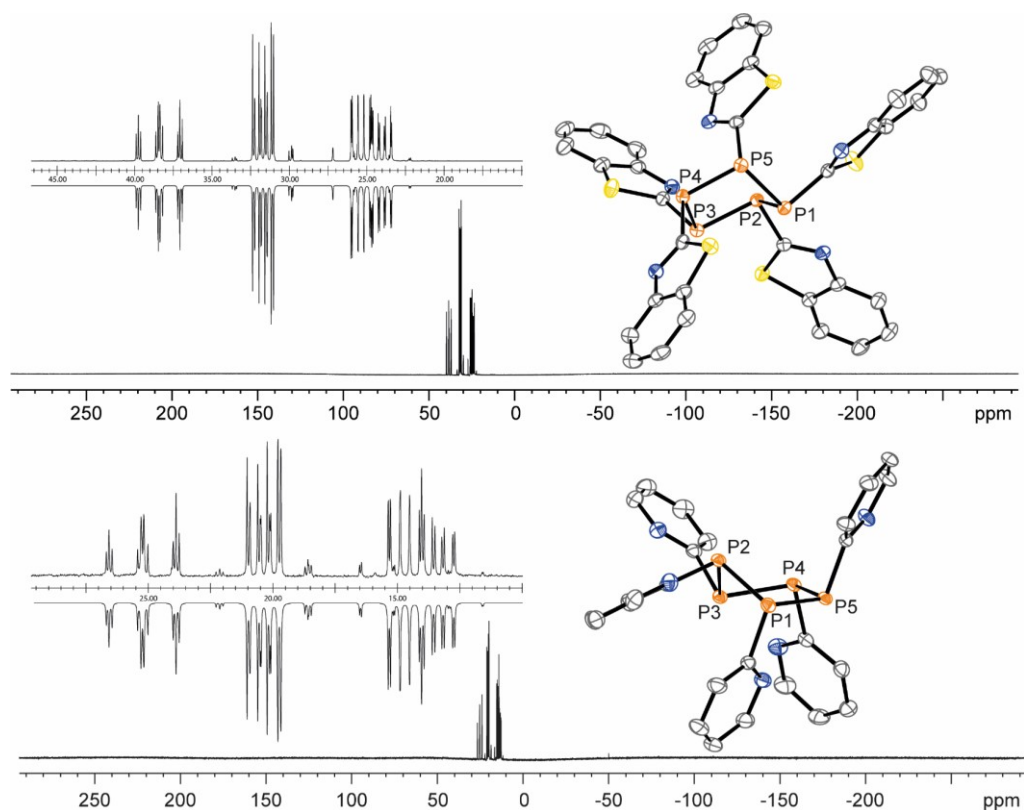


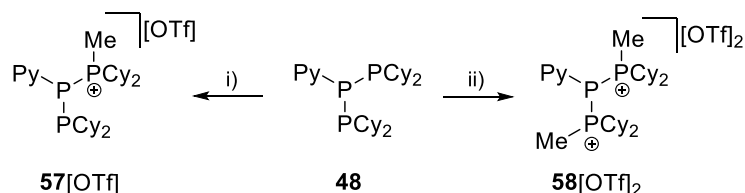
Figure 12. ^{31}P NMR spectra of **52** (bottom) and **56** (top) (Both: CD_2Cl_2 , 300 K, insets on the left show the corresponding AA'BB'C spin system of the experimental (upwards) and fitted spectra (downwards)). Molecular structure of **52** (bottom, right) and **56** in $56^{*1/2}$ CH_2Cl_2 (top, right) (hydrogen atoms and solvate molecules are omitted for clarity; thermal ellipsoids are displayed at 50% probability). Selected bond lengths (\AA) and angles ($^\circ$) for **52**: P1–P2 2.2222(4), P2–P3 2.2200(5); P3–P4 2.22200(5), P4–P5 2.2078(4), P1–P2–P3 97.254(15), P2–P3–P4 95.594(16), P3–P4–P5 102.27(2), P4–P5–P1 106.776(17), P5–P1–P2 97.144(19); **56**: P1–P2 2.2336(6), P2–P3 2.2232(6), P3–P4 2.338(6), P4–P5 2.2069(6), P5–P1 2.2288(6), P1–P2–P3 93.54(2), P2–P3–P4 100.29(2), P3–P4–P5 107.27(2), P4–P5–P1 96.32(2), P5–P1–P2 96.85(2).

Both compounds **52** and **56** reveal the typical envelope conformation of the P_5 -ring featuring the substituents in all-*trans* position. The P–P bond lengths observed for both pentaphospholanes **52** (av. P–P 2.218 \AA) and **56** (av. P–P 2.2461 \AA) are in a range known for pentaphospholanes such as $(\text{PhP})_5$ (av. 2.217 \AA); also the P–P–P angles are in good accordance with the reported data of $(\text{PhP})_5$.⁴⁹ As already indicated by the aforementioned scrambling reaction between **48**, Cy_4P_2 and **52** (see Scheme 20), the use of **52** as PyP-synthon for insertion reactions into P–P bonds is envisioned (*vide infra*).

4.4. Methylation Reactions of Triphosphane **48** and P–P/P–P Bond

Metathesis Reaction

As scrambling reactions like those mentioned before might also be expected for triphosphanium and triphosphanediiium salts, triphosphane **48** was methylated with different amounts of MeOTf. The ^{31}P NMR spectrum of the 1:1 reaction of **48** with MeOTf gives rise to an AMX spin system ($\delta(\text{P}_\text{A}) = -46.2$ ppm, $\delta(\text{P}_\text{M}) = -12.9$ ppm and $\delta(\text{P}_\text{X}) = 34.2$ ppm ($^1J(\text{P}_\text{A}\text{P}_\text{M}) = -290$ Hz, $^1J(\text{P}_\text{A}\text{P}_\text{X}) = -281$ Hz, $^2J(\text{P}_\text{M}\text{P}_\text{X}) = 58$ Hz), suggesting the methylation of a phosphorus atom rather than the nitrogen atom of the pyridyl-substituent. After removal of all volatiles *in vacuo* triphosphan-1-ium triflate salt **57**[OTf] can be isolated in quantitative yield as colorless powder. A second methylation is achieved when **48** is reacted with an excess of MeOTf under solvent free conditions (Scheme 22).



Scheme 22. Methylation reactions of **48**; i) MeOTf, Et₂O, r.t., 99%; ii) 5 eq. MeOTf, neat, r.t., 97%.

Similar to the mono-methylation reaction, only the dicyclohexyl-substituted phosphorus atoms are methylated giving triphosphan-1,3-diiiumtriflate salt **58**[OTf]₂. As both dicyclohexylphosphaneyl moieties are methylated, the ^{31}P NMR spectrum of **48**[OTf]₂ shows an AX₂ spin system with resonances at $\delta(\text{P}_\text{A}) = -67.9$ ppm and $\delta(\text{P}_\text{X}) = 44.0$ ppm ($^1J(\text{P}_\text{A}\text{P}_\text{X}) = -315$ Hz). The molecular structures of cation **57**⁺ and dication **58**²⁺ are depicted in Figure 13.

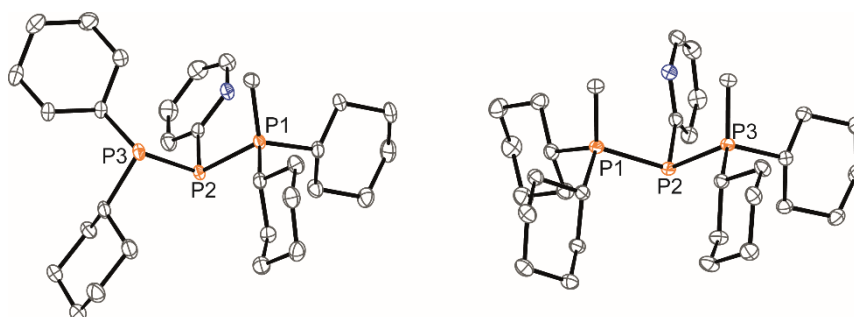
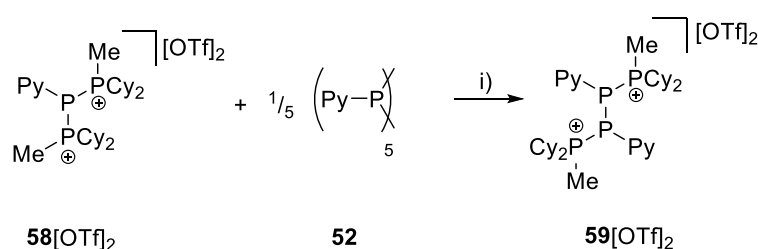


Figure 13. Molecular structures of **57**⁺ in **57**[OTf] (left) and **58**²⁺ in **58**[OTf]₂ (hydrogen atoms and anions are omitted for clarity; thermal ellipsoids are displayed at 50% probability). Selected bond lengths (Å) and angles (°) for **57**⁺: P1–P2 2.1956(5), P2–P3 2.2362(5), P1–P2–P3 97.89(2); **58**²⁺: P1–P2 2.2152(4), P2–P3 2.2182(4), P1–P2–P3 107.439(13).

Note that only a small number of triphosphanediiium salts are reported in the literature,^{62,63} however, compound **57**[OTf] is the first structurally characterized triphosphan-1-ium salt and extends the library of cationic, catenated polyphosphorus compounds.⁶² The P1–P2 bond length in cation **57**⁺ (P1–P2 2.1956(5) Å) is shortened whereas the P2–P3 bond (P2–P3 2.2362(5) Å) is comparable to those in **48** (P1–P2 2.2301(3) Å, P1–P3 2.2371(3) Å) or similar diphosphanium cations (compare [Ph₂P–PPh₃]⁺: 2.2302(13) Å).⁶³ The P–P–P bond angle in **57**⁺ (97.89(2)°) is similar to that of compound **48** (97.16(6)°). The P–P bond lengths in **58**²⁺ (P1–P2 2.2152(4) Å, P2–P3 2.2182(4) Å) are marginally shorter compared to those in **48** but in accordance with bond lengths reported for similar triphosphane-1,3-diiium cations (compare [Me₃P–P(Cy)–PMe₃]²⁺: 2.1979(5) Å and 2.1976(6) Å).⁶² The P–P–P bond angle in **58**²⁺ (107.439(13)°) is significantly wider compared to **48** and [Me₃P–P(Cy)–PMe₃]²⁺ (103.11(2)°). In order to investigate the envisioned [Py–P] transfer into a P–P bond, **52** is reacted with 5 equivalents **88**[OTf]₂ in MeCN (Scheme 23).



Scheme 23. Synthesis of tetraphosphane-1,4-diiium triflate salt **59**[OTf]₂; i) MeCN, r.t., 51%.

Upon addition of **52** to a colorless MeCN solution of **58**[OTf]₂ the reaction mixture turns from a deep red color to pale yellow. The ³¹P NMR spectrum of the reaction mixture after 24 h shows two AA'XX' spin systems which are attributed to two isomers of tetraphosphane-1,4-diiium cations **59**²⁺ (Figure 14), stating the successful [Py–P] transfer via P–P/P–P bond metathesis reaction. The A part of the prominent AA'XX' spin system at δ(P_A) = -55.1 ppm is assigned to the inner pyridyl-substituted P nuclei and the X part at δ(P_X) = 40.7 ppm to the tetra-coordinate phosphorus atoms which is similar to known tetraphosphane-1,4-diiium salts.⁶⁴ The minor spin system resonates at δ(P_A) = -40.1 ppm and δ(P_X) = 39.8 ppm, respectively. After work-up compound **49**[OTf]₂ can be isolated analytically pure in 51% yield. X-ray analysis revealed that the centrosymmetric *meso*-isomer **49**²⁺ crystallized showing central torsion angles of 180° (Figure 14). The P–P bond lengths in **49**²⁺ (P1–P2 2.2347(12) Å, P2–P2' 2.2327(16) Å) are in good agreement with the reported data of comparable tetraphosphane-1,4-diiium cations (compare [Ph₃P–(PPh)₂–PPh₃]²⁺: P1–P2 2.2583(10) Å, P2–P2' 2.2214(13) Å).⁶⁴

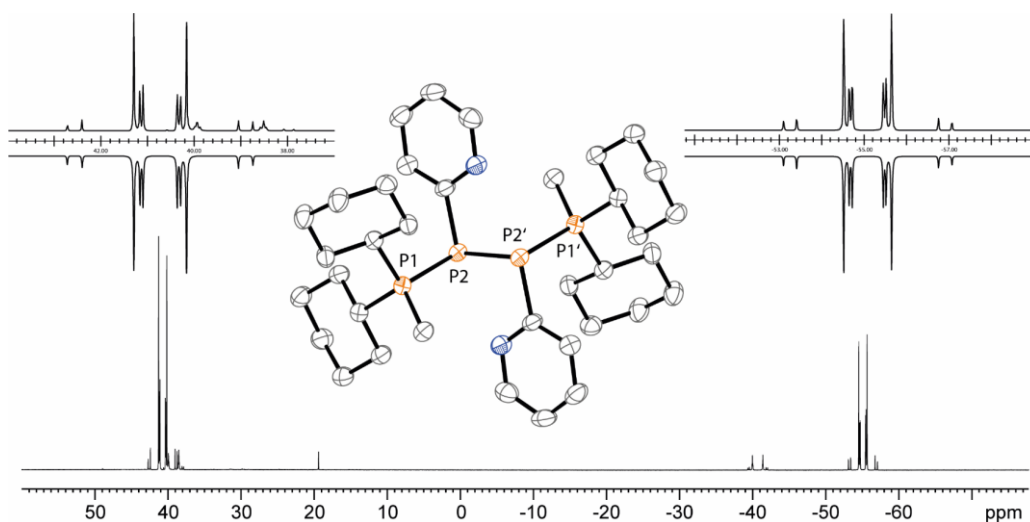


Figure 14. ^{31}P NMR spectrum of dication $\mathbf{59}[\text{OTf}]_2$ (CD_2Cl_2 , 300 K, insets show the AA'XX' spin system of the experimental (upwards) and fitted spectra (downwards) of the most prominent isomer of $\mathbf{59}[\text{OTf}]_2$); centered: Molecular structure of $\mathbf{59}^{2+}$ in $\mathbf{59}[\text{OTf}]_2$ (hydrogen atoms and anions are omitted for clarity; thermal ellipsoids are displayed at 50% probability). Selected bond lengths (\AA) and angles ($^\circ$): P1–P2 2.2347(12), P2–P2' 2.2327(16), P1–P2–P2' 97.60(6).

Similar to the reported [Ph–P] transfer from $(\text{PhP})_5$ to a NHC,⁶⁵ $\mathbf{52}$ can be used as a PyP-synthon, thus, featuring an additional reaction or coordination site. While keeping compound $\mathbf{59}[\text{OTf}]_2$ in a CD_3CN solution for 14 days, the ^{31}P NMR spectrum gives rise to three rearrangement products (Figure 15).

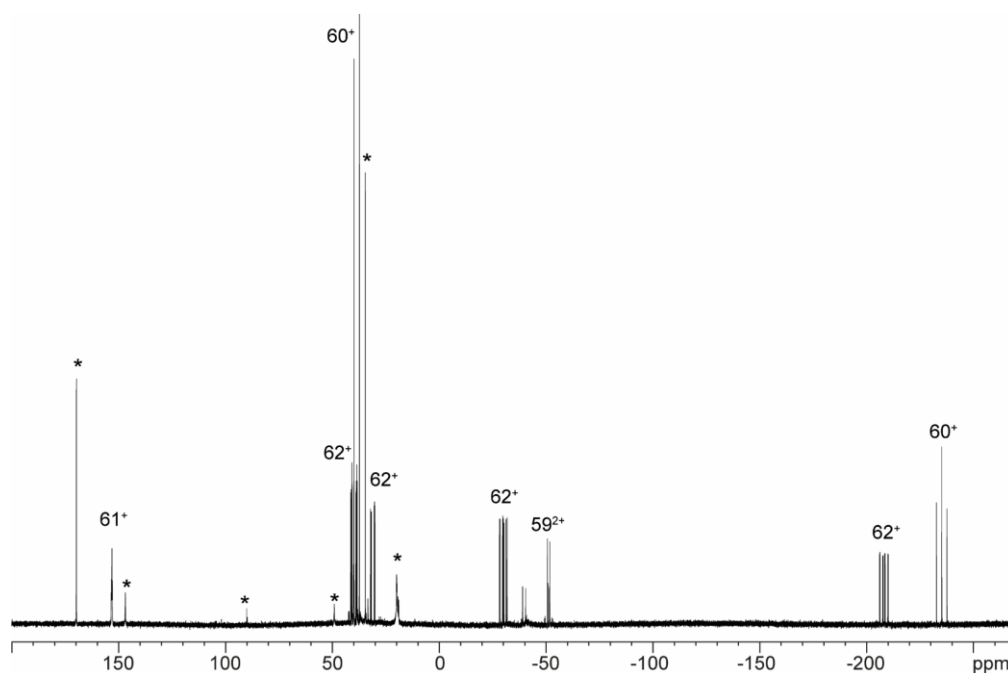


Figure 15. ^{31}P NMR spectrum of a solution of $\mathbf{59}[\text{OTf}]_2$ in CD_3CN after 14 days.

Next to an AX₂ spin system ($\delta(\text{P}_A) = -235.3$ ppm and $\delta(\text{P}_X) = 38.8$ ppm ($^1J(\text{P}_A\text{P}_X) = -501$ Hz)), a *pseudo* triplet resonance ($\delta(\text{P}) = 153.1$ ppm; $^1J(\text{PN}) = 50$ Hz) and an AMXY spin system ($\delta(\text{P}_A) = -208.2$ ppm, $\delta(\text{P}_M) = -30.0$ ppm, $\delta(\text{P}_X) = 31.1$ ppm, $\delta(\text{P}_Y) = 39.8$ ppm; $^1J(\text{P}_A\text{P}_Y) = -490$ Hz, $^1J(\text{P}_M\text{P}_X) = -342$ Hz, $^1J(\text{P}_A\text{P}_M) = -298$ Hz, $^2J(\text{P}_M\text{P}_Y) = 91$ Hz, $^2J(\text{P}_A\text{P}_X) = 45$ Hz, $^3J(\text{P}_X\text{P}_Y) = 34$ Hz) are observed. The AX₂ spin system can be attributed to a 3 λ^5 -triphosph-2-en-1-ium cation **60**⁺, as the spectroscopic parameters are in the range for those observed for [Ph₃P-P-PPh₃]⁺ ($\delta(\text{P}_A) = -174$ ppm, $\delta(\text{P}_X) = 30$ ppm; $^1J(\text{P}_A\text{P}_X) = -500$ Hz) which was first reported by Schmidpeter and co-workers.⁶⁶ A variety of similar derivatives has been synthesized and reported by the group of Macdonald.⁶⁷ Slow vapor diffusion of Et₂O into the CD₃CN solution yielded crystals suitable for X-ray analysis confirming the structural connectivity of **60**⁺ (Figure 16).

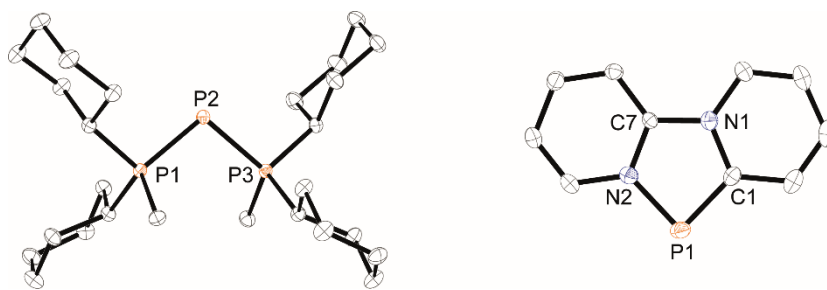


Figure 16. Molecular structure of the 3 λ^5 -triphosph-2-en-1-ium **60**⁺ in **60**[OTf] (left) and 1,4,2-diazaphospholium **61**⁺ in **61**[OTf] (right) (hydrogen atoms and anions are omitted for clarity, thermal ellipsoids are displayed at 50% probability). Selected bond lengths (Å) and angles (°) for **60**⁺: P1–P2 2.134(4), P2–P3 2.1382(4), P1–P2–P3 103.859(19); **61**⁺: P1–C1 1.7333(14), P1–N2 1.7413(13), C1–P1–N2 87.08(6).

The structural parameters of **60**⁺ are similar to those observed for cation [Ph₃P-P-PPh₃]⁺, i.e. slightly shortened P–P bond lengths (P1–P2 2.134(4), P2–P3 2.1382(4) Å) and a P–P–P bond angle of 103.859(19)°.⁶⁶ By co-crystallization, a further product was identified as the triflate salt of diazaphospholium cation **61**⁺ (Figure 16). This species is assigned to the *pseudo* triplet resonance observed in the ³¹P NMR spectrum (Figure 15). The P–C bond distance of 1.7333(14) Å is slightly exceeding the upper limit of typical P=C bond length (1.61–1.71 Å),⁶⁸ while the P–N bond length of P1–N2 1.7413(13) Å is indicating a P–N single bond (P–N: 1.78 Å).⁶⁹ Furthermore, the structure of **61**⁺ reveals an acute angle around the P atom (C1–P1–N2 87.08(6)°) and a planar arrangement, suggesting a delocalized π -system. The AMXY spin system is assigned to asymmetric tetraphosphanediium dication **62**²⁺, most likely formed by an intramolecular aromatic substitution reaction of **59**²⁺. This can be attributed to be the first step of the rearrangement reaction of **59**²⁺ to form **60**⁺ and **61**⁺. We further studied this rearrangement reaction using the TURBOMOLE 7.0 program at the

PB86-D3/def2-TZVP level of theory and taking into consideration solvent effects by using the Conductor-like Screening Model (COSMO). The calculations started from 62^{2+} and show that the cleavage of Cy_2PMe is energetically quite costly. This is in accordance with the ^{31}P NMR spectrum as Cy_2PMe is not observable ($\delta(\text{P}) = -19.8$ ppm).⁷⁰ More likely and energetically favored is a [1,2]-shift of the Cy_2PMe group to form $\text{iso-}62^{2+}$ with a reaction barrier of +22.0 kcal/mol. Figure 17 is showing the optimized structures for this [1,2]- Cy_2PMe shift reaction.

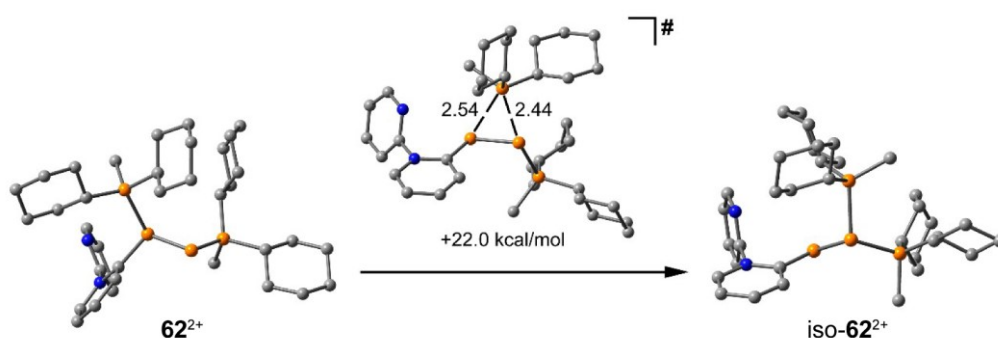
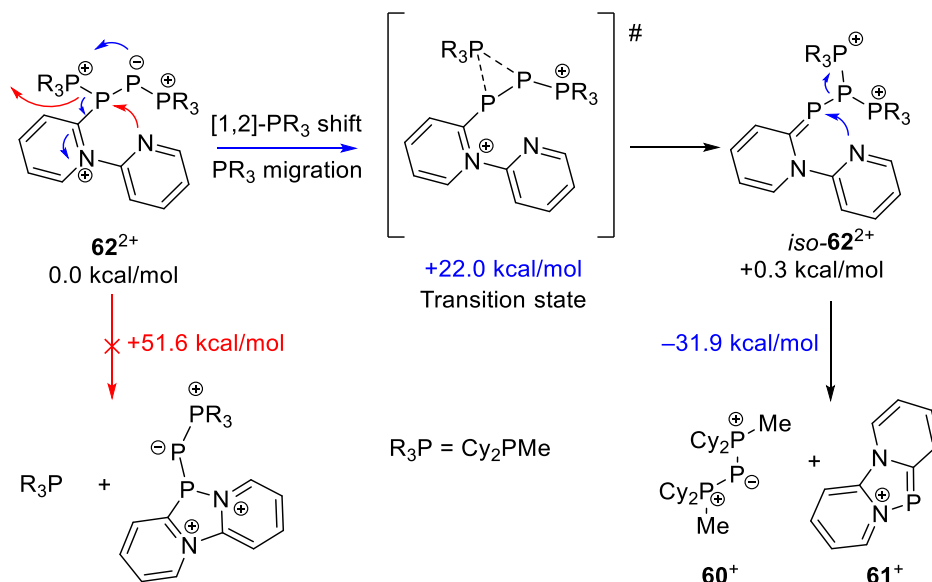


Figure 17. Optimized structures of 62^{2+} , $\text{iso-}62^{2+}$ and the transition state; distances are given in Å.

It is noteworthy, that similar [1,2]- and [1,3]- PR_3 shifts have been reported.⁷¹ Compared to 62^{2+} , $\text{iso-}62^{2+}$ is almost isoenergetic and readily decomposes in an exergonic step (-31.9 kcal/mol) to form cations 60^+ and 61^+ with a low barrier of only 1.9 kcal/mol (Scheme 24).



Scheme 24. Rearrangement reaction from 62^{2+} towards 60^+ and 61^+ calculated at the PB86-D3/def2-TZVP level of theory.

In contrast to the well-established chemistry of $3\lambda^5$ -triphosph-2-en-1-ium cations like **60**⁺ the number of cationic, annulated diazaphospholium salts like **61**[OTf] is scarce. This and the recent interest in Polycyclic Aromatic Hydrocarbons (PAHs), motivated investigations towards a general synthesis yielding 1,4,2-diazaphospholium cations like **61**⁺.

5. 1,4,2-Diazaphospholium Triflates – Synthesis and Reactivity

Polycyclic aromatic hydrocarbons have gathered considerable impact within the last two decades as they reveal diverse electronic and optoelectronic properties.⁷² The size of the π -conjugated system and/or the choice of lateral aliphatic substituents has a tremendous impact.⁷³ An alternative approach to modify the properties of extended π -conjugated systems involves the incorporation of heteroatoms⁷⁴ such as boron,⁷⁵ nitrogen,⁷⁶ oxygen⁷⁷ and sulfur⁷⁸. In this regard, also phosphorus containing PAHs have been investigated in which the central scaffold is based on a phosphole skeleton featuring a σ^3, λ^3 -P atom (**I**; Chart 4).^{79,80}

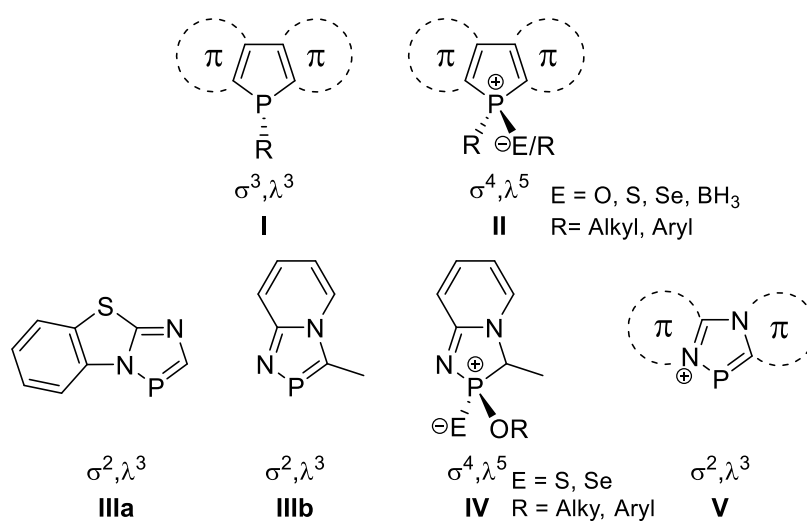


Chart 4. π -extended phosphole derivatives **I** and **II** and examples of annulated diazaphospholes **IIIa,b** and **IV** and asymmetric diannulated 1,4,2-diazaphospholium cations **V**.

The electronic and optical properties of the latter can be further tuned by oxidation (**II**, E = O, S, Se),⁸¹ alkylation (**II**, R = alkyl, aryl)⁸² or adduct formation (**II**, E = e.g. BH₃, metal complexation)⁸³ yielding a σ^4, λ^5 -P atom which has a significant influence on the overall aromaticity of the conjugated system.⁸⁴ Diazaphospholes featuring a dicoordinated σ^2, λ^3 -P atom such as 1,4,2-diazaphospholes (**IIIa,b**),⁸⁵ represent interesting backbones for the construction of N,P-doped π -extended PAHs.² However, the class of annulated 1,4,2-diazaphospholes with an extended π -conjugated system (e.g. **IIIa,b**) are scarce due to limited synthetic protocols. Very few examples of annulated azaphospholes of type **IIIb** are e.g. reported by Karaghioshoff and co-workers and are accessible from cyclocondensation reactions of 1,2-disubstituted cycloiminium salts and PCl₃ in the presence of NEt₃ as base.^{85c} So far extension of the ring system is limited to a [2+4]-cycloaddition of 1,3-dienes with

certain phospholes of type **III**.^{85a} Subsequent functionalization of the σ^2, λ^3 -P atom mainly concentrates on the *in situ* alcoholysis and oxidation with S or Se to derivatives of type **IV**⁸⁵ with a σ^4, λ^5 -P atom. These generally appear to be non-planar, with only very few examples being discussed where the σ^4, λ^5 -P system is forced into planarity.⁸⁶ As diannulated 1,4,2-diazaphospholium triflate salt **61**[OTf] represents a prototypical N,P-doped π -extended PAH (**V**), a systematic protocol towards these compounds is investigated.

5.1. One-Pot Synthesis of 1,4,2-Diazaphospholium Triflate Salts

The targeted synthesis of the diannulated 1,4,2-diazaphospholium triflate salts **61**[OTf], **62**[OTf], **63**[OTf] and **64**[OTf] is achieved by a Me₃SiOTf-mediated self-condensation of the respective dichlorophosphaneyl aza-(Poly)cyclic Aromatic Hydrocarbon (aza-(P)AHs; namely: pyridine (**40**), quinoline (**65**), phenanthridine (**66**) and benzo[*d*]thiazole(**42**)) along with the release of PCl₃ (Table 3). The aforementioned synthesis of compounds **40** and **42** is also used for the synthesis of dichlorophosphanes **65** and **66**. Aside dichlorophosphaneylpyridine **42**, which is a colorless oil best stored at -30 °C, **42**, **65** and **66** are obtained as air-sensitive solids. Suitable crystals for X-ray crystallography are obtained either from vacuum sublimation (**42** and **66**) or recrystallization from CH₂Cl₂ and *n*-pentane (**65**). The molecular structures are depicted in Figure 18, showing the expected pyramidal geometry for P(III) compounds.

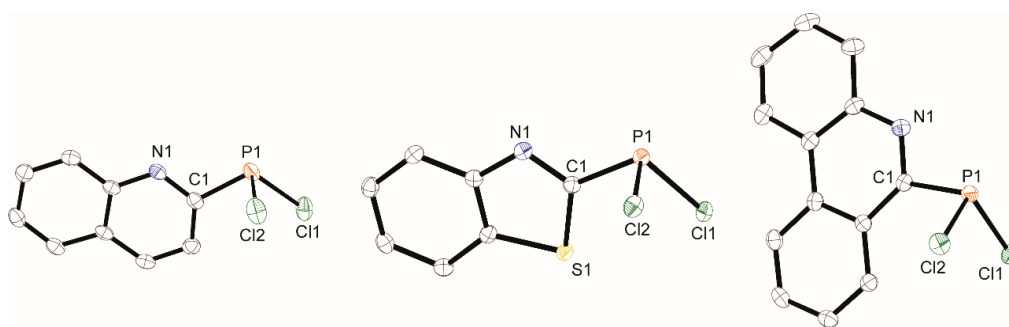


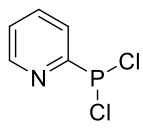
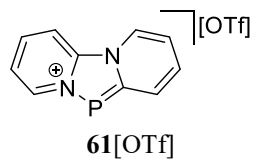
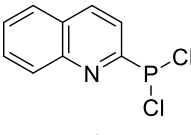
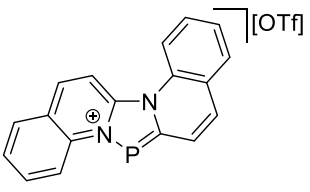
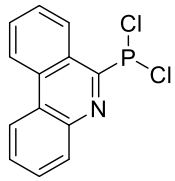
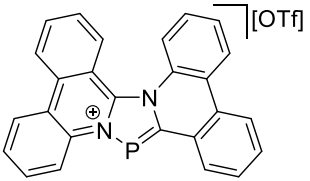
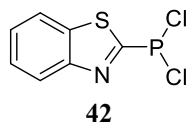
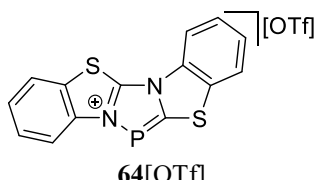
Figure 18. Molecular structures of dichlorophosphanes **65** (left), **42** (middle) and **66** (right) (hydrogen atoms are omitted for clarity; thermal ellipsoids are displayed at 50% probability). Selected bond lengths (Å) and angles (°) for **65**: P1–Cl1 2.0588(8), P1–Cl2 2.0675(8), P1–C1 1.835(2), Cl1–P1–Cl2 98.56(3), C1–P1–Cl1 101.39(7), C1–P1–Cl2 97.52(7); **42**: P1–Cl1 2.0623(5), P1–Cl2 2.0697(5), P1–C1 1.8231(14), Cl1–P1–Cl2 99.727(19), C1–P1–Cl1 98.26(5), C1–P1–Cl2 98.23(4); **66**: P1–Cl1 2.0723(4), P1–Cl2 2.0694(4), P1–C1 1.8419(12), Cl1–P1–Cl2 101.086(18), C1–P1–Cl1 101.13(4), C1–P1–Cl2 100.46(4).

The P–C bond lengths of **65** and **66** (P1–C1 1.835(2) and P1–C1 1.8419(12) Å) are slightly elongated compared to the P–C bond lengths reported for tris(2-pyridyl)phosphane (1.824(3)-1.834(3) Å).⁴⁴ The P–C bond in **42** is a little shorter (P1–C1 1.8231(14) Å) and comparable to the P–C bonds in tris(2-benzothiazolyl)phosphane (P–C 1.820(2) Å).⁴⁵ The P–Cl bonds in **65**, **42** and **66** are all within a range of 2.0588(8)-2.0723(4) Å and thus comparable to the P–Cl bonds in chlorophosphanes **44** and **45**.

For the synthesis of 1,4,2-diazaphospholium triflates **61-64**[OTf], mixtures of dichlorophosphanes **40**, **42**, **65** or **66** and two eq. of Me₃SiOTf in 1,2-dichlorobenzene are heated to 110 °C for 16 h, resulting in yellow to orange colored solutions. After cooling to ambient temperature, the products are isolated as analytically pure yellow to orange

(**61-63**[OTf]) or colorless (**64**[OTf]) powders in good to very good yields after removal of all volatiles *in vacuo* (Table 3).

Table 3. Synthesis of the diazaphospholium triflate salts **61-64**[OTf].

Educt	Product	Yield in % ^a	$\delta(^{31}\text{P})$ in ppm
 <p>40</p>	 <p>61[OTf]</p>	86	152.9
 <p>65</p>	 <p>62[OTf]</p>	50	140.8
 <p>66</p>	 <p>63[OTf]</p>	79	146.3
 <p>42</p>	 <p>64[OTf]</p>	76	141.7

i) $-\text{Me}_3\text{SiCl}$, $-\text{PCl}_3$, $1,2\text{-C}_6\text{H}_4\text{Cl}_2$, $110\text{ }^\circ\text{C}$; a) isolated yield.

All compounds show a good solubility in typical aprotic polar solvents (e.g. MeCN, CH_2Cl_2 , $\text{C}_6\text{H}_5\text{F}$, $1,2\text{-C}_6\text{H}_4\text{F}_2$) and can be readily crystallized by vapor diffusion of Et_2O into concentrated MeCN solutions at $-30\text{ }^\circ\text{C}$. The $^{31}\text{P}\{^1\text{H}\}$ NMR spectra of the isolated materials show resonances ranging from $\delta(\text{P}) = 141.7$ to 152.9 ppm (Table 3) which are significantly high-field shifted compared to known 1,4,2-diazaphospholes (e.g. **IIIb**: $\delta(\text{P}) = 195.0$ ppm^{85a}),^{85a,b} Figure 19 shows the molecular structures of cations **61-64**⁺. While cations **61**⁺ and **64**⁺ are completely planar, **62**⁺ and **63**⁺ are significantly bent.⁷⁴ The P–C bond lengths ($1.711(4)$ – $1.7333(14)$ Å) are slightly longer compared to a typical P=C bond (1.61 – 1.71 Å)⁶⁸ whereas the observed P–N bond lengths ($1.7413(13)$ – $1.7811(15)$ Å) are in the range of a typical P–N single bond (P–N: 1.78 Å; Table 4).⁶⁹

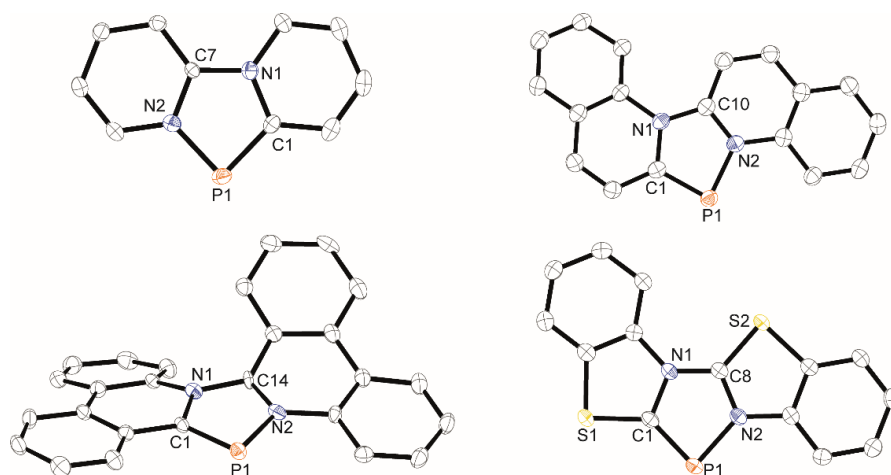


Figure 19. Molecular structures of diazaphospholium cations **61-64⁺** in **61[OTf]** (top left), **62[OTf]*MeCN** (top right), **63[OTf]** (bottom left) and **64[OTf]*MeCN** (bottom right), respectively (hydrogen atoms, solvate molecules and anions are omitted for clarity, thermal ellipsoids are displayed at 50% probability). Selected bond lengths (Å) and angles (°) are listed in Table 4.

Table 4. Selected geometrical parameters of crystallographically characterized diazaphospholium triflate salts **61-64[OTf]**.

	61[OTf]	62[OTf]	63[OTf]	64[OTf]
C1–P1 in Å	1.7333(14)	1.7238(16)	1.711(4)	1.7281(19)
N2–P1 in Å	1.7413(13)	1.7538(14)	1.740(3)	1.7811(15)
C1–P1–N2' in °	87.08(6)	86.83(7)	87.14(12)	85.28(8)

The N-P-C angles range from 85.28° to 87.14° and are unsurprisingly the smallest within the diazaphosphole rings. To verify the aromatic features of the diannulated 1,4,2-diazaphospholium cations **61-64⁺**, NICS values at 0.6 Å and 1.0 Å from the ring centroid are calculated using the B3LYP level of theory with the B3LYP/6-311+G* basis and are compared with the calculated values for benzene (Table 5). The NICS value of **61⁺** shows an aromaticity comparable to that of benzene at 1.0 Å. Cations **62-64⁺** are less aromatic, which is shown by the decreasing magnitude of their NICS values, yet they maintain a strong aromatic character at the five membered rings.

Table 5. Nucleus Independent Chemical Shifts (NICS) computed at the five-membered ring in compounds **61-64⁺** and benzene (COSMO B3LYP/6-311+G*).

	NICS (0.0 Å) in ppm	NICS (0.6 Å) in ppm	NICS (1.0 Å) in ppm
61⁺	-13.2	-13.0	-10.7
62⁺	-10.7	-10.2	-8.4
63⁺	-8.63	-8.8	-7.5
64⁺	-10.6	-9.8	-7.8
C ₆ H ₆	-8.0	-10.2	-10.1

Salt **64**[OTf] shows an interesting feature in the solid state. A fluorescence was detected with an emission maximum at 490 nm (excitation wave length 350 nm) and a fluorescence quantum yield of $\theta = 14.0\%$ (Figure 20). Complete quenching of the fluorescence is observed when dissolving **64**[OTf] in MeCN or CH₂Cl₂.

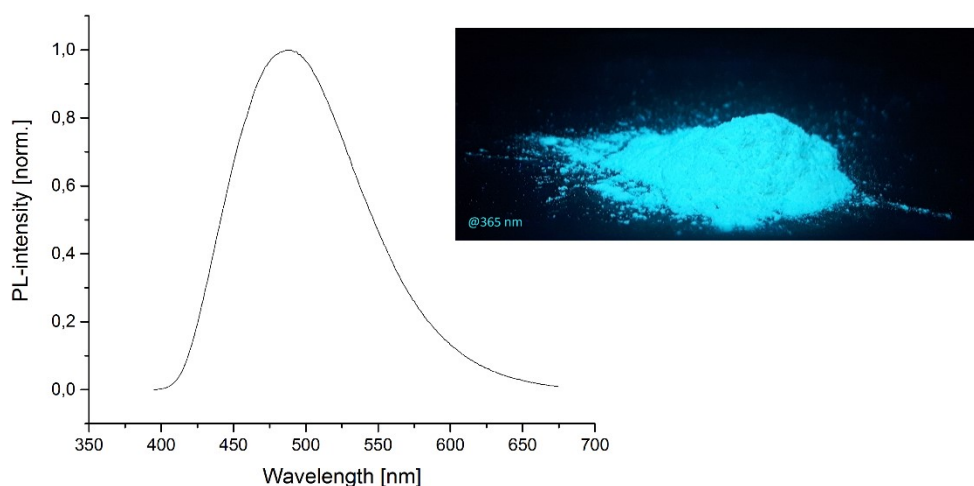


Figure 20. Emission spectra of **64**[OTf] with an excitation wavelength of 350 nm (left) and a sample of microcrystalline **64**[OTf] under an UV lamp (365 nm).

Detailed DFT calculations (B3LYP/6-311+G*) helped to understand the mechanism towards the formation of cations **61-64**⁺. Initial investigations of the Molecular Electrostatic Potential (MEP) plotted onto the van der Waals surface of dichlorophosphane **40** were used to examine the electrophilic as well as the nucleophilic areas of the molecule (Figure 21).

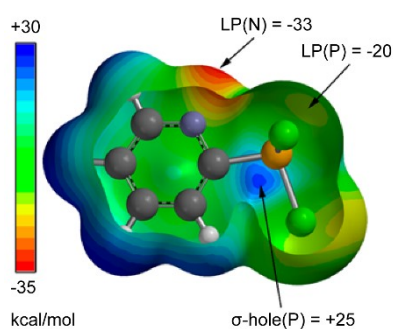


Figure 21. MEP open surface of **40** at the B3LYP/6-311+G*. Isosurface 0.01 a.u. The MEP values at selected points are given in kcal/mol.

As expected, the most negative MEP value is located at the nitrogen atom of the pyridyl-substituent, while a σ -hole is observed at the phosphorus atom (a well-defined positively charged region in extension to the P–Cl bond) indicating the most reactive site towards

suitable nucleophiles.^{18e,87} The optimized intermediates and the proposed mechanism were calculated at the BP86-D3/def2TZVP level of theory considering solvent effects using the COSMO continuum model (1,2-dichlorobenzene). Based on the aforementioned findings, formation of a homo dimeric, noncovalent complex **A** is anticipated, which is stabilized by pnictogen bonding interactions involving the σ -hole at the P atom (-6.1 kcal/mol; N–P 2.80 Å; Figure 22).

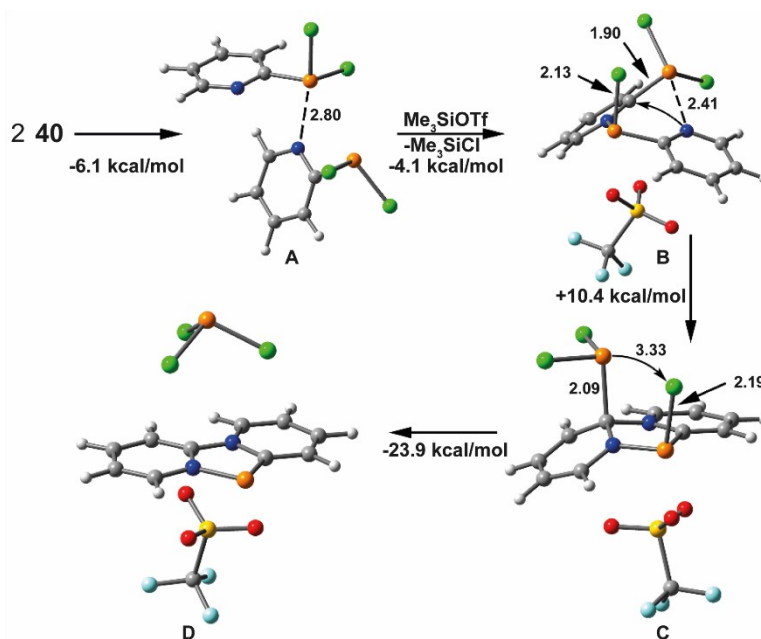
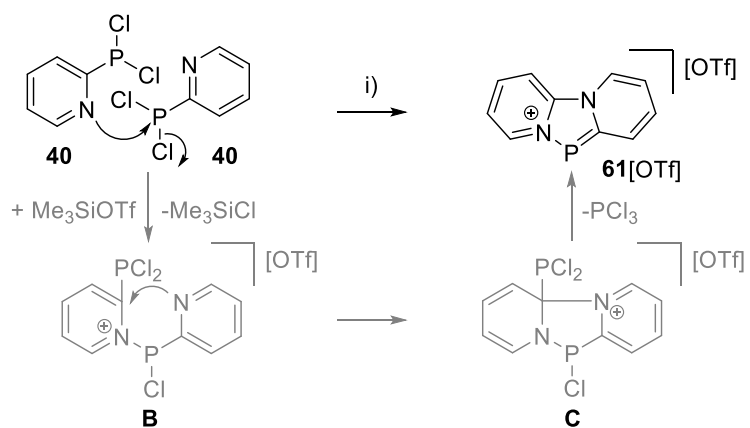


Figure 22. Calculated mechanism of the formation of **61**[OTf]; distances are given in Å.

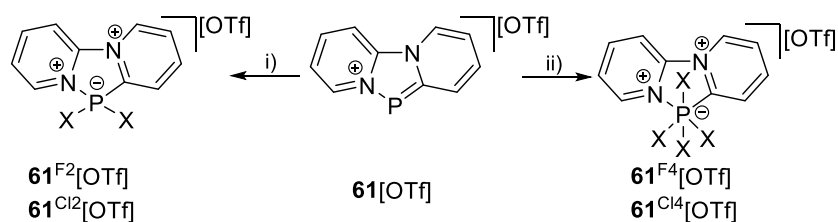
The subsequent substitution reaction promoted by Me_3SiOTf is thermodynamically favored (-4.1 kcal/mol) and gives intermediate **B** which again shows an intramolecular pnictogen bonding interaction (N–P 2.41 Å). This preorganization of intermediate **B** favors a nucleophilic attack of the N atom to the P-bound carbon atom yielding intermediate **C**. This rate determining step is endergonic (+10.4 kcal/mol) due to the loss of aromaticity of the pyridine ring and differs only +0.2 kcal/mol from the starting material **40**. Intermediate **C** reveals elongated C–P (2.09 Å) and P–Cl (2.19 Å) bond lengths and a comparatively close contact (3.33 Å; sum of van der Waals radii of Cl and P (3.55 Å))⁵⁶ between the PCl_2 moiety and the Cl atom, facilitating the formation of PCl_3 . The final step is calculated to be highly exergonic with -23.9 kcal/mol due to liberation of PCl_3 via a 1,3-elimination and aromatization of the molecule. The complete reaction sequence is summarized in Scheme 25 for the formation of **61**[OTf].



Scheme 25. Reaction of 2 eq. **40** with Me_3SiOTf to **61[OTf]** and PCl_3 ; i) 2 eq. Me_3SiOTf , $-\text{Me}_3\text{SiCl}$, $-\text{PCl}_3$, 1,2- $\text{C}_6\text{H}_4\text{Cl}_2$, 110 °C.

5.2. Halogenation Reactions of **61**[OTf]

The presence of a highly polarized P=C double bond in the diannulated 1,4,2-diazaphospholium salts motivates to investigate halogenation reactions of **61**[OTf] using XeF₂ or SO₂Cl₂ as readily available sources for F₂ and Cl₂, respectively. **61**[OTf] reacts with either XeF₂ or SO₂Cl₂ *via* a 1,1-addition to the corresponding phosphoranides **61**^{F₂}[OTf], **61**^{Cl₂}[OTf], and surprisingly also to phosphates **61**^{F₄}[OTf], **61**^{Cl₄}[OTf] depending on the applied reactant ratio (Scheme 26).



Scheme 26. Halogenation reactions **61**[OTf] with one eq. (left) and two eq. (right) XeF₂ or SO₂Cl₂; i) for X = F: XeF₂, -Xe, MeCN, -40 °C to r.t., not isolated; for X = Cl: SO₂Cl₂, -SO₂, MeCN, -40 °C to r.t., 74% ii) for X = F: 2 XeF₂, -2 Xe, MeCN, -40 °C to r.t., quant; for X = Cl: 2 SO₂Cl₂, -2 SO₂, MeCN, -40 °C to r.t., quant..

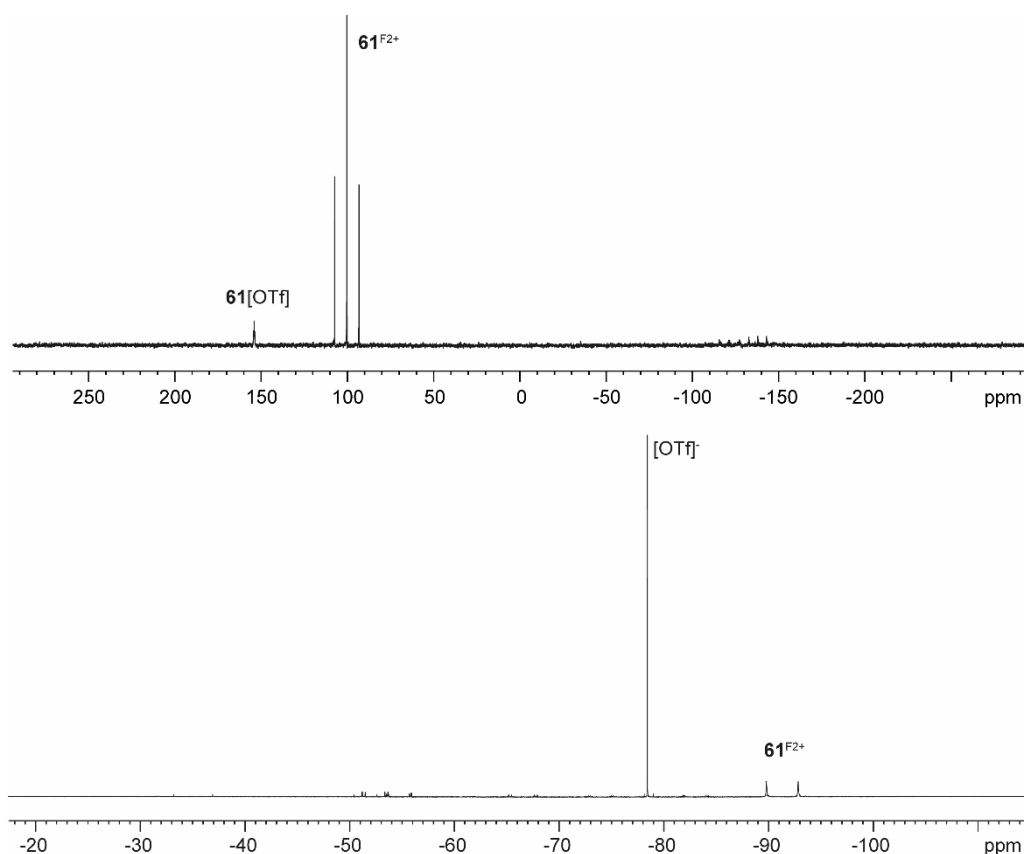


Figure 23. ³¹P NMR spectrum (top) and ¹⁹F NMR spectrum (bottom) of the reaction mixture of **61**[OTf] and XeF₂ in a 1 : 1 ratio.

The 1:1 reaction of **61a**[OTf] and XeF₂ in MeCN at -40 °C yields mainly cation **61**^{F2+} as indicated by ¹⁹F and ³¹P NMR spectroscopic investigations ($\delta(\text{F}) = -91.4$ ppm, (d, $^1J_{\text{FP}} = 1135$ Hz); $\delta(\text{P}) = 96.5$ (t, $^1J_{\text{PF}} = 1135$ Hz)). Small amounts of unidentified side-products as well as the presence of phosphate **61a**^{F4+} indicate the highly reactive nature of cation **61**^{F2+} and explain the problems that encountered during attempts of isolation. Cation **61**^{F2+} readily undergoes a disproportionation reaction to **61**[OTf] and **61**^{F4}[OTf] (*vide infra*) during work-up. The ¹⁹F and ³¹P NMR spectra of the reaction mixture (Figure 23) indicate two equivalent fluorine atoms for cation **61**^{F2+} in solution, which follows the expected VSEPR model, placing the two fluoro-substituents in the axial position of the bisphenoidal bonding environment of the phosphorus atom (Chart 5, left). A slightly different outcome is observed, when **61**[OTf] is reacted with SO₂Cl₂ in MeCN at -40 °C. From this reaction, phosphoranide derivative **61**^{Cl2}[OTf] is readily obtained as voluminous orange precipitate in a good yield of 74% after filtration of the reaction mixture and subsequent addition of Et₂O. Single crystals of **61**^{Cl2}[OTf] suitable for X-ray diffraction were obtained as bright orange plates from the filtrate of the reaction over the course of three days at -30 °C. The molecular structure of **61**^{Cl2+} shows also the expected bisphenoidal geometry of the phosphorus atom (Chart 5, right).

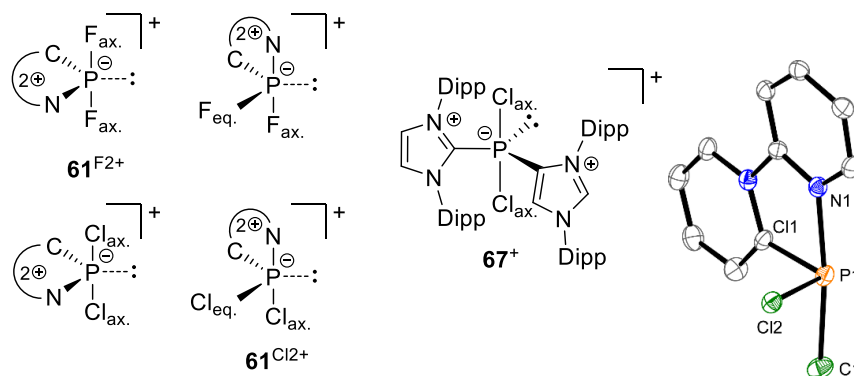


Chart 5. Possible structural isomers of cations **61**^{X2+} (X = F, Cl) according to VSEPR and cation **67**⁺ as an example of a previously reported cationic phosphoranide (left);⁸⁸ and molecular structure of cation **61**^{Cl2+} in **61**^{Cl2}[OTf] (right; hydrogen atoms and anions are omitted for clarity, thermal ellipsoids are displayed at 50% probability); selected bond lengths (Å) and angles (°): P1–Cl1 2.200(1), P1–Cl2 2.0717(9), P1–C1 1.870(3), P1–N1 2.110(3), C1–P1–N1 79.0(1), Cl1–P1–N1 173.41(8), Cl1–P1–Cl2 92.09(4).

However, one of the chloro-substituents and the nitrogen atom are now located in axial positions in accordance to the electronegativity of the donor atoms (Chart 5). The bond length between the pyridyl nitrogen atom and the P atom (P1–N1 2.110(3) Å) is significantly elongated compared to **61**[OTf] or **61**^{Cl4}[OTf] (P1–N2 1.7413(13) Å and P1–N1 1.930(4) Å, *vide infra*) suggesting an intramolecular Lewis acid-base adduct. The ³¹P NMR spectrum of dissolved **61**^{Cl2}[OTf] shows a singlet resonance at $\delta(\text{P}) = 56.6$ ppm (CD₃CN), which is

similar to cyclic phosphoranides⁸⁹ and significantly shifted to lower field compared to related acyclic chloro-substituted phosphoranide derivatives.^{90,88} Our group reported on cationic phosphoranide **67**⁺ (Dipp = 2,6-di*is*opropylphenyl; Chart 5)^{88b} with a chemical shift of $\delta(\text{P}) = -98.9$ ppm (CD_2Cl_2). The significant $\Delta\delta$ of ~ 150 ppm is explained by the chelating effect of the bidentate C, N-ligand in **61**^{Cl2+} causing a very acute C1-P1-Cl2 angle of $92.09(4)^\circ$ vs. the corresponding much wider C-P-C angle of $113.47(7)^\circ$ in cation **67**⁺. Fluorination of **61**[OTf] with 2 eq. XeF_2 in MeCN at -40°C gives salt **61**^{F4}[OTf] quantitatively as analytically pure, beige colored powder after removal of all volatiles *in vacuo*. The ³¹P NMR spectrum of cation **61**^{F4+} shows at $\delta(\text{P}) = -138.7$ ppm a resonance with a ddt splitting due to the coupling with two chemically inequivalent fluorine atoms ($\text{F}_{\text{eq.}}$) in the equatorial position and the two axial fluorine atoms ($\text{F}_{\text{ax.}}$). Accordingly, the ¹⁹F NMR spectrum displays the expected ABM₂ spin system ($\delta(\text{F}_\text{M}) = -55.6$ ppm, $\delta(\text{F}_\text{B}) = -74.8$ ppm, $\delta(\text{F}_\text{A}) = -83.8$ ppm), which matches literature reported assymmetrically substituted tetrafluorophosphate salts.⁹¹ The iteratively fitted ³¹P and ¹⁹F NMR spectra of **61**^{F4}[OTf] are depicted in Figure 24 including the coupling constants in the caption. Chlorination of **61**[OTf] with two eq. of SO_2Cl_2 in MeCN at -40°C proceeds in the same manner and gives quantitatively **61**^{Cl4}[OTf] as off-white powder after removing all volatiles *in vacuo*.

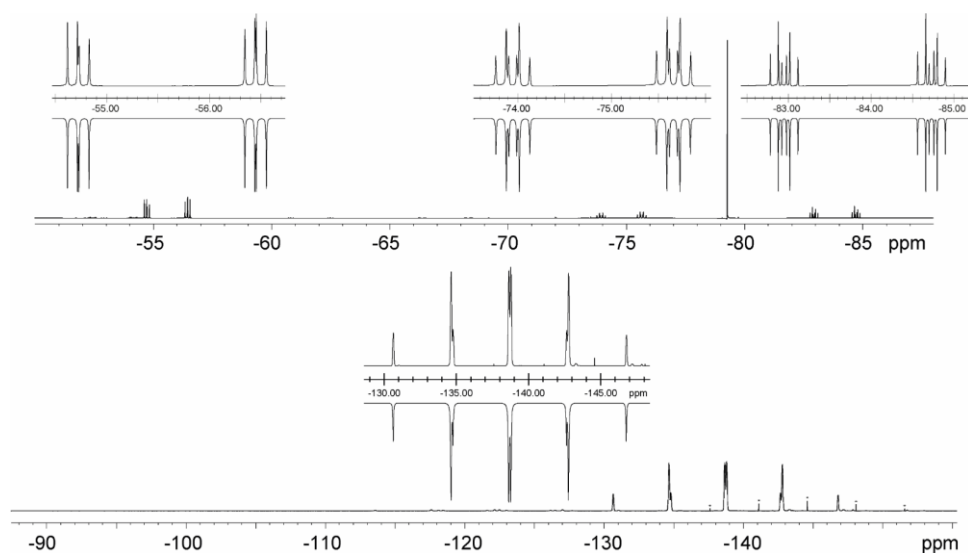


Figure 24. ¹⁹F NMR spectrum of **61**[OTf] (top; CD_3CN , 300 K, insets show the ABM₂ spin system of the experimental (upwards) and the fitted spectra (downwards); $\delta(\text{F})$ in ppm = -55.6 (2F, ddd, $^1J_{\text{FP}} = 812$ Hz, $^2J_{\text{Fax.Feq.}} = 52$ Hz, $^2J_{\text{Fax.Feq.}} = 46$ Hz, $\text{F}_{\text{ax.}}$), -74.8 (1F, ddt, $^1J_{\text{FP}} = 806$ Hz, $^2J_{\text{Feq.Feq.}} = 65$ Hz, $^2J_{\text{Feq.Fax.}} = 52$ Hz, $\text{F}_{\text{eq.}}$), -79.3 (3F, s, CF_3), -83.8 (1F, ddt, $^1J_{\text{FP}} = 838$ Hz, $^2J_{\text{Feq.Feq.}} = 65$ Hz, $^2J_{\text{Feq.Fax.}} = 46$ Hz, $\text{F}_{\text{eq.}}$). ³¹P NMR spectrum of **61**^{F4}[OTf] (bottom; CD_3CN , 300 K, inset shows the dtd of triplet of doublet resonance of the experimental (upwards) and the fitted spectra (downwards); $\delta(\text{P})$ in ppm = -138.7 (1P, dtd, $^1J_{\text{PFeq.}} = 838$ Hz, $^1J_{\text{PFax.}} = 812$ Hz, $^1J_{\text{PFax.}} = 806$ Hz), -144.6 (small impurities of PF_6^- , indicated as *).

The singlet resonance for $\mathbf{61}^{\text{Cl}4+}$ ($\delta(\text{P}) = -208.9$ ppm) is shifted to lower field compared to the related 2,2'-bipyridinyl-tetrachlorophosphate ion (2,2-bipy)PCl₄⁺ ($\delta(\text{P}) = 191.5$ ppm).⁹² Single crystals suitable for X-ray diffraction are obtained by diffusion of Et₂O into saturated MeCN solution of both triflate salts at -30 °C. The molecular structures of the cations are depicted in Figure 25 displaying the expected distorted octahedral arrangement of the phosphorus centers.

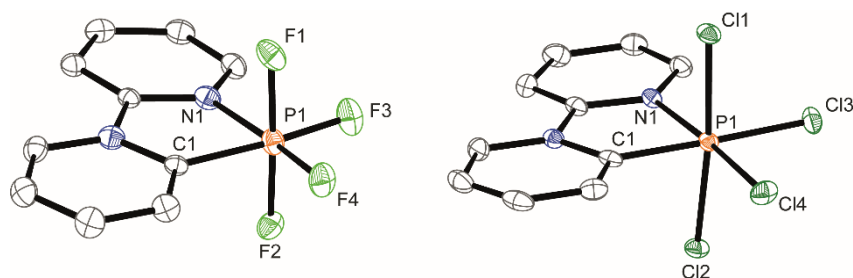
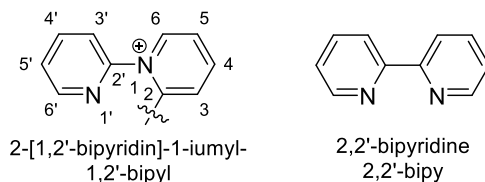


Figure 25. Molecular structures of cations $\mathbf{61}^{\text{F}4+}$ in $\mathbf{61}^{\text{F}4}[\text{OTf}]$ (left) and $\mathbf{61}^{\text{Cl}4+}$ in $\mathbf{61}^{\text{Cl}4}[\text{OTf}]$ (right) (hydrogen atoms and anions are omitted for clarity, thermal ellipsoids are displayed at 50% probability); selected bond lengths (Å) and angles (°) for $\mathbf{61}^{\text{F}4+}$: P1–F1 1.6386(19), P1–F2 1.6088(17), P1–F3 1.5720(17), P1–F4 1.5843(16), P1–N1 1.889(2), P1–C1 1.865(3), C1–P1–N2 85.53(10), F3–P1–F4 93.05(10), F1–P1–F2 176.90(9) and $\mathbf{61}^{\text{Cl}4+}$: P1–Cl1 2.1231(14), P1–Cl2 2.1447(14), P1–Cl3 2.0926(14), P1–Cl4 2.1044(14), P1–N1 1.930(4), P1–C1 1.896(4), C1–P1–N2 83.10(16), Cl3–P1–Cl4 91.14(6), Cl1–P1–Cl2 174.21(7).

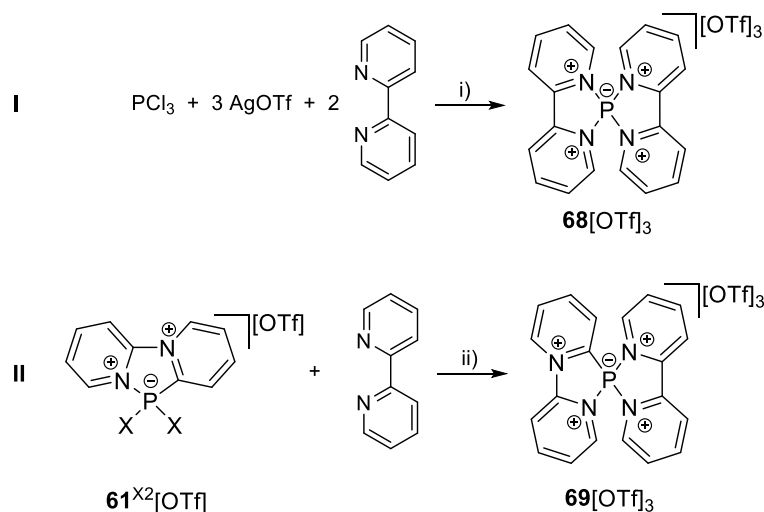
In both cases angles $X_{\text{ax.}}\text{-P-}X_{\text{ax.}}$ ($\mathbf{61}^{\text{F}4+}$: 176.90(9)°, $\mathbf{61}^{\text{Cl}4+}$: 174.21(7)°) and $X_{\text{eq.}}\text{-P-}X_{\text{eq.}}$ ($\mathbf{61}^{\text{F}4+}$: 85.53(10)-93.05(10)°, $\mathbf{61}^{\text{Cl}4+}$: 83.10(6)-93.5(1)°) are slightly distorted as a result of the chelating C, N-ligand. Compared to $\mathbf{61}^+$ (P–N 1.7413(13) Å, P–C 1.7333(14) Å) the P–N and the P–C bonds are significantly elongated ($\mathbf{61}^{\text{F}4+}$: P–N 1.889(2) Å, P–C 1.865(3) Å; $\mathbf{61}^{\text{Cl}4+}$: P–N 1.930(4) Å, P–C 1.896(4) Å).

5.3. Substitution Reactions of $\mathbf{61}^{\text{Cl}_2}[\text{OTf}]$

Particularly $\mathbf{61}^{\text{Cl}_2}[\text{OTf}]$ is an interesting starting compound for the introduction of the cationic 2-(1,2'-bipyridin)-1-iumyl ligand (1,2'-bipyl) which represents the monocationic structural isomer of the prototypical 2,2'-bipyridine ligand (2,2'-bipy).



The 2,2'-bipy ligand offers relatively high basicity and oxidative resistance, making it an important ligand in main group and transition metal coordination chemistry.⁹³ It has also been used to stabilize element triflates $\text{E}(\text{OTf})_n$, which are widely used as Lewis acids,⁹⁴ oxidizing agents⁹⁵⁻⁹⁷ and sources of E^{n+} cations.⁹⁸⁻¹⁰¹ Thus, Burford and co-workers reported on the synthesis of the bis-2,2'-bipy complex $\mathbf{68}^{3+}$ of *in situ* generated $\text{P}(\text{OTf})_3$ from PCl_3 and AgOTf (Scheme 27, I).¹⁰²



Scheme 27. I: Synthesis of the bis-2,2'-bipy complex $\mathbf{68}[\text{OTf}]_3$ according to reference [102]; i) MeCN, -3 AgCl, r.t., 40%; **II:** Synthesis of the mixed bis-2,2'-bipy/1,2'-bipyl complex $\mathbf{69}[\text{OTf}]_3$ from $\mathbf{61}^{\text{X}_2}[\text{OTf}]$; ii) for X = F: *in situ* preparation of $\mathbf{61}^{\text{F}_2}[\text{OTf}]$, +2 Me_3SiOTf , -2 Me_3SiCl , MeCN, r.t., 46%; for X = Cl: +2 Me_3SiOTf , -2 Me_3SiCl , CH_2Cl_2 , r.t., 99%.

The mixed 2,2'-bipy/1,2'-bipyl complex $\mathbf{69}[\text{OTf}]_3$ forms quantitatively from the reaction of either *in situ* formed $\mathbf{61}^{\text{F}_2}[\text{OTf}]$ or $\mathbf{61}^{\text{Cl}_2}[\text{OTf}]$ with 1 eq. 2,2'-bipy and 2 eq. Me_3SiOTf (Scheme 27, II). The switch from the N_4 - to CN_3 -coordination mode of the spirocyclic environment of cation $\mathbf{68}^{3+}$ vs. $\mathbf{69}^{3+}$ causes an upfield shift from $\delta(\text{P}) = 33.9 \text{ ppm}$ ¹⁰² to $\delta(\text{P}) = 20.5 \text{ ppm}$ as a result of the decreased electron density of the 1,2'-bipyl-backbone in $\mathbf{69}^{3+}$ resulting in a significant shielding of the P nucleus.

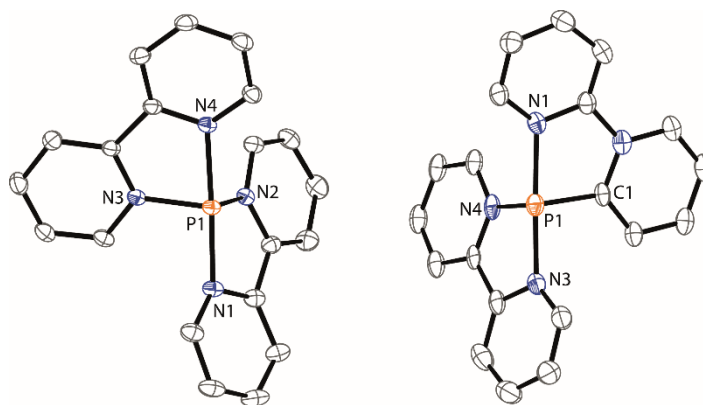
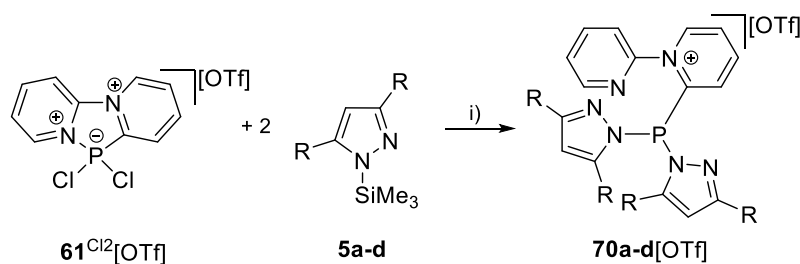


Figure 26. Molecular structure of 68^{3+} in $68[\text{OTf}]_3 \cdot 2 \text{ MeCN}$ (left) as reported by Burford et al.¹⁰² and molecular structure of cation 69^{3+} in $69[\text{OTf}]_3 \cdot 2 \text{ MeCN}$ (right) (hydrogen atoms, solvate molecules and anions are omitted for clarity, thermal ellipsoids are displayed at 50% probability). Selected bond lengths (Å) and angles (°) for 68^{3+} : P1–N1 1.9389(16), P1–N2 1.8111(18), P1–N3 1.8157(18), P1–N4 1.9735(17), N1–P1–N4 173.09(8), N1–P1–N2 82.80(9), N3–P1–N4 82.03(9), N2–P1–N3 99.57(9) and 69^{3+} : P1–N1 1.992(3), P1–N3 1.942(3), P1–N4 1.836(3), P1–C1 1.852(3), N1–P1–N3 173.44(11), N1–P1–C1 81.83(12), N3–P1–N4 82.34(12), N4–P1–C1 98.41(11).

The molecular structure of cation 69^{3+} in $69[\text{OTf}]_3 \cdot 2 \text{ MeCN}$ is comparable to that of 68^{3+} in $68[\text{OTf}]_3 \cdot 2 \text{ MeCN}$ with the presence of the stereochemical lone pair at the phosphorus atom in each case (Figure 26). As expected, the P–N bond lengths to the axial N-substituents (P1–N1 1.992(3), P1–N3 1.942(3) Å) in 69^{3+} are elongated compared to the equatorial P–N bond (P1–N4 1.836(3) Å). Compared to 68^{3+} ,¹⁰² the P–N bond lengths of 69^{3+} are slightly elongated (69^{3+} : P1–N1 1.992(3), P1–N3 1.942(3), P1–N4 1.836(3) Å; 68^{3+} : P1–N4 1.9735(17), P1–N1 1.9389(16), P1–N2 1.8111(18), P1–N3 1.8157(18) Å), which is caused by the substitution of one nitrogen donor with a carbon donor. Furthermore, the P–N bond in equatorial position in 69^{3+} (P1–N4 1.836(3) Å) is clearly exceeding the length of a typical P–N single bond (P–N: 1.78 Å),⁶⁹ indicating a rather coordinative character of this bond. In contrast, the P–C bond (P1–C1 1.852(3) Å) is slightly shortened compared to a typical P–C single bond (P–C: 1.87 Å).¹⁰³

Compound $61^{\text{Cl}_2}[\text{OTf}]$ can also be used for the synthesis of 2-(1,2'-bipyridin)-1-iumyl-substituted dipyrazolylphosphanes **70a-d**[OTf], a class of novel cationic ligands and examples of cationic *SynPhos* type II phosphanes (Scheme 28).



Scheme 28. Reaction of $61^{\text{Cl}_2}[\text{OTf}]$ with 2 eq. of **5a-d**; i) -2 Me₃SiCl, Et₂O, r.t., 91–98%.

Salts **70a-d**[OTf] are synthesized by the reaction of **61**^{Cl₂}[OTf] with two equivalents of the respective 3,5-alkyl/aryl-1-(trimethylsilyl)pyrazole in Et₂O at ambient temperature. The released chloro(trimethyl)silane can be removed under reduced pressure after 16-120 h and no further purification is necessary. All phosphanes **70a-d**[OTf] are conveniently prepared in excellent yields (91-98%). The ³¹P NMR spectra of **70a-d**[OTf] display singlet resonances (**70a**[OTf]: δ(P) = 38.6 ppm; **70b**[OTf]: δ(P) = 41.6 ppm; **70c**[OTf]: δ(P) = 61.4 ppm; **70d**[OTf]: δ(P) = 44.1 ppm), which are in good agreement with aforementioned dipyrazolyl-substituted phosphanes **41** and **43**. All compounds can be readily re-crystallized from concentrated MeCN or CH₂Cl₂ solutions *via* Et₂O diffusion yielding X-ray quality single crystals. The molecular structures of **70a-d**⁺ are depicted in Figure 27 with selected geometrical parameters presented in Table 6, stating that in all four cases the 1,2'-bipyl substituent is solely bound to the phosphorus *via* its carbon atom. The P–C bond lengths in **70a-d**⁺ range from 1.862(2)-1.8684(13) Å (Table 6) and are thus only slightly shorter than a typical P–C single bond (P–C: 1.87 Å).¹⁰³ Yet, the neutral nitrogen (N2, see Figure 27) of the 1,2'-bipyl-moiety is still in close contact with the phosphorus atom in all cations **70a-d**⁺, ranging from 2.3897(17)-2.8520(13) Å (Table 6), being well inside the sum of the van der Waals radii of N and P (3.35 Å).⁵⁶ This coordination of the N2 atom towards P1 leads to an elongation of the P1–N4 bond compared to the P1–N3 bond in all **70a-d**⁺ (Table 6). This P1–N4 bond stretching is especially larger, when the observed torsion angle of the 1,2'-bipyl-moiety (N2-C2-N1-C1) is smaller. Thus, in **70d**⁺ the smallest torsion angle (N2-C2-N1-C1 16.2(2)°) and the largest P1–N4 bond (1.7787(17) Å) are observed. On the other hand, shorter P1–N4 bonds are observed for **70b**⁺ and **70c**⁺, which both show larger torsion angles (Table 6).

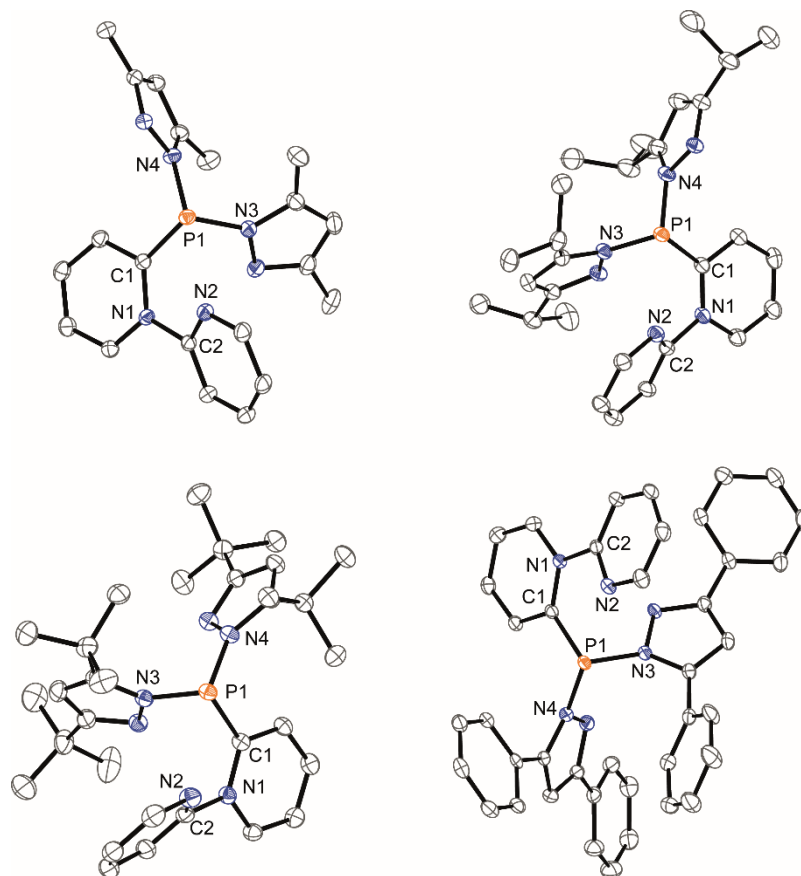


Figure 27. Molecular structures of **70a⁺** in **70a[OTf]** (top left), **70b⁺** in **70b[OTf]*Et₂O** (top right), **70c⁺** in **70c[OTf]*Et₂O** (bottom left) and **70d⁺** in **70d[OTf]** (bottom right; hydrogen atoms, solvate molecules and anions are omitted for clarity, thermal ellipsoids are displayed at 50% probability). Selected bond lengths (Å) and angles (°) are listed in Table 6.

Table 6. Selected geometrical parameters of crystallographically characterized **70a-d[OTf]**.

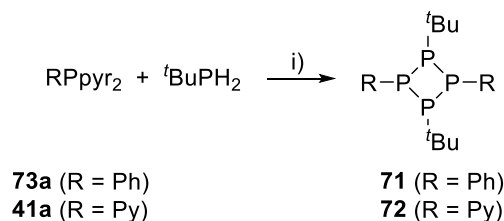
	70a[OTf]	70b[OTf]*Et₂O	70c[OTf]*Et₂O	70d[OTf]
P1–C1 in Å	1.8653(12)	1.862(2)	1.8684(13)	1.866(2)
P1–N3 in Å	1.7276(10)	1.7188(17)	1.7183(12)	1.7493(17)
P1–N4 in Å	1.7442(10)	1.7307(17)	1.7305(11)	1.7787(17)
P1–N2 in Å	2.5096(9)	2.705(2)	2.8520(13)	2.3897(17)
N2–C2–N1–C1 in °	25.15(14)	36.0(3)	48.84(17)	16.2(2)

6. Dipyrazolylphosphanes in Condensation Reactions with Primary Phosphanes

In chapter 4 the versatile use of dipyrazolyl-substituted phosphanes as [P₁]-building block is described. The controlled reactions of dipyrazolylphosphanes **41a** and **43a** with secondary phosphanes yields triphosphanes **48-50** and triphospholane **51** *via* condensation or pentaphospholanes **52** and **56** *via* a P–N/P–P bond metathesis reaction. Extending this protocol towards primary phosphanes should allow the formation of cyclophosphanes, which are most commonly synthesized by chemical¹⁰⁴ or electrochemical¹⁰⁵ reduction of corresponding dihalophosphanes RPX₂ (X = halogen) yielding symmetrical, homosubstituted rings.^{4a,106} The obtained cyclophosphanes (RP)_n typically undergo rearrangement to the respective more stable ring-sizes (typically four- of five-membered rings), depending on the substituents and the polarity of the used solvents.^{4a,106,107} Sterically demanding substituted dihalophosphanes give access to diphosphenes RP=PR which under certain circumstances are isolatable¹⁰⁸ but typically tend to dimerize to tetraphosphetanes.¹⁰⁹ Thus, following the classical routes and using mixtures of dihalophosphanes allows the introduction of two different substituents yielding mixed-substituted tetraphosphetanes, however, very often unselective and in low yields. There are only a handful reports on mixed-substituted tetraphosphetanes using specialized synthetic protocols.^{14a,109-111} Therefore, a more general route with readily available P-precursors would certainly be beneficial for further exploration of the chemistry of this type of compounds.

6.1. Synthesis of Mixed-substituted Tetraphosphetanes

The mixed-substituted tetraphosphetanes (RP-P^tBu)₂ **71** (R = Ph) and **72** (R = Py) form readily from the reaction of ^tBuPH₂ and the respective dipyrazolylphosphanes **41a** or **73a** when mixed in equimolar ratios in MeCN at -30 °C (Scheme 29).



Scheme 29. Preparation of tetraphosphetanes **71** and **72**; i) -2 **1a**, MeCN, -30 °C, 16 h, 69% (**71**), 53% (**72**).

After evaporating the solvent and subsequent sublimation of the by-product 3,5-dimethylpyrazole (**1a**), both tetraphosphetanes **71** and **72** are obtained as colorless powders in quantitative yields and acceptable purities of >90%, deduced by the integral ratios in the ³¹P NMR spectra. Washing of the crude products with cold MeCN gives analytically pure materials, however, reduces the isolated yield significantly (**71**: 69%, **72**: 53%).

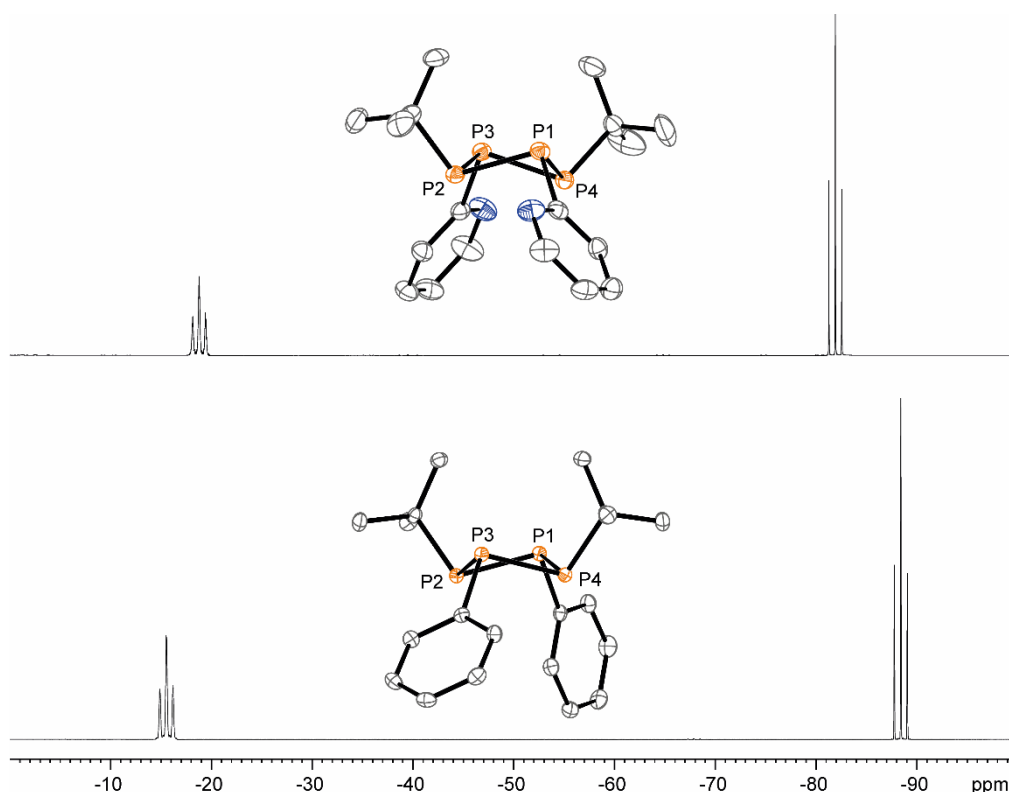
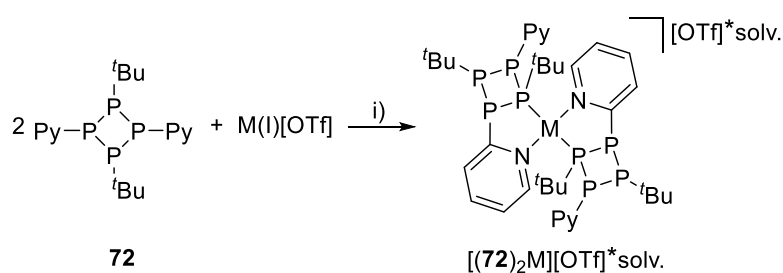


Figure 28. ³¹P NMR spectra of **71** (bottom; CD₂Cl₂, 300 K) and **72** (top; CD₂Cl₂, 300 K). Centred: Molecular structures of **71** (bottom) and **72** (top; hydrogen atoms and anions are omitted for clarity; thermal ellipsoids are displayed at 50% probability). Selected bond lengths (Å) and angles (°) are listed in Table 9.

The formation of other ring sizes is not observed and for both compounds the observation of an A_2X_2 spin system in the ^{31}P NMR spectrum (**71**: $\delta(\text{P}_A) = -88.4$ ppm, $\delta(\text{P}_X) = -15.5$ ppm; $^1J(\text{P}_A\text{P}_X) = -130$ Hz; **72**: $\delta(\text{P}_A) = -81.9$ ppm, $\delta(\text{P}_X) = -18.8$ ppm; $^1J(\text{P}_A\text{P}_X) = -131$ Hz; Figure 28) confirms the C_{2v} symmetry of the molecules. The structural connectivity is moreover confirmed by single crystal X-ray analysis and the molecular structures of **71** and **72** are depicted in Figure 28. The structural parameters of the P_4 -cores of **71** and **72** are listed in Table 9 (*vide infra*) and compare well with known symmetrically, homosubstituted tetraphosphetanes such as $(\text{PhP})_4$ ¹¹² and $(\text{CyP})_4$ ¹¹³ which reasons abstaining from a detailed discussion.

6.2. Coinage Metal Complexes of Tetraphosphetane **72**

While the coordination behavior of tetraphosphetanes of type (RP)₄ (R = Me, Et, Ph) has been extensively explored,¹¹⁴ corresponding investigations with mixed-substituted derivatives are scarce and, to the best of knowledge, did not involve derivatives with pyridyl-substituents. The additional nitrogen-based donor site of the pyridyl-units in **72** makes it a suitable multi-dentate ligand for metal coordination with selected Cu(I), Ag(I) and Au(I) triflate salts. Thus, **72** is reacted in a 2 : 1 ratio in CH₂Cl₂ with [Cu(MeCN)₄][OTf] and Ag[OTf] and in the case of Au(I), with the corresponding triflate salt which was *in situ* prepared from (tht)AuCl and MeSiOTf (Scheme 30).



Scheme 30. Reaction of **72** with selected coinage metal triflate salts “M(I)[OTf]”; i) CH₂Cl₂, r.t., 1 h; M = Cu, M[OTf] = [Cu(MeCN)₄][OTf], -4 MeCN, 89%; M = Ag, M[OTf] = Ag[OTf], 76%; M = Au, M[OTf] = (tht)AuCl + Me₃SiOTf, -Me₃SiCl, -tht, 74%.

Vapor diffusion of *n*-pentane into the reaction mixtures at -30 °C yields crystals of [(**72**)₂Cu][OTf]*CH₂Cl₂, [(**72**)₂Ag][OTf]*CH₂Cl₂ and [(**72**)₂Au][OTf]*CH₂Cl₂ in good to very good yields (74–89%). Crystals of [(**72**)₂Cu][OTf]*CH₂Cl₂ and [(**72**)₂Au][OTf]*CH₂Cl₂ are suitable for X-ray analysis, however, better quality crystals of [(**72**)₂Ag][OTf] are obtained as MeCN mono-solvate *via* recrystallization from MeCN/Et₂O. The molecular structures are depicted in Figure 29 and structural parameters are summarized in Table 7. In all three cases the molecular structures reveal mononuclear metal complexes where the metal center M(I) is coordinated by two tetraphosphetanes *via* one ^tBuP-moiety and the nitrogen atom of one pyridyl-substituent each. The P–P bond lengths in the complexes remain virtually unchanged compared to the free tetraphosphetane **72**. The average P–M contacts in [(**72**)₂M][OTf] (2.2621 Å (Cu), 2.4100 Å (Ag) and 2.2982 Å (Au)) are comparable to the coinage metal complexes of **48**, mentioned in chapter 4.2. [(**72**)₂Cu]⁺ shows a distorted tetrahedral geometry around the copper atom with a N–Cu–N angle of 94.55(6)° and a P–Cu–P angle of 127.26(2)°. This distortion causes a slight elongation of the Cu–N bond lengths in [(**72**)₂Cu]⁺ (av. 2.1124 Å) compared to tetrakis(pyridine)copper(I) hexafluorophosphate (Cu–N 2.061(3) Å), which shows an almost perfect tetrahedral

coordination geometry.¹¹⁵ Cations $[(72)_2Ag]^+$ and $[(72)_2Au]^+$ show wider P-M-P angles ($[(72)_2Ag]^+$: $141.14(2)^\circ$ and $[(72)_2Au]^+$: $154.71(2)^\circ$) and more acute N-M-N angles ($[(72)_2Ag]^+$: $85.18(5)^\circ$ and $[(72)_2Au]^+$: $75.42(6)^\circ$), causing a further elongation of the N-M distances ($[(72)_2Ag]^+$: 2.4458 \AA and $[(72)_2Au]^+$: 2.6262 \AA (average values)). This states a decreasing participation of the pyridine nitrogen and *vice versa* an increasing involvement of the phosphorus in the coordination of silver and gold, which is in consistency with Pearsons' concept.¹¹⁶

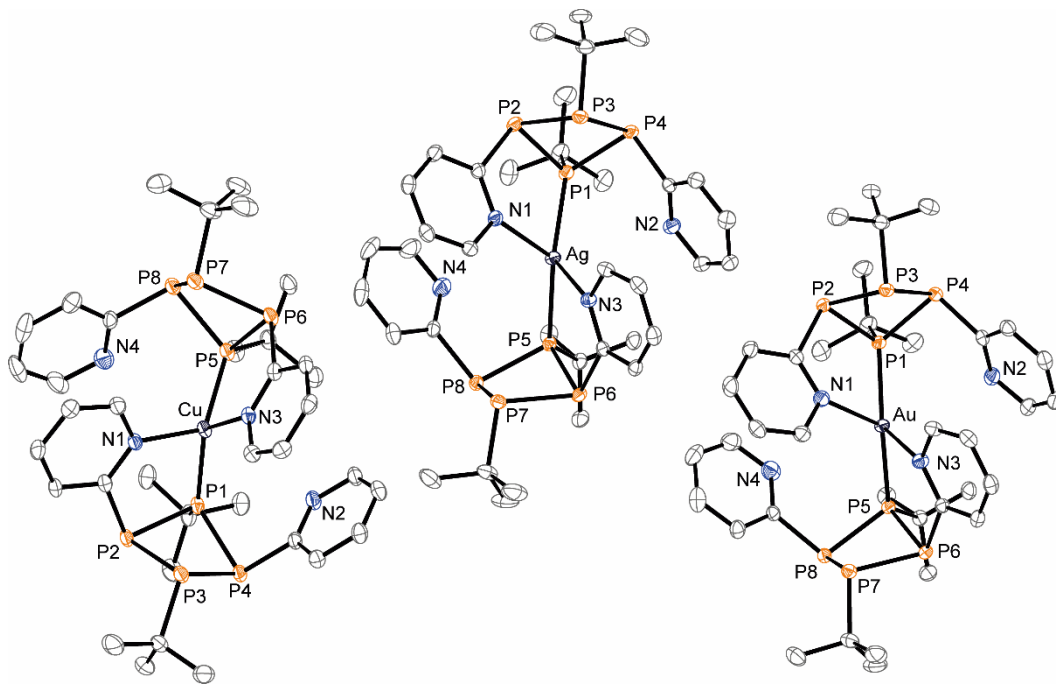


Figure 29. Molecular structures of $[(72)_2Cu]^+$ in $[(72)_2Cu][OTf] \cdot CH_2Cl_2$ (left), $[(72)_2Ag]^+$ in $[(72)_2Ag][OTf] \cdot MeCN$ (middle) and $[(72)_2Au]^+$ in $[(72)_2Au][OTf] \cdot CH_2Cl_2$ (right) (hydrogen atoms, anions and solvate molecules are omitted for clarity, thermal ellipsoids are displayed at 50% probability); selected bond lengths (\AA) and angles ($^\circ$) are given in Table 7.

Table 7. Selected geometrical parameters of crystallographically characterized coinage metal complexes $[(72)_2Cu][OTf] \cdot CH_2Cl_2$, $[(72)_2Ag][OTf] \cdot MeCN$ and $[(72)_2Au][OTf] \cdot CH_2Cl_2$.

	$[(72)_2Cu][OTf]$	$[(72)_2Ag][OTf]$	$[(72)_2Au][OTf]$
P-P ^a in \AA	2.2204	2.2183	2.2191
P-M ^a in \AA	2.2621	2.4100	2.2982
N-M ^a in \AA	2.1124	2.4458	2.6262
N-M-N in $^\circ$	94.55(6)	85.18(5)	75.42(6)
P-M-P in $^\circ$	127.26(2)	141.14(2)	154.71(2)

[a] average bond lengths and angles are given.

Coordination complexes $[(72)_2Cu][OTf]$, $[(72)_2Ag][OTf]$ and $[(72)_2Au][OTf]$ were further analyzed by multinuclear NMR spectroscopy at various temperatures. All three complexes $[(72)_2Cu][OTf]$, $[(72)_2Ag][OTf]$ and $[(72)_2Au][OTf]$ show a dynamic behavior in CD_2Cl_2

solution at 290 K. In the ^1H NMR spectra four resonances for the pyridyl moieties are observed in each case of the three coordination complexes, stating the fast exchange of the pyridyl moieties coordinating the respective metal cation. Upon cooling, this exchange is slowing down, leading to eight different resonances for the pyridyl moieties.

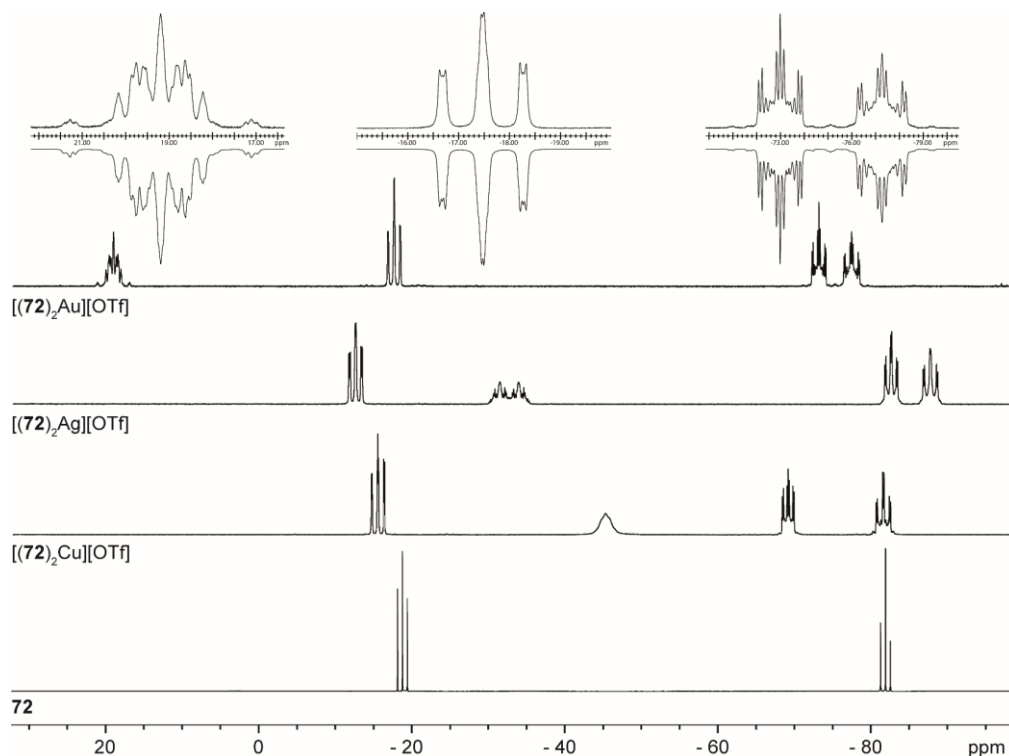


Figure 30. $^{31}\text{P}\{^1\text{H}\}$ spectra of **72** (CD_2Cl_2 , 300 K) and $[(\mathbf{72})_2\text{Cu}][\text{OTf}]$, $[(\mathbf{72})_2\text{Ag}][\text{OTf}]$ and $[(\mathbf{72})_2\text{Au}][\text{OTf}]$ (form bottom to top; CD_2Cl_2 , 190 K); insets show the AA'BB'MM'XX' spin system of the experimental (upwards) and fitted spectra (downwards) of $[(\mathbf{72})_2\text{Au}][\text{OTf}]$.

Table 8. Chemical shifts of **72**, $[(\mathbf{72})_2\text{Cu}][\text{OTf}]$, $[(\mathbf{72})_2\text{Ag}][\text{OTf}]$ and $[(\mathbf{72})_2\text{Au}][\text{OTf}]$ in ppm; entries with a grey background indicate resonances of the 'Bu-P moiety coordinating the metal(I) cation.

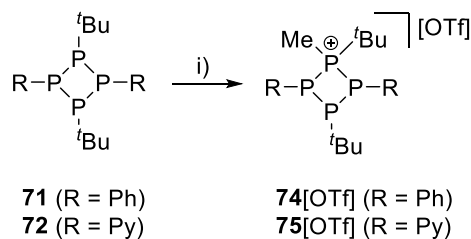
	72	$[(\mathbf{72})_2\text{Cu}][\text{OTf}]$	$[(\mathbf{72})_2\text{Ag}][\text{OTf}]$	$[(\mathbf{72})_2\text{Au}][\text{OTf}]$
$\delta(\text{P}_\text{A})$	-81.9	-81.4	-87.6	-77.3
$\delta(\text{P}_\text{B})$	-	-68.9	-82.4	-73.0
$\delta(\text{P}_\text{M})$	-	-45.1	-32.5	-17.5
$\delta(\text{P}_\text{X})$	-18.8	-15.4	-12.4	19.2

While two pyridyl groups are coordinating the metal cation, the other two are not, making them chemically inequivalent. The ^1H NMR spectra of $[(\mathbf{72})_2\text{Cu}][\text{OTf}]$, $[(\mathbf{72})_2\text{Ag}][\text{OTf}]$ and $[(\mathbf{72})_2\text{Au}][\text{OTf}]$ at temperatures from 290-190 K are depicted in chapter 12.5, showing coalescence temperatures of 260K for $[(\mathbf{72})_2\text{Cu}][\text{OTf}]$ and of 210 K for $[(\mathbf{72})_2\text{Ag}][\text{OTf}]$ and $[(\mathbf{72})_2\text{Au}][\text{OTf}]$. These findings are also observed in the ^{31}P NMR spectra (see chapter 12.5). $[(\mathbf{72})_2\text{Au}][\text{OTf}]$ and $[(\mathbf{72})_2\text{Cu}][\text{OTf}]$ show three broadened resonances at 300 K due to

dynamic processes and additionally for [(**72**)₂Cu][OTf] due to the fast quadrupole relaxation of the ⁶³Cu nucleus.⁵⁹ For [(**72**)₂Ag][OTf] two resonances are observed at 300 K. Measuring the ³¹P NMR spectra at 190 K reveals an AA'BB'MM'XX' spin system for each coinage metal complex [(**72**)₂M][OTf] (see Figure 30 and Table 8). Details on the coupling constants for [(**72**)₂Au][OTf], acquired by iteratively fitting the spectrum, are reported in the experimental details (chapter 12.5.5). Severe line broadening in the spectra of [(**72**)₂Cu][OTf] due to the fast quadrupole relaxation of the ⁶³Cu nuclei,⁵⁹ and further line splitting in the spectra of [(**72**)₂Ag][OTf] as a result of the complexation with the ¹⁰⁷Ag/¹⁰⁹Ag nuclei reasons refraining from iteratively fitting these spectra. It is noteworthy that the resonance of the ^tBu-P moiety in [(**72**)₂M][OTf] coordinating the metal cation shows a significant shift compared to the ^tBu-P moiety of the free ligand **72**. Coordination to Cu(I) and Ag(I) cause upfield shifts of $\Delta\delta = -26.3$ ppm and $\Delta\delta = -13.7$ ppm, respectively. Yet coordination to Au(I) is observed by a downfield shift of $\Delta\delta = +38.0$ ppm (Figure 30; Table 8).

6.3. Methylation Reactions of Tetraphosphetanes **71** and **72**

Further investigations on the donor ability of compounds **71** and **72** focused on methylation reactions with an equimolar ratio of MeOTf in Et₂O (Scheme 31).



Scheme 31. Monomethylation reaction of **71** and **72**; i) +MeOTf, Et₂O, r.t., 16 h, 87% (**74[OTf]**), 91% (**75[OTf]**).

For both compounds, colorless precipitates are obtained, which after filtration and subsequent recrystallization from MeCN/Et₂O were identified as tetraphosphetan-1-ium triflate salts **74[OTf]** and **75[OTf]**. Both salts are obtained in very good yield (**74[OTf]**: 87%; **75[OTf]**: 91%) and their ³¹P {¹H} NMR spectra display an A₂MX spin system each (**74[OTf]**: δ(P_A) = -81.2 ppm, δ(P_M) = -39.8 ppm, δ(P_X) = 22.0 ppm; ¹J(P_AP_X) = -248 Hz, ¹J(P_AP_M) = -127 Hz, ²J(P_MP_X) = 23 Hz; **75[OTf]**: δ(P_A) = -70.5 ppm, δ(P_M) = -24.9 ppm, δ(P_X) = 24.2 ppm; ¹J(P_AP_X) = -225 Hz, ¹J(P_AP_M) = -132 Hz, ²J(P_MP_X) = 15 Hz) as expected for the monomethylation of one of the ^tBu-P moieties. X-ray analysis of both salts confirms the structural connectivity of cations **74**⁺ and **75**⁺ as shown in Figure 31. Their structural parameters are in good agreement with those reported for related monomethylated tetraphosphetanium cations (Table 9).^{35c,d}

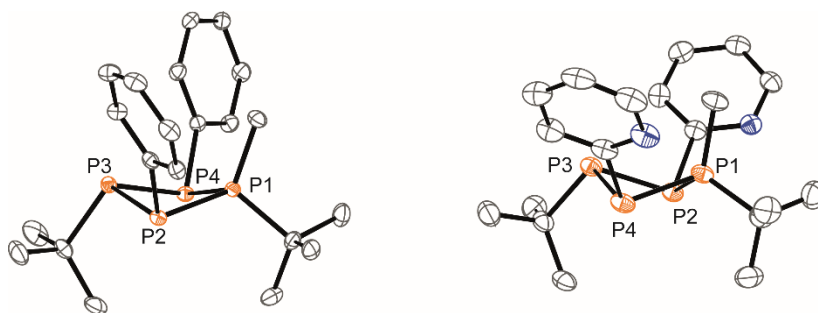
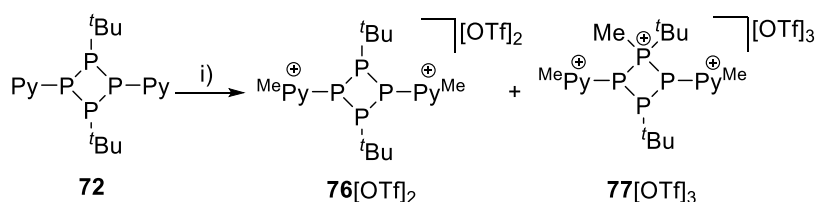


Figure 31. Molecular structures of **74[OTf]** (left) and **75[OTf]** (right) (hydrogen atoms and anions are omitted for clarity; thermal ellipsoids are displayed at 50% probability); selected bond lengths and angles are given in Table 9.

In thought of further methylation of **71** and **72** harsher reaction conditions are attempted by reacting them in a slurry of a fivefold excess of MeOTf, similarly to reports by Burford and co-workers.^{35d} In case of **71**, only the exclusive formation of the monomethylated salt

$74[\text{OTf}]$ is observed with no indication for the formation of other compounds. However, in case of **72** the formation of two distinct different cations is observed as indicated by the $^{31}\text{P}\{^1\text{H}\}$ NMR spectrum of the heterogeneous reaction mixture dissolved in CD_3NO_2 (Figure 32). The presence of an A_2X_2 spin system suggests the formation of the C_{2v} symmetric cation 76^{2+} ($\delta(\text{P}_\text{A}) = -96.4$ ppm, $\delta(\text{P}_\text{X}) = -4.3$ ppm; $^1J(\text{P}_\text{A}\text{P}_\text{X}) = -132$ Hz; Figure 32) and the observed A_2MX spin system ($\delta(\text{P}_\text{A}) = -89.8$ ppm, $\delta(\text{P}_\text{M}) = -17.4$ ppm, $\delta(\text{P}_\text{X}) = 42.6$ ppm; $^1J(\text{P}_\text{A}\text{P}_\text{X}) = -249$ Hz, $^1J(\text{P}_\text{A}\text{P}_\text{M}) = -129$ Hz, $^2J(\text{P}_\text{M}\text{P}_\text{X}) = 22$ Hz; Figure 32, highlighted in red) is significantly different from that of the monomethylated cation 75^+ suggesting the formation of tricationic 77^{3+} (Scheme 32).



Scheme 32. Reaction of **72** with excess MeOTf; i) 5 eq. MeOTf, neat, r.t., 16h; unbalanced equation.

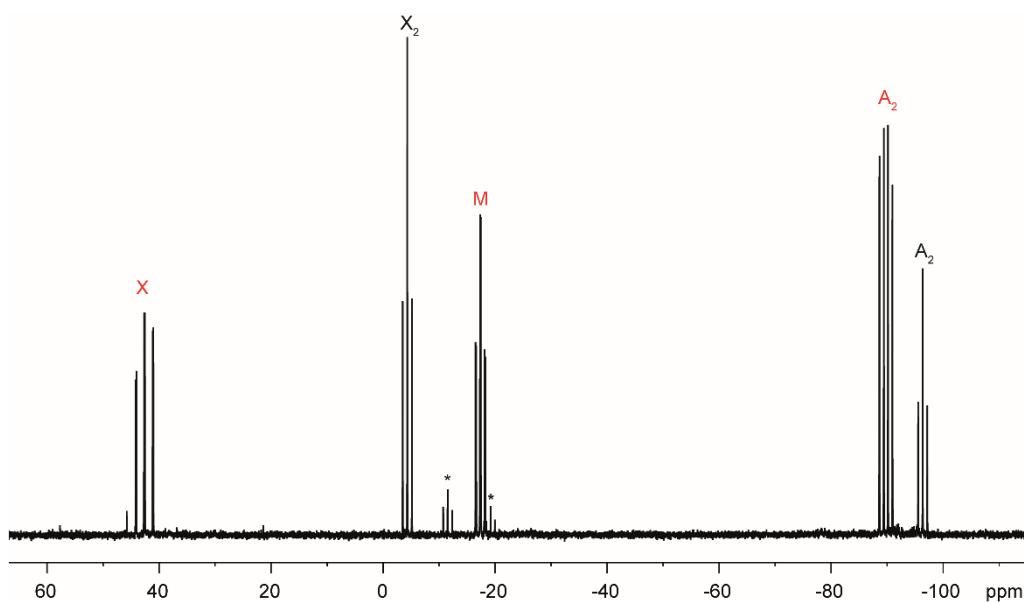


Figure 32. $^{31}\text{P}\{^1\text{H}\}$ NMR spectrum of the reaction of **72** with 5 eq. MeOTf (CD_3NO_2 ; 300K); small amounts of unidentified compounds are indicated by asterisks.

The findings are justified by the observed shifts of the A_2X_2 spin system which are in the region of tri-coordinated phosphorus atoms, whereas the resonance at $\delta(\text{P}_\text{X}) = 42.6$ ppm for cation 77^{3+} is typical for a tetra-coordinated phosphorus atom.¹¹⁷ This assumption is confirmed by X-ray analysis since both salts could be crystallized, however, repeatedly as mixtures. After removal of the excess MeOTf from the reaction mixture, crystals of $76[\text{OTf}]_2$

suitable for X-ray analysis grew from a MeCN solution by slow vapor diffusion of Et₂O at -30 °C next to the deposition of copious amounts of amorphous material. If the reaction mixture is dissolved with excess of MeOTf in MeNO₂ followed by Et₂O addition *via* slow vapor diffusion at -30 °C, suitable crystals of 77[OTf]₃*2 MeNO₂ could be harvested. The separation of 76[OTf]₂ from 77[OTf]₃ by fractional crystallization was not possible so far, thus, hampering the isolation of analytically pure salts. Figure 33 displays the molecular structures of the cations 76²⁺ and 77³⁺.

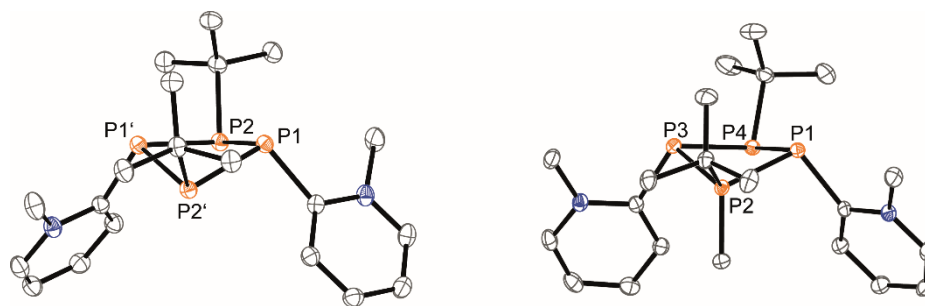


Figure 33. Molecular structures of 76²⁺ in 76[OTf]₂ (left) and 77³⁺ in 77[OTf]₃*2 MeNO₂ (right; hydrogen atoms, anions and solvate molecules are omitted for clarity, thermal ellipsoids are displayed at 50% probability); selected bond lengths and angles are given in Table 9.

Table 9. Selected geometrical parameters of crystallographically characterized 71, 72, 74[OTf], 75[OTf], 76[OTf]₂, 77[OTf]₃*2 MeNO₂, 78[OTf]₃*MeNO₂ and 82[OTf]₃; bond lengths are given in (Å), angles are given in (°); entries with a grey background indicate λ³P–λ⁴P⁺ bond lengths and λ³P–λ⁴P⁺–λ³P bond angles.

	71	72	74[OTf]	75[OTf]	76[OTf] ₂	77[OTf] ₃	78[OTf] ₃	82[OTf] ₃
P1 – P2	2.2236(4)	2.2226(4)	2.1983(6)	2.1899(6)	2.2187(5)	2.2034(5)	2.247(2)	2.2398(7)
P2 – P3	2.2222(4)	2.2232(5)	2.2341(6)	2.2419(6)	2.2345(5) _a	2.2120(5)	2.238(2)	2.2194(7)
P3 – P4	2.2198(4)	2.2195(4)	2.2333(5)	2.2397(6)	-	2.2420(5)	2.203(2)	2.2224(7)
P4 – P1	2.2313(4)	2.2191(4)	2.1938(6)	2.1861(6)	-	2.2351(5)	2.204(2)	2.2257(7)
P1-P2-P3	87.87(1)	85.55(2)	83.97(2)	82.46(2)	86.30(2) ^a	90.33(2)	83.61(6)	82.92(3)
P2-P3-P4	85.94(1)	85.14(2)	90.28(2)	85.89(2)	87.21(2) ^a	84.12(2)	81.51(6)	84.44(3)
P3-P4-P1	87.73(1)	85.72(2)	84.09(2)	82.59(2)	-	88.76(2)	85.44(6)	83.17(9)
P4-P1-P2	85.63(1)	85.16(2)	92.77(2)	88.49(2)	-	84.48(2)	81.29(5)	83.88(2)

[a] P1' ≅ P3, P2' ≅ P4

The P–P bond lengths in dicationic 76²⁺ are comparable to those of tetraphosphetanes 71 and 72 (Table 9). The P-P-P angles differ only slightly indicating only a minor influence of the methylation of the pyridyl-substituents to the structural parameters of the P₄-core. Consistent

with our findings, the structural parameters of trication 77^{3+} are very similar to those of mono-methylated tetraphosphetanium cations 74^+ and 75^+ (Table 9).

Attempting to selectively synthesize $77[\text{OTf}]_3$, **72** was stirred in a twenty-two-fold excess of MeOTf at elevated temperature (80 °C; microwave). After 4 h, a red-colored solution was obtained, and, although the $^{31}\text{P}\{^1\text{H}\}$ NMR spectrum showed a rather complex mixture of compounds, one very dominant A_2MX spin system ($\delta(\text{P}_A) = -73.5$ ppm, $\delta(\text{P}_M) = -12.0$ ppm, $\delta(\text{P}_X) = 19.9$ ppm; $^1J(\text{P}_A\text{P}_X) = -228$ Hz, $^1J(\text{P}_A\text{P}_M) = -118$ Hz, $^2J(\text{P}_M\text{P}_X) = 31$ Hz) indicated the formation of a new compound in high yields. After the addition of Et₂O to the reaction mixture, copious amounts of a colorless precipitate are obtained. Washing with CH₂Cl₂ gives the analytically pure product in high yields (91%) which was identified as $77[\text{OTf}]_3$ after recrystallization from a MeNO₂ solution and slow vapor diffusion of Et₂O or CH₂Cl₂ at -30 °C (Figure 34).

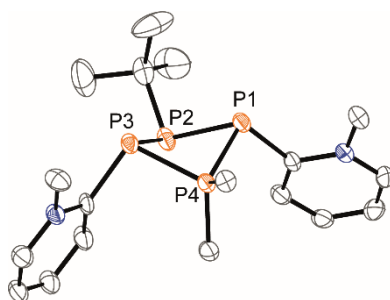
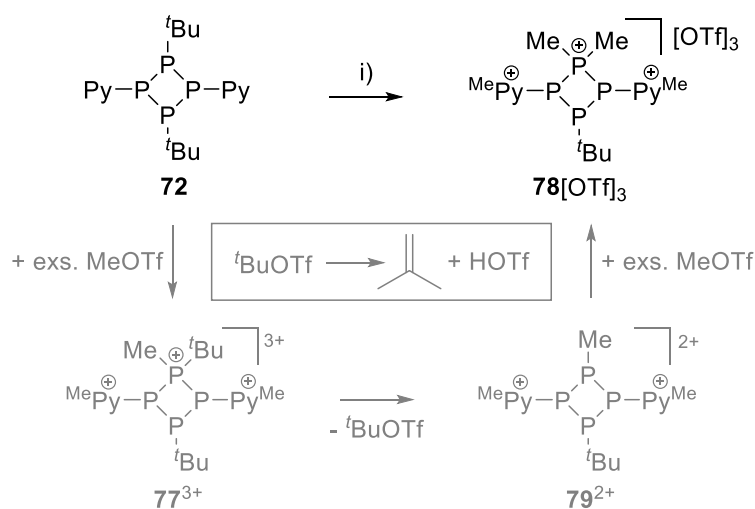


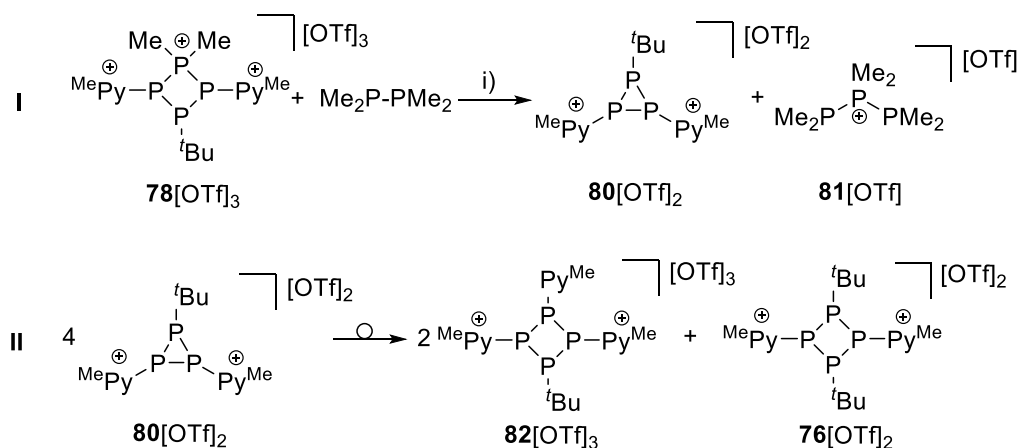
Figure 34. Molecular structure of 78^{3+} in $78[\text{OTf}]_3 \cdot \text{MeNO}_2$ (hydrogen atoms, solvate molecules and anions are omitted for clarity, thermal ellipsoids are displayed at 50% probability). Selected bond lengths and angles are given in Table 9.

The formation of cation 78^{3+} is likely to proceed according to Scheme 33 *via* a series of alkylation and dealkylation reactions in which the first step is the formation of the trimethylated trication 77^{3+} . Due to the high charge of cation 77^{3+} , the nucleophilic attack of one triflate anion and elimination of *t*BuOTf is supported and leads to the formation of dication 79^{2+} . At temperatures above -30 °C *t*BuOTf is known to decompose to *t*butene and HOTf.¹¹⁸ The formation of the latter can be traced by multi-nuclear NMR spectroscopy of the reaction mixture ($\delta(\text{H}) = 15.42$ ppm (br), $\delta(\text{F}) = -76.0$ ppm (s)).^{118b} In the last step, dication 79^{2+} is regioselectively methylated due to the excess of MeOTf to trication 78^{3+} .



Scheme 33. Proposed mechanism of the formation of **78[OTf]₃** from the reaction of **72** with MeOTf at elevated temperatures; i) 22 eq. MeOTf, neat, 80 °C, 4 h, -*t*-butene, -HOTf, 91%.

The molecular structure of **78³⁺** is shown in Figure 34. The $\lambda^3\text{P}-\lambda^4\text{P}^+$ bond lengths in **78³⁺** (P3–P4 2.203(2) Å, P4–P1 2.204(2) Å) are marginally shorter compared to the $\lambda^3\text{P}-\lambda^4\text{P}^+$ bond lengths in **77³⁺** (P1–P2 2.2034(5) Å and P2–P3 2.2120(5) Å). Moreover, they are considerably shorter than the other P–P bond lengths in **78³⁺** (P1–P2 2.247(2) Å, P2–P3 2.238(2) Å) which is caused by the polarization in the $\lambda^3\text{P}-\lambda^4\text{P}^+$ bond. This leads to a large $\lambda^3\text{P}-\lambda^4\text{P}^+-\lambda^3\text{P}$ bond angle (P3–P4–P1 85.44(6)°) compared to the smaller P–P–P angles in **78³⁺** (P1–P2–P3 83.61(6)°, P2–P3–P4 81.51(6)°, P4–P1–P2 81.29(5)°), which is consistent with the findings for the tetraphosphetan-1-ium salts **74[OTf]** and **75[OTf]** (Table 9). Further investigations aimed to see, if ring contraction of **78³⁺** by phosphonium abstraction gives access to the three-membered dication **80²⁺**. Related approaches have been demonstrated by the Burford group which reacted tetraphosphetanium salt **33[OTf]** with PMe_3 and observed the formation of the respective ring contracted triphosphirane and diphosphanium salt **35[OTf]** (Scheme 11).^{35a,d} In this approach the more basic diphosphane $\text{Me}_2\text{P}-\text{PMe}_2$ is chosen and an equimolar amount is added to a solution of **78[OTf]₃** in MeCN. A deep red-colored reaction mixture is observed immediately which showed after a reaction time of 4 h at ambient temperature three main products as judged from the $^{31}\text{P}\{^1\text{H}\}$ NMR spectrum. Hexamethyltriphosphan-2-ium cation **81⁺** can be identified by its characteristic A_2X spin system ($\delta(\text{P}_\text{A}) = -59.2$ ppm, $\delta(\text{P}_\text{X}) = 10.5$ ppm; $^1J(\text{P}_\text{A}\text{P}_\text{X}) = 298$ Hz)^{35a} and is the product of the successful phosphonium abstraction from **78³⁺**.



Scheme 34. Suggested mechanism of the formation of $\mathbf{82[OTf]}_3$ from the reaction of $\mathbf{78[OTf]}_3$ with Me_2PPMe_2 via P–P/P–P bond metathesis (**I**) and a rearrangement reaction of the *in situ* generated triphosphirane $\mathbf{80}^{2+}$ (**II**); i) MeCN, r.t., 4 h, 45%.

In addition, the presence of a known A_2X_2 spin system identifies the formation of dicationic $\mathbf{76}^{2+}$ ($\delta(\text{P}_\text{A}) = -96.4$ ppm, $\delta(\text{P}_\text{X}) = -4.3$ ppm; $^1J(\text{P}_\text{A}\text{P}_\text{X}) = -132$ Hz) and a new A_2MX spin system ($\delta(\text{P}_\text{A}) = -68.3$ ppm, $\delta(\text{P}_\text{M}) = -51.1$ ppm, $\delta(\text{P}_\text{X}) = 2.7$ ppm; $^1J(\text{P}_\text{A}\text{P}_\text{X}) = -123$ Hz, $^1J(\text{P}_\text{A}\text{P}_\text{M}) = -100$ Hz, $^2J(\text{P}_\text{M}\text{P}_\text{X}) = 91$ Hz) is assigned to tricationic $\mathbf{82}^{3+}$ (Scheme 34). At first glance, these findings are different from the aforementioned assumption, which does not agree with the observation of cation $\mathbf{76}^{2+}$ and the new cation $\mathbf{82}^{3+}$. In order to shed light on this outcome, the reaction was performed at -30 °C and the progress of the reaction was monitored NMR spectroscopically during the warm-up to room temperature (Figure 35). At -30 °C the $^{31}\text{P}\{^1\text{H}\}$ NMR spectrum shows mainly the resonances for cation $\mathbf{81}^+$ and a characteristic A_2X spin system ($\delta(\text{P}_\text{A}) = -138.3$ ppm, $\delta(\text{P}_\text{X}) = -106.5$ ppm; $^1J(\text{P}_\text{A}\text{P}_\text{X}) = -199$ Hz) which is consistent with a triphosphirane, and thus, is assigned to dication $\mathbf{80}^{2+}$ (Scheme 34, **I**). During warm-up, the resonances for $\mathbf{80}^{2+}$ completely vanish and the resonances of cation $\mathbf{76}^{2+}$ and $\mathbf{82}^{3+}$ appear. It is known that cyclo-polyphosphanes can undergo interconversion reactions in protic solvents to give thermodynamically more favored ring-sizes.^{104d} Therefore ring-interconversion of $\mathbf{80}^{2+}$ is assumed as a result of a P–P/P–P bond metathesis to form cations $\mathbf{82}^{3+}$ and $\mathbf{76}^{2+}$ (Scheme 34, **II**).^{21e,f} Salt $\mathbf{82[OTf]}_3$ could be separated from the reaction mixture in yields of 45% *via* slow vapor diffusion of CH_2Cl_2 into the reaction mixture at -30 °C. The obtained clear, yellow-colored crystals were suitable for X-ray analysis and the molecular structure of $\mathbf{82}^{3+}$ is depicted in Figure 36. The P–P bond lengths in $\mathbf{82}^{3+}$ are in the expected range of P–P single bonds and comparable to the P–P bonds in **71**, **72** and $\mathbf{76}^{2+}$ (Table 9).

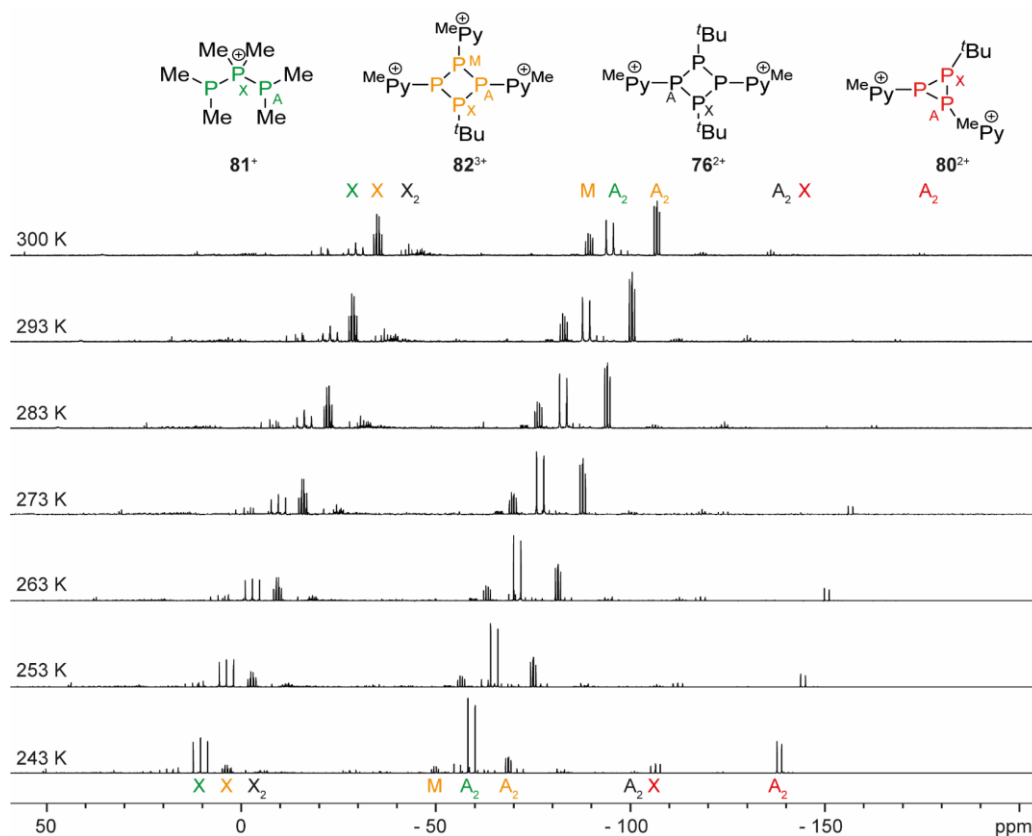


Figure 35. $^{31}\text{P}\{^1\text{H}\}$ spectra of the reaction mixture of $78[\text{OTf}]_3$ and $\text{Me}_2\text{P-PMe}_2$ in MeCN measured at temperatures from 243–300 K. Identified resonances are assigned to the respective molecules by their spin systems in the same color as the phosphorus atoms in the molecules shown atop the spectra.

Compared to 76^{2+} (P1-P2-P1' $86.30(2)^\circ$, P2-P1-P2' $87.21(2)^\circ$) the exchange of one *tert*-butyl moiety for one methylpyridiniumyl-substituent leads to smaller P-P-P angles in 82^{3+} (P1-P2-P3 $82.92(3)^\circ$, P2-P3-P4 $84.44(3)^\circ$, P3-P4-P1 $83.17(9)^\circ$, P4-P1-P3 $83.88(2)^\circ$), as the methylpyridiniumyl group is sterically less demanding.

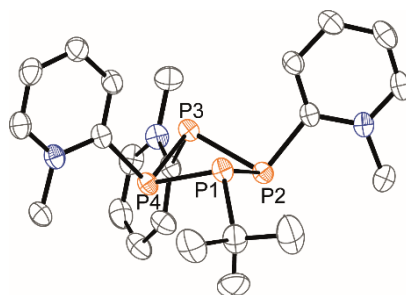
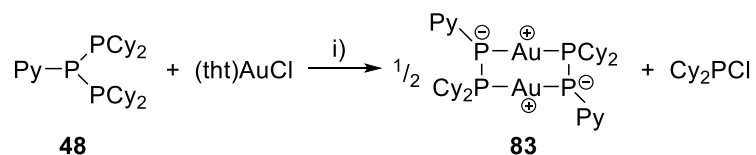


Figure 36. Molecular structure of 82^{3+} in $82[\text{OTf}]_3$ (hydrogen atoms, solvate molecules and anions are omitted for clarity, thermal ellipsoids are displayed at 50% probability); selected bond lengths and angles are given in Table 9.

7. Gold Chloride induced Cleavage of P–P Bonds

The coordination chemistry of triphosphane **48** towards coinage metal salts is presented in chapter 4.2., with regard to coinage metal triflate and bromide salts. Investigating its coordination chemistry towards chloride salt (tbt)AuCl, a degradation reaction of the triphosphane **48** is observed. Reacting **48** with (tbt)AuCl in THF in an equimolar ratio gives a clear, yellow solution. ^{31}P NMR spectroscopy indicates the formation of $\text{Cy}_2\text{P}(\text{Cl})$, observed by its singlet resonance at $\delta(\text{P}) = 127.8$ ppm,¹¹⁹ next to an AA'XX' spin system ($\delta(\text{P}_\text{A}) = -67.4$ ppm, $\delta(\text{P}_\text{X}) = 58.1$ ppm; $^1J(\text{P}_\text{A}\text{P}_\text{X}) = -356$ Hz, $^1J(\text{P}_\text{A}'\text{P}_\text{X}') = -355$ Hz, $^2J(\text{P}_\text{A}\text{P}_\text{X}') = 131$ Hz, $^1J(\text{P}_\text{A}'\text{P}_\text{X}) = 135$ Hz, $^3J(\text{P}_\text{A}\text{P}_\text{A}') = 0$ Hz, $^3J(\text{P}_\text{X}\text{P}_\text{X}') = 0$ Hz; Figure 37) which is assigned to diphosphan-1-ide gold complex **83** (Scheme 35).



Scheme 35. Reaction of **48** with (tbt)AuCl; i) –tbt, THF, r.t., **83** is not isolated.

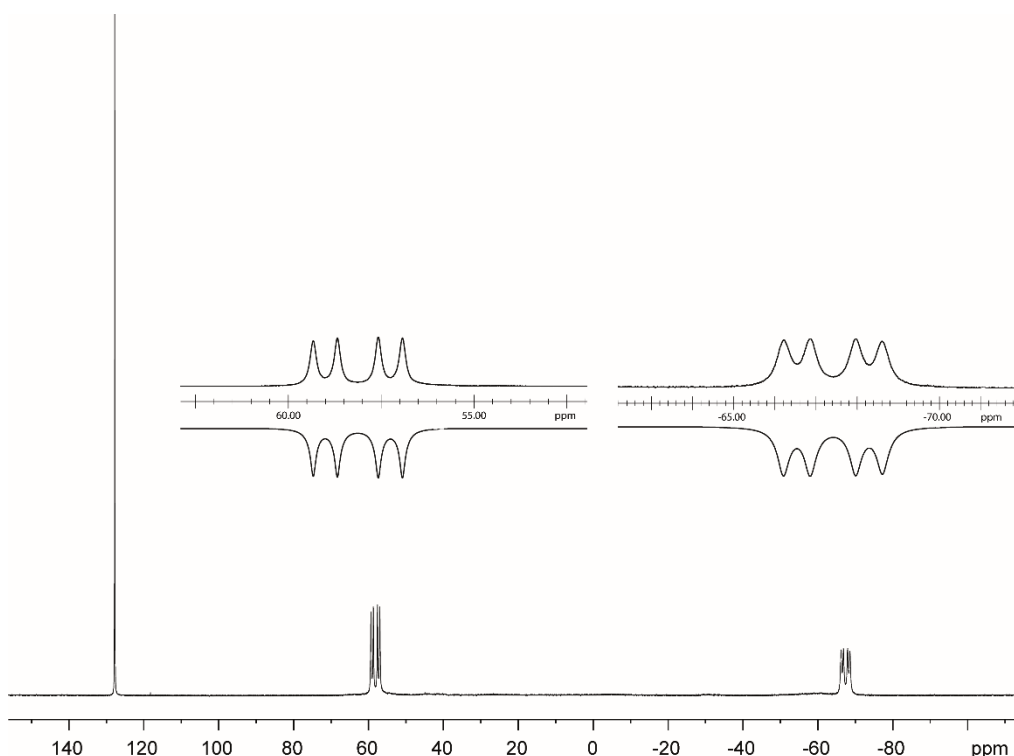
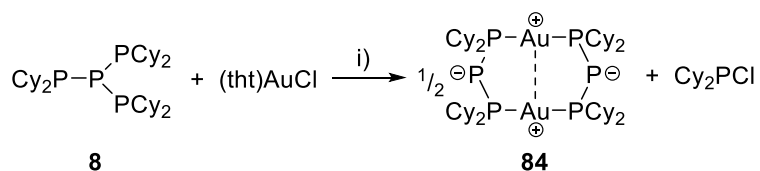


Figure 37. $^{31}\text{P}\{^1\text{H}\}$ NMR spectrum of the reaction described in Scheme 33. (THF, C_6D_6 -capillary, 300 K); insets show the AA'XX' spin system of the experimental (upwards) and fitted spectra (downwards) of **83** in the reaction mixture.

Compound **83** forms *via* a chloride induced P–P bond cleavage, which is known from similar P–P bond cleavage reactions by hydrogen chloride,¹²⁰ thionyl chloride,¹²¹ carbon tetrachloride,¹²² or other phosphorus chlorides,¹²³ next to one very recently reported cleavage by (tbt)AuCl.^{21f} As of now **83** could not be isolated successfully, as various attempts lead to the formation of complex mixtures of products including (PyP)_n (n = 3-5) and Cy₄P₂. Further investigations on gold chloride induced P–P bond cleavage reactions in polyphosphanes focused on the reaction of *iso*-tetraphosphane **8** and (tbt)AuCl according to Scheme 36. Figure 38 shows the ³¹P NMR spectrum of this reaction, showing the formation of two products. Next to the resonance of Cy₂PCL a highly symmetric spin system of higher order is observed, which is assigned to dinuclear gold complex **84** which is isolated in very good yields of 89% as a beige-colored powder on a gram scale after a reaction time of 15 minutes.



Scheme 36. Reaction of **8** with (tbt)AuCl; i) –tbt, THF, r.t., 89%.

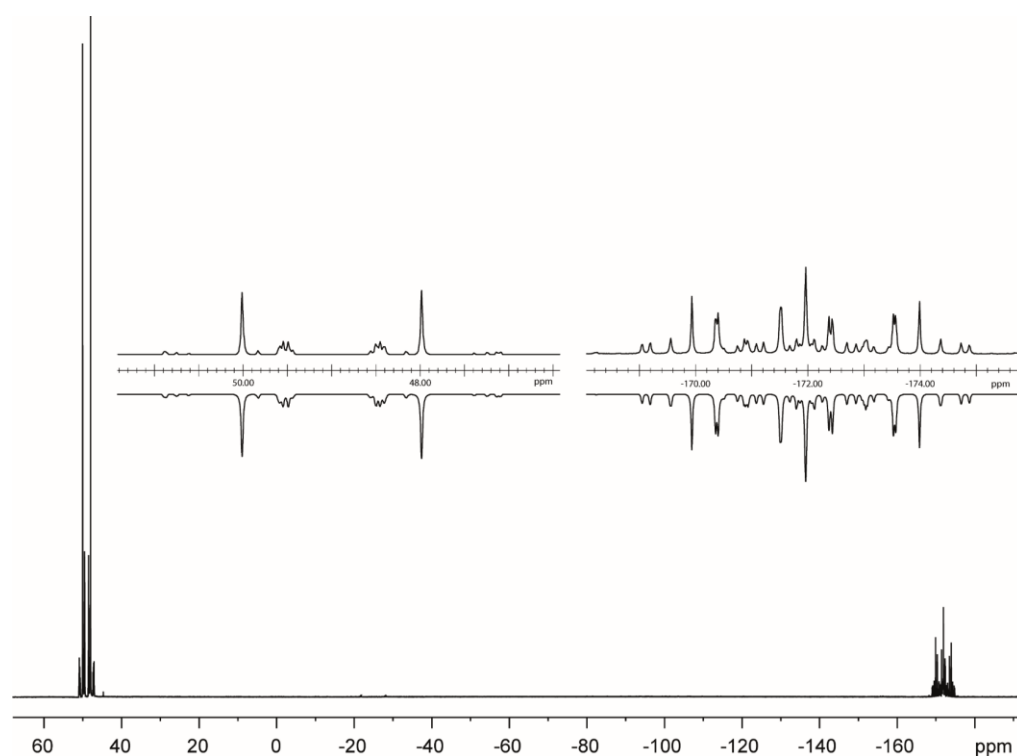


Figure 38. ³¹P{¹H} NMR spectrum of **84** (THF-d₈, 300 K); insets show the AA'XX'X''X''' spin system of the experimental (upwards) and fitted spectra (downwards).

The spin system of **84** observed in the $^{31}\text{P}\{^1\text{H}\}$ spectrum was iteratively fitted to be an AA'XX'X''X''' spin system ($\delta(\text{P}_A) = -172.0$ ppm, $\delta(\text{P}_X) = 49.0$ ppm; coupling constants are reported in chapter 12.6.1). Figure 38 shows the experimental as well as the fitted spectra. Crystals in X-ray quality of **84** are obtained by slow vapor diffusion of *n*-pentane into a saturated CH_2Cl_2 solution at -30 °C. The molecular structure of **84** is depicted in Figure 39.

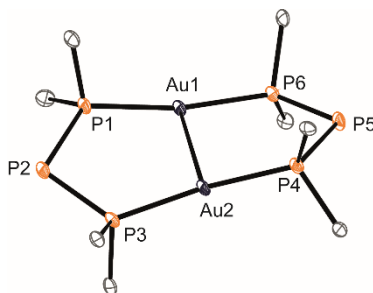
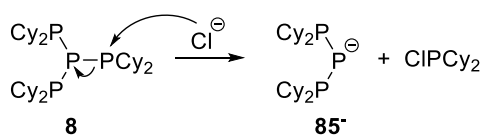


Figure 39. Molecular structure of **84** (hydrogen atoms, solvate molecules and anions omitted for clarity, cyclohexyl groups are depicted by their P–C bound carbon atom only, thermal ellipsoids are displayed at 50% probability). Selected bond lengths (Å) and angles (°): P1–P2 2.1481(17), P2–P3 2.1505(17), P4–P5 2.1454(17), P5–P6 2.1402(17), P1–Au1 2.3324(12), P6–Au1 2.3298(12), P3–Au2 2.3254(11), P4–Au2 2.3167(12), Au1–Au2 2.9048(2), P1–P2–P3 100.83(7), P4–P5–P6 103.22(7), P1–Au1–P6 168.72(4), P3–Au2–P4 171.65(4).

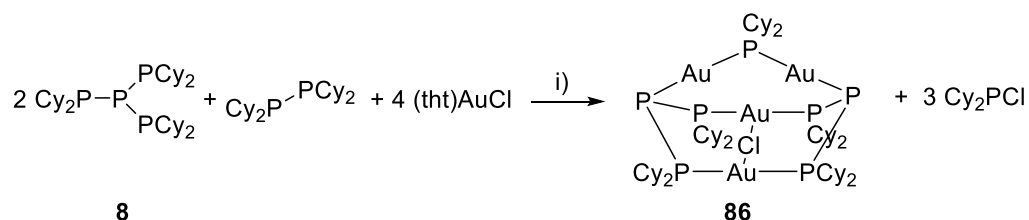
The P–P bond lengths in **84** range from 2.1402(17)-2.1505(17) Å, which is shorter than the P–P bonds observed for a similar diphosphanide gold complex (2.1900(14)-2.1958(13) Å)^{21f} and comparable to the P–P bond lengths reported for triphosphenium ion $[\text{Ph}_3\text{P}-\text{P}-\text{PPh}_3]^+$ (2.128(6)-2.141(6) Å).⁶⁶ Also the P–P–P angles in **84** (100.83(7) and 103.22(7)°) are in the range of the P–P–P angles reported for $[\text{Ph}_3\text{P}-\text{P}-\text{PPh}_3]^+$ (102.2(2) and 103.0(3)°).⁶⁶ The P–Au bond lengths and the P–Au–P angles in **84** (2.3167(12)-2.3324(12) Å, 168.72(4) and 171.65(4)°) are in good comparison to the P–Au bond lengths and the P–Au–P angle observed in $[(\mathbf{48Au})_2]^{2+}$ (2.3033(8) and 2.3198(8) Å, 171.52(3)°). The distance of 2.9048(2) Å between the gold atoms shows an aurophilic interaction.⁵⁵

Mechanistically the formation of **84** is considered a result of a P–P bond cleavage by nucleophilic attack of a chloride anion. Through chloride mediated cleavage of one P–P bond in **8**, $\text{Cy}_2\text{P}\text{Cl}$ is formed next to anionic tetracyclohexyltriphosphan-1-ide **85⁻** which coordinates to a Au(I) cation followed by a dimerization (Scheme 37).



Scheme 37. Nucleophilic attack of a chloride on **8**.

Interestingly the Au(I) cation in **84** is coordinated *via* the dicyclohexylphosphaneyl moieties of the *in situ* generated tetracyclohexyltriphosphan-1-ide **85**⁻ and not *via* the phosphanide moiety. This is best described by Pearsons' concept.¹¹⁶ With two phosphanide moieties, **84** has two more coordination sites which should allow for further coordination. Reacting *iso*-tetraphosphane **8** with (tth)AuCl in the presence of tetracyclohexyldiphosphane yields tetranuclear gold complex **86** in an excellent yield of 96% (Scheme 38).



Scheme 38. Reaction of **8** with (tth)AuCl and Cy₂P–PCy₂; i) -4 tth, THF, r.t., 96%.

Two equivalents of *iso*-tetraphosphane **8** react with one equivalent of Cy₂P–PCy₂ and four equivalents of (tth)AuCl forming **86** by chloride mediated cleavage of one P–P bond in **8** and the P–P bond in Cy₂P–PCy₂. The ³¹P{¹H} NMR spectrum of **86** shows an AA'XX'X''X'''Z spin system (δ(P_A) = -113.0 ppm, δ(P_X) = 36.4 ppm, δ(P_Z) = 65.1 ppm; coupling constants are reported in chapter 12.6.2.) and is depicted in Figure 40 together with the iteratively fitted resonances.

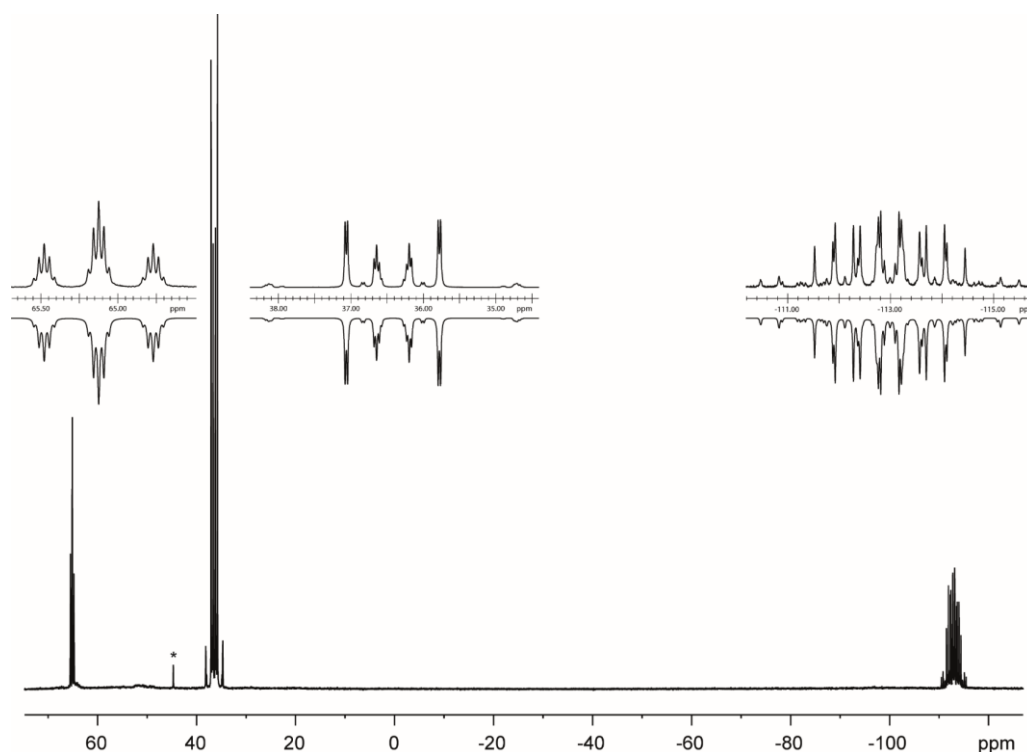


Figure 40. ³¹P{¹H} NMR spectrum of **86** (THF-d₈, 300 K); insets show the AA'XX'X''X'''Z spin system of the experimental (upwards) and fitted spectra (downwards). Trace impurity is marked with an asterisk.

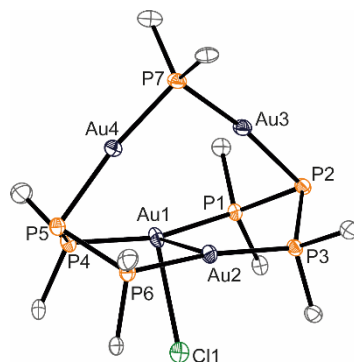


Figure 41. Molecular structure of **86** in $86 \cdot 2$ THF (hydrogen atoms, solvate molecules and anions omitted for clarity, cyclohexyl groups are depicted by their P–C bound carbon atom only, thermal ellipsoids are displayed at 50% probability). Selected bond lengths (Å) and angles (°): P1–P2 2.201(2), P2–P3 2.2011(19), P4–P5 2.206(2), P5–P6 2.200(2), P1–Au1 2.3175(14), P4–Au1 2.3214(14), P3–Au2 2.3073(14), P6–Au2 2.3151(14), P7–Au4 2.3110(14), P7–Au3 2.3085(15), P5–Au4 2.3848(15), P2–Au3 2.3849(14), Au1–Au2 3.0036(3), Au1–Cl1 2.9154(16), Au2–Cl1 3.4512(17), P1–P2–P3 98.36(7), P4–P5–P6 98.41(8), P1–Au1–P4 164.47(5), P3–Au2–P6 171.86(5), P7–Au3–P2 172.35(5), P7–Au4–P5 171.45(5), Cl1–Au1–Au2 71.32(4), Au1–Au2–Cl1 53.15(3), Au1–Cl1–Au2 55.53(3).

Crystals suitable for X-Ray analysis grew from a saturated THF solution by slow vapor diffusion of *n*-pentane at -30 °C as $86 \cdot 2$ THF. The molecular structure is depicted in Figure 41. The P–P bond lengths observed for **86** (2.200(2)–2.206(2) Å) are elongated compared to **84** and well within the range of a typical P–P single bond.¹²⁴ The P–P–P angles (98.36(7) and 98.41(8)°) are comparable to the P–P–P angle observed for triphosane gold complex $[(48 \cdot Au)_2]^{2+}$ (98.29(5)°). While the dicyclohexylphosphaneyl and dicyclohexylphosphanideyl P–Au bond lengths in **86** (2.3073(14)–2.3214(14) Å) are comparable to those observed in **84** and cation $[(48Au)_2]^{2+}$ (*vide supra*), the bis(dicyclohexylphosphaneyl)-phosphanideyl P–Au bond lengths are significantly elongated (P5–Au4: 2.3848(15) and P2–Au3: 2.3849(14) Å). The P–Au–P angles in **86** all differ only slightly from the expected linear geometry around gold (P3–Au2–P6 171.86(5), P7–Au3–P2 172.35(5) and P7–Au4–P5 171.45(5)°), with an exception of the P1–Au1–P4 angle which is more acute (164.47(5)°), due to the additional interaction of the chlorido-substituent with the gold atom (Au1–Cl1 2.9154(16) Å). This bond length is well inside the sum of the van der Waals radii of gold and chlorine (3.41 Å),⁵⁶ yet significantly elongated compared to the two Au–Cl bonds observed for (tht)AuCl (2.274(8) and 2.292(13) Å).¹²⁵ The chloride in **86** is directing to the center of the Au1–Au2 bond (Cl1–Au1–Au2 71.32(4)°). Nevertheless a contact of the chloride with the Au2 atom is to be excluded, as the distance between them (3.4512(17) Å) is exceeding the sum of the van der Waals radii of gold and chlorine (3.41 Å).⁵⁶ Compound **86** is a stable solid when kept under inert gas like Ar or N₂, yet in solution formation of Cy₂PCL is observed. This indicates a further nucleophilic attack of the chloride

in **86** in an intramolecular reaction. As this reaction is taking some time at room temperature, **86** is stirred in toluene for 24 h at 100 °C, yielding an orange-red-colored solution. Figure 42 is showing the $^{31}\text{P}\{^1\text{H}\}$ NMR spectrum of this reaction mixture.

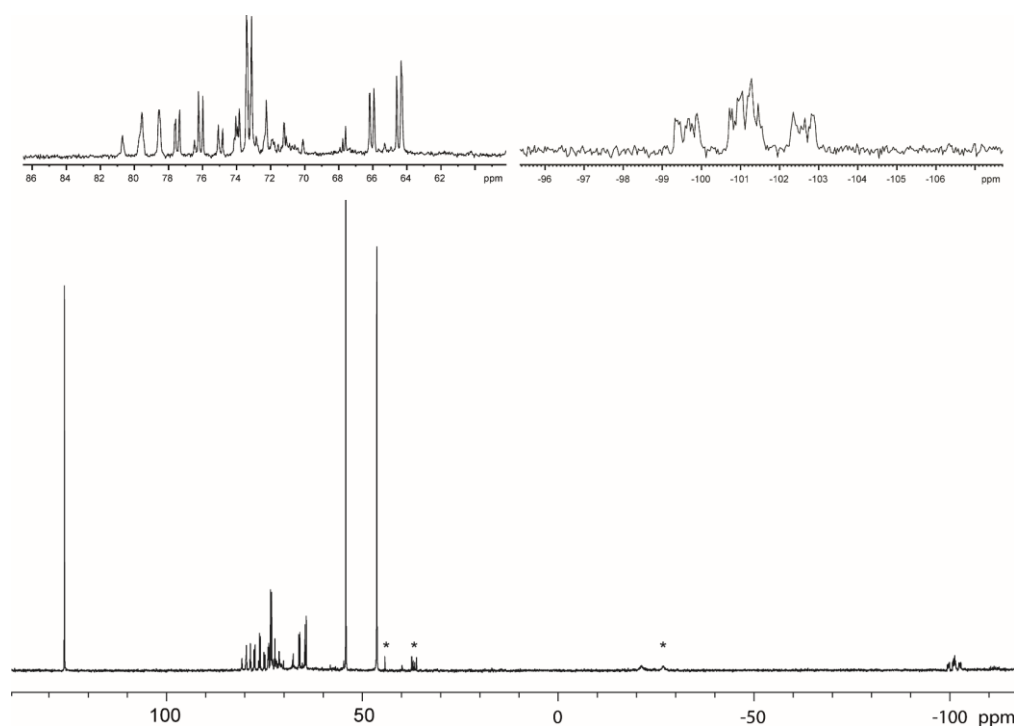
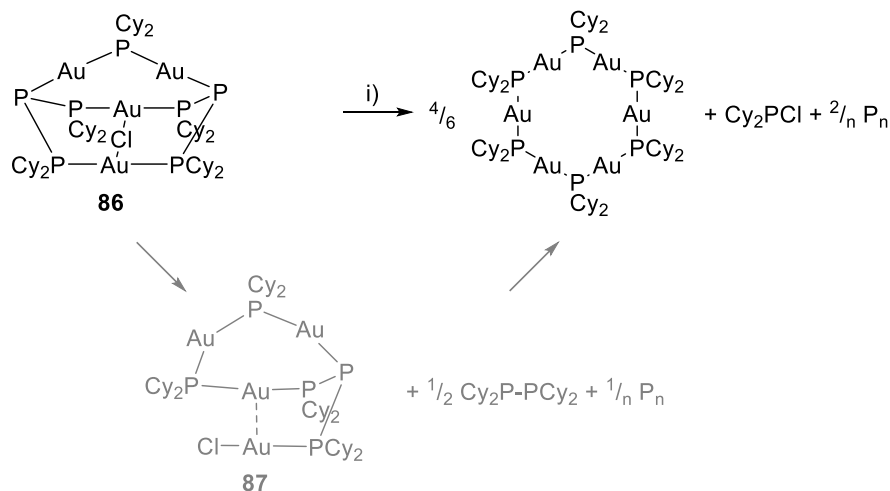


Figure 42. $^{31}\text{P}\{^1\text{H}\}$ NMR spectrum of **86** in toluene stirred at 100 °C for 24 h; asterisks indicate unidentified resonances; insets are showing the resonances of the AUVWXYZ spin system of **87**.

Formation of $\text{Cy}_2\text{P}\text{Cl}$ is observed according to the singlet resonance at $\delta(\text{P}) = 127.8 \text{ ppm}$,¹¹⁹ next to a small, broadened resonance at $\delta(\text{P}) = -21.0 \text{ ppm}$, indicating formation of trace amounts of $\text{Cy}_2\text{P}-\text{PCy}_2$.^{18e} The two singlet resonances at $\delta(\text{P}) = 46.3 \text{ ppm}$ and $\delta(\text{P}) = 54.2 \text{ ppm}$ are assigned to cyclic compounds $(\text{Cy}_2\text{P}-\text{Au})_n$, with $(\text{Cy}_2\text{P}-\text{Au})_6$ being the major product at $\delta(\text{P}) = 54.2 \text{ ppm}$.¹²⁶ These compounds were first reported by Rheingold and co-workers, who synthesized them by treatment of $(\text{Cy}_2\text{PH})\text{AuCl}$ with ammonium hydroxide.¹²⁶ Next to these singlet resonances more complex resonances at $\delta(\text{P}) = -101.1, 64.4, 66.1$ and $70.0-81.0 \text{ ppm}$ are observed, which integrate in a 1 : 1 : 1 : 4 ratio, resembling a AUVWXYZ spin system. These resonances are assigned to compound **87**, which is proposed to be an intermediate in the reaction from **86** to $(\text{Cy}_2\text{P}-\text{Au})_n$, with $(\text{Cy}_2\text{P}-\text{Au})_6$ being the thermodynamically favoured ring size. Initially, **86** forms **87**, $\text{Cy}_2\text{P}-\text{PCy}_2$ and $1/n \text{ P}_n$ of which the constitution of the latter is unknown. Compound **87** and $\text{Cy}_2\text{P}-\text{PCy}_2$ then react further to form $\text{Cy}_2\text{P}\text{Cl}$ and $(\text{Cy}_2\text{P}-\text{Au})_n$ next to another equivalent of $1/n \text{ P}_n$ (Scheme 39). Since the formation of P_4 is not observed by ^{31}P NMR spectroscopy, the formation of amorphous red phosphorus P_n is conceivable and could be the reason of the orange-red-colored reaction

mixture. Compound **87** crystallizes from the reaction mixture upon addition of *n*-hexane *via* slow vapor diffusion at -30 °C in form of clear, colorless blocks that are suitable for X-Ray analysis, next to copious amounts of amorphous material, attributed to (Cy₂P–Au)_n, hampering the isolation of pure **87**. The molecular structure of **87** is depicted in Figure 43.



Scheme 39. Decomposition of **86** *via* formation of **87**; i) PhMe, 100 °C, 24 h.

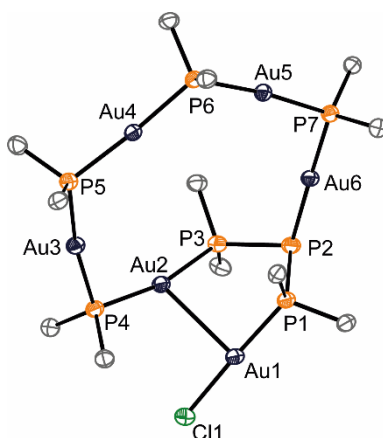


Figure 43. Molecular structure of **87** in $\text{87} \cdot n\text{-C}_6\text{H}_{14}$ (hydrogen atoms and solvate molecules are omitted for clarity, cyclohexyl groups are depicted by their P–C bound carbon atom only, thermal ellipsoids are displayed at 50% probability). Selected bond lengths (Å) and angles (°): Au1–Au2 2.9980(3), Au1–Cl1 2.3080(13), Au1–P1 2.2496(12), Au2–P3 2.3289(12), Au2–P4 2.3167(12), Au3–P4 2.3268(12), Au3–P5 2.3197(12), Au4–P5 2.3241(12), Au4–P6 2.3279(12), Au5–P6 2.3223(11), Au5–P7 2.3220(11), Au6–P7 2.3183(12), Au6–P2 2.3552(12), P2–P3 2.1996(18), P2–P1 2.1967(17), P1–P2–P3 98.62(6), Cl1–Au1–Au2 92.35(3), P1–Au1–Cl1 177.06(5), P3–Au2–P4 166.47(4), P4–Au3–P5 170.91(4), P5–Au4–P6 173.25(4), P6–Au5–P7 174.20(4), P7–Au6–P2 178.16(4), P1–Au1–Au2 89.75(3), P3–Au2–Au1 86.21(3), P4–Au2–Au1 107.25(3), Au2–P4–Au3 103.72(5), Au3–P5–Au4 115.38(5), Au4–P6–Au5 118.31(5), Au5–P7–Au6 105.83(5).

The P–P bond lengths observed for **87** (2.1967(17)–2.1996(18) Å) are comparable to the P–P bond lengths observed for **86** (2.200(2)–2.206(2) Å) as well as the P–P–P angle of **87** (98.62(6)°) is comparable to the P–P–P angles in **86** (98.36(7) and 98.41(8)°). The dicyclohexylphosphaneyl P–Au bond lengths in **87** (2.3167(12)–2.3289(12) Å) are

comparable to those observed in **84**, **86** and $[(48\text{Au})_2]^{2+}$ (*vide supra*), with an exception of the P1–Au1 bond, which is shorter in comparison (2.2496(12) Å), likely due to a trans effect of the Cl1 atom bound to Au1. Moreover, the bis(dicyclohexylphosphaneyl)phosphanideyl P–Au bond length in **87** is elongated (P2–Au6 2.3552(12) Å), which is similarly observed for **86**. The Au1–Cl1 bond in **87** (2.3080(13) Å) is significantly shortened compared to **86** (Au1–Cl1 2.9154(16) Å), and thus comparable to the two Au–Cl bonds in (tht)AuCl (2.274(8) and 2.292(13) Å).¹²⁵ The P–Au–P angles in **87** are in the expected range from 166.47(4)–178.16(4)°. The Cl1–Au1–Au2 in **87** (92.35(3)°) is significantly larger than the one observed in **86** (Cl1–Au1–Au2 71.32(4)°), thus an interaction between Cl1 and Au2 can be excluded.

8. Reactivity studies of Pyridyl-substituted Polyphosphanes towards PdCl₂ and PtCl₂

The coordination chemistry of pyridyl-substituted triphosphane **48** and tetraphosphetane **72** was comprehensively studied with respect to coinage metal salts M(I) (M = Cu, Ag, Au) (*vide supra*). Especially the P–P bond cleavage reactions induced by metal chlorides in combination with the coordination of that metal by the *in situ* formed poly-phosphorus fragment as described in chapter 7 is an intriguing reaction pathway for the formation of a plethora of fascinating metal complexes of polyphosphanes. As there are already interesting reports on the coordination chemistry of polyphosphanes and platinum metals,^{127,128} further investigations focused on the reactivity of pyridyl-substituted polyphosphanes towards palladium(II) and platinum(II) chloride.

The following reactions were performed on a small scale and are unoptimized. They require further experimental work in thought of isolating analytically pure compounds in higher yields. However, some preliminary results are presented in the following.

Reaction of **48** with (PhCN)₂PtCl₂ at ambient temperature in CH₂Cl₂ reveals formation of at least three different compounds as observed ³¹P NMR spectroscopy after 16 h (Figure 44).

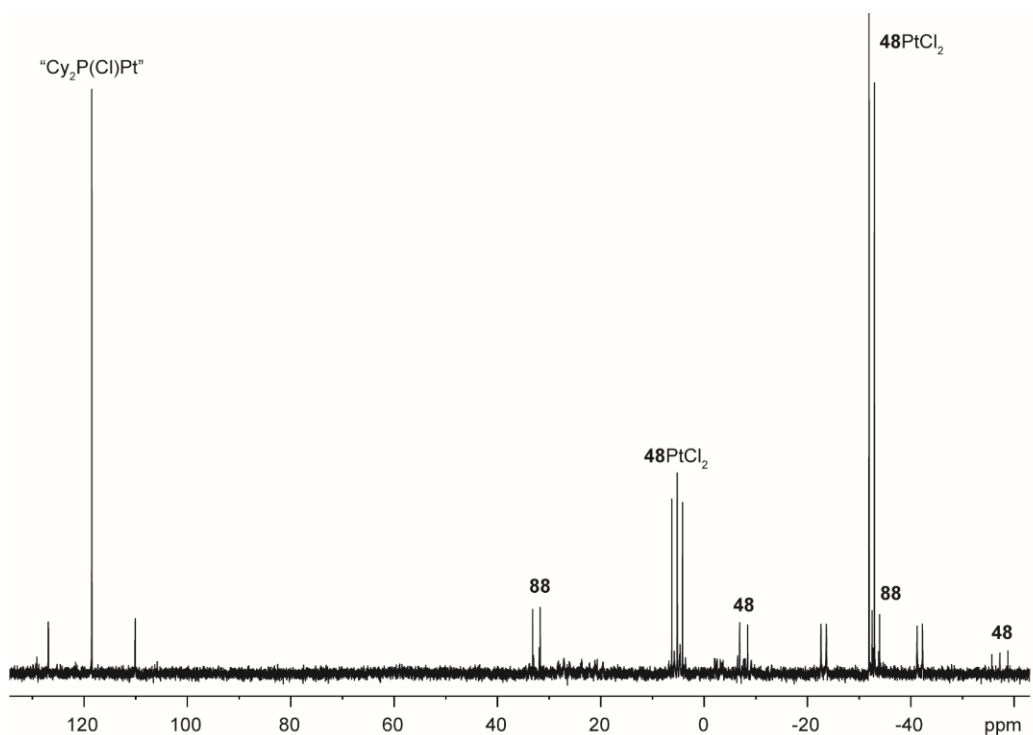
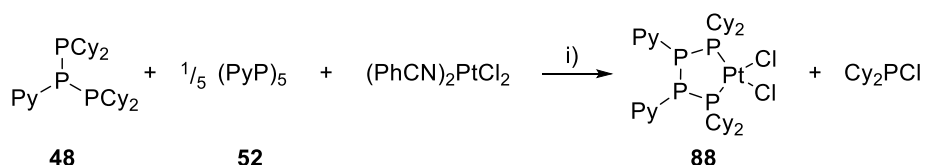


Figure 44. ³¹P{¹H} NMR spectrum of a mixture of **48** and (PhCN)₂PtCl₂ in an equimolar ratio in CH₂Cl₂ after 16 h at ambient temperature.

The A₂M spin system observed ($\delta(P_A) = -32.5$ (2P), $\delta(P_M) = 5.2$ (1P) ppm, $^1J_{AM} = 168$ Hz) indicates formation of the coordination complex **48**PtCl₂. The characteristic ¹⁹⁵Pt satellites of the A-part suggest coordination of Pt(II) by the two dicyclohexylphosphaneyl moieties. This is confirmed by X-Ray analysis of a few crystals of **48**PtCl₂*PhMe, that grew from a concentrated toluene solution of an equimolar mixture of **48** and (PhCN)₂PtCl₂ cooled from ambient temperature to -30 °C. The molecular structure of **48**PtCl₂ is shown in Figure 46. The singlet resonance at $\delta(P) = 118.5$ ppm with a set of ¹⁹⁵Pt satellites indicates formation of Cy₂PtCl, which is coordinating Pt(II).¹²⁹ Moreover an AA'MM' spin system is observed ($\delta(P_A) = -33.2$ (2P), $\delta(P_M) = 32.4$ (2P) ppm). This AA'MM' spin system is attributed to (PyP)₂(Cy₂P)₂PtCl₂ **88**, which is most likely formed *via* a P–P/P–P bond metathesis reaction. To further investigate on this behalf, **48** is reacted with (PhCN)₂PtCl₂ in the presence of **52** in thought of a selective [Py–P] transfer (Scheme 40). This reaction is giving a mixture of **88** and **48**PtCl₂ (see the experimental section for details). In order to increase formation of **88**, the reaction mixture stirred in PhF at 100 °C for 14 h (Scheme 40), giving a dark green solution.



Scheme 40. Reaction towards **88**; i) -2 PhCN, PhF, 100 °C, 14 h; equation is unbalanced.

The ³¹P{¹H} NMR spectrum of this solution is depicted in Figure 45 and only shows the AA'MM' spin system of **88** next to the resonance of Cy₂PtCl ($\delta(P) = 127.8$ ppm).¹¹⁹

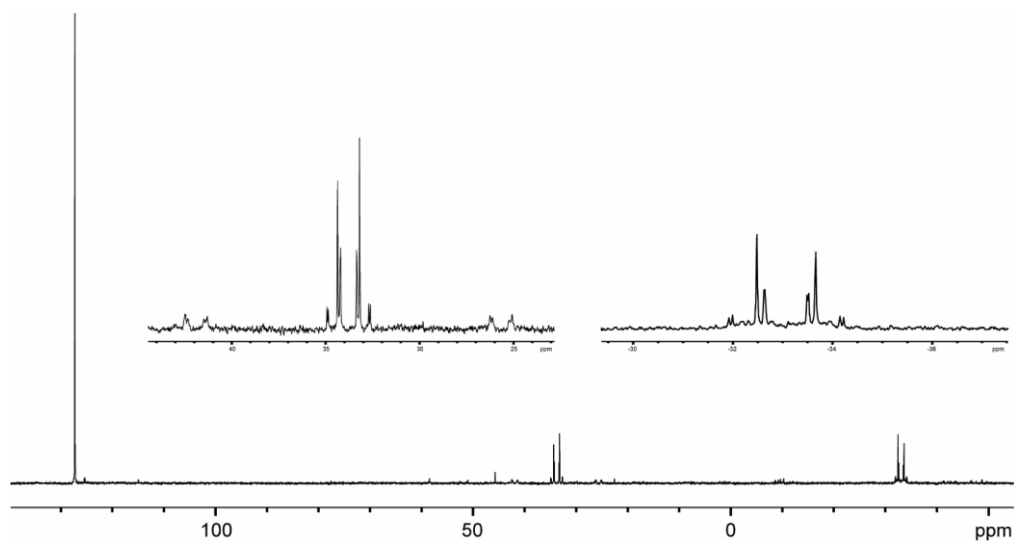


Figure 45. ³¹P{¹H} NMR spectrum of the reaction described in Scheme 47. Insets show the AA'XX' spin system of **88**.

Upon addition of *n*-pentane a voluminous, green precipitate appears, which after collection is recrystallized. Thus, by slow vapor addition of Et₂O to a CH₂Cl₂ solution of the crude product a few crystals of **88**·3 CH₂Cl₂ are obtained as clear, colorless blocks. Figure 46 shows the molecular structure of **88**, as well as that of the aforementioned **48PtCl₂**. Both complexes are square planar coordinated about their central platinum atom, as expected for Pt(II) complexes. In contrast to the coinage metal complexes of pyridyl-substituted polyphosphanes (*vide supra*), the pyridyl nitrogen is not taking part in the coordination of the metal ion. The P–P bond lengths are in the typical range of P–P single bonds for both complexes **48PtCl₂** and **88**. The Pt–Cl bond lengths observed for both complexes (**48PtCl₂**: Pt1–Cl1 2.3701(5), Pt1–Cl2 2.3633(8); **88**: Pt1–Cl1 2.3526(6), Pt1–Cl2 2.3647(6) Å) are only slightly elongated compared to those observed for *cis*-(Ph₃P)₂PtCl₂.¹³⁰

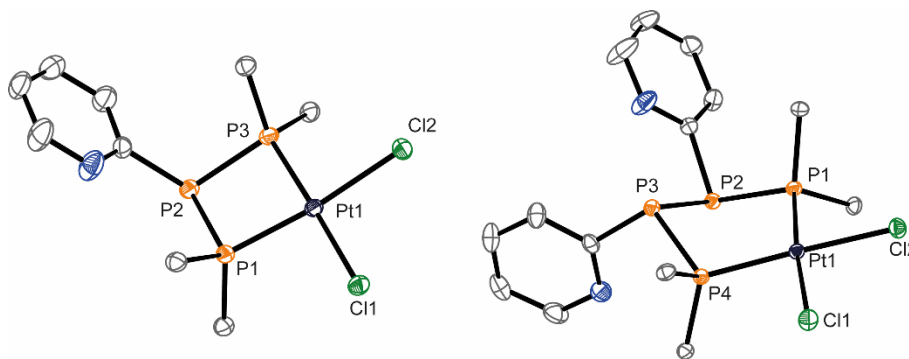
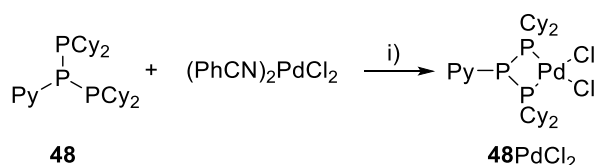


Figure 46. Molecular structure of **48PtCl₂** in **48PtCl₂**·PhMe (left) and **88** in **88**·3 CH₂Cl₂ (right; hydrogen atoms and solvate molecules are omitted for clarity, cyclohexyl groups are depicted by their P–C bound carbon atom only, thermal ellipsoids are displayed at 50% probability). Selected bond lengths (Å) and angles (°) for **48PtCl₂**: Pt1–Cl1 2.3701(5), Pt1–Cl2 2.3633(8), Pt1–P1 2.2409(6), Pt1–P3 2.2236(5), P1–P2 2.2281(8), P2–P3 2.2114(8), P1–P2–P3 81.79(3), P2–P3–Pt1 98.11(3), Pt1–P1–P2 97.11(3), P3–Pt1–P1 81.23(2), P3–Pt1–Cl2 92.18(2), Cl2–Pt1–Cl1 89.37(2), Cl1–Pt1–P1 97.20(2); **88**: Pt1–Cl1 2.3526(6), Pt1–Cl2 2.3647(6), Pt1–P1 2.2410(6), Pt1–P4 2.2439(6), P1–P2 2.2196(8), P2–P3 2.2002(8), P3–P4 2.2180(8), Pt1–P1–P2 110.88(3), P1–P2–P3 96.34(3), P2–P3–P4 96.76(3), P3–P4–Pt1 109.48(3), P4–Pt1–P1 95.56(2), P1–Pt1–Cl2 88.00(2), Cl2–Pt1–Cl1 87.73(2), Cl1–Pt1–P4 88.76(2).

Consequently in both cases the Pt–P bonds (**48PtCl₂**: Pt1–P1 2.2409(6), Pt1–P3 2.2236(5); **88**: Pt1–P1 2.2410(6), Pt1–P4 2.2439(6) Å) are slightly shortened compared to those observed for *cis*-(Ph₃P)₂PtCl₂.¹³⁰ While the dicyclohexylphosphaneyl-phosphorus atoms show an almost ideal tetrahedral geometry in **88**, a certain distortion is observed for the respective atoms in **48PtCl₂**. This is due to the ring contraction in **48PtCl₂**, which is also responsible for the almost 20° more acute P–P–P angle in **48PtCl₂** when compared to **48**.

Further studies were performed with respect to the reactivity of **48** towards (PhCN)₂PdCl₂. ³¹P NMR spectroscopic investigations on a solution containing of an equimolar mixture of **48** and (PhCN)₂PdCl₂ revealed an A₂M spin system (δ(P_A) = -25.8 (2P), δ(P_M) = -12.8 (1P))

ppm, $^1J_{AM} = 179$ Hz) which is assigned to **48**PdCl₂ (Scheme 41). Slow vapor diffusion of *n*-pentane into this reaction mixture gave crystals of **48**PdCl₂·3CH₂Cl₂ confirming the structural connectivity. The molecular structure is depicted in Figure 47.



Scheme 41. Synthesis of **48**PdCl₂; i) -2 PhCN, CH₂Cl₂, r.t..

After three weeks at -30 °C further crystals grew from the same mixture. These were identified to be crystals of **89**·3 CH₂Cl₂·½ *n*-pentane. The molecular structure of **89** is depicted in Figure 47.

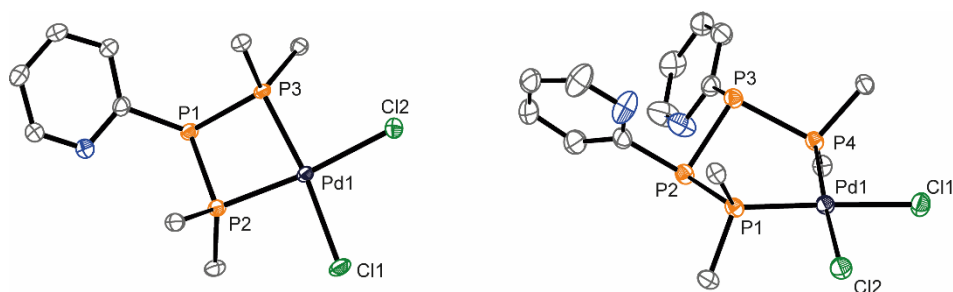


Figure 47. Molecular structure of **48**PdCl₂ in **48**PdCl₂·3 CH₂Cl₂ (left) and **89** in **89**·3 CH₂Cl₂·½ *n*-pentane (right; hydrogen atoms and solvate molecules are omitted for clarity, cyclohexyl groups are depicted by their P–C bound carbon atom only, thermal ellipsoids are displayed at 50% probability). Selected bond lengths (Å) and angles (°) for **48**PdCl₂: Pd1–Cl1 2.3699(8), Pd1–Cl2 2.3578(8), Pd1–P2 2.2459(8), Pd1–P3 2.2332(8), P1–P2 2.2028(11), P1–P3 2.2026(11), P2–P1–P3 82.58(4), P1–P3–Pd1 95.39(4), P1–P2–Pd1 95.03(4), P3–Pd1–P2 80.93(3), P3–Pd1–Cl2 92.51(3), Cl2–Pd1–Cl1 94.50(3), Cl1–Pd1–P2 92.06(3); **89**: Pd1–Cl1 2.3505(10), Pd1–Cl2 2.3631(10), Pd1–P1 2.2566(10), Pd1–P4 2.2614(10), P1–P2 2.2180(14), P2–P3 2.2013(14), P3–P4 2.2191(14), Pd1–P1–P2 110.98(5), P1–P2–P3 96.00(5), P2–P3–P4 96.91(5), P3–P4–Pd1 109.45(5), P4–Pd1–P1 94.96(4), P1–Pd1–Cl2 87.00(3), Cl2–Pd1–Cl1 90.47(4), Cl1–Pd1–P4 87.58(4).

Both complexes **48**PdCl₂ and **89** show the expected square planar geometry of the central palladium atoms and are isostructural compared to their platinum derivatives **48**PtCl₂ and **88**. Bond lengths and angles within the palladacycle of **48**PdCl₂ and **89** are almost the same as in **48**PtCl₂ and **88**, respectively, and therefore not discussed in detail. In thought of a selective synthesis of **89**, the reaction of **48**, (PhCN)₂PdCl₂ and **52** in a 1 : 1 : 1/5 ratio in PhF is investigated. Figure 48 shows the $^{31}\text{P}\{^1\text{H}\}$ NMR spectrum of this reaction mixture after stirring for 16 h at ambient temperature. Formation of **89** is observed by an AA'MM' spin system ($\delta(\text{P}_A) = -23.8$, $\delta(\text{P}_M) = 54.2$). This reaction is repeatedly giving mixtures of **48**PdCl₂ and **89**, even if the reaction time is increased to five days.

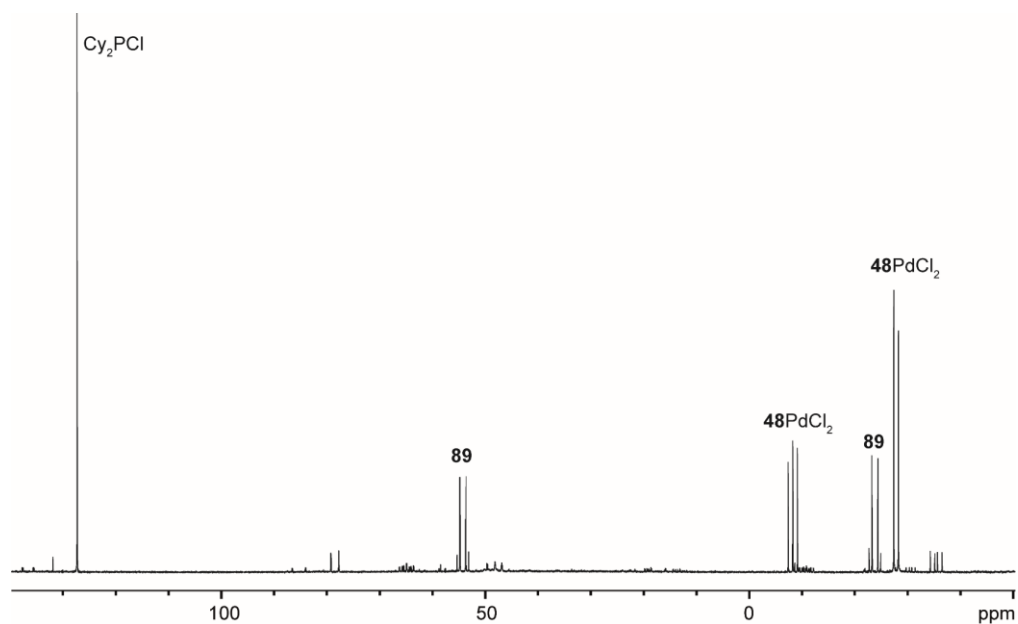
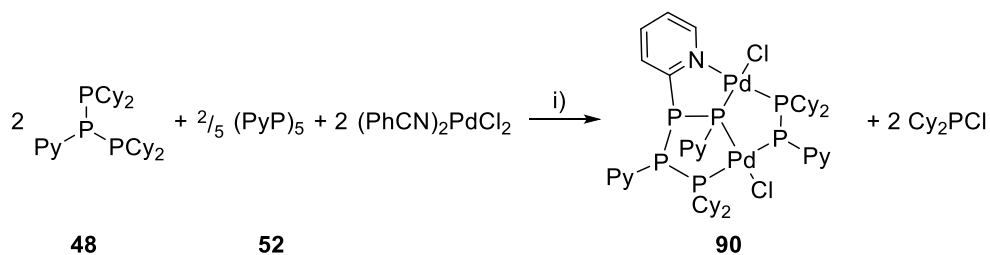


Figure 48. $^{31}\text{P}\{^1\text{H}\}$ NMR spectrum of the reaction of **48**, $(\text{PhCN})_2\text{PdCl}_2$ and **52** in a 1 : 1 : $1/5$ ratio in PhF after 16 h at ambient temperature.

In thought of increasing the amount of **89**, the reaction mixture is stirred for 3 h at 100 °C yielding a deep red-colored solution (Scheme 42).



Scheme 42. Synthesis of **90**; i) -2 PhCN, PhF, 100 °C, 3 h.

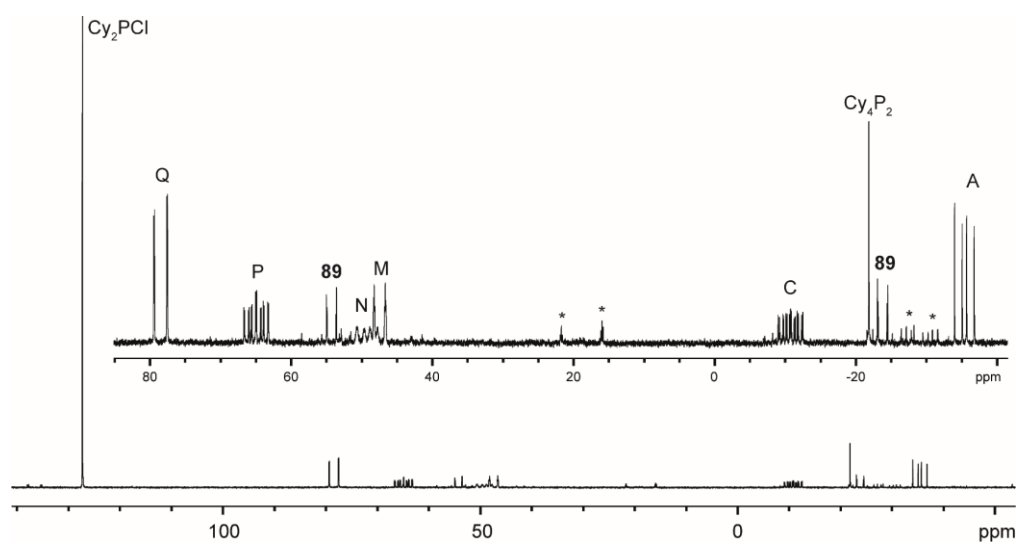


Figure 49. $^{31}\text{P}\{^1\text{H}\}$ NMR spectrum of the reaction described in Scheme 42.

^{31}P NMR spectroscopy of this reaction mixture shows a dominant ACMNPQ spin system ($\delta(\text{P}_A) = -35.4$, $\delta(\text{P}_C) = -10.7$, $\delta(\text{P}_M) = 47.4$, $\delta(\text{P}_N) = 49.3$, $\delta(\text{P}_P) = 64.9$, $\delta(\text{P}_Q) = 78.5$ ppm) which is assigned to compound **90**, next to Cy_4P_2 , $\text{Cy}_2\text{P}(\text{Cl})$ and only small amounts of **89** (Figure 49). In this case formation of $\text{Cy}_2\text{P}(\text{Cl})$ is observed as it is the co-product in the formation of **90**. While the isolation of **90** is hampered due to impurities of **89**, few single crystals of **90** could be obtained from a 1,2- $\text{C}_6\text{H}_4\text{F}_2$ solution upon slow vapor addition of *n*-hexane in form of clear, yellow blocks of $\text{90}^{*3/2} \cdot 1,2\text{-C}_6\text{H}_4\text{F}_2^{*1/2} \cdot n\text{-hexane}$. The molecular structure of **90** is depicted in Figure 50.

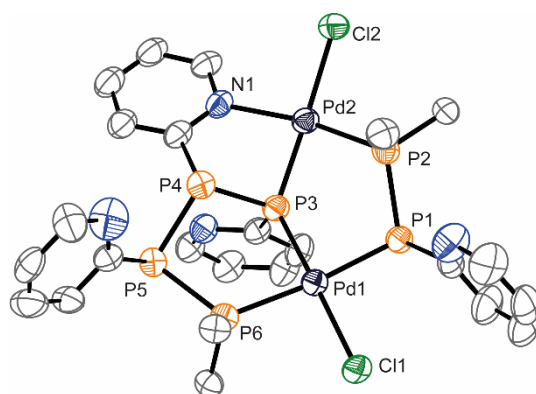
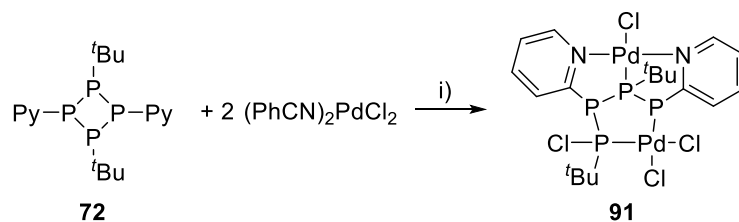


Figure 50. Molecular structure of **90** in $\text{90}^{*3/2} \cdot 1,2\text{-C}_6\text{H}_4\text{F}_2^{*1/2} \cdot n\text{-hexane}$ (hydrogen atoms and solvate molecules are omitted for clarity, cyclohexyl groups are depicted by their P–C bound carbon atom only, thermal ellipsoids are displayed at 50% probability). Selected bond lengths (Å) and angles ($^\circ$): Pd1–Cl1 2.3649(9), Pd1–P1 2.3531(10), Pd1–P3 2.2042(9), Pd1–P6 2.3703(10), Pd2–Cl2 2.3924(9), Pd2–P2 2.2617(10), Pd2–P3 2.2166(10), Pd2–N1 2.172(3), P1–P2 2.2038(14), P3–P4 2.1653(14), P4–P5 2.2049(14), P5–P6 2.2651(14), P1–Pd1–Cl1 93.91(3), Cl1–Pd1–P6 92.08(3), P6–Pd1–P3 89.60(3), P3–Pd1–P1 84.50(3), N1–Pd2–Cl2 93.17(10), Cl2–Pd2–P2 97.06(4), P2–Pd2–P3 86.42(4), P3–Pd2–N1 83.88(10), Pd1–P3–Pd2 131.87(4), Pd1–P3–P4 110.53(5), Pd2–P3–P4 94.03(5).

The molecular structure of **90** shows that the square planar geometry for Pd1 and Pd2 is slightly distorted, with angles of 84.50(3)–93.91(3) $^\circ$ around Pd1 and 83.88(10)–97.06(4) $^\circ$ around Pd2. The Pd–Cl bond lengths are comparable to those observed for **48PdCl₂** and **90** and the Pd–N bond length in **90** (Pd2–N1 2.172(3) Å) is slightly elongated compared to other Pd–N bond lengths reported for pyridyl coordinated Pd(II) compounds.¹³¹ The Pd2–P2 and Pd2–P3 bond lengths (2.2617(10) and 2.2166(10) Å) are comparable to the Pd–P bond lengths in **48PdCl₂** and **89**, as well as the Pd1–P3 bond length (2.2042(9) Å), which is only marginally shortened. Yet the Pd1–P1 and Pd1–P6 bond lengths are significantly elongated (Pd1–P1 2.3531(10), Pd1–P6 2.3703(10) Å).

Dipalladium complex **90** is formed *via* a chloride induced P–P bond cleavage reaction as described in chapter 7, observed by the co-produced $\text{Cy}_2\text{P}(\text{Cl})$. A similar chloride induced P–P bond cleavage is observed by reacting **72** with $(\text{PhCN})_2\text{PdCl}_2$ (Scheme 43). When reacted in an equimolar ratio in CH_2Cl_2 at ambient temperature a red-colored solution is formed.

Upon addition of Et₂O a voluminous precipitate forms, which is isolated and recrystallized from MeCN and Et₂O, yielding a few crystals of **91***MeCN in X-Ray quality. The molecular structure of **91** is depicted in Figure 51.



Scheme 43. Reaction of **72** with (PhCN)₂PdCl₂; i) -2 PhCN, CH₂Cl₂, r.t..

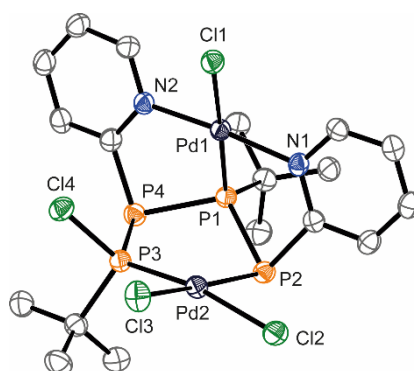


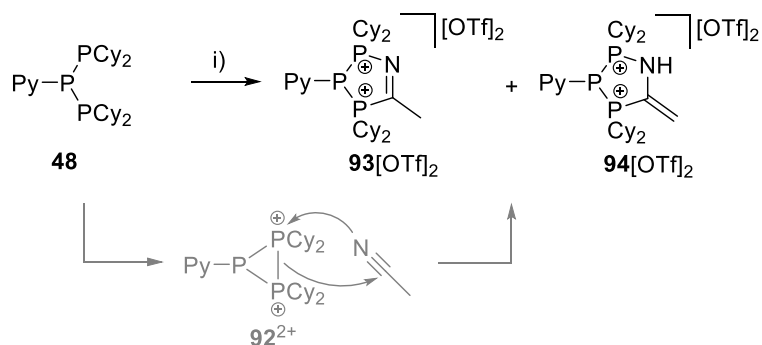
Figure 51. Molecular structure of **91** in **91***MeCN (hydrogen atoms and solvate molecules are omitted for clarity; thermal ellipsoids are displayed at 50% probability). Selected bond lengths (Å) and angles (°): Pd1–Cl1 2.3782(11), Pd1–P1 2.1923(12), Pd1–N1 2.062(4), Pd1–N2 2.062(4), Pd2–Cl2 2.3509(11), Pd2–Cl3 2.3635(13), Pd2–P2 2.2941(12), Pd2–P3 2.2163(11), P1–P2 2.1993(15), P3–P4 2.2507(16), P4–P1 2.1819(16), P1–Pd1–N1 84.57(12), N1–Pd1–Cl1 94.67(12), Cl1–Pd1–N2 93.92(12), N2–Pd1–P1 86.92(12), P2–Pd2–Cl2 83.16(4), Cl2–Pd2–Cl3 91.22(5), Cl3–Pd2–P3 91.61(4), P3–Pd2–P2 95.20(4).

Similarly to the structure of **90**, the Pd atoms in **91** show a slightly disordered square planar geometry with angles of 84.57(12)-94.67(12)° around Pd1 and 83.16(4)-95.20(4)° around Pd2. The two Pd–N bond lengths Pd1–N1 and Pd1–N2 are equidistant (2.062(4) Å) and in a good agreement with those reported for similar Pd(II) complexes.¹³¹

9. Oxidation of **48** and Subsequent Deprotonation Studies

Next to the metathesis, methylation and coordination chemistry presented for **48**, its chemistry towards oxidizing agents promises a rich and fascinating chemistry. First studies were performed by reacting **48** with the strong oxidizing agent $[\text{Ph}_3\text{As}][\text{OTf}]_2$ in MeCN. The results presented are preliminary and need to be finalized.

Addition of $[\text{Ph}_3\text{As}][\text{OTf}]_2$ to a suspension of **48** in MeCN gives a yellow-colored suspension that turns to a red-colored solution within one hour. Addition of Et_2O gives a slightly yellow-colored precipitate of a mixture of imine **93** $[\text{OTf}]_2$ and enamine **94** $[\text{OTf}]_2$. This mixture is isolated in 86% yield (Scheme 44). Mechanistically the one electron oxidation of each of the dicyclohexylphosphaneyl moieties of **48** is anticipated, forming dicationic triphosphiranedium **92** $^{2+}$ intermediary. Dicationic **92** $^{2+}$ is a highly reactive compound, which readily reacts with MeCN, similar to the reported reactivity of a triphosphirane with MeCN in the presence of a Lewis acid (Scheme 44).¹⁰



Scheme 44. Reaction towards **93** $[\text{OTf}]_2$ and **94** $[\text{OTf}]_2$; i) $[\text{Ph}_3\text{As}][\text{OTf}]_2$, $-\text{Ph}_3\text{As}$, MeCN, r.t. 1 h.

Crystals suitable for X-ray crystallography of **93** $[\text{OTf}]_2 \cdot 2 \text{ MeCN}$ grew *via* slow vapor diffusion of Et_2O into a saturated MeCN solution of the mixture of **93** $[\text{OTf}]_2$ and **94** $[\text{OTf}]_2$ at $-30\text{ }^\circ\text{C}$. The molecular structure of **93** $^{2+}$ is depicted in Figure 52. The P–P bond lengths observed in **93** $^{2+}$ (P1–P2 2.2318(5), P1–P3 2.2041(5) Å) are in the typical range of P–P single bonds, as well as the endocyclic P–C bond length (P3–C30 1.8642(14) Å) is in the range of a P–C single bond. Yet the P–N (P2–N2 1.6914(13) Å) lies in between the typical values for a P–N single bond (1.78 Å)⁶⁹ and for a P=N double bond (1.54 Å).⁶⁹ As expected C30 is sp^2 -hybridized indicated by the angles around C30 (N2–C30–P3 119.47(11), N2–C30–C31 122.01(13), C31–C30–P3 118.52(10) $^\circ$) and the C30–C31 bond lengths (1.491(2) Å), being marginally shorter than the ideal sp^3 - sp^2 C–C bond length of 1.50 Å.¹³² The C–N bond length (C30–N2 1.2692(19) Å) is indicating strong double bond character. Thus, the imine tautomer **93** $^{2+}$ crystallizes from the mixture of tautomers.

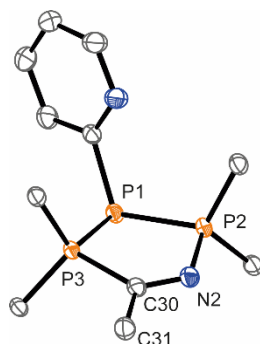
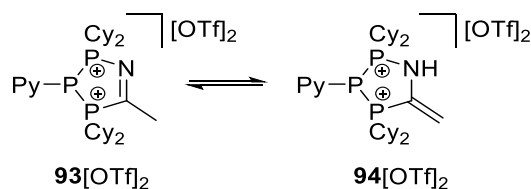


Figure 52. Molecular structure of 93^{2+} in $93[OTf]_2 \cdot 2 \text{ MeCN}$ (hydrogen atoms and solvate molecules are omitted for clarity; thermal ellipsoids are displayed at 50% probability). Selected bond lengths (Å) and angles (°): P1–P2 2.2318(5), P1–P3 2.2041(5), P3–C30 1.8642(14), P2–N2 1.6914(13), C30–N2 1.2692(19), C30–C31 1.491(2), P3–P1–P2 88.817(17), C30–N2–P2 122.55(10), N2–C30–P3 119.47(11), N2–C30–C31 122.01(13), C31–C30–P3 118.52(10).



Scheme 45. Tautomerism of imine $93[OTf]_2$ and enamine $94[OTf]_2$.

However, multi-nuclear NMR spectroscopy reveals tautomerism of 93^{2+} and 94^{2+} , with 93^{2+} being the minor tautomer in CD_3CN solution (Scheme 45). The ^1H NMR spectrum of CD_3CN solution of the product obtained from the reaction described above, majorly shows the enamine form $94[OTf]_2$, as observed by the characteristic methylene protons ($\delta = 5.51$ (1H, dd, $^4J_{\text{HH}} = 11.43$ Hz, $^2J_{\text{HH}} = 4.14$ Hz), 6.17 (1H, dd, $^3J_{\text{HP}} = 34.04$ Hz, $^2J_{\text{HH}} = 4.14$ Hz)) and the nitrogen bound proton ($\delta = 8.53$ (1H, dd, $^2J_{\text{HP}} = 23.36$ Hz, $^4J_{\text{HH}} = 11.43$ Hz)) (Figure 53). The minor imine tautomer $93[OTf]_2$ is observed in the ^1H NMR spectrum by resonances of some of the pyridyl protons, while the resonance of the methyl protons is superimposed by the resonances of the cyclohexyl groups.

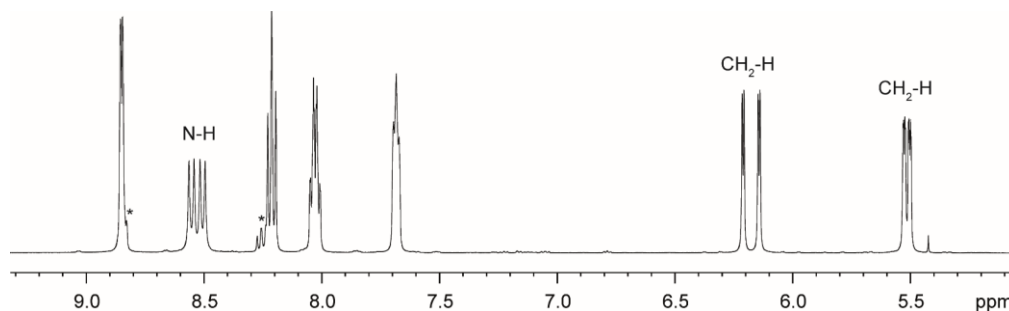


Figure 53. ^1H NMR spectrum of $94[OTf]_2$ (CD_3CN , 300 K), majorly showing the enamine form $94[OTf]_2$. Asterisks are marking resonances assigned to the imine form $93[OTf]_2$.

However, in the ^{31}P NMR spectrum both tautomers are clearly visible by an AXZ spin system each. The dominant AXZ spin system ($\delta(\text{P}_\text{A}) = -84.3$ ppm, $\delta(\text{P}_\text{X}) = 44.1$ ppm, $\delta(\text{P}_\text{Z}) = 77.4$ ppm; $^1J(\text{P}_\text{A}\text{P}_\text{X}) = (^1J(\text{P}_\text{A}\text{P}_\text{Z}) = -295$ Hz, $^2J(\text{P}_\text{X}\text{P}_\text{Z}) = 7$ Hz) is attributed to the enamine form $\mathbf{94}^{2+}$, while the minor AXZ spin system ($\delta(\text{P}_\text{A}) = -95.2$ ppm, $\delta(\text{P}_\text{X}) = 96.2$ ppm, $\delta(\text{P}_\text{Z}) = 119.2$ ppm; $^1J(\text{P}_\text{A}\text{P}_\text{X}) = -350$ Hz, $^1J(\text{P}_\text{A}\text{P}_\text{Z}) = -330$ Hz, $^2J(\text{P}_\text{X}\text{P}_\text{Z}) = 32$ Hz) is attributed to the imine form $\mathbf{93}^{2+}$ (Figure 54).

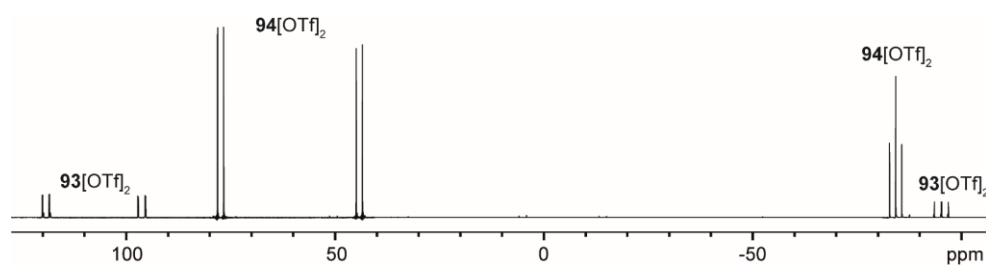
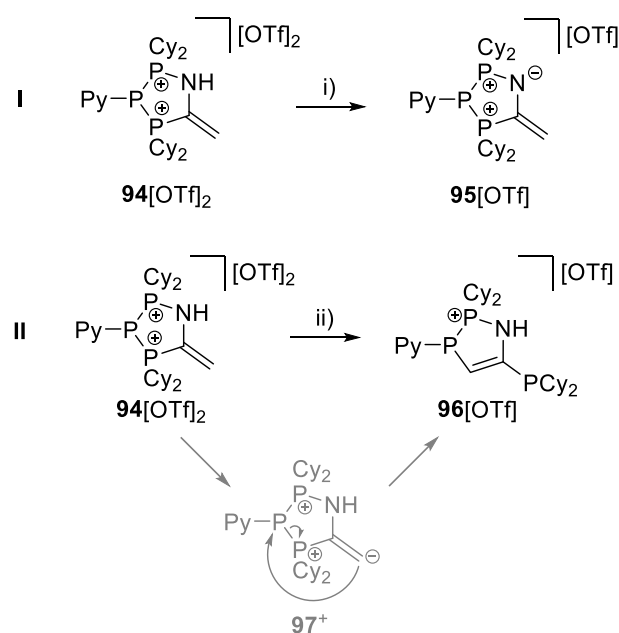


Figure 54. ^{31}P NMR spectrum of $\mathbf{93}[\text{OTf}]_2$ and $\mathbf{94}[\text{OTf}]_2$ (CD_3CN , 300 K).

Of both tautomers especially $\mathbf{94}[\text{OTf}]_2$ should be conveniently deprotonated. Assuming that both tautomers are in a state of equilibrium in solution, a mixture of $\mathbf{93}[\text{OTf}]_2$ and $\mathbf{94}[\text{OTf}]_2$ is reacted with one equivalent of NaO^tBu (Scheme 46; I). The $^{31}\text{P}\{^1\text{H}\}$ NMR spectrum of this reaction mixture shows only one AXY spin system ($\delta(\text{P}_\text{A}) = -84.0$ ppm, $\delta(\text{P}_\text{X}) = 68.9$ ppm, $\delta(\text{P}_\text{Y}) = 72.3$ ppm; $^1J(\text{P}_\text{A}\text{P}_\text{X}) = -306$ Hz, $^1J(\text{P}_\text{A}\text{P}_\text{Y}) = -265$ Hz, $^2J(\text{P}_\text{X}\text{P}_\text{Y}) = 44$ Hz; Figure 55, top). Considering that the nitrogen bound proton of $\mathbf{94}[\text{OTf}]_2$ is most prone to deprotonation, this AXY spin system is assigned to compound $\mathbf{95}[\text{OTf}]$ (Scheme 46; I).



Scheme 46. Deprotonation reactions of tautomeric mixtures of $\mathbf{93}[\text{OTf}]_2$ and $\mathbf{94}[\text{OTf}]_2$, displayed by the major tautomer $\mathbf{94}[\text{OTf}]_2$; i) NaO^tBu , $-\text{Na}[\text{OTf}]$, $-\text{HO}^t\text{Bu}$, CH_2Cl_2 ; ii) NaH , $-\text{Na}[\text{OTf}]$, $-\text{H}_2$, Et_2O .

In another reaction the mixture of tautomers **93**[OTf]₂ and **94**[OTf]₂ was reacted with an equimolar amount of NaH (Scheme 46; **I**). The ³¹P NMR spectrum of this reaction mixture shows an AMX spin system ($\delta(P_A) = -46.2$ ppm, $\delta(P_M) = 8.9$ ppm, $\delta(P_X) = 86.0$ ppm; $^1J(P_AP_X) = -306$ Hz, $^3J(P_AP_M) = 10$ Hz, $^3J(P_MP_Y) = 10$ Hz; Figure 55, bottom), which is attributed to **96**[OTf]. Formation of **96**[OTf] is proposed to proceed *via* deprotonation of the exocyclic methylene carbon atom of **94**[OTf]₂ forming **97**⁺, which undergoes a subsequent rearrangement reaction (Scheme 46; **II**), yielding dicyclophosphaneyl-substituted azadiphospholium triflate salt **96**[OTf].

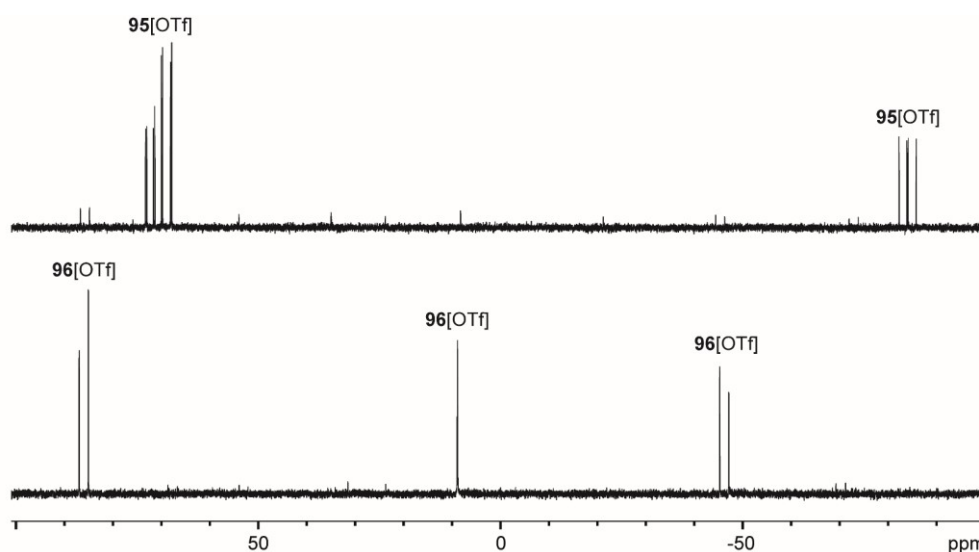


Figure 55. ³¹P{¹H} NMR spectrum of the reaction mixture according to Scheme 46; **I** (top) and according to Scheme 46; **II** (bottom).

Filtration of the reaction mixture described in Scheme 46; **II** and subsequent evaporation of all volatiles *in vacuo* yields a colorless solid, which is recrystallized from PhF *via* slow vapor addition of *n*-pentane at -30 °C yielding X-ray quality crystals of **96**[OTf]*PhF.

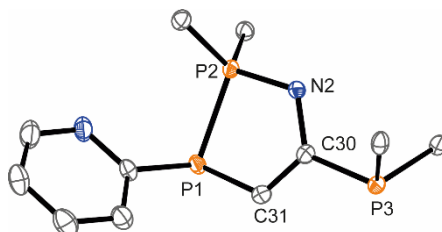


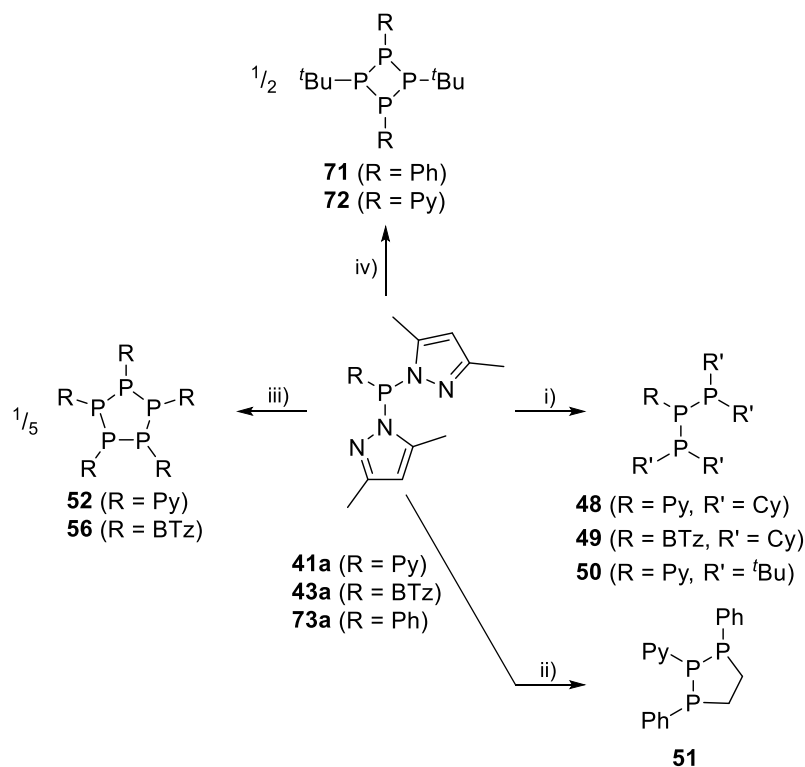
Figure 56. Molecular structure of **96**⁺ in **96**[OTf]*PhF (hydrogen atoms and solvate molecules are omitted for clarity; thermal ellipsoids are displayed at 50% probability). Selected bond lengths (Å) and angles (°): P1–P2 2.2092(8), P1–C31 1.815(3), P2–N2 1.662(2), C30–N2 1.410(3), C30–C31 1.350(4), C31–P1–P2 88.73(9), P1–P2–N2 96.45(8), P2–N2–C30 117.07(8), N2–C30–C31 118.6(2), C30–C31–P1 118.3(2).

The molecular structure of **96**⁺ is depicted in Figure 56 confirming the structural connectivity. The endocyclic P–C bond observed for **96**⁺ (P1–C31 1.815(3) Å) is slightly

shorter than the typical P–C single bond (1.83 Å),¹³³ while the P–N bond (P2–N2 1.662(2) Å) is elongated compared to a typical P=N bond length (P=N 1.54 Å),⁶⁹ but still shorter than a P–N single bond (1.78 Å). Both endocyclic carbon atoms are sp² hybridized as indicated by the C30–C31 bond length of 1.350(4) Å, typical for C=C double bonds.¹³²

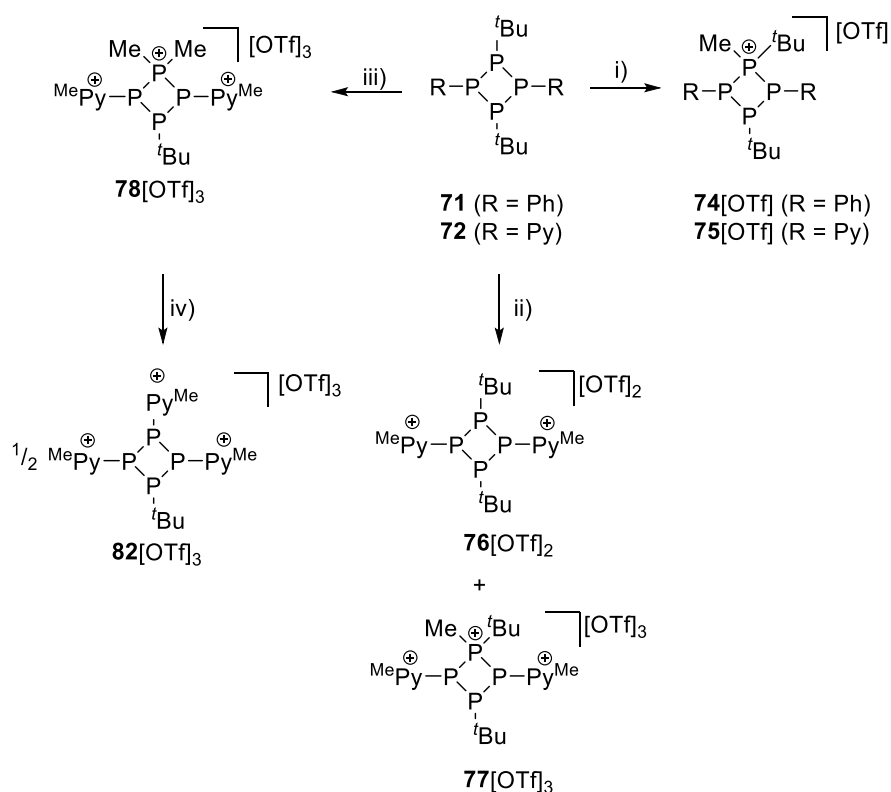
10. Summary

SynPhos type II phosphanes **41a** and **43a** as well as dipyrazolylphosphane **73a** could be established as useful and versatile [R-P] building blocks in polyphosphorus chemistry. Triphosphanes **48-50**, triphospholane **51** and tetraphosphetanes **71** and **72** are conveniently prepared in high yields *via* condensation reactions, next to pentaphospholanes **52** and **56** which are the products of highly selective P-N/P-P bond metathesis reactions (Scheme 47).

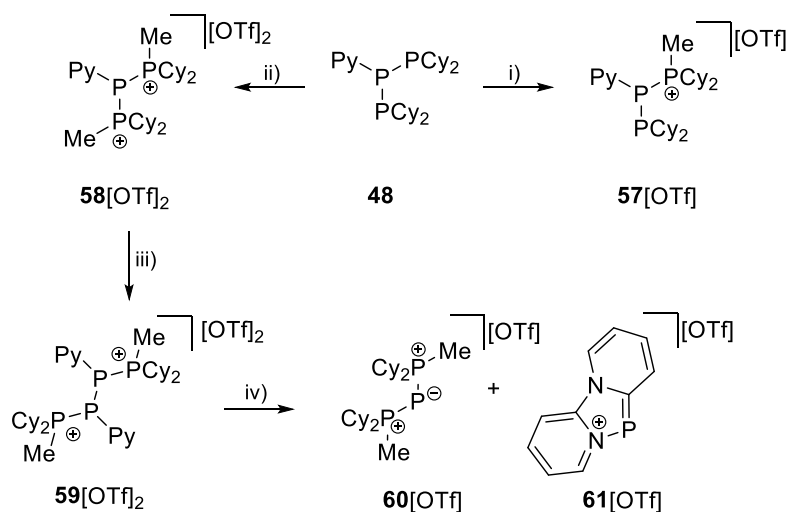


Scheme 47. Dipyrazolylphosphanes in P-P bond formation reactions; i) 2 eq. R'₂PH, -2 **1a**, MeCN, r.t., 96% (**48**), 93% (**49**), 77% (**50**); ii) 1 eq. PhPH(CH₂)₂PPh, -2 **1a**, MeCN, r.t., 69% (**51**); iii) 1 eq. Cy₂PH, -**1a**, -**26**, Et₂O, 98% (**52**), CH₂Cl₂, 72% (**56**); iv) 1 eq. ^tBuPH₂, -2 **1a**, MeCN, -30 °C, 16 h, 69% (**71**), 53% (**72**).

Methylation reactions were performed with a focus on triphosphane **48** and tetraphosphetanes **71** and **72**. Studying the behaviour of the latter two in methylation reactions revealed the fascinating properties introduced by the pyridyl-substituent. While both tetraphosphetanes **71** and **72** are forming **74**[OTf] and **75**[OTf] *via* monomethylation, further methylation is only observed for **72**. Stirring **72** in an excess of MeOTf gives repeatedly mixtures of dicationic **76**[OTf]₂ and tricationic **77**[OTf]₃. By stirring **72** in a twenty-two-fold excess of MeOTf at elevated temperatures **78**[OTf]₃ is feasible *via* elimination of ^tbutene and HOTf. Reacting **78**[OTf]₃ with Me₂P-PMe₂ gives rise to tricationic **82**[OTf]₃ in a series of P-P/P-P bond metathesis reactions (Scheme 48).



Scheme 48. Methylation reactions of tetraphosphetanes **71** and **72** reactions; i) +MeOTf, Et₂O, r.t., 16 h, 87% (**74[OTf]**), 91% (**75[OTf]**); ii) R = Py, 5 eq. MeOTf, neat, r.t., 16h; unbalanced equation **76[OTf]₂** and **77[OTf]₃** are isolated as mixtures; iii) 22 eq. MeOTf, neat, 80 °C, 4 h, ^{*i*}-butene, -HOTf, 91%; iv) +Me₂P-PMe₂, -**81[OTf]**, -^{1/4} **76[OTf]₂**, MeCN, r.t., 4 h, 45%.



Scheme 49. Methylation reactions of **48**; i) MeOTf, Et₂O, r.t., 99%; ii) 5 eq. MeOTf, neat, r.t., 97%; iii) ^{1/5} (PyP)₅, MeCN, r.t., 51%; iv) CD₃CN, 14 d.

Methylation of triphosphane **48** readily gave triphosphanium **57[OTf]** and triphosphanediiium **58[OTf]₂** as triflate salt each in excellent yields. Reacting **58[OTf]₂** with **52** yields tetraphosphanediiium triflate salts **59[OTf]** via P-P/P-P bond metathesis reaction

(Scheme 49). $59[\text{OTf}]_2$ undergoes a rearrangement reaction *via* a [1,2]-Cy₂PMe shift towards triphosphenium triflate salt $60[\text{OTf}]$ and diazaphospholium triflate salt $61[\text{OTf}]$. This interesting rearrangement was studied by ³¹P NMR spectroscopy and theoretical investigations.

The following investigations focused on a more convenient and general synthesis of diazaphospholium salts like $61[\text{OTf}]$. This led to a Me₃SiOTf mediated self-condensation reaction of dichlorophosphanes **40**, **42**, **65** and **66** to P, N-doped polycyclic aromatic hydrocarbons **61-64**[OTf] in good to excellent yields (Chart 6).

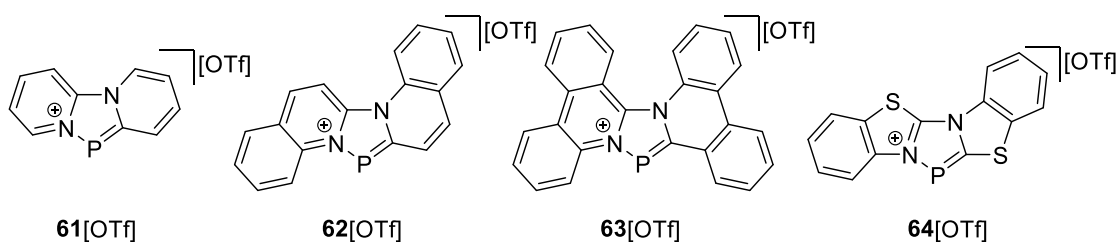
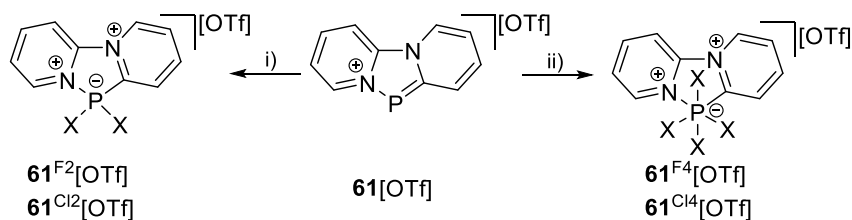
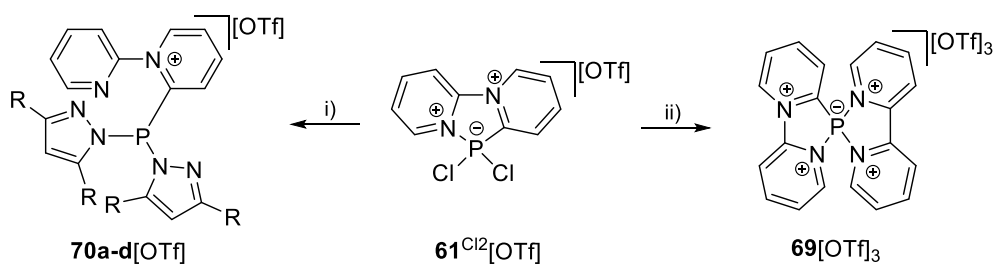


Chart 6. P,N-doped polycyclic aromatic hydrocarbons **61-64**[OTf].

Mechanistic insights into the formation of $61[\text{OTf}]$ are derived from quantum mechanical calculations. Further reactivity studies included halogenation of $61[\text{OTf}]$ with XeF₂ or SO₂Cl₂ yielding cationic dihalophosphoranes $61^{\text{X}2}[\text{OTf}]$ and cationic tetrahalophosphate salts $61^{\text{X}4}[\text{OTf}]$ (Scheme 50). $61^{\text{Cl}2}[\text{OTf}]$ is accessible on a multi-gram scale and was therefore investigated in substitution reactions. Reacting $61^{\text{Cl}2}[\text{OTf}]$ with **5a-d** yields dipyrazolylyphosphanes **70a-d**[OTf], bearing the interesting, cationic 1,2'-bipyridiniumyl substituent, while the reaction of $61^{\text{Cl}2}[\text{OTf}]$ with 2,2'-bipyridine in the presence of Me₃SiOTf yields the mixed 2,2'-bipy/1,2'-bipyl complex **69**[OTf]₃ quantitatively (Scheme 51).

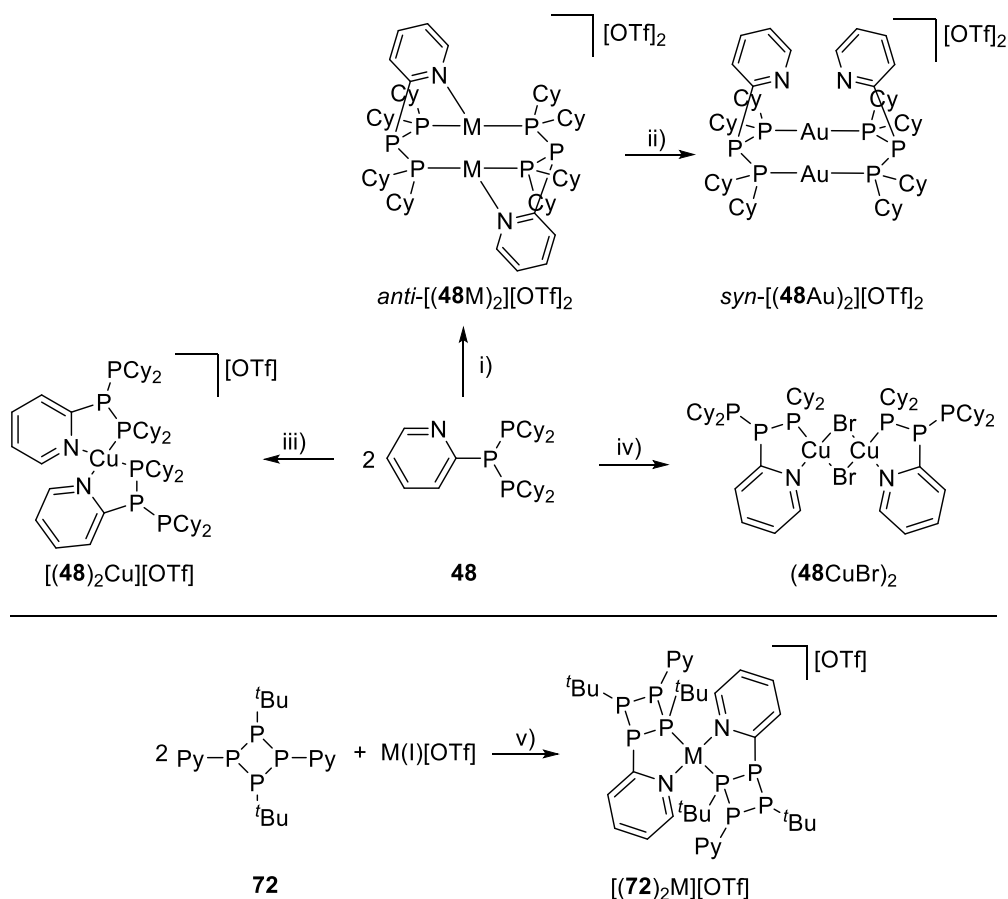


Scheme 50. Halogenation reactions $61[\text{OTf}]$ with one eq. (left) and two eq. (right) XeF₂ or SO₂Cl₂; i) for X = F: XeF₂, -Xe, MeCN, -40 °C to r.t., not isolated; for X = Cl: SO₂Cl₂, -SO₂, MeCN, -40 °C to r.t., 74% ii) for X = F: 2 XeF₂, -2 Xe, MeCN, -40 °C to r.t., quant; for X = Cl: 2 SO₂Cl₂, -2 SO₂, MeCN, -40 °C to r.t., quant.



Scheme 51. Substitution reactions of **61**^{Cl₂}[OTf]; i) 2 eq. **5a-d**, -2 Me₃SiCl, Et₂O, r.t., 91-98%; ii) +2,2'-bipy, +2 Me₃SiOTf, -2 Me₃SiCl, CH₂Cl₂, r.t., 99%.

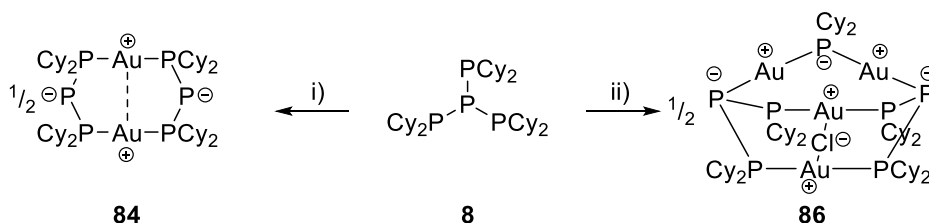
Aside methylation reactions, triphosphane **48** and tetraphosphetane **72** were studied with respect to their coordination chemistry towards coinage metal salts. This led to a small library of coordination complexes with pyridyl-substituted polyphosphanes as ligands (Scheme 52).



Scheme 52. Synthesis of coinage metal coordination complexes starting from triphosphane **48** (top); i) 2 eq. Ag[OTf], PhF (M = Ag), 99%; 2 eq. [(MeCN)₄Cu][OTf], -8 MeCN, CH₂Cl₂ (M = Cu), 94%; ii) 2 eq. (tht)AuCl, -2 tht, -2 AgCl, MeCN, 64%; iii) 1 eq. [(MeCN)₄Cu][OTf], -4 MeCN, CH₂Cl₂, 93%; iv) 2 eq. (tht)CuBr, -2 tht, THF, 93%; Reaction of **72** with selected coinage metal triflate salts “M(I)[OTf]” (bottom); v) CH₂Cl₂, r.t., 1 h; M = Cu, M[OTf] = [Cu(MeCN)₄][OTf], -4 MeCN, 89%; M = Ag, M[OTf] = Ag[OTf], 76%; M = Au, M[OTf] = (tht)AuCl + Me₃SiOTf, -Me₃SiCl, -tht, 74%.

All coinage metal complexes depicted in Scheme 52 were isolated in good to excellent yields and are fully characterized by X-ray analysis and multi-nuclear NMR spectroscopy at various temperatures.

While investigating the coordination chemistry of polyphosphanes on coinage metal salts, complexes **84** and **86** were isolated in excellent yields *via* an unprecedented chloride mediated P–P bond cleavage reaction starting from *iso*-tetraphosphane **8** and (tht)AuCl (Scheme 53).

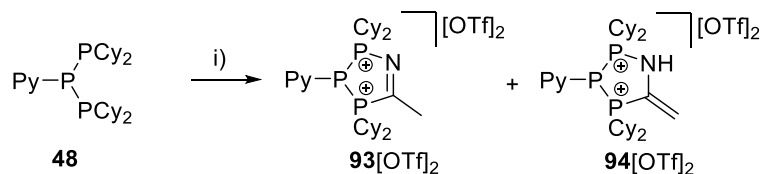


Scheme 53. Synthesis of gold complexes **84** and **86**; i) +(tht)AuCl, –tht, –Cy₂PCL, THF, r.t., 89%; ii) +4 (tht)AuCl, + Cy₂P–PCy₂, –4 tht, –3 Cy₂PCL, THF, r.t., 96%.

Both coordination complexes **84** and **86** are formed quantitatively within minutes at ambient temperature.

Moreover, preliminary studies showed the intriguing chemistry of pyridyl-substituted polyphosphanes towards PdCl₂ and PtCl₂. Besides chloride mediated P–P bond cleavage reactions also P–P/P–P bond metathesis reactions are observed in the formation of Pd(II) and Pt(II) complexes of polyphosphanes.

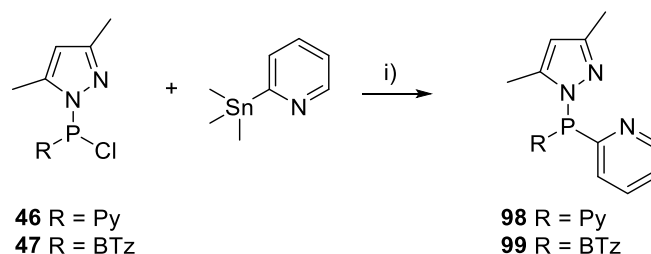
Further initial studies on triphosphane **48** stated its promising chemistry in oxidation reactions as shown by the reaction of **48** with [Ph₃As][OTf]₂ in MeCN giving a mixture of tautomers **93**[OTf]₂ and **94**[OTf]₂ (Scheme 54).



Scheme 54. Reaction towards **93**[OTf]₂ and **94**[OTf]₂; i) [Ph₃As][OTf]₂, –Ph₃As, MeCN, r.t. 1 h.

11. Prospect

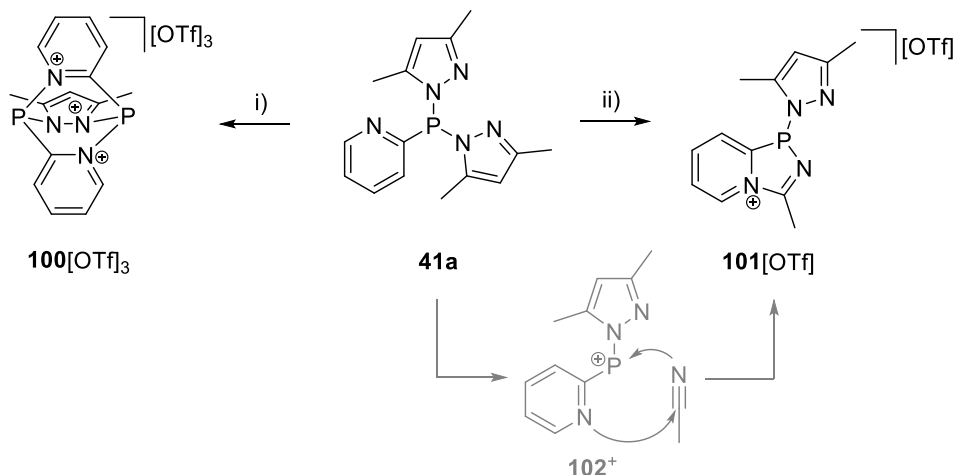
The application of *SynPhos* type II phosphanes as [R–P] building blocks in P–P bond formation reactions towards triphosphanes, tetraphosphetanes and phospholanes is demonstrated in chapters 4 and 6 of this thesis. Following this work the synthesis of the still unknown *SynPhos* type III phosphanes is highly desirable, as these are promising [R₂P] building blocks. As the reaction of dichlorophosphane like **40** and 2-pyridyl-magnesiumhalides might yield a mixture of *SynPhos* type III and type IV phosphanes a more selective synthesis is desirable. Starting from pyrazolylphosphane **46** or **47** and selectively addressing the chloro-substituent in a substitution reaction is a promising way towards *SynPhos* type III phosphanes like **98** or **99** (Scheme 55).



Scheme 55. Possible reaction towards **98** and **99**; i) –Me₃SnCl.

As lithium organyls and Grignard reagents are known to react not only with the chloro- but also with the pyrazolyl-substituent a milder pyridyl source like 2-(trimethylstannyl)-pyridine might be used. This way *SynPhos* type III phosphanes bearing different carbon bound heterocycles might be accessible.

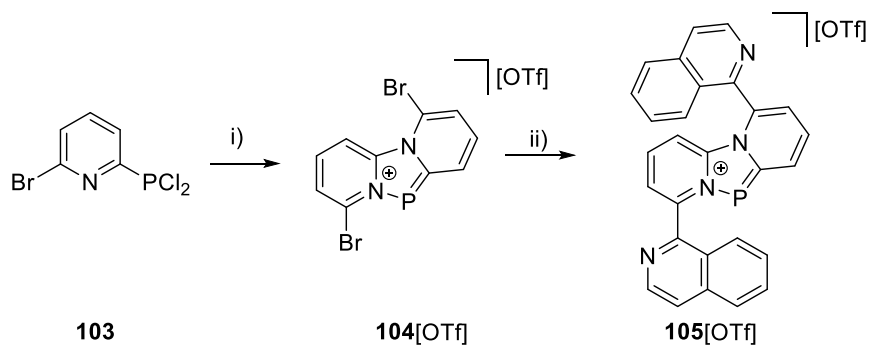
Moreover the protonation of *SynPhos* type II phosphanes might offer a promising chemistry.



Scheme 56. Possible protonation reactions from **41a**; i) ²/₃ HOTf, ⁻²/₃ **1a**; ii) HOTf, MeCN, **-1a**.

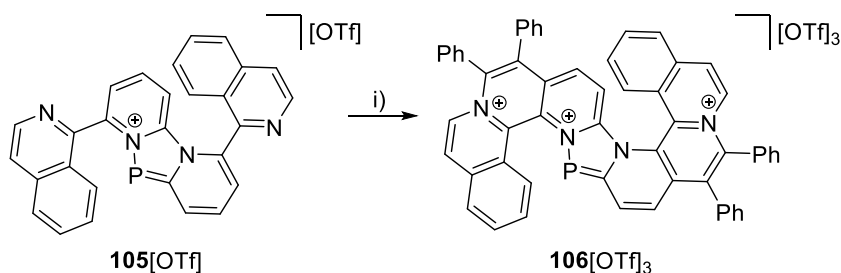
Reacting two equivalents of **41a** with three equivalent HOTf in an aprotic solvent such as PhF or CH₂Cl₂ might give diphosphorus trication **100**[OTf]₃ and three equivalents pyrazole **1a** (Scheme 56). On the other hand, protonation of **41a** in MeCN might yield diazaphospholium salt **101**[OTf] *via* formation of phosphonium cation **102**⁺ which is reacting with MeCN in a 1,3-dipolar cycloaddition reaction. Formation of pyrazolyl-substituted diazaphospholium salts like **102**[OTf] is of special interest with the diazaphospholium cations described in chapter 5.

The self condensation towards P, N-doped PAHs presented in chapter 5 itself also allows for further modification. Reacting dichlorophosphanes like **103** in this self condensation reaction opens up new possibilities to functionalized diazaphospholium triflate salts like **104**[OTf] (Scheme 57).



Scheme 57. Reaction towards functionalized diazaphospholium triflate salt and possible follow up reactions; i) Me₃SiOTf, -Me₃SiCl, -PCl₃; ii) 1-(trialkylstannyl)-isoquinoline, Stille-coupling.

Such a functionalized diazaphospholium salt **104**[OTf] could then be reacted, e.g. in a Stille coupling reaction to **105**[OTf]. Starting from **105**[OTf] multiply charged P, N-doped helical nanographenes like **106**[OTf]₃ might be accessible *via* Rhodium catalyzed annulation reactions (Scheme 58).



Scheme 58. Conceivable Rh-catalyzed annulation towards P, N-doped helical nanographenes; i) diphenylethyne, [Cp*RhCl₂]₂, AgOTf.

These fundamental new derivatives combine the chemistry of π -extended PAHs and other intriguing carbon-based systems such as helicenes with new synthetic strategies in

phosphorus chemistry to allow the introduction of heteroatoms such as phosphorus and nitrogen. The results expected will therefore have a scientific impact on several areas (helicenes, P, N-doped π -extended PAHs, emissive π -conjugated systems, asymmetric catalysis, *et cetera*). Strongly improved performances in luminescence and CPL activity are expectable due to the presence of the heteroatoms in addition to possible donor sites for metal coordination. Thus, also a conception of chiral optoelectronic devices based on the resulting systems would be possible, which results in a high added value. In addition, the development of efficient methods in asymmetric catalysis using new, chiral complexes based on P, N-doped π -extended PAHs ligands will not only be an important proof of concept but will also be a breakthrough in applied chemistry ultimately give impetus maybe for conception of new chiral multifunctional devices.

12. Experimental Details

12.1. Materials and Methods

12.1.1. General Remarks

All manipulations were performed in a Glovebox MB Unilab or using Schlenk techniques under an atmosphere of purified argon or nitrogen. Dry, oxygen-free solvents were distilled either from molecular sieves 3 Å (MeNO₂), from CaH₂ (CH₂Cl₂, MeCN, C₆H₅F, *o*-C₆H₄Cl₂), from potassium/benzophenone (Et₂O, THF, C₆H₆, PhMe) or from potassium (*n*-pentane, *n*-hexane). Deuterated benzene (C₆D₆) was purchased from Sigma-Aldrich and distilled from potassium/benzophenone. Anhydrous CD₃CN, CD₃NO₂, CDCl₃ and CD₂Cl₂ were purchased from Sigma-Aldrich. With the exception of MeNO₂ and CD₃NO₂ all distilled and deuterated solvents were stored over molecular sieves (4 Å: CH₂Cl₂, C₆H₅F, *o*-C₆H₄Cl₂, THF, *n*-hexane, *n*-pentane, Et₂O, C₆D₆, CD₂Cl₂; 3 Å: CD₃CN, MeCN). All glassware was oven-dried at 160 °C prior to use. Quinoline, 2-(dimethylamino)ethanol and 2-Bromopyridine were purchased from TCI and distilled under inert conditions prior to use. 2,2'-bipyridine was purchased from TCI and sublimated prior to use. PCl₃, Et₃SiH, and SO₂Cl₂ were purchased from Sigma Aldrich and distilled under inert conditions prior to use. MeOTf and Me₃SiOTf were purchased from Manchester Organics and distilled under inert conditions prior to use. Me₃SiCl (purified by redistillation, 99%), *n*-butyl lithium (2.5 M in hexanes), Ag[OTf] and [Cu(MeCN)₄][OTf] were purchased by Sigma Aldrich and used as received. Di-*tert*-butylphosphine was purchased from Cytec Solvay Group and used as received. Dicyclohexylphosphine was purchased from Strem Chemicals and used as received. 2-Isocyano-1,1'-biphenyl,¹³⁴ 2-(Trimethylsilyl)benzo[*d*]thiazol,¹³⁵ 1,2-Bis(phenylphosphanyl)ethane,¹³⁶ *tert*-butylphosphane,¹³⁷ tetramethyldiphosphane,¹³⁸ (tht)AuCl,¹²⁵ P(PCy₂)₃^{21b} were prepared as described in the literature. NMR spectra were measured on a Bruker AVANCE III HD Nanobay 400 MHz UltraShield (¹H: 400.13 MHz, ¹³C: 100.61 MHz, ³¹P: 161.98 MHz, ¹⁹F: 376.50 MHz, ⁷⁷Se: 76.31 Hz), or on a Bruker AVANCE III HDX, 500 MHz Ascend (¹H: 500.13 MHz, ¹³C: 125.75 MHz, ³¹P: 202.45 MHz, ¹⁹F: 470.59 MHz). Reported numbers assigning atoms in the ¹³C spectra were indirectly deduced from the cross-peaks in 2D correlation experiments (HMBC, HSQC). Chemical shifts are referenced to δ(Me₄Si) = 0.00 ppm (¹H, ¹³C, externally), δ(CFCl₃) = 0.00 ppm (externally) and δ(H₃PO₄, 85%) = 0.00 ppm (externally). Unless stated otherwise, all NMR spectra were measured at 300 K. Chemical shifts (δ) are reported in ppm. Coupling constants (*J*) are

reported in Hz. The designation of the spin systems is performed by convention. The furthest downfield resonance is denoted by the latest letter in the alphabet and the furthest upfield by the earliest letter. Melting points were recorded on an electrothermal melting point apparatus (Büchi Switzerland, Melting point M-560) in sealed capillaries under Nitrogen atmosphere and are uncorrected. Infrared (IR) and Raman spectra were recorded at ambient temperature using a Bruker Vertex 70 instrument equipped with a RAM II module (Nd: YAG laser, 1064 nm). The Raman intensities are reported in percent relative to the most intense peak and are given in parenthesis. An ATR unit (diamond) was used for recording IR spectra. The intensities are reported relative to the most intense peak and are given in parenthesis using the following abbreviations: vw = very weak, w = weak, m = medium, s = strong, vs = very strong. Elemental analyses were performed on a Vario MICRO cube Elemental Analyzer by Elementar Analysatorsysteme GmbH in CHNS modus.

12.1.2. X-ray Diffraction Refinements

Suitable single crystals were coated with Paratone-N oil or Fomblin Y25 PFPE oil, mounted using either a glass fiber or a nylon loop and frozen in the cold nitrogen stream. Crystals were measured at low temperature on several diffractometers. Crystal and data collection details are given in Tables 10-32, including information about the used diffractometer. Data reduction and absorption correction was performed either with CrysAlisPro¹³⁹ software or Bruker SMART¹⁴⁰ or Bruker SADABS¹⁴¹. Using Olex2,¹⁴² the structures were solved with SHELXS/T¹⁴³ by direct methods and refined with SHELXL¹⁴⁴ by least-square minimization against F^2 using first isotropic and later anisotropic thermal parameters for all non-hydrogen atoms. Hydrogen atoms bonded to carbon atoms were added to the structure models on calculated positions using the riding model. All other hydrogen atoms were localized in the difference Fourier map. Images of the structures were produced with Olex2¹⁴² software. Crystals of compounds **61**^{Cl2}[OTf], **63**[OTf] and **70b**[OTf]·Et₂O were integrated and refined as twins with component ratios of 60:40, 63:37 and 52:48, respectively.

12.1.3. Details on the computational methods for quantum chemical calculations

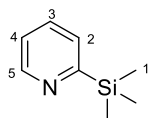
Concerning chapter 4. The geometry optimization has been performed at the BP86-D3/def2-TZVP level of theory without symmetry constrains by means of the Turbomole version 7.0 program.¹⁴⁵ The minimum nature or transition state condition of the compounds has been checked by using frequency analysis. Solvent effects have been taken into consideration by using Conductor-like Screening Model (COSMO).¹⁴⁶

Concerning chapter 5. The geometries and energies of all systems included in this study were fully optimized at the BP86-D3/def2-TZVP level of theory. The calculations have been performed by using the program TURBOMOLE version 7.0.¹⁴⁵ For the calculations the BP86 functional with the latest available correction for dispersion (D3) was used.¹⁴⁷ The NICS (Nucleus Independent Chemical Shift) calculations¹⁴⁸ were computed at the B3LYP/6-311+G* level of theory using the Gaussian 09¹⁴⁹ calculation package. In order to reproduce solvent effects, we have used the conductor-like screening model COSMO,¹⁴⁶ which is a variant of the dielectric continuum solvation models.¹⁵⁰ We have used dichlorobenzene as solvent. The molecular electrostatic potential surface has been calculated using the Spartan'10, v. 1.10 software at the B3LYP/6-311+G* level of theory.

12.2. Syntheses and Characterization Data regarding Compounds in Chapter 3

The syntheses and characterization data of **40** and dipyrazolyolphosphanes **41a-f** are mentioned in addition and completion to the syntheses and characterization data presented in my master's thesis.⁴¹

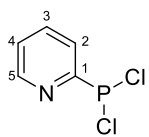
12.2.1. Preparation of 2-(Trimethylsilylpyridine)



A solution of 2-Bromopyridine (24.4 ml, 250 mmol) in THF (300 ml) is cooled to -78 °C. A solution of *n*-butyllithium in hexanes (100 ml, 250 mmol) is added dropwise and the reaction mixture is stirred for 15 min at -78 °C to form a dark red suspension. To this suspension Trimethylsilylchloride (31.8 ml, 250 mmol) is added dropwise and the reaction mixture is allowed to rise to room temperature. After evaporating all volatile compounds, the crude product is distilled (T = 75 °C; p = 30 mbar) from the residue to obtain the product as a clear, colorless oil. The spectral data are in accordance with the ones reported in the literature.¹⁵¹

Yield: 22.4 g (59 %); **¹H NMR (CD₃CN, 300 K, in ppm):** δ = 0.39 (9H, s, C1-H), 7.05-7.10 (1H, m, C4-H), 7.47-7.48 (1H, m, C2-H), 7.48-7.49 (1H, m, C3-H), 8.77-8.78 (1H, m, C5-H). **²⁹Si{¹H} NMR (CD₃CN, 300 K, in ppm):** δ = -5.8 (1Si, s).

12.2.2. Preparation of **40**

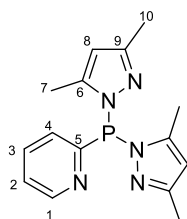


2-(Trimethylsilyl)pyridine (22.4 g, 148 mmol) and PCl₃ (38.8 ml, 444 mmol) are placed in a Schlenk flask and heated under reflux for 48 h. After evaporation of all volatiles the crude product is distilled (T = 48 °C, p = 1.1 x

10^{-2} mbar) to afford the product as a clear, colorless oil that turns yellow upon standing at room temperature within 20-30 minutes. Hence, 2-(dichlorophosphaneyl)pyridine (**40**) is stored at -30 °C under an inert atmosphere.

Yield: 21.5 g (81 %); **Raman (100 mW, 298 K, in cm^{-1}):** $\nu = 3128$ (12), 3064 (58), 3052 (61), 2988 (9), 2972 (8), 2899 (10), 1572 (36), 1564 (38), 1447 (7), 1276 (11), 1243 (6), 1154 (21), 1126 (12), 1086 (8), 1044 (78), 989 (100), 723 (18), 617 (15), 503 (61), 462 (27), 420 (9), 285 (31), 243 (15), 188 (31), 149 (38); **IR (ATR, 298 K, in cm^{-1}):** $\nu = 2361$ (vw), 1572 (vw), 1446 (vw), 1424 (vw), 1202 (vs), 1147 (vs), 1044 (vw), 988 (vw), 850 (vw), 764 (vw), 739 (vw), 722 (vw), 638 (m), 626 (m), 554 (m), 498 (vs), 422 (vw); **^1H NMR (CD_2Cl_2 , 300 K, in ppm):** $\delta = 7.42$ -7.45 (1H, m, C4-H), 7.88-7.93 (1H, m, C3-H), 8.10-8.12 (1H, m, C2-H), 8.73-8.74 (1H, m, C5-H); **$^{13}\text{C}\{^1\text{H}\}$ NMR (CD_2Cl_2 , 300 K, in ppm):** $\delta = 126.1$ (1C, d, $^2J_{\text{CP}} = 15.0$ Hz, C2), 126.3 (1C, d, $^4J_{\text{CP}} = 1.2$ Hz, C4), 138.78 (1C, s, C3), 150.24 (1C, d, $^3J_{\text{CP}} = 18.4$ Hz, C5), 163.44 (1C, d, $^1J_{\text{CP}} = 31.7$ Hz, C1); **^{31}P NMR (CD_2Cl_2 , 300 K, in ppm):** $\delta = 138.7$ (1P, s).

12.2.3. Preparation of **41a**

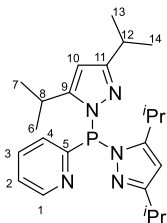


To dichlorophosphane **40** (4.4 g, 24.4 mmol) **5a** (8.4 g, 50.1 mmol) is added while cooling with an ice bath. The suspension is stirred for 16 h at room temperature. After evaporation of all volatiles *in vacuo* the product is obtained as an off-white solid.

Yield: 7.08 g (97 %); **m.p.:** 109 °C; **Raman (100 mW, 298 K, in cm^{-1}):** $\nu = 3132$ (18), 3101(22), 3071(26), 3054(29), 3039(37), 2988(31), 2921(100), 2860(16), 2729(8), 1572(62), 1464(33), 1439(43), 1380(17), 1274(9), 1158(19), 1139(24), 1088(11), 1046(43), 1020(26), 991(86), 960(9), 741(10), 721(18), 635(11), 618(16), 588(58), 558(10), 477(17), 463(15), 399(16), 374(14), 358(9), 305(10), 237(24), 220(17), 196(25), 156(25), 125(54); **IR (ATR, 298 K, in cm^{-1}):** $\nu = 3134$ (vw), 3038(vw), 2920(vw), 1564(m), 1446(w), 1425(w), 1406(w), 1366(vw), 1323(vw), 1309(w), 1291(m), 1155(w), 1131(m), 1087(vw), 1079(vw), 1043(vw), 1021(w), 990(w), 960(w), 895(vw), 847(vw), 806(m), 776(w), 761(w), 747(m), 720(vw), 659(vw), 633(vw), 617(vw), 600(vw), 588(w), 556(m), 491(s), 473(s), 446(m); **^1H NMR (CD_3Cl , 300 K, in ppm):** $\delta = 2.20$ (6H, s, C10-H), 2.41 (6H, s, C7-H), 5.89 (2H, s, C8-H), 7.20-7.23 (1H, m, C2-H), 7.40-7.42 (1H, m, C4-H), 7.63-7.68 (1H, m, C3-H), 8.68-8.70 (1H, m, C1-H); **$^{13}\text{C}\{^1\text{H}\}$ NMR (CD_3Cl , 300 K, in ppm):** $\delta = 12.5$ (2C, d, $^3J_{\text{CP}} = 13.8$ Hz, C7), 13.9 (2C, s, C10), 108.6 (2C, s, C8), 132.2 (1C, s, C2), 127.5 (1C, d, $^2J_{\text{CP}} = 16.9$ Hz, C4), 135.9 (1C, s, C3), 148.4 (2C, d, $^2J_{\text{CP}} = 17.2$ Hz, C6), 150.0 (1C, d, $^3J_{\text{CP}} = 14.4$ Hz, C1), 153.7 (2C, d, $^3J_{\text{CP}} = 5.8$ Hz, C9), 159.6 (1C, d, $^1J_{\text{CP}} = 23.1$

Hz, C5); ^{31}P NMR (CD_3Cl , 300 K, ppm): $\delta = 44.8$ (1P, s); **elemental analysis**: calcd. for $\text{C}_{15}\text{H}_{18}\text{N}_5\text{P}$: C: 60.19, H: 6.06, N: 23.40; found: C: 60.13, H: 6.34, N 22.91.

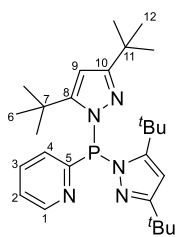
12.2.4. Preparation of **41b**



To dichlorophosphane **40** (0.500 g, 2.78 mmol) **5b** (1.31 g, 5.83 mmol) is added. The reaction mixture is stirred for 16 h at room temperature. After evaporation of all volatiles *in vacuo* a colorless oil is obtained. This oil is dissolved in *n*-hexane (2 ml) and cooled to -30°C . After 16 h colorless crystals grow which are isolated and washed with chilled *n*-hexane to afford the product after evaporation of all volatiles *in vacuo*.

Yield: 730 mg (64 %); **m.p.**: 54°C ; **Raman (100 mW, 298 K, in cm^{-1})**: $\nu = 3132(16)$, 3097(9), 3067(25), 3049(30), 2967(100), 2938(51), 2911(73), 2884(81), 2865(70), 2755(7), 2712(10), 1574(39), 1560(27), 1477(31), 1464(31), 1447(43), 1424(24), 1383(9), 1346(12), 1303(24), 1280(13), 1237(6), 1154(12), 1131(18), 1107(24), 1049(36), 1035(12), 990(60), 960(15), 922(9), 878(39), 724(13), 706(9), 686(9), 619(12), 585(10), 541(6), 519(7), 474(12), 424(6), 397(7), 250(18), 218(13), 182(16), 140(28); **IR (ATR, 298 K, in cm^{-1})**: $\nu = 3086(\text{vw})$, 3043(vw), 2964(w), 2927(vw), 2887(vw), 2865(vw), 1573(w), 1556(w), 1468(w), 1447(w), 1422(w), 1381(w), 1362(w), 1345(w), 1300(w), 1269(w), 1246(w), 1180(vw), 1162(vw), 1143(w), 1127(m), 1104(w), 1065(w), 1049(w), 1031(w), 983(m), 960(vw), 921(vw), 876(vw), 798(m), 771(w), 742(w), 724(w), 705(w), 683(vw); **^1H NMR (CD_2Cl_2 , 300 K, in ppm)**: $\delta = 1.12$ (6H, d, $^3J_{\text{HH}} = 6.9$ Hz, C7–H), 1.23 (12H, d, $^3J_{\text{HH}} = 6.9$ Hz, C13/C14–H), 1.24 (6H, d, $^3J_{\text{HH}} = 6.9$ Hz, C6–H), 2.94 (2H, sept., $^3J_{\text{HH}} = 6.9$ Hz, C12–H), 3.52 (2H, sept.d, $^3J_{\text{HH}} = 6.8$ Hz, $^4J_{\text{HP}} = 3.4$ Hz, C8–H), 6.05 (2H, s, C10–H), 7.24–7.28 (1H, m, C2–H), 7.36–7.38 (1H, m, C4–H), 7.66–7.71 (1H, m, C3–H), 8.67–8.69 (1H, m, C1–H); **$^{13}\text{C}\{^1\text{H}\}$ NMR (CD_2Cl_2 , 300 K, in ppm)**: $\delta = 22.8$ (2C, s, C13/C14), 23.0 (2C, s, C13/C14), 23.4 (2C, s, C7), 24.6 (2C, d, $^4J_{\text{CP}} = 2.3$ Hz, C6), 27.0 (2C, d, $^3J_{\text{CP}} = 12.1$ Hz, C8), 28.8 (2C, s, C12), 102.1 (2C, d, $^4J_{\text{CP}} = 0.5$ Hz, C10), 132.9 (1C, d, $^4J_{\text{CP}} = 1.9$ Hz, C2), 127.9 (1C, d, $^2J_{\text{CP}} = 16.2$ Hz, C4), 136.3 (1C, s, C3), 150.4 (1C, d, $^3J_{\text{CP}} = 14.9$ Hz, C1), 160.6 (2C, d, $^2J_{\text{CP}} = 13.8$ Hz, C9), 160.9 (1C, d, $^1J_{\text{CP}} = 20.1$ Hz, C5), 164.0 (2C, d, $^3J_{\text{CP}} = 6.4$ Hz, C11); **^{31}P NMR (CD_2Cl_2 , 300 K, ppm)**: $\delta = 45.9$ (1P, s); **elemental analysis**: calcd. for $\text{C}_{23}\text{H}_{34}\text{N}_5\text{P}$: C: 67.13, H: 8.33, N: 17.02; found: C: 66.82, H: 8.49, N 16.67.

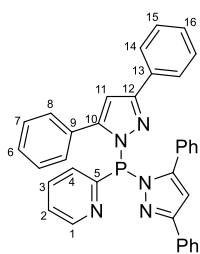
12.2.5. Preparation of 41c



To dichlorophosphane **40** (0.500 g, 2.78 mmol) **5c** (1.47 g, 5.83 mmol) is added. The suspension is stirred for 16 h at room temperature, filtered and the residue is washed with Et₂O (3 x 2 ml). After evaporation of all volatiles *in vacuo* the product is obtained as a colorless solid.

Yield: 870 mg (67 %); **m.p.:** 171 °C; **Raman (100 mW, 298 K, in cm⁻¹):** $\nu = 3128(16), 3071(18), 3050(34), 2967(100), 2928(68), 2904(85), 2859(34), 2775(8), 2713(15), 1577(29), 1562(19), 1535(10), 1486(21), 1465(34), 1446(45), 1420(27), 1392(15), 1364(10), 1307(10), 1291(11), 1276(16), 1251(11), 1227(14), 1204(41), 1154(14), 1135(18), 1089(14), 1048(38), 1029(12), 991(49), 931(29), 840(14), 824(51), 725(19), 618(15), 566(37), 522(12), 506(16), 416(12), 373(15), 260(29), 223(26), 204(19), 168(29), 139(30)$; **IR (ATR, 298 K, in cm⁻¹):** $\nu = 2966(s), 2955(vs), 2927(s), 2902(s), 2868(s), 1576(s), 1559(s), 1535(s), 1476(s), 1453(s), 1423(s), 1393(s), 1361(s), 1307(s), 1291(s), 1275(s), 1250(s), 1225(s), 1203(s), 1193(s), 1125(vs), 1108(vs), 1087(s), 1048(s), 1019(s), 984(vs), 932(s), 800(vs), 764(vs), 739(s), 723(s), 693(s), 655(s), 617(s)$; **¹H NMR (CD₂Cl₂, 300 K, in ppm):** $\delta = 11.14 (18H, s, C12-H), 1.39 (18H, s, C6-H), 5.99 (2H, d, ^4J_{PH} = 1.9 \text{ Hz}, C9-H), 7.20-7.23 (2H, m, C2/C4-H), 7.59-7.64 (1H, m, C3-H), 8.60-8.62 (1H, m, C1-H)$; **¹³C{¹H} NMR (CD₂Cl₂, 300 K, in ppm):** $\delta = 30.5 (6C, s, C12), 31.5 (6C, d, ^4J_{CP} = 8.6 \text{ Hz}, C6), 32.6 (2C, s, C11), 32.8 (2C, bs, C7), 103.1 (2C, s, C9), 123.8 (1C, s, C2), 129.5 (1C, d, ^3J_{CP} = 8.8 \text{ Hz}, C1), 135.4 (1C, s, C3), 149.1 (1C, d, ^2J_{CP} = 20.9 \text{ Hz}, C4), 160.5 (2C, d, ^2J_{CP} = 14.0 \text{ Hz}, C8), 163.1 (1C, d, ^1J_{CP} = 22.2 \text{ Hz}, C5), 164.0 (2C, d, ^3J_{CP} = 0.8 \text{ Hz}, C10)$; **³¹P NMR (CD₂Cl₂, 300 K, ppm):** $\delta = 63.9 (1P, s)$; **elemental analysis:** calcd. for C₂₇H₄₂N₅P: C: 69.35, H: 9.05, N: 14.98; found: C: 69.18, H: 8.88, N 14.69.

12.2.6. Preparation of 41d

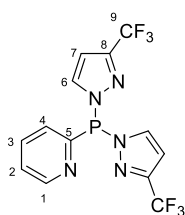


To dichlorophosphane **40** (0.500 g, 2.78 mmol) in CH₂Cl₂ **5d** (1.71 g, 5.83 mmol) is added. After stirring for 16 h at room temperature all volatiles are evaporated *in vacuo*. The residue is recrystallized from CH₂Cl₂/*n*-hexane and washed with *n*-hexane. After evaporating all volatiles *in vacuo* the product is obtained as a colorless solid.

Yield: 1.39 g (91 %); **m.p.:** 191 °C; **Raman (100 mW, 298 K, in cm⁻¹):** $\nu = 3129(3), 3064(24), 1605(100), 1576(9), 1551(15), 1512(38), 1448(13), 1430(44), 1400(13), 1223(5), 1179(5), 1158(8), 1126(3), 1051(6), 1029(8), 1001(47), 980(12), 951(22), 846(4), 770(3), 714(4), 668(4), 619(5), 536(5), 405(4), 286(4), 250(8), 236(7), 211(7), 186(7), 150(13)$; **IR**

(ATR, 298 K, in cm^{-1}): $\nu = 3057(\text{vw}), 3042(\text{vw}), 1574(\text{vw}), 1550(\text{w}), 1483(\text{w}), 1455(\text{w}), 1446(\text{w}), 1423(\text{w}), 1399(\text{w}), 1334(\text{vw}), 1318(\text{w}), 1294(\text{vw}), 1269(\text{w}), 1221(\text{vw}), 1141(\text{w}), 1123(\text{m}), 1071(\text{w}), 1054(\text{w}), 1026(\text{w}), 1001(\text{vw}), 978(\text{w}), 950(\text{w}), 916(\text{w}), 820(\text{w}), 808(\text{w}), 759(\text{s}), 740(\text{w}), 714(\text{w}), 698(\text{m}), 688(\text{m}), 669(\text{w}), 619(\text{vw});$ **^1H NMR (CD_2Cl_2 , 300 K, in ppm):** $\delta = 6.78$ (2H, d, $^4J_{\text{PH}} = 2.2$ Hz, C11–H), 7.29–7.46 (17H, m, C2/C6/C7/C8/C15/C16–H), 7.76–7.81 (1H, m, C3–H), 7.86–7.88 (4H, m, C14–H), 8.07–8.09 (1H, m, C4–H), 8.70–8.71 (1H, m, C1–H); **$^{13}\text{C}\{^1\text{H}\}$ NMR (CD_2Cl_2 , 300 K, in ppm):** $\delta = 106.4$ (2C, d, $^3J_{\text{CP}} = 1.4$ Hz, C11), 124.6, (1C, s, C2), 126.8 (4C, s, C14), 128.8 (4C, s, C15), 128.9 (2C, s, C16), 129.2 (4C, s, C7), 129.4 (2C, s, C6), 129.5 (1C, d, $^2J_{\text{CP}} = 13.7$ Hz, C4), 130.3 (4C, d, $^4J_{\text{CP}} = 4.8$ Hz, C8), 130.8 (2C, d, $^3J_{\text{CP}} = 3.6$ Hz, C9), 133.6 (2C, d, $^4J_{\text{CP}} = 0.7$ Hz, C13), 136.4 (1C, s, C3), 150.2 (1C, d, $^3J_{\text{CP}} = 18.8$ Hz, C1), 154.4 (2C, d, $^2J_{\text{CP}} = 22.6$ Hz, C10), 156.4 (2C, d, $^3J_{\text{CP}} = 1.4$ Hz, C12), 160.1 (1C, d, $^1J_{\text{CP}} = 22.7$ Hz, C5); **^{31}P NMR (CD_2Cl_2 , 300 K, ppm):** $\delta = 52.3$ (1P, s); **elemental analysis:** calcd. for $\text{C}_{35}\text{H}_{26}\text{N}_5\text{P}$: C: 76.77, H: 4.79, N: 12.79; found: C: 76.20, H: 4.80, N: 12.56.

12.2.7. Preparation of 41e

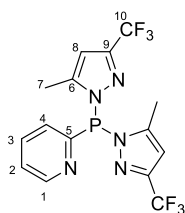


To dichlorophosphane **40** (0.500 g, 2.78 mmol) **5e** (1.22 g, 5.83 mmol) is added. The suspension is stirred for 16 h at room temperature. After evaporation of all volatiles *in vacuo* a colorless oil is obtained. This oil is dissolved in *n*-hexane (2 ml) and cooled to -30 °C. After 16 h colorless crystals grow which are isolated and washed with chilled *n*-hexane to afford the product after evaporation of all volatiles *in vacuo*.

Yield: 747 mg (71 %); **m.p.:** 51 °C; **Raman (100 mW, 298 K, in cm^{-1}):** $\nu = 3159(29), 3142(20), 3118(24), 3078(22), 3060(49), 3043(53), 3016(8), 2992(12), 2976(8), 2862(12), 1575(61), 1536(22), 1474(33), 1455(10), 1429(10), 1391(59), 1341(16), 1286(12), 1245(8), 1233(8), 1159(27), 1137(29), 1092(12), 1046(63), 990(92), 972(100), 956(24), 744(47), 720(24), 618(29), 544(14), 523(10), 501(12), 437(10), 421(10), 400(16), 353(20), 306(29), 273(20), 251(39), 239(20), 208(24), 196(22), 139(84);$ **IR (ATR, 298 K, in cm^{-1}):** $\nu = 3160(\text{vw}), 3141(\text{vw}), 3117(\text{vw}), 3042(\text{vw}), 1574(\text{w}), 1563(\text{vw}), 1536(\text{vw}), 1471(\text{w}), 1454(\text{vw}), 1428(\text{w}), 1390(\text{m}), 1339(\text{w}), 1286(\text{vw}), 1231(\text{m}), 1179(\text{w}), 1161(\text{s}), 1135(\text{vs}), 1114(\text{vs}), 1041(\text{s}), 988(\text{w}), 970(\text{m}), 957(\text{s}), 872(\text{w}), 768(\text{s}), 741(\text{s}), 724(\text{w}), 639(\text{w}), 623(\text{w});$ **^1H NMR (CD_2Cl_2 , 300 K, in ppm):** $\delta = 6.72$ (2H, d, $^3J_{\text{HH}} = 2.6$ Hz, C7–H), 7.30–7.32 (1H, m, C4–H), 7.40–7.43 (1H, m, C2–H), 7.78–7.83 (1H, m, C3–H), 8.11–8.12 (1H, m, C6–H), 8.73–8.75 (1H, m, C1–H); **$^{13}\text{C}\{^1\text{H}\}$ NMR (CD_2Cl_2 , 300 K, in ppm):** 107.4 (2C, *pseudo*-

quint., C7), 121.5 (2C, q, $^1J_{CF} = 269.4$ Hz, C9), 125.8 (1C, bs, C2), 127.9 (1C, d, $^2J_{CP} = 22.6$ Hz, C4), 137.3 (1C, d, $^3J_{CP} = 2.8$ Hz, C3), 139.7 (2C, d, $^2J_{CP} = 11.9$ Hz, C6), 148.5 (2C, qd, $^2J_{CF} = 38.5$ Hz, $^3J_{CP} = 8.1$ Hz, C8), 151.4 (1C, d, $^3J_{CP} = 13.5$ Hz, C1), 157.5 (1C, d, $^1J_{CP} = 14.0$ Hz, C5); ^{19}F NMR (CD_2Cl_2 , 300 K, in ppm): $\delta = -62.9$ (6F, s); ^{31}P NMR (CD_2Cl_2 , 300 K, in ppm): $\delta = 64.2$ (1P, s); **elemental analysis**: calcd. for $\text{C}_{13}\text{H}_8\text{F}_6\text{N}_5\text{P}$: C: 41.18, H: 2.13, N: 18.47; found: C: 40.99, H: 2.11, N 17.90.

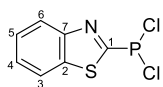
12.2.8. Preparation of 41f



To dichlorophosphane **40** (280 mg, 1.57 mmol) **5f** (730 mg, 3.3 mmol) is added. The suspension is stirred for 16 h at room temperature, filtered and the residue is washed with *n*-hexane (3 x 2 ml). After evaporation of all volatiles *in vacuo* the product is obtained as a colorless solid.

Yield: 567 mg (89 %); **m.p.**: 116 °C; **Raman (100 mW, 298 K, in cm^{-1})**: $\nu = 3147(9)$, 3097(11), 3081(17), 3052(12), 3001(12), 2958(9), 2936(18), 2919(17), 1578(24), 1566(26), 1484(25), 1458(16), 1438(17), 1386(7), 1282(8), 1238(7), 1164(9), 1143(12), 1128(14), 1090(11), 1050(26), 991(58), 960(20), 723(7), 688(32), 621(11), 495(7), 462(7), 327(26), 291(7), 269(7), 243(9), 216(21), 200(20), 178(11), 129(100); **IR (ATR, 298 K, in cm^{-1})**: $\nu = 3124(\text{vs})$, 3094(vs), 3052(vs), 2996(vs), 1577(vs), 1564(vs), 1483(vs), 1452(vs), 1430(vs), 1325(vs), 1309(vs), 1234(vs), 1172(vs), 1140(vs), 1124(vs), 1101(vs), 1082(vs), 1039(vs), 988(vs), 957(vs), 896(vs), 850(vs), 802(vs), 757(vs), 741(vs), 725(vs), 684(vs); **^1H NMR (CD_2Cl_2 , 300 K, in ppm)**: $\delta = 2.41$ (6H, s, C7–H), 6.42 (2H, s, C8–H), 7.38–7.41 (1H, m, C2–H), 7.43–7.45 (1H, m, C4–H), 7.77–7.82 (1H, m, C3–H), 8.73–8.74 (1H, m, C1–H); **$^{13}\text{C}\{^1\text{H}\}$ NMR (CD_2Cl_2 , 300 K, in ppm)**: 13.0 (2C, d, $^3J_{CP} = 11.1$ Hz, C7), 106.9 (2C, q, $^3J_{CF} = 1.8$ Hz, C8), 121.6 (2C, q, $^1J_{CF} = 269.8$ Hz, C10), 125.3 (1C, d, $^4J_{CP} = 1.3$ Hz, C2), 128.3 (1C, d, $^2J_{CP} = 17.1$ Hz, C4), 137.1 (1C, s, C3), 151.2 (1C, d, $^3J_{CP} = 12.9$ Hz, C1), 157.3 (1C, d, $^1J_{CP} = 19.1$ Hz, C5); ^{19}F NMR (CD_2Cl_2 , 300 K, in ppm): $\delta = -63.3$ (6F, s); ^{31}P NMR (CD_2Cl_2 , 300 K, in ppm): $\delta = 56.5$ (1P, s); **elemental analysis**: calcd. for $\text{C}_{15}\text{H}_{12}\text{F}_6\text{N}_5\text{P}$: C: 44.24, H: 2.97, N: 17.20; found: C: 44.13, H: 2.84, N 16.80.

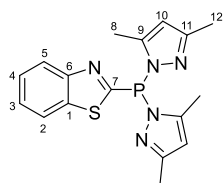
12.2.9. Preparation of 42



2-(Trimethylsilyl)benzo[*d*]thiazol (1.060 g, 5.112 mmol) and PCl_3 (1.3 ml, 15.336 mmol) are placed in a Schlenk flask and heated under reflux for 48 h. After evaporation of all volatiles the residue is sublimed ($T = 55$ °C, $p = 9 \times 10^{-3}$ mbar) to yield the product as colorless crystals. The spectral data are in accordance with the ones reported in the literature.⁴³

Yield: 808 mg (67 %); **¹H NMR (C₆D₆, 300 K, in ppm):** δ = 6.90-6.94 (1H, m, C4-H), 7.01-7.05 (1H, m, C5-H), 7.23-7.26 (1H, m, C6-H), 7.93-7.95 (1H, m, C3-H); **¹³C{¹H} NMR (CD₂Cl₂, 300 K, in ppm):** δ = 122.0 (1C, s, C6), 125.1 (1C, s, C4), 127.0 (1C, s, C5), 127.1 (1C, s, C4), 137.7 (1C, d, ³J_{CP} = 2.7 Hz, C7), 155.1 (1C, d, ³J_{CP} = 15.8 Hz, C2), 173.1 (1C, d, ¹J_{CP} = 63.4 Hz, C1); **³¹P NMR (C₆D₆, 300 K, in ppm):** δ = 132.0 (1P, s).

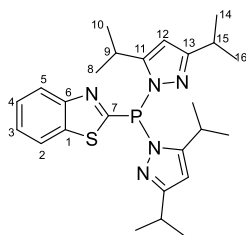
12.2.10. Preparation of 43a



To a suspension of dichlorophospane **42** (2.500 g, 10.59 mmol) in Et₂O **5a** (3.740 g, 22.24 mmol) is added. After stirring for 16 h all volatiles are evaporated *in vacuo* to yield the product as a light-yellow powder.

Yield: 3.620 g (96%); **m.p.:** 102 °C ; **Raman (100 mW, 298 K, in cm⁻¹):** ν = 3097 (12), 3055 (33), 3009 (7), 2970 (15), 2928 (37), 1589 (7), 1571 (9), 1550 (32), 1467 (14), 1452 (28), 1441 (27), 1400 (100), 1384 (12), 1375 (8), 1314 (13), 1272 (23), 1232 (52), 1158 (7), 1125 (12), 1016 (15), 1006 (37), 853 (13), 762 (7), 707 (20), 631 (6), 590 (19), 579 (5), 516 (5), 507 (15), 459 (11), 419 (5), 366 (10), 219 (9), 203 (10), 175 (17); **IR (ATR, 298 K, in cm⁻¹):** ν = 3071 (w), 3053 (w), 2976 (w), 2926 (w), 1569 (s), 1455 (m), 1440 (m), 1398 (s), 1367 (m), 1305 (m), 1284 (s), 1230 (m), 1154 (m), 1129 (vs), 1085 (m), 1068 (m), 1035 (w), 1016 (s), 1005 (m), 956 (vs), 852 (m), 813 (s), 773 (vs), 759 (s), 738 (s), 706 (m), 675 (w), 659 (m), 604 (w), 577 (m), 534 (s), 516 (s), 486 (vs), 458 (vs), 431 (vs), 417 (vs); **¹H NMR (CD₂Cl₂, 300 K, in ppm):** δ = 2.25 (6H, s, C12-H), 2.50 (6H, s, C8-H), 5.98 (2H, s, C10-H), 7.44-7.48 (1H, m, C3-H), 7.50-7.54 (1H, m, C4-H), 7.98-8.00 (1H, m, C5-H), 8.10-8.12 (1H, m, C2-H); **¹³C{¹H} NMR (CD₂Cl₂, 300 K, in ppm):** δ = 12.8 (2C, d, ³J_{CP} = 14.9 Hz, C8), 14.1 (2C, s, C12), 109.5 (2C, d, ³J_{CP} = 1.8 Hz, C10), 122.1 (1C, s, C5), 124.3 (1C, s, C2), 126.5 (1C, s, C3), 126.7 (1C, s, C4), 138.5 (1C, d, ³J_{CP} = 1.7 Hz, C1), 149.9 (2C, d, ²J_{CP} = 20.8 Hz, C9), 154.7 (2C, d, ³J_{CP} = 5.4 Hz, C11), 154.8 (1C, d, ³J_{CP} = 19.1 Hz, C6), 168.6 (1C, d, ¹J_{CP} = 5.0 Hz, C7); **³¹P NMR (CD₂Cl₂, 300 K, in ppm):** δ = 38.0 (1P, s); **elemental analysis:** calcd. for C₁₇H₁₈N₅PS: C: 57.45, H: 5.11, N: 19.71, S: 9.02; found: C: 57.70, H: 5.11, N: 19.25, S: 9.33.

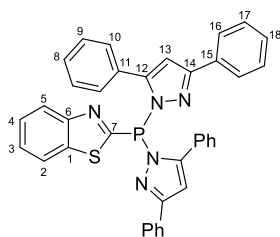
12.2.11. Preparation of 43b



To a suspension of dichlorophospane **42** (236 mg, 1.000 mmol) in Et₂O **5b** (471 mg, 2.100 mmol) is added. After stirring for 16 h all volatiles are evaporated *in vacuo* to yield a light-yellow oil. After addition of *n*-pentane the oil solidifies. The colorless solid is filtered off, washed with *n*-pentane and dried *in vacuo* to yield the product.

Yield: 397 mg (85%); **m.p.:** 109 °C ; **Raman (100 mW, 298 K, in cm⁻¹):** $\nu = 3111$ (5), 3081 (7), 3062 (25), 3028 (6), 2968 (40), 2923 (29), 2868 (34), 2711 (5), 1591 (13), 1554 (29), 1474 (17), 1450 (52), 1410 (100), 1382 (8), 1368 (7), 1314 (18), 1274 (35), 1237 (53), 1162 (5), 1126 (22), 1109 (10), 1049 (7), 1002 (31), 989 (10), 959 (6), 878 (19), 853 (9), 707 (18), 670 (5), 504 (18), 443 (5), 377 (7), 214 (8), 174 (15), 124 (33); **IR (ATR, 298 K, in cm⁻¹):** $\nu = 2964$ (s), 2928 (m), 2868 (m), 2324 (w), 1555 (m), 1448 (m), 1409 (m), 1381 (w), 1364 (m), 1313 (m), 1297 (w), 1248 (s), 1207 (w), 1181 (w), 1164 (m), 1144 (s), 1117 (s), 1089 (w), 1067 (s), 1043 (m), 1016 (m), 1002 (w), 982 (s), 942 (w), 924 (w), 877 (w), 852 (m), 813 (m), 803 (m), 763 (vs), 731 (s), 703 (m), 682 (w), 670 (w), 616 (m), 578 (m), 558 (w), 526 (s), 508 (vs), 495 (vs), 435 (s), 421 (vs); **¹H NMR (CD₂Cl₂, 300 K, in ppm):** $\delta = 1.04$ (6H, d, ³J_{HH} = 6.82 Hz, C8/C10-H), 1.16 (6H, d, ³J_{HH} = 6.82 Hz, C8/C10-H), 1.26 (12H, d, ³J_{HH} = 7.03 Hz, C16-H), 2.95 (2H, sept., ³J_{HH} = 7.03 Hz, C15-H), 3.68 (2H, sept. d, ³J_{HH} = 6.82 Hz, ⁴J_{HP} = 3.09 Hz, C9), 5.90 (2H, s, C12-H), 6.93-6.97 (1H, m, C3-H) 7.04-7.07 (1H, m, C4-H), 7.42-7.44 (1H, m, C5-H), 7.99-8.02 (1H, m, C2-H); **¹³C{¹H} NMR (CD₂Cl₂, 300 K, in ppm):** $\delta = 22.8$ (4C, d, ⁵J_{CP} = 11.4 Hz, C14/C16), 23.6 (2C, s, C10), 24.5 (2C, d, ⁴J_{CP} = 3.2 Hz, C8), 27.1 (2C, d, ³J_{CP} = 11.6 Hz, C9), 29.1 (2C, s, C15), 103.0 (2C, d, C12), 121.9 (1C, s, C5), 124.7 (1C, s, C2), 126.3 (1C, s, C3), 126.5 (1C, s, C4), 139.1 (1C, s, C1), 155.3 (1C, d, ³J_{CP} = 19.4 Hz, C6), 160.0 (1C, d, ²J_{CP} = 13.8 Hz, C11), 163.9 (1C, d, ³J_{CP} = 6.5 Hz, C13), 169.5 (1C, s, C7); **³¹P NMR (CD₂Cl₂, 300 K, in ppm):** $\delta = 39.3$ (1P, s); **elemental analysis:** calcd. for C₂₅H₃₄N₅PS: C: 64.21, H: 7.33, N: 14.98, S: 6.86; found: C: 64.33, H: 7.11, N: 14.75, S: 6.63.

12.2.12. Preparation of 43d

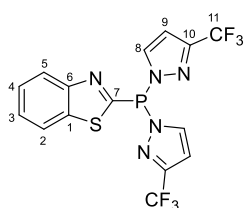


To a suspension of dichlorophospane **42** (236 mg, 1.0 mmol) in Et₂O **5d** (614 mg, 2.10 mmol) is added. After stirring for 16 h the resulting suspension is filtered. The residue is washed with Et₂O (3 x 2 ml). All volatiles are evaporated *in vacuo* to yield the product as a colorless powder.

Yield: 442 mg (73%); **m.p.:** 169 °C ; **Raman (100 mW, 298 K, in cm⁻¹):** $\nu = 3097$ (12), 3055 (33), 3009 (7), 2970 (15), 2928 (37), 1589 (7), 1571 (9), 1550 (32), 1467 (14), 1452 (28), 1441 (27), 1400 (100), 1384 (12), 1375 (8), 1314 (13), 1272 (23), 1232 (52), 1158 (7), 1125 (12), 1016 (15), 1006 (37), 853 (13), 762 (7), 707 (20), 631 (6), 590 (19), 579 (5), 516 (5), 507 (15), 459 (11), 419 (5), 366 (10), 219 (9), 203 (10), 175 (17); **IR (ATR, 298 K, in cm⁻¹):** $\nu = 3071$ (w), 3053 (w), 2976 (w), 2926 (w), 1569 (s), 1455 (m), 1440 (m), 1398 (s), 1367 (m), 1305 (m), 1284 (s), 1230 (m), 1154 (m), 1129 (vs), 1085 (m), 1068 (m), 1035 (w),

1016 (s), 1005 (m), 956 (vs), 852 (m), 813 (s), 773 (vs), 759 (s), 738 (s), 706 (m), 675 (w), 659 (m), 604 (w), 577 (m), 534 (s), 516 (s), 486 (vs), 458 (vs), 431 (vs), 417 (vs); **¹H NMR (CD₂Cl₂, 300 K, in ppm):** δ = 6.76 (2H, d, ⁴J_{HP} = 2.42 Hz, C13–H), 7.29–7.33 (4H, m, C9–H), 7.36–7.42 (8H, m, C8/C10/C18–H), 7.44–7.48 (4H, m, C17–H), 7.48–7.54 (2H, m, C3/C4–H), 7.96–7.99 (4H, m, C16–H), 8.05–8.08 (1H, m, C2–H), 8.13–8.15 (1H, m, C5–H); **¹³C{¹H} NMR (CD₂Cl₂, 300 K, in ppm):** δ = 106.6 (2C, d, ³J_{CP} = 1.7 Hz, C13), 122.2 (1C, s, C2), 124.6 (1C, s, C5), 126.6 (1C, s, C3), 126.8 (5C, s, C4/C16), 129.0 (4C, s, C9), 129.2 (2C, s, C18), 129.3 (4C, s, C17), 129.6 (2C, s, C8), 130.2 (2C, d, ³J_{CP} = 3.1 Hz, C11), 130.3 (4C, d, ⁴J_{CP} = 4.5 Hz, C10), 133.2 (2C, s, C15), 139.5 (1C, s, C1), 153.9 (2C, d, ²J_{CP} = 23.8 Hz, C12), 154.2 (1C, d, ³J_{CP} = 24.4 Hz, C6), 156.5 (2C, s, C14), 168.3 (1C, d, ¹J_{CP} = 2.4 Hz, C7); **³¹P NMR (CD₂Cl₂, 300 K, in ppm):** δ = 43.4 (1P, s); **elemental analysis:** calcd. for C₃₇H₂₆N₅PS x 0.15 CH₂Cl₂: C: 72.39, H: 4.30, N: 11.36, S: 5.20; found: C: 72.45, H: 4.39, N: 11.42, S: 5.09.

12.2.13. Preparation of **43e**

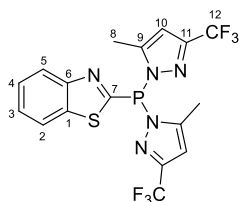


To a suspension of dichlorophospane **42** (236 mg, 1.00 mmol) in Et₂O **5e** (437 g, 2.10 mmol) is added. After stirring for 16 h all volatiles are evaporated *in vacuo* to yield a colorless oil. After addition of *n*-pentane the oil solidifies. The colorless solid is filtered off, washed with *n*-pentane and dried *in vacuo* to yield the product as a colorless powder.

Yield: 224 mg (51%); **m.p.:** 111 °C ; **Raman (100 mW, 298 K, in cm⁻¹):** ν = 3161 (167), 3144 (33), 3115 (83), 3074 (250), 3061 (17), 3033 (50), 1592 (117), 1555 (317), 1535 (33), 1464 (883), 1423 (600), 1399 (183), 1388 (67), 1346 (67), 1316 (117), 1275 (283), 1236 (783), 1158 (50), 1124 (217), 1074 (33), 1046 (67), 1014 (167), 972 (600), 851 (100), 761 (33), 742 (233), 726 (17), 709 (217), 676 (50), 635 (17), 623 (17), 610 (83), 586 (33), 541 (83), 526 (17), 503 (233), 457 (17), 433 (17), 418 (50), 401 (50), 373 (83), 347 (100), 308 (100), 282 (67), 248 (17), 241 (150); **IR (ATR, 298 K, in cm⁻¹):** ν = 3160 (vw), 3143 (vw), 3115 (vw), 1466 (w), 1399 (w), 1389 (w), 1344 (vw), 1316 (vw), 1225 (m), 1147 (vs), 1130 (vs), 1116 (vs), 1035 (s), 970 (m), 958 (s), 886 (vw), 868 (vw), 851 (vw), 784 (m), 759 (s), 741 (m), 729 (m), 709 (vw), 676 (w), 635 (w), 623 (w), 609 (w), 591 (w), 543 (m), 524 (m), 502 (m), 456 (m), 432 (w), 417 (w), 406 (vw); **¹H NMR (CD₂Cl₂, 300 K, in ppm):** δ = 6.75 (2H, d, ⁴J_{HP} = 2.60 Hz, C9–H), 7.53–7.58 (1H, m, C4–H), 7.58–7.62 (1H, m, C3–H), 8.02–8.08 (1H, m, C2–H), 8.16–8.18 (1H, m, C5–H), 8.24 (2H, bs, C8–H); **¹³C{¹H} NMR (CD₂Cl₂, 300 K, in ppm):** δ = 107.9 (2C, *pseudo t*, C9), 121.3 (2C, q, ¹J_{CF} = 267.5 Hz,

C11), 122.5 (1C, s, C2), 125.0 (1C, s, C5), 127.7 (1C, s, C4), 127.8 (1C, s, C3), 138.0 (1C, s, C1), 139.7 (2C, d, $^2J_{CP} = 13.3$ Hz, C8), 148.9 (2C, qd, $^2J_{CF} = 38.5$ Hz, $^3J_{CP} = 8.3$ Hz, C10), 155.1 (1C, d, $^3J_{CP} = 17.1$ Hz, C6), 165.1 (1C, d, $^1J_{CP} = 3.3$ Hz, C7); **^{31}P NMR (CD₂Cl₂, 300 K, in ppm):** $\delta = 54.1$ (1P, s); **^{19}F NMR (CD₂Cl₂, 300 K, in ppm):** $\delta = -63.0$ (3F, s); **elemental analysis:** calcd. for C₁₅H₈F₆N₅PS: C: 41.39, H: 1.85, N: 16.09, S: 7.37; found: C: 41.13, H: 1.86, N: 15.88, S: 7.50.

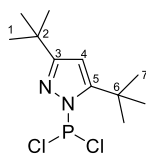
12.2.14. Preparation of 43f



To a suspension of dichlorophospane **42** (236 mg, 1.00 mmol) in Et₂O **5f** (467 g, 2.10 mmol) is added. After stirring for 16 h all volatiles are evaporated *in vacuo* to yield a colorless oil. After addition of *n*-pentane the oil solidifies. The colorless solid is filtered off, washed with *n*-pentane and dried *in vacuo* to yield the product as a colorless powder.

Yield: 267 mg (58%); **m.p.:** 133 °C ; **Raman (100 mW, 298 K, in cm⁻¹):** $\nu = 3146$ (9), 3111 (5), 3071 (25), 3005 (6), 2978 (6), 2935 (21), 1594 (12), 1554 (29), 1483 (16), 1456 (37), 1410 (100), 1388 (10), 1322 (15), 1277 (30), 1240 (58), 1174 (5), 1127 (19), 1088 (7), 1026 (14), 1010 (45), 987 (6), 960 (12), 854 (9), 709 (23), 688 (17), 675 (10), 644 (5), 579 (7), 504 (16), 479 (8), 413 (6), 329 (15), 266 (5), 199 (13), 164 (10), 150 (13), 132 (22); **IR (ATR, 298 K, in cm⁻¹):** $\nu = 3147$ (vw), 3070 (vw), 3005 (vw), 1615 (vw), 1560 (vw), 1484 (m), 1446 (w), 1410 (vw), 1386 (vw), 1362 (vw), 1313 (w), 1234 (s), 1173 (vs), 1131 (vs), 1102 (vs), 1083 (s), 1040 (w), 1025 (w), 1010 (w), 986 (w), 957 (m), 873 (vw), 855 (w), 808 (m), 760 (s), 731 (w), 723 (w), 708 (vw), 686 (vw), 675 (vw), 644 (vw), 603 (w), 578 (w), 529 (m), 507 (m), 497 (s), 477 (s), 433 (w); **^1H NMR (CD₂Cl₂, 300 K, in ppm):** $\delta = 2.52$ (6H, s, C8–H), 6.45 (2H, s, C10–H), 7.51–7.55 (1H, m, C4–H), 7.55–7.59 (1H, m, C3–H), 8.02–8.05 (1H, m, C2–H), 8.14–8.16 (1H, m, C5–H); **$^{13}\text{C}\{^1\text{H}\}$ NMR (CD₂Cl₂, 300 K, in ppm):** $\delta = 12.9$ (2C, d, $^3J_{CP} = 11.5$ Hz, C8), 107.2 (2C, d, $^3J_{CP} = 1.9$ Hz, C10), 121.5 (2C, q, $^1J_{CF} = 268.9$ Hz, C12), 122.5 (1C, s, C2), 124.7 (1C, s, C5), 127.3 (1C, s, C3), 127.4 (1C, s, C4), 138.5 (1C, d, $^3J_{CP} = 1.7$ Hz, C1), 148.1 (2C, qd, $^2J_{CF} = 38.1$ Hz, $^3J_{CP} = 6.2$ Hz, C11), 150.9 (2C, d, $^2J_{CP} = 16.2$ Hz, C9), 154.9 (1C, d, $^3J_{CP} = 19.7$ Hz, C6), 165.2 (1C, d, $^1J_{CP} = 2.3$ Hz, C7); **^{31}P NMR (CD₂Cl₂, 300 K, in ppm):** $\delta = 49.0$ (1P, s); **^{19}F NMR (CD₂Cl₂, 300 K, in ppm):** $\delta = -63.4$ (3F, s); **elemental analysis:** calcd. for C₁₇H₁₂F₆N₅PS: C: 44.07, H: 2.61, N: 15.12, S: 6.92; found: C: 44.19, H: 2.65, N: 14.74, S: 7.00.

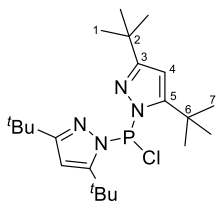
12.2.15. Preparation of 44



To PCl_3 (2.0 ml, 22.86 mmol) **5c** (2.90 g, 11.43 mmol) is added. The reaction mixture is stirred at r.t. for 16 h resulting in a thick, colorless suspension. After evaporation of all volatiles the product is obtained as colorless solid.

Yield: 3.18 g (99 %); **m.p.:** 80 °C; **Raman (100 mW, 298 K, in cm^{-1}):** $\nu = 3139$ (100), 3107 (99), 2972 (95), 2928 (93), 2906 (93), 2864 (91), 2784 (89), 2717 (87), 1563 (50), 1485 (47), 1464 (47), 1442 (46), 1415 (45), 1395 (44), 1368 (44), 1286 (41), 1251 (40), 1221 (39), 1203 (38), 1040 (33), 1029 (33), 1013 (32), 974 (31), 931 (30), 837 (27), 823 (26), 687 (22), 657 (21), 570 (18), 505 (16), 477 (15), 442 (14), 416 (13), 376 (12), 331 (11), 286 (9), 262 (8), 242 (8), 177 (6); **IR (ATR, 298 K, in cm^{-1}):** $\nu = 2962$ (m), 2930 (w), 2904 (w), 2866 (vw), 1561 (m), 1462 (w), 1413 (vw), 1398 (w), 1364 (m), 1284 (m), 1250 (m), 1221 (w), 1188 (m), 1128 (s), 1107 (m), 1039 (vw), 1012 (w), 972 (m), 931 (vw), 822 (m), 725 (vw), 686 (vw), 656 (w), 568 (m), 501 (vs), 471 (vs), 440 (s); **$^1\text{H NMR}$ (CD_2Cl_2 , 300 K, in ppm):** $\delta = 1.31$ (9H, s, C1-H), 1.43 (9H, s, C7-H), 6.02 (1H, d, $^4J_{\text{HP}} = 2.0$ Hz, C4-H); **$^{13}\text{C}\{^1\text{H}\}$ NMR (CD_2Cl_2 , 300 K, in ppm):** $\delta = 30.3$ (3C, s, C1), 31.7 (3C, d, $^4J_{\text{CP}} = 14.0$ Hz, C7), 32.6 (1C, s, C6), 33.5 (1C, s, C2), 104.9 (1C, d, $^3J_{\text{CP}} = 2.0$ Hz, C4), 161.7 (1C, d, $^2J_{\text{CP}} = 16.7$ Hz, C5), 168.9 (1C, d, $^3J_{\text{CP}} = 2.6$ Hz, C3); **$^{31}\text{P NMR}$ (CD_2Cl_2 , 300 K, ppm):** $\delta = 148.5$ (1P, s); **elemental analysis:** calcd. for $\text{C}_{11}\text{H}_{19}\text{Cl}_2\text{N}_2\text{P}$: C: 46.99, H: 6.81, N: 9.96; found: C: 46.97, H: 6.39, N 9.62.

12.2.16. Preparation of 45

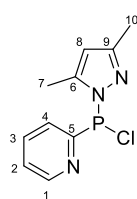


To **5c** (2.30 g, 9.10 mmol) PCl_3 (0.4 ml, 4.55 mmol) is added. The reaction mixture is stirred at r.t. for 72 h resulting in a thick, colorless suspension. After evaporation of all volatiles the product is obtained as colorless solid.

Yield: 1.91 g (99 %); **m.p.:** 135 °C; **Raman (100 mW, 298 K, in cm^{-1}):** $\nu = 3136$ (14), 2971 (100), 2926 (87), 2906 (76), 2864 (32), 2782 (7), 2714 (13), 1558 (10), 1485 (19), 1463 (41), 1449 (53), 1414 (10), 1403 (11), 1366 (5), 1291 (5), 1278 (6), 1250 (10), 1219 (15), 1204 (41), 1181 (11), 1127 (5), 1038 (12), 1026 (15), 981 (19), 928 (33), 837 (19), 822 (59), 688 (5), 656 (11), 578 (15), 564 (38), 503 (38), 486 (31), 452 (9), 414 (7), 372 (14), 328 (11), 288 (21), 262 (24), 245 (16), 225 (14), 196 (18), 175 (24); **IR (ATR, 298 K, in cm^{-1}):** $\nu = 3231$ (vw), 2965 (m), 2928 (w), 2904 (w), 2867 (w), 1557 (m), 1475 (vw), 1460 (w), 1400 (vw), 1361 (m), 1289 (w), 1278 (w), 1249 (m), 1220 (w), 1194 (w), 1178 (w), 1122 (s), 1106 (s), 1038 (vw), 1011 (w), 975 (s), 928 (vw), 848 (vw), 811 (m), 722 (w), 686 (vw),

652 (m), 578 (w), 551 (w), 501 (vs), 484 (vs), 451 (m), 432 (w); **¹H NMR (CD₂Cl₂, 300 K, in ppm):** δ = 1.25 (18H, s, C1–H), 1.42 (18H, s, C7–H), 6.03 (2H, d, ⁴J_{HP} = 2.08 Hz, C4–H); **¹³C{¹H} NMR (CD₃Cl, 300 K, in ppm):** δ = 30.4 (6C, s, C1), 31.6 (6C, d, ⁴J_{CP} = 10.5 Hz, C7), 32.7 (2C, s, C6), 33.0 (2C, s, C2), 104.7 (2C, d, ³J_{CP} = 2.9 Hz, C4), 160.7 (2C, d, ²J_{CP} = 16.7 Hz, C5), 165.6 (2C, d, ³J_{CP} = 2.74 Hz, C3); **³¹P NMR (CD₂Cl₂, 300 K, ppm):** δ = 106.4 (1P, s); **elemental analysis:** calcd. for C₂₂H₃₈ClN₄P: C: 62.17, H: 9.01, N: 13.18; found: C: 61.92, H: 8.59, N 13.00.

12.2.17. Preparation of 46

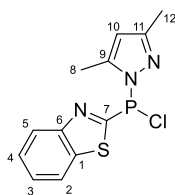


To a solution of dichlorophosphane **40** (3.60 g, 20.0 mmol) in *n*-pentane (10 ml) a solution of **5a** (3.20 g, 19.0 mmol) in *n*-pentane (10 ml) is added at -30 °C.

After that the reaction mixture is stirred at r.t. for 16 h. The resulting colorless precipitate is filtered off and washed with *n*-pentane (2 x 5 ml). After evaporation of all volatiles the product is obtained as colorless solid.

Yield: 3.81 g (84 %); **m.p.:** 69 °C; **Raman (100 mW, 298 K, in cm⁻¹):** ν = 3131 (12), 3101 (13), 3088 (13), 3070 (38), 3040 (45), 2975 (15), 2923 (55), 2858 (9), 1575 (34), 1567 (48), 1446 (38), 1384 (11), 1375 (11), 1304 (11), 1278 (14), 1250 (11), 1163 (21), 1136 (16), 1087 (15), 1046 (52), 1017 (15), 991 (100), 966 (12), 774 (12), 759 (10), 721 (18), 635 (11), 617 (21), 591 (37), 519 (18), 492 (29), 473 (61), 447 (18), 408 (28), 374 (15), 286 (45), 235 (29), 214 (23), 197 (20); **IR (ATR, 298 K, in cm⁻¹):** ν = 3038 (vw), 2921 (vw), 1563 (m), 1445 (w), 1427 (w), 1402 (w), 1370 (w), 1322 (w), 1300 (m), 1277 (w), 1155 (w), 1132 (m), 1081 (w), 1044 (vw), 1015 (w), 989 (w), 963 (w), 897 (vw), 860 (vw), 802 (m), 777 (m), 760 (m), 721 (vw), 660 (vw), 634 (vw), 616 (vw), 590 (vw), 557 (vw), 520 (s), 489 (vs), 467 (vs), 440 (s), 408 (m); **¹H NMR (CD₂Cl₂, 300 K, in ppm):** δ = 2.15 (3H, s, C10–H), 2.38 (3H, s, C7–H), 5.94 (1H, s, C8–H), 7.34-7.38 (1H, m, C2–H), 7.83-7.88 (1H, m, C4–H), 8.08-8.14 (1H, m, C3–H), 8.67-8.69 (1H, m, C1–H); **¹³C{¹H} NMR (CD₂Cl₂, 300 K, in ppm):** δ = 12.7 (1C, s, C7), 14.1 (1C, s, C10), 109.8 (1C, s, C8), 124.9 (1C, s, C2), 126.9 (1C, s, C4), 136.9 (1C, s, C3), 149.3 (1C, s, C6), 150.3 (1C, d, ³J_{CP} = 16.8 Hz, C1), 155.6 (1C, s, C9), 160.6 (1C, s, C5); **³¹P NMR (CD₂Cl₂, 300 K, ppm):** δ = 80.1 (1P, s); **elemental analysis:** calcd. for C₁₀H₁₁ClN₃P: C: 50.12, H: 4.63, N: 17.53; found: C: 50.44, H: 4.31, N 17.45.

12.2.18. Preparation of 47

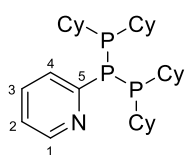


To a suspension of dichlorophosphane **42** (250 mg, 1.06 mmol) in *n*-pentane **5a** (178 mg, 1.06 mmol) is added. After 16 h the resulting thick, colorless suspension is filtered. The residue is washed with *n*-pentane (3 x 1 ml) and dried *in vacuo* to yield the product as a colorless solid.

Yield: 297 mg (95 %); **m.p.:** 104 °C; **Raman (100 mW, 298 K, in cm⁻¹):** $\nu = 3107$ (20), 3065 (70), 2982 (15), 2961 (22), 2924 (73), 1593 (18), 1575 (17), 1554 (46), 1457 (75), 1436 (28), 1415 (100), 1384 (14), 1317 (22), 1281 (18), 1238 (96), 1126 (30), 1021 (30), 1011 (60), 852 (16), 763 (22), 709 (51), 601 (13), 587 (31), 504 (25), 483 (53), 477 (66), 460 (45), 402 (14), 371 (25), 243 (35), 189 (30); **IR (ATR, 298 K, in cm⁻¹):** $\nu = 3063$ (w), 2979 (w), 2956 (w), 2923 (w), 2656 (w), 2363 (w), 1574 (m), 1553 (w), 1454 (m), 1399 (m), 1368 (w), 1315 (m), 1295 (s), 1237 (w), 1167 (w), 1153 (m), 1129 (s), 1090 (m), 1078 (w), 1034 (w), 1016 (m), 957 (m), 940 (w), 861 (w), 850 (w), 801 (s), 758 (vs), 727 (s), 707 (w), 673 (w), 657 (w), 634 (w), 599 (m), 586 (w), 574 (m), 526 (m), 483 (s), 472 (vs), 454 (vs), 424 (vs); **¹H NMR (CD₂Cl₂, 300 K, in ppm):** $\delta = 2.24$ (3H, s, C12-H), 2.47 (3H, s, C8-H), 6.00 (1H, s, C10-H), 7.48-7.53 (1H, m, C3-H), 7.53-7.58 (1H, m, C4-H), 8.02-8.05 (1H, m, C5-H), 8.11-8.14 (1H, m, C2-H); **¹³C{¹H} NMR (CD₂Cl₂, 300 K, in ppm):** $\delta = 12.5$ (1C, d, ³J_{CP} = 14.9 Hz, C8), 14.2 (1C, s, C12), 110.4 (1C, s, C10), 122.4 (1C, s, C5), 124.7 (1C, s, C2), 127.1 (2C, s, C3/C4), 138.4 (1C, s, C1), 149.3 (1C, d, ²J_{CP} = 21.7 Hz, C9), 155.1 (1C, d, ³J_{CP} = 17.8 Hz, C6), 156.7 (1C, d, ³J_{CP} = 5.0 Hz, C11), 171.0 (1C, d, ¹J_{CP} = 27.9 Hz, C7); **³¹P NMR (CD₂Cl₂, 300 K, ppm):** $\delta = 76.1$ (1P, s); **elemental analysis:** calcd. for C₁₂H₁₁ClN₃PS: C: 48.74, H: 3.75, N: 14.21, S: 10.84; found: C: 48.65, H: 3.36, N: 13.84, S: 11.34.

12.3. Syntheses and Characterization Data regarding Compounds in Chapter 4

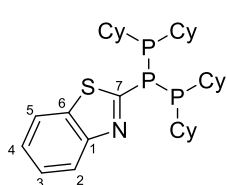
12.3.1. Preparation of 48



To a solution of dipyrazolyphosphane **41a** (2.00 g, 6.682 mmol) in 20 ml of MeCN dicyclohexylphosphane (2.9 ml, 13.364 mmol) is added while stirring vigorously. After a few moments a colorless precipitate forms. The reaction mixture is stirred for 16 h. After that the precipitate is filtered off and washed with MeCN (3 x 10 ml). Evaporation of all volatiles *in vacuo* yields the product as a colorless powder.

Yield: 3.239 g (96%); **m.p.:** 122 °C; **Raman (100 mW, 298 K, in cm⁻¹):** $\nu = 3057$ (13), 3033 (18), 2928 (80), 2916 (79), 2890 (45), 2848 (100), 2649 (6), 1569 (30), 1460 (5), 1443 (30), 1420 (5), 1343 (8), 1328 (9), 1298 (10), 1274 (20), 1189 (8), 1179 (6), 1153 (5), 1122 (11), 1080 (5), 1043 (21), 1025 (21), 986 (22), 848 (9), 815 (17), 735 (8), 714 (10), 697 (6), 505 (6), 464 (10), 444 (5), 401 (5), 364 (5), 211 (11), 160 (9), 132 (16), 122 (19); **IR (ATR, 298 K, in cm⁻¹):** $\nu = 3056$ (w), 3032 (w), 2916 (vs), 2847 (s), 1568 (m), 1558 (w), 1443 (vs), 1420 (m), 1339 (w), 1293 (w), 1262 (w), 1212 (vw), 1188 (w), 1177 (w), 1169 (w), 1153 (w), 1121 (w), 1080 (w), 1045 (w), 1028 (vw), 997 (m), 953 (vw), 914 (vw), 902 (vw), 884 (w), 849 (w), 814 (vw), 763 (s), 747 (w), 735 (vw), 714 (w), 621 (w), 504 (w), 484 (w), 464 (w), 454 (vw), 438 (vw); **¹H NMR (CD₂Cl₂, 300 K, in ppm):** $\delta = 1.08$ -1.42 (20H, m, CH₂), 1.59-1.65 (4H, m, CH₂), 1.65-1.78 (12H, m, CH₂), 1.78-1.89 (8H, m, CH, CH₂), 7.07-7.11 (1H, m, C2-H), 7.51-7.55 (1H, m, C3-H), 7.81-7.83 (1H, m, C4-H), 8.57-8.59 (1H, m C1-H); **¹³C{¹H} NMR (CD₂Cl₂, 300 K, in ppm):** $\delta = 27.0$ (m, CH₂), 28.1 (m, CH₂), 31.8 (m, CH₂), 32.7 (m, CH₂), 33.9 (4C, m, CH), 121.9 (1C, s, C2), 130.3 (1C, dt, ²J_{CP} = 18.5 Hz, ³J_{CP} = 5.7 Hz, C4), 134.8 (1C, d, ³J_{CP} = 3.8 Hz, C3), 150.0 (1C, d, ³J_{CP} = 11.4 Hz, C1), 163.6 (1C, dt, ¹J_{CP} = 22.3 Hz, ²J_{CP} = 8.1 Hz, C5); **³¹P NMR (CD₂Cl₂, 300 K, in ppm):** AX₂ spin system: $\delta(P_A) = -57.3$ (1P), $\delta(P_X) = -7.7$ (2P); ¹J(P_AP_X) = -251.3 Hz; **elemental analysis:** calcd. for C₂₉H₄₈NP₃: C: 69.16, H: 9.61, N: 2.78; found: C: 68.85, H: 9.33, N: 2.80.

12.3.2. Preparation of 49



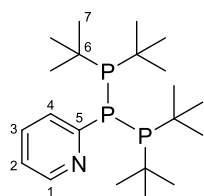
To a solution of dipyrazolylphosphane **43a** (500 mg, 1.407 mmol) in 10 ml of MeCN dicyclohexylphosphane (0.57 ml, 2.814 mmol) is added while stirring vigorously. After a few moments a slightly yellow oil forms which solidifies over the course of approximately five minutes;

this can be supported by means of ultra sonification. The suspension is then stirred for 16 h. After that the precipitate is filtered off and washed with MeCN (3 x 5 ml). Evaporation of all volatiles *in vacuo* yields the product as a pale-yellow powder.

Yield: 731 mg (93%); **m.p.:** 99 °C; **Raman (100 mW, 298 K, in cm⁻¹):** $\nu = 3058$ (29), 2931 (100), 2882 (7), 2848 (61), 1557 (7), 1448 (18), 1408 (61), 1268 (11), 1231 (18), 1022 (11), 961 (11), 501 (7); **IR (ATR, 298 K, in cm⁻¹):** $\nu = 2919$ (vs), 2846 (s), 1446 (m), 1413 (m), 1314 (w), 1301 (w), 1265 (w), 1241 (w), 1192 (w), 1181 (w), 1158 (w), 1015 (w), 997 (m), 964 (s), 884 (w), 847 (m), 757 (vs), 726 (s), 652 (w), 599 (w), 510 (w), 453 (w), 433 (w); **¹H NMR (CD₂Cl₂, 300 K, in ppm):** $\delta = 1.11$ -1.30 (12H, m, CH₂), 1.34-1.47 (8H, m, CH₂), 1.60-1.66 (4H, m, CH₂), 1.68-1.76 (8H, m, CH₂), 1.76-1.82 (4H, m, CH₂), 1.88-1.95 (4H, m, CH₂), 1.98-2.07 (4H, m, CH), 7.32-7.36 (1H, m, C4-H), 7.42-7.46 (1H, m, C3-H), 7.86-

7.89 (1H, m, C2–H), 7.98–8.00 (1H, m, C5–H); $^{13}\text{C}\{^1\text{H}\}$ NMR (CD_2Cl_2 , 300 K, in ppm): $\delta = 26.9$ (m, CH_2), 28.0 (m, CH_2), 31.7 (m, CH_2), 32.6 (m, CH_2), 34.2 (4C, m, CH), 121.6 (1C, s, C2), 123.0 (1C, s, C5), 125.1 (1C, s, C4), 126.2 (1C, s, C3), 137.8 (1C, dt, $^3J_{\text{CP}} = 5.1$ Hz, $^4J_{\text{CP}} = 2.1$ Hz, C6), 155.9 (1C, d, $^3J_{\text{CP}} = 11.7$ Hz, C1), 173.6 (1C, dt, $^1J_{\text{CP}} = 50.2$ Hz, $^2J_{\text{CP}} = 15.2$ Hz, C7); ^{31}P NMR (CD_2Cl_2 , 300 K, in ppm): AX_2 spin system: $\delta(\text{P}_\text{A}) = -58.1$ (1P), $\delta(\text{P}_\text{X}) = -0.7$ (2P); $^1J(\text{P}_\text{A}\text{P}_\text{X}) = -268.8$ Hz; **elemental analysis**: calcd. for $\text{C}_{31}\text{H}_{48}\text{NP}_3\text{S}$: C: 66.52, H: 8.64, N: 2.50, S: 5.73; found: C: 66.16, H: 8.20, N: 2.45, S: 5.36.

12.3.3. Preparation of **50**

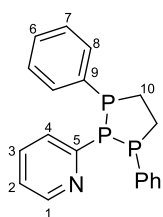


To a solution of dipyrzolyolphosphane **41a** (485 mg, 1.62 mmol) in 3 ml of MeCN di-*tert*-butylphosphane (0.6 ml, 3.24 mmol) is added while stirring. After stirring for 5 h the solution is stored at -30°C for five days. During this time large colorless crystals of **50** are growing. These crystals

are isolated by decantation, washed with MeCN (2 x 1 ml) and dried *in vacuo* to afford **50**. The mother liquor is again stored at -30°C for a second crop of crystals to grow which are isolated as described.

Yield: 501 mg (77%); **m.p.**: 142°C ; **Raman (100 mW, 298 K, in cm^{-1})**: $\nu = 3114$ (5), 3081 (6), 3056 (20), 3044 (24), 2986 (31), 2941 (59), 2892 (100), 2861 (70), 2766 (9), 2701 (12), 1569 (51), 1557 (19), 1472 (28), 1459 (31), 1445 (30), 1413 (10), 1389 (7), 1362 (7), 1278 (10), 1202 (22), 1190 (22), 1172 (33), 1145 (18), 1114 (17), 1079 (7), 1046 (36), 1015 (10), 989 (50), 932 (25), 808 (59), 707 (10), 620 (9), 569 (43), 509 (13), 481 (16), 395 (15), 379 (10), 361 (9), 257 (27), 237 (23), 190 (20); **IR (ATR, 298 K, in cm^{-1})**: $\nu = 2992$ (m), 2940 (s), 2889 (s), 2857 (s), 2703 (w), 1567 (s), 1556 (m), 1466 (s), 1450 (s), 1412 (s), 1384 (s), 1360 (vs), 1272 (w), 1201 (w), 1169 (vs), 1144 (m), 1111 (m), 1079 (w), 1044 (m), 1015 (m), 987 (m), 930 (m), 806 (s), 760 (vs), 742 (s), 705 (m), 621 (m); **^1H NMR (CD_2Cl_2 , 300 K, in ppm)**: $\delta = 1.26$ (36H, d, $^3J_{\text{HP}} = 11.1$ Hz, C7–H), 7.07–7.10 (1H, m, C2–H), 7.46–7.51 (1H, m, C3–H), 8.17–8.20 (1H, m, C4–H), 8.53–8.55 (1H, m C1–H); **$^{13}\text{C}\{^1\text{H}\}$ NMR (CD_2Cl_2 , 300 K, in ppm)**: $\delta = 32.2$ (12C, m, C7), 36.5 (4C, m, CH_2), 122.4 (1C, s, C2), 132.6 (1C, dt, $^2J_{\text{CP}} = 20.8$ Hz, $^3J_{\text{CP}} = 5.8$ Hz, C4), 135.0 (1C, d, $^3J_{\text{CP}} = 4.7$ Hz, C3), 149.7 (1C, dt, $^3J_{\text{CP}} = 12.6$ Hz, $^4J_{\text{CP}} = 0.9$ Hz, C1), 164.9 (1C, dt, $^1J_{\text{CP}} = 22.5$ Hz, $^2J_{\text{CP}} = 9.3$ Hz, C5); **^{31}P NMR (CD_2Cl_2 , 300 K, in ppm)**: AX_2 spin system: $\delta(\text{P}_\text{A}) = -44.1$ (1P), $\delta(\text{P}_\text{X}) = 37.0$ (2P); $^1J(\text{P}_\text{A}\text{P}_\text{X}) = -307.4$ Hz; **elemental analysis**: calcd. for $\text{C}_{21}\text{H}_{48}\text{NP}_3$: C: 63.14, H: 10.09, N: 3.51; found: C: 62.98, H: 10.13, N: 3.56.

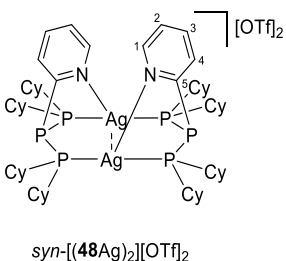
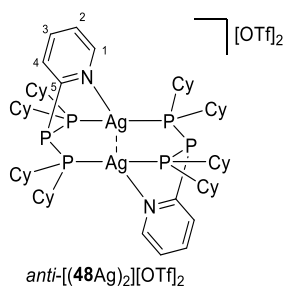
12.3.4. Preparation of **51**



To a solution of dipyrazolylphosphane **41a** (599 mg, 0.2 mmol) in 3 ml of MeCN 1,2-bis(phenylphosphaneyl)ethane (492 mg, 0.2 mmol) is added while stirring. After stirring for 5 min the solution is stored at -30 °C for 24 h. During this time colorless crystals of **51** are growing. These crystals are isolated by decantation, washed with MeCN (2 x 1 ml) and dried *in vacuo* to afford **51**. The mother liquor is again stored at -30 °C for a second crop of crystals to grow which are isolated as described.

Yield: 489 mg (69%); **m.p.:** 101 °C; **Raman (100 mW, 298 K, in cm⁻¹):** $\nu = 3054$ (68), 3037 (29), 3001 (5), 2955 (11), 2941 (17), 2896 (77), 1584 (71), 1570 (40), 1407 (12), 1276 (7), 1185 (8), 1152 (13), 1116 (17), 1099 (36), 1045 (26), 1027 (44), 1000 (100), 874 (5), 714 (8), 690 (7), 650 (15), 639 (18), 619 (17), 509 (8), 488 (20), 459 (39), 423 (46), 398 (8), 381 (10), 303 (8), 282 (17), 244 (11), 225 (33), 205 (35), 179 (28); **IR (ATR, 298 K, in cm⁻¹):** $\nu = 3063$ (w), 3045 (w), 3035 (w), 3014 (w), 2982 (w), 2953 (w), 2940 (w), 2895 (w), 1984 (w), 1952 (w), 1892 (w), 1821 (w), 1757 (w), 1657 (w), 1583 (w), 1567 (m), 1558 (w), 1473 (w), 1444 (w), 1429 (m), 1413 (m), 1326 (w), 1304 (w), 1273 (w), 1224 (w), 1181 (w), 1146 (w), 1110 (w), 1096 (w), 1080 (w), 1069 (w), 1044 (w), 1023 (w), 998 (w), 987 (w), 974 (w), 921 (w), 910 (w), 893 (w), 873 (w), 854 (w), 781 (m), 759 (m), 740 (s), 694 (s); **¹H NMR (CD₂Cl₂, 300 K, in ppm):** $\delta = 2.69$ -2.79 (4H, m, C10-H), 7.15-7.18 (1H, m, C2-H), 7.19-7.22 (6H, m, C6/C7-H), 7.34-7.38 (4H, m, C8-H), 7.59-7.63 (1H, m, C3-H), 7.86-7.89 (1H, m, C4-H), 8.63-8.65 (1H, m C1-H); **¹³C{¹H} NMR (CD₂Cl₂, 300 K, in ppm):** $\delta = 33.0$ (2C, m, C10), 122.5 (1C, bs, C2), 128.2 (2C, m, C6), 128.8 (4C, m, C7), 129.3 (1C, dt, ²J_{CP} = 27.9 Hz, ³J_{CP} = 7.7 Hz, C4), 132.5 (4C, m, C8), 135.9 (1C, d, ³J_{CP} = 6.2 Hz, C3), 137.5 (2C, m, C9), 150.8 (1C, d, ³J_{CP} = 7.2 Hz, C1), 163.6 (1C, dt, ¹J_{CP} = 8.8 Hz, ²J_{CP} = 14.7 Hz, C5); **³¹P NMR (CD₂Cl₂, 300 K, in ppm):** AX₂ spin system: $\delta(P_A) = -12.1$ (1P), $\delta(P_X) = 14.5$ (2P); ¹J(P_AP_X) = -260.7 Hz; **elemental analysis:** calcd. for C₁₉H₁₈NP₃: C: 64.60, H: 5.14, N: 3.96; found: C: 64.47, H: 5.05, N: 4.02.

12.3.5. Preparation of [(48Ag)₂][OTf]₂



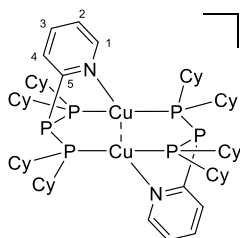
To triphosphane **48** (1007 mg, 2.00 mmol) in PhF (5 ml) Ag[OTf] (513.9 mg, 2 mmol) is added. After stirring for 16 h the colorless suspension is filtered and the residue is washed with PhF (1 x 2 ml) and *n*-pentane (2 x 2 ml). The precipitate is subsequently dried *in vacuo* to afford the product as a colorless powder.

Yield: 1504 mg (99%); **m.p.:** 263 °C (dec.); **Raman (100 mW, 50 scans, 298 K, in cm⁻¹):** $\nu = 3073$ (25), 3058 (24), 3046 (19), 2955 (80), 2935 (91), 2923 (94), 2893 (51), 2881 (56), 2854 (78), 1603 (17), 1592 (15), 1574 (32), 1560 (33), 1445 (65), 1350 (26), 1329 (24), 1294 (31), 1266 (38), 1213 (29), 1200 (26), 1176 (21),

1159 (19), 1110 (24), 1085 (23), 1050 (42), 1030 (100), 999 (76), 851 (40), 816 (41), 752 (28), 734 (19), 710 (31), 573 (18), 512 (31), 457 (15), 437 (16), 426 (15), 388 (16), 348 (26), 315 (26), 233 (36), 192 (22), 168 (62); **IR (ATR, 298 K, in cm⁻¹):** $\nu = 3069$ (vw), 2920 (m), 2847 (w), 1590 (vw), 1573 (w), 1486 (vw), 1446 (w), 1424 (vw), 1348 (vw), 1327 (vw), 1292 (w), 1282 (m), 1258 (vs), 1219 (m), 1196 (w), 1177 (vw), 1147 (s), 1122 (vw), 1084 (vw), 1070 (vw), 1045 (vw), 1029 (vs), 997 (w), 916 (vw), 888 (vw), 853 (vw), 806 (w), 778 (w), 762 (m), 752 (w), 734 (vw), 705 (vw), 690 (vw), 633 (vs), 572 (w), 516 (m), 466 (m), 438 (vw), 419 (vw), 409 (vw); **¹H NMR (CD₃CN, 263 K, in ppm):** $\delta = 0.85$ -1.16 (m, CH/CH₂), 1.18-1.36 (m, CH/CH₂), 1.36-1.46 (m, CH/CH₂), 1.46-1.56 (m, CH/CH₂), 1.58-1.66 (m, CH/CH₂), 1.66-1.88 (m, CH/CH₂), 2.00-2.07 (m, CH/CH₂), 2.07-2.17 (m, CH/CH₂), 7.09-7.14 (m, C2-H), 7.17-7.21 (m, C2-H), 7.37-7.43 (m, C3-H), 7.60-7.64 (m, C3-H), 7.73-7.78 (m, C3-H), 8.01-8.08 (m, C4-H), 8.11-8.16 (m, C4/C1-H), 8.83-8.87 (m, C1-H); **¹³C{¹H} NMR (CD₃CN, 263 K, in ppm):** $\delta = 25.9$ (m, CH/CH₂), 26.1 (m, CH/CH₂), 27.9 (m, CH/CH₂), 28.2 (m, CH/CH₂), 28.4 (m, CH/CH₂), 28.8 (m, CH/CH₂), 32.6 (m, CH/CH₂), 32.8 (m, CH/CH₂), 33.5 (m, CH/CH₂), 33.7 (m, CH/CH₂), 34.6 (m, CH/CH₂), 34.9 (m, CH/CH₂), 36.2 (m, CH/CH₂), 36.9 (m, CH/CH₂), 116.2 (d, ⁴J_{CP} = 21 Hz, C2), 122.1 (2C, q, ¹J_{CF} = 320 Hz, CF₃), 125.5 (d, ⁴J_{CP} = 3 Hz, C2), 128.2 (d, ³J_{CP} = 40 Hz, C3), 131.4 (d, ³J_{CP} = 8 Hz, C3), 137.0 (dd, ²J_{CP} = 51 Hz, ³J_{CP} = 17 Hz, C4), 140.7 (dd, ²J_{CP} = 64 Hz, ³J_{CP} = 13 Hz, C4), 153.9 (s, C1), 154.8 (s, C1), 155.8 (dt, ¹J_{CP} = 98 Hz, ²J_{CP} = 30 Hz, C5); **¹⁹F NMR (CD₃CN, 263 K, in ppm):** $\delta = -78.5$ (3F, s); **³¹P NMR (CD₃CN, 263 K, in ppm):** isomer 1: AA'XX'X''X''' spin system: $\delta(P_A) = -48.5$ (2P), $\delta(P_X) = 29.3$ (4P); isomer 2 AA'XX'X''X''' spin system: $\delta(P_A) = -51.5$ (2P), $\delta(P_X) = 36.1$ (4P); coupling constants

could not be determined; **elemental analysis**: calcd. for $C_{60}H_{96}Ag_2F_6N_2O_6P_6S_2$: C: 47.38, H: 6.36, N: 1.84, S: 4.22; found: C: 47.59, H: 6.14, N: 1.96, S: 3.75.

12.3.6. Preparation of $[(48Cu)_2][OTf]_2$

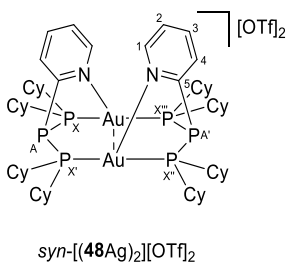
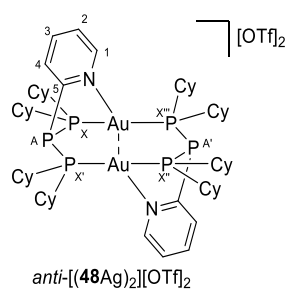


To triphosphane **48a** (100 mg, 0.199 mmol) in CH_2Cl_2 (2 ml) $[(MeCN)_4Cu][OTf]$ (75 mg, 0.199 mmol) is added to form a yellow solution. After stirring for 1 h all volatiles are evaporated *in vacuo*. The yellow residue is recrystallized by slow vapor diffusion of *n*-pentane into a CH_2Cl_2 solution at $-30\text{ }^\circ\text{C}$. This yields the product

as light-yellow crystals which are isolated by filtration, washing with *n*-pentane (2 x 1 ml) and subsequent evaporation of all volatiles.

Yield: 134 mg (94%); **m.p.:** $266\text{ }^\circ\text{C}$ (dec.); **Raman (100 mW, 50 scans, 298 K, in cm^{-1}):** $\nu = 3127$ (5), 3063 (17), 2933 (100), 2857 (98), 2660 (6), 1579 (14), 1560 (13), 1446 (37), 1356 (10), 1343 (10), 1292 (13), 1267 (25), 1224 (10), 1200 (14), 1174 (11), 1111 (7), 1083 (8), 1045 (16), 1031 (43), 1005 (52), 850 (15), 815 (19), 754 (12), 707 (20), 640 (7), 572 (7), 520 (19), 462 (6), 437 (7), 372 (6), 347 (10), 311 (9), 286 (5), 235 (10), 216 (10), 192 (16); **IR (ATR, 298 K, in cm^{-1}):** $\nu = 2926$ (w), 2853 (w), 1578 (w), 1448 (w), 1420 (vw), 1355 (vw), 1326 (vw), 1257 (vs), 1221 (m), 1154 (s), 1088 (vw), 1053 (vw), 1028 (s), 1002 (m), 917 (vw), 891 (w), 850 (vw), 816 (vw), 782 (w), 753 (vw), 733 (w), 703 (vw), 635 (vs); **1H NMR (CD_2Cl_2 , 300 K, in ppm):** $\delta = 0.96$ -1.14 (16H, m, CH_2), 1.28-1.49 (8H, m, CH_2), 1.53-1.57 (2H, m, CH_2), 1.62-1.69 (4H, m, CH_2), 1.73-1.82 (6H, m, CH_2), 1.90-2.02 (8H, m, CH_2), 2.03-2.25 (8H, m, CH), 8.17-8.27 (2H, m, C2-H), 8.29-8.40 (4H, m, C3/C4-H), 8.93-8.96 (2H, m, C1-H); **$^{13}C\{^1H\}$ NMR (CD_2Cl_2 , 300 K, in ppm):** $\delta = 25.2$ (m, CH/ CH_2), 27.6 (m, CH/ CH_2), 32.7 (m, CH/ CH_2), 36.1 (m, CH/ CH_2), 120.9 (2C, d, $^1J_{CF} = 321$ Hz, CF_3), 128.8 (2C, d, $^4J_{CP} = 13$ Hz, C2), 135.6 (2C, m, C4), 141.7 (2C, m, C3), 153.1 (2C, s, C1), 158.1 (2C, d, $^1J_{CP} = 39$ Hz, C5); **^{19}F NMR (CD_2Cl_2 , 300 K, in ppm):** $\delta = -78.8$ (6F, s); **^{31}P NMR (CD_2Cl_2 , 300 K, in ppm):** AA'XX'X''X''' spin system: $\delta(P_A) = -39.1$ (2P), $\delta(P_X) = 15.4$ (4P); coupling constants could not be determined; **elemental analysis**: calcd. for $C_{60}H_{96}Cu_2F_6N_2O_6P_6S_2 \cdot 0.5 CH_2Cl_2$: C: 49.27, H: 6.63, N: 1.90, S: 4.35; found: C: 49.09, H: 6.76, N: 1.98, S: 4.26.

12.3.7. Preparation of $[(48Au)_2][OTf]_2$



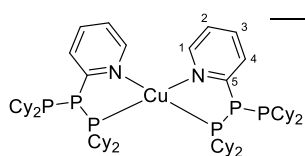
To silver complex $[(48Ag)_2][OTf]_2$ (456 mg, 0.30 mmol) in MeCN (3 ml) (tbt)AuCl (192 mg, 0.60 mmol) is added. The occurring precipitate is filtered off. To the filtrate Et₂O is added until the formation of a faint mist. The mixture is stored at -30 °C. After 16 h colorless crystals of the product are formed which are isolated by filtration and subsequent washing with Et₂O (2 x 2 ml). After evaporation of all volatiles *in vacuo* the product is obtained as a colorless, crystalline solid.

Yield: 327 mg (64%); **m.p.:** 266 °C (dec.); **Raman (100 mW, 50 scans, 298 K, in cm⁻¹):** $\nu = 3076$ (9), 3045 (17), 2944 (100), 2918 (67), 2851 (74), 2666 (6), 1560 (22), 1444 (35), 1351 (14), 1328

(12), 1293 (22), 1270 (31), 1224 (11), 1209 (16), 1178 (14), 1160 (6), 1110 (21), 1080 (10), 1044 (40), 1030 (62), 1003 (21), 986 (38), 851 (21), 816 (30), 754 (16), 742 (12), 707 (22), 620 (7), 572 (8), 542 (15), 519 (9), 437 (9), 396 (11), 373 (5), 348 (14), 334 (12), 313 (15), 220 (19); **IR (ATR, 298 K, in cm⁻¹):** $\nu = 3043$ (vw), 2921 (w), 2848 (w), 1565 (w), 1444 (w), 1422 (w), 1352 (vw), 1326 (vw), 1260 (vs), 1221 (m), 1177 (w), 1148 (vs), 1076 (w), 1043 (w), 1028 (s), 1000 (w), 985 (w), 918 (w), 891 (w), 851 (w), 820 (vw), 777 (m), 752 (w), 635 (vs), 571 (w), 516 (m), 466 (m), 420 (vw); **¹H NMR (CD₂Cl₂, 243 K, in ppm):** $\delta = 0.90$ -1.05 (m, CH/CH₂), 1.08-1.19 (m, CH/CH₂), 1.22-1.42 (m, CH/CH₂), 1.49-1.56 (m, CH/CH₂), 1.56-1.65 (m, CH/CH₂), 1.65-1.73 (m, CH/CH₂), 1.76-1.86 (m, CH/CH₂), 1.94-2.02 (m, CH/CH₂), 2.04-2.14 (m, CH/CH₂), 2.14-2.22 (m, CH/CH₂), 2.28-2.37 (m, CH/CH₂), 7.60-7.64 (m, C2-H), 7.65-7.69 (m, C2-H), 7.90-7.95 (m, C3-H), 7.97-8.02 (m, C4-H), 8.02-8.07 (m, C3/C4-H), 8.47-8.50 (m, C1-H), 8.74-8.77 (m, C1-H); **¹³C{¹H} NMR (CD₂Cl₂, 243 K, in ppm):** $\delta = 25.2$ (m, CH/CH₂), 25.5 (m, CH/CH₂), 27.1 (m, CH/CH₂), 27.7 (m, CH/CH₂), 31.1 (m, CH/CH₂), 31.5 (m, CH/CH₂), 32.7 (m, CH/CH₂), 33.1 (m, CH/CH₂), 33.6 (m, CH/CH₂), 36.9 (m, CH/CH₂), 37.1 (m, CH/CH₂), 121.0 (2C, q, ¹J_{CF} = 321 Hz, CF₃), 126.9 (d, ⁴J_{CP} = 8 Hz, C2), 127.4 (d, ⁴J_{CP} = 9 Hz, C2), 134.0 (m, C3), 135.1 (m, C3), 138.8 (m, C4), 139.2 (m, C4), 151.8 (bs, C1), 152.1 (d, ¹J_{CP} = 22 Hz); **¹⁹F NMR (CD₂Cl₂, 243 K, in ppm):** $\delta = -79.0$ (6F, s); **³¹P NMR (CD₂Cl₂, 243 K, in ppm):** Isomer 1: AA'XX'X''X''' spin system: $\delta(P_A) = \delta(P_{A'}) = -34.2$, $\delta(P_X) = \delta(P_{X'}) = 52.5$, $\delta(P_{X''}) = \delta(P_{X'''}) = 52.6$, ⁴J(P_AP_{A'}) = -5.9 Hz, ¹J(P_AP_X) = -232.0 Hz, ¹J(P_AP_{X'}) = -188.3 Hz, ³J(P_AP_{X''}) = -23.8 Hz, ³J(P_AP_{X'''}) = -23.9 Hz, ³J(P_{A'}P_X) = -3.0 Hz, ³J(P_{A'}P_{X'}) = 50.7 Hz, ¹J(P_{A'}P_{X''}) = -270.6 Hz, ¹J(P_{A'}P_{X'''}) = -245.2 Hz, ²J(P_XP_{X'}) = 40.4 Hz, ⁴J(P_XP_{X''}) = -11.7 Hz, ²J(P_XP_{X'''}) =

244.5 Hz, $^2J(\text{P}_X\text{P}_{X'}) = 261.5$ Hz, $^4J(\text{P}_X\text{P}_{X'}) = 33.4$ Hz, $^2J(\text{P}_{X'}\text{P}_{X''}) = 7.5$ Hz; isomer 2: AA'XX'X''X''' spin system: $\delta(\text{P}_A) = \delta(\text{P}_{A'}) = -37.8$, $\delta(\text{P}_X) = \delta(\text{P}_{X'}) = \delta(\text{P}_{X''}) = \delta(\text{P}_{X'''}) = 50.3$, $^4J(\text{P}_A\text{P}_{A'}) = 0.1$ Hz, $^1J(\text{P}_A\text{P}_X) = -250.4$ Hz, $^1J(\text{P}_A\text{P}_{X'}) = -262.3$ Hz, $^3J(\text{P}_A\text{P}_{X''}) = 12.4$ Hz, $^3J(\text{P}_A\text{P}_{X'''}) = -8.0$ Hz, $^3J(\text{P}_{A'}\text{P}_X) = 29.5$ Hz, $^3J(\text{P}_{A'}\text{P}_{X'}) = -22.7$ Hz, $^1J(\text{P}_{A'}\text{P}_{X''}) = -241.2$ Hz, $^1J(\text{P}_{A'}\text{P}_{X'''}) = -283.2$ Hz, $^2J(\text{P}_X\text{P}_{X'}) = 26.2$ Hz, $^4J(\text{P}_X\text{P}_{X''}) = 1.5$ Hz, $^2J(\text{P}_X\text{P}_{X''}) = 261.0$ Hz, $^2J(\text{P}_X\text{P}_{X'''}) = 251.8$ Hz, $^4J(\text{P}_{X'}\text{P}_{X''}) = 16.1$ Hz, $^2J(\text{P}_{X'}\text{P}_{X''}) = 23.7$ Hz; **elemental analysis:** calcd. for $\text{C}_{60}\text{H}_9\text{Au}_2\text{F}_6\text{N}_2\text{O}_6\text{P}_6\text{S}_2$: C: 42.41, H: 5.69, N: 1.65, S: 3.77; found: C: 42.51, H: 5.67, N: 1.70, S: 3.76.

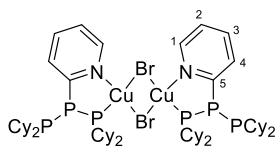
12.3.8. Preparation of [(48)₂Cu][OTf]



To triphosphane **48** (200 mg, 0.397 mmol) in CH_2Cl_2 (0.5 ml) $[(\text{MeCN})_4\text{Cu}][\text{OTf}]$ (75 mg, 0.199 mmol) is added to form a yellow solution. Slow vapor diffusion of *n*-pentane into the reaction mixture at -30 °C over the course of three days leads to the formation of colorless crystals. These are isolated by filtration, washing with *n*-pentane (2 x 1 ml) and evaporation of all volatiles.

Yield: 225 mg (93%); **m.p.:** 189 °C (dec.); **Raman (100 mW, 50 scans, 298 K, in cm^{-1}):** $\nu = 3112$ (7), 3068 (13), 3044 (9), 2934 (99), 2891 (45), 2850 (100), 2659 (7), 1580 (44), 1551 (34), 1443 (44), 1416 (8), 1338 (12), 1293 (18), 1271 (23), 1201 (11), 1169 (6), 1156 (7), 1121 (33), 1087 (10), 1048 (27), 1027 (35), 1000 (46), 850 (15), 817 (20), 751 (6), 736 (10), 722 (11), 710 (15), 633 (6), 510 (5), 470 (11), 433 (9), 379 (6), 347 (6), 313 (8), 227 (13), 207 (13), 179 (12); **IR (ATR, 298 K, in cm^{-1}):** $\nu = 2920$ (s), 2848 (m), 1579 (m), 1551 (w), 1446 (s), 1414 (m), 1340 (w), 1265 (vs), 1221 (m), 1198 (w), 1179 (w), 1143 (s), 1119 (m), 1086 (w), 1048 (w), 1030 (vs), 998 (m), 915 (w), 887 (w), 849 (m), 815 (w), 760 (m), 735 (w), 722 (w), 710 (w), 636 (vs); **^1H NMR (CD_2Cl_2 , 300 K, in ppm):** $\delta = 1.06$ -1.53 (44H, m, CH_2), 1.62-1.73 (20H, m, CH_2), 1.77-1.90 (16H, m, CH_2), 2.00-2.11 (8H, m, CH), 7.11-7.15 (2H, m, C2-H), 7.65-7.70 (2H, m, C3-H), 7.72-7.78 (2H, m, C4-H), 8.35-8.38 (2H, m, C1-H); **$^{13}\text{C}\{^1\text{H}\}$ NMR (CD_2Cl_2 , 300 K, in ppm):** $\delta = 26.6$ (m, CH_2), 27.7 (m, CH_2), 31.2 (m, CH_2), 32.3 (m, CH_2), 34.0 (8C, m, CH), 121.7 (1C, q, $^1J_{\text{CF}} = 321$ Hz, CF_3), 123.1 (2C, s, C2), 130.9 (2C, d, $^2J_{\text{CP}} = 38$ Hz, C4), 137.0 (2C, d, $^3J_{\text{CP}} = 9$ Hz, C3), 151.8 (2C, bs, C1), 161.4 (2C, d, $^1J_{\text{CP}} = 32$ Hz, C5); **^{31}P NMR (CD_2Cl_2 , 300 K, in ppm):** AX₂ spin system: $\delta(\text{P}_A) = -44.8$ ppm (2P), $\delta(\text{P}_X) = -8.9$ ppm (4P); $^1J(\text{P}_A\text{P}_X) = -275$ Hz; **^{19}F NMR (CD_3CN , 300 K, in ppm):** $\delta = -78.9$ (3F, s); **elemental analysis:** calcd. for $\text{C}_{59}\text{H}_9\text{CuF}_3\text{N}_2\text{O}_3\text{P}_6\text{S}$: C: 58.09, H: 7.93, N: 2.30, S: 2.63; found: C: 57.67, H: 7.55, N: 2.61, S: 2.54.

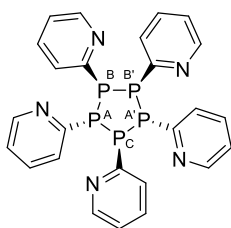
12.3.9. Preparation of (48CuBr)₂



To triphosphane **48** (100 mg, 0.199 mmol) in THF (0.5 ml) (tbt)CuBr (46 mg, 0.199 mmol) is added to form a yellow solution. Slow vapor diffusion of *n*-pentane into the reaction mixture at -30 °C over the course of three days leads to the formation of colorless crystals. These are isolated by filtration, washing with *n*-pentane (2 x 1 ml) and evaporation of all volatiles.

Yield: 120 mg (93%); **m.p.:** 154 °C (dec.); **Raman (100 mW, 50 scans, 298 K, in cm⁻¹):** $\nu = 3051$ (17), 2934 (100), 2894 (39), 2850 (95), 2657 (6), 1575 (23), 1556 (14), 1462 (6), 1443 (27), 1343 (7), 1330 (8), 1298 (9), 1268 (12), 1206 (6), 1187 (8), 1175 (7), 1153 (6), 1118 (9), 1086 (6), 1047 (19), 1027 (18), 1000 (42), 850 (10), 815 (15), 742 (6), 705 (10), 634 (5), 516 (5), 477 (6), 437 (5), 423 (7), 358 (5), 329 (5), 229 (6), 182 (11); **IR (ATR, 298 K, in cm⁻¹):** $\nu = 2919$ (vs), 2846 (vs), 1574 (m), 1555 (w), 1460 (w), 1445 (s), 1416 (m), 1339 (w), 1290 (w), 1267 (w), 1222 (w), 1174 (w), 1152 (w), 1116 (w), 1069 (w), 1046 (w), 1029 (w), 998 (m), 914 (w), 886 (w), 850 (m), 815 (w), 755 (vs), 711 (w), 633 (w); **¹H NMR (CD₂Cl₂, 300 K, in ppm):** $\delta = 1.10$ -1.44 (44H, m, CH₂), 1.60-1.78 (36H, m, CH₂), 1.93-2.05 (8H, m, CH), 7.23-7.35 (2H, m, C2-H), 7.66-7.40 (2H, m, C3-H), 7.74-7.76 (2H, m, C4-H), 8.80-9.00 (2H, m C1-H); **¹³C{¹H} NMR (CD₂Cl₂, 300 K, in ppm):** $\delta = 26.6$ (s, CH₂), 27.7 (m, CH₂), 31.4 (m, CH₂), 32.5 (m, CH₂), 33.9 (8C, m, CH), 123.7 (2C, s, C2), 131.4 (2C, d, ²J_{CP} = 43 Hz, C4), 137.3 (2C, d, ³J_{CP} = 10.4 Hz, C3), 151.3 (2C, bs, C1), 160.3 (2C, bs, C5); **³¹P NMR (CD₂Cl₂, 300 K, in ppm):** AX₂ spin system: $\delta(P_A) = -46.6$ ppm (2 P), $\delta(P_X) = -6.2$ ppm (4P); ¹J(P_AP_X) = -253 Hz; **elemental analysis:** calcd. for C₅₈H₉₆Cu₂Br₂N₂P₆: C: 53.83, H: 7.48, N: 2.16; found: C: 54.12, H: 7.65, N: 1.98.

12.3.10. Preparation of **52**

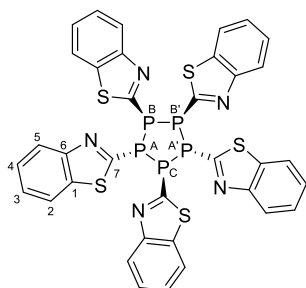


To a solution of dipyrazolylphosphane **41a** (2.275 g, 7.600 mmol) in 20 ml of Et₂O dicyclohexylphosphane (1.5 ml, 7.600 mmol) is added while stirring. After a few moments a colorless precipitate forms. The reaction mixture is stirred for 16 h. After that the precipitate is filtered off and washed with Et₂O (3 x 10 ml). Evaporation of all volatiles *in vacuo* yields the product as a colorless powder.

Yield: 810 mg (98%); **m.p.:** 197 °C; **Raman (100 mW, 298 K, in cm⁻¹):** $\nu = 3133$ (7), 3114 (10), 3042 (76), 2977 (11), 2954 (7), 1571 (69), 1555 (27), 1446 (8), 1417 (15), 1271 (11), 1151 (13), 1129 (31), 1083 (8), 1052 (31), 1044 (41), 986 (100), 712 (14), 619 (13), 517 (8), 493 (7), 439 (42), 417 (15), 408 (15), 399 (15), 383 (20), 290 (7), 271 (14), 243 (11), 230

(13), 203 (25), 161 (35), 133 (41); **IR (ATR, 298 K, in cm^{-1}):** $\nu = 3035$ (w), 2919 (s), 2844 (s), 1569 (s), 1553 (m), 1444 (s), 1413 (s), 1333 (w), 1267 (m), 1191 (w), 1179 (w), 1147 (m), 1120 (w), 1043 (w), 1000 (w), 987 (m), 885 (m), 851 (w), 755 (vs), 739 (s), 711 (m), 618 (m), 514 (w), 483 (s), 463 (w); **^1H NMR (CD_3CN , 300 K, in ppm):** $\delta = 6.98$ -7.02 (2H, m, C2-H), 7.14-7.17 (1H, m, C2-H), 7.17-7.21 (2H, m, C2-H), 7.25-7.29 (2H, m, C4-H), 7.33-7.37 (2H, m, C3-H), 7.58-7.67 (3H, m, C3-H), 7.99-8.03 (3H, m, C4-H), 8.04-8.07 (2H, m, C1-H), 8.44-8.46 (2H, m, C1-H), 8.46-8.49 (1H, m, C1-H); **$^{13}\text{C}\{^1\text{H}\}$ NMR (CD_3CN , 300 K, in ppm):** $\delta = 123.0$ (1C, s, C2), 123.6 (2C, s, C2), 123.7 (2C, s, C2), 127.8 (1C, m, C4), 129.5 (4C, m, C4), 136.5 (1C, s, C3), 136.6 (2C, s, C3), 137.0 (2C, s, C3), 150.3 (2C, m, C1), 150.6 (1C, m, C1), 150.9 (2C, m, C1), 162.0 (2C, m, C5), 164.5 (2C, m, C5), 165.2 (1C, m, C5); **^{31}P NMR (CD_3CN , 300 K, in ppm):** AA'BB'C spin system: $\delta(\text{P}_A) = \delta(\text{P}_{A'}) = 14.1$ (2P), $\delta(\text{P}_B) = \delta(\text{P}_{B'}) = 20.3$ (2P), $\delta(\text{P}_C) = 25.1$ (1P); $^2J(\text{P}_A\text{P}_{A'}) = -2.59$ Hz, $^1J(\text{P}_A\text{P}_B) = ^1J(\text{P}_{A'}\text{P}_{B'}) = -242.59$ Hz, $^2J(\text{P}_A\text{P}_{B'}) = ^2J(\text{P}_{A'}\text{P}_B) = -6.74$ Hz, $^1J(\text{P}_A\text{P}_C) = ^1J(\text{P}_{A'}\text{P}_C) = -275.37$ Hz, $^1J(\text{P}_B\text{P}_{B'}) = -327.59$ Hz, $^2J(\text{P}_B\text{P}_C) = ^2J(\text{P}_{B'}\text{P}_C) = 28.00$ Hz; **elemental analysis:** calcd. for $\text{C}_{25}\text{H}_{20}\text{N}_5\text{P}_5$: C: 55.06, H: 3.70, N: 12.84; found: C: 54.87, H: 3.67, N: 12.60.

12.3.11. Preparation of **56**



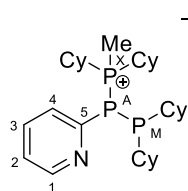
To a solution of diphosphazolyphosphane **43a** (2.00 g, 5.627 mmol) in 20 ml of CH_2Cl_2 dicyclohexylphosphane (1.14 ml, 5.627 mmol) is added while stirring. After stirring for 16 h the reaction mixture is reduced to half of its volume *in vacuo*. Et_2O (10 ml) is added and the reaction mixture is stored at $-30\text{ }^\circ\text{C}$ for 16 h to form a colorless precipitate. The precipitate is filtered off, washed with

n-pentane (2 x 5 ml) and dried *in vacuo* to yield the product as a colorless solid.

Yield: 669 mg (72%); **m.p.:** $188\text{ }^\circ\text{C}$; **Raman (100 mW, 298 K, in cm^{-1}):** $\nu = 3059$ (15), 3026 (5), 1589 (15), 1555 (22), 1454 (45), 1447 (40), 1412 (100), 1312 (8), 1272 (27), 1236 (54), 1124 (20), 1015 (10), 986 (28), 849 (16), 708 (18), 504 (17), 485 (7), 467 (6), 440 (9), 412 (37), 396 (12), 371 (16), 354 (7), 280 (6), 248 (6), 229 (5), 194 (12), 160 (12), 136 (20), 126 (24); **IR (ATR, 298 K, in cm^{-1}):** $\nu = 3058$ (w), 2920 (w), 1555 (vw), 1447 (w), 1412 (m), 1311 (w), 1272 (w), 1234 (w), 1157 (w), 1122 (w), 1073 (w), 1014 (w), 979 (m), 940 (w), 848 (w), 757 (vs), 727 (s), 706 (w), 668 (m), 594 (w), 579 (w), 532 (w), 523 (w), 504 (vw), 458 (vw), 430 (m); **^1H NMR (CD_2Cl_2 , 300 K, in ppm):** $\delta = 7.12$ -7.16 (2H, m, C2-H), 7.17-7.21 (2H, m, C5-H), 7.27-7.31 (1H, m, C5-H), 7.35-7.38 (2H, m, C4-H), 7.39-7.41 (2H, m, C5-H), 7.41-7.42 (1H, m, C2-H), 7.43-7.47 (2H, m, C2-H), 7.63-7.69 (3H, m, C3-

H), 7.83-7.86 (1H, m, C4-H), 7.86-7.89 (2H, m, C3-H), 7.90-7.93 (2H, m, C4-H); $^{13}\text{C}\{^1\text{H}\}$ NMR (CD_2Cl_2 , 300 K, in ppm): $\delta = 121.6$ (2C, s, C3), 121.7 (1C, s, C3), 122.1 (2C, s, C3), 123.1 (1C, s, C4), 123.3 (2C, s, C4), 123.6 (2C, s, C4), 125.7 (1C, s, C5), 126.1 (2C, s, C5), 126.3 (2C, s, C5), 126.6 (2C, s, C2), 126.8 (1C, s, C2), 127.0 (2C, s, C2), 137.8 (1C, m, C1), 138.4 (2C, m, C1), 138.5 (2C, m, C1), 154.5 (2C, m, C6), 155.6 (3C, m, C6), 169.9 (2C, m, C7), 168.5 (2C, m, C7), 165.4 (1C, m, C7); ^{31}P NMR (CD_2Cl_2 , 300 K, in ppm): AA'BB'C spin system: $\delta(\text{P}_A) = \delta(\text{P}_{A'}) = 24.8$ (2P), $\delta(\text{P}_B) = \delta(\text{P}_{B'}) = 31.6$ (2P), $\delta(\text{P}_C) = 38.3$ (1P); $^2J(\text{P}_A\text{P}_{A'}) = 2.35$ Hz, $^1J(\text{P}_A\text{P}_B) = ^1J(\text{P}_{A'}\text{P}_{B'}) = -240.58$ Hz, $^2J(\text{P}_A\text{P}_{B'}) = ^2J(\text{P}_{A'}\text{P}_B) = -2.59$ Hz, $^1J(\text{P}_A\text{P}_C) = ^1J(\text{P}_{A'}\text{P}_C) = -274.52$ Hz, $^1J(\text{P}_B\text{P}_{B'}) = -335.67$ Hz, $^2J(\text{P}_B\text{P}_C) = ^2J(\text{P}_{B'}\text{P}_C) = 32.07$ Hz; **elemental analysis**: calcd. for $\text{C}_{35}\text{H}_{20}\text{N}_5\text{P}_5\text{S}_5$: C: 50.91, H: 2.44, N: 8.48. S: 19.41; found: C: 50.99, H: 2.62, N: 8.30, S: 18.98.

12.3.12. Preparation of 57[OTf]

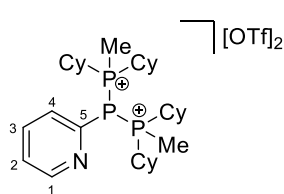


To a solution of **48** (504 mg, 1 mmol) in 3 ml of Et_2O MeOTf (164 mg, 1 mmol) is added while stirring. After 16 h a colorless suspension is formed. The precipitate is filtered off and washed with Et_2O (3 x 3 ml). Evaporation of all volatiles *in vacuo* yields the product as a colorless powder.

Yield: 658 mg (99%); **m.p.:** 127 °C dec.; **Raman (100 mW, 298 K, in cm^{-1}):** $\nu = 3058$ (23), 3019 (6), 2987 (20), 2942 (85), 2923 (77), 2875 (50), 2853 (100), 2680 (5), 2658 (6), 1571 (30), 1561 (21), 1445 (33), 1419 (7), 1330 (9), 1302 (14), 1293 (12), 1274 (22), 1220 (11), 1205 (7), 1191 (7), 1181 (8), 1155 (9), 1122 (19), 1085 (10), 1047 (34), 1029 (45), 991 (33), 973 (5), 849 (13), 819 (23), 752 (13), 734 (8), 715 (15), 700 (11), 623 (6), 572 (8), 517 (6), 481 (12), 468 (13), 455 (10), 433 (8), 401 (11); **IR (ATR, 298 K, in cm^{-1}):** $\nu = 3056$ (w), 3032 (w), 2916 (vs), 2847 (s), 1568 (m), 1558 (w), 1443 (vs), 1420 (m), 1339 (w), 1293 (w), 1262 (w), 1212 (vw), 1188 (w), 1177 (w), 1169 (w), 1153 (w), 1121 (w), 1080 (w), 1045 (w), 1028 (vw), 997 (m), 953 (vw), 914 (vw), 902 (vw), 884 (w), 849 (w), 814 (vw), 763 (s), 747 (w), 735 (vw), 714 (w), 621 (w), 504 (w), 484 (w), 464 (w), 454 (vw), 438 (vw); **^1H NMR (CD_3CN , 300 K, in ppm):** $\delta = 1.10$ -1.40 (14H, m, CH_2), 1.43-1.56 (6H, m, CH_2), 1.61-1.75 (9H, m, CH_2), 1.80-1.88 (7H, m, CH_2), 1.99-2.09 (6H, m, CH, CH_2), 2.59-2.81 (2H, m, CH), 7.41-7.45 (1H, m, C2-H), 7.65-7.69 (1H, m, C4-H), 7.85-7.90 (1H, m, C3-H), 8.63-8.65 (1H, m C1-H); **$^{13}\text{C}\{^1\text{H}\}$ NMR (CD_3CN , 300 K, in ppm):** $\delta = 4.7$ (1C, ddd, $^1J_{\text{CP}} = 39.2$ Hz, $^2J_{\text{CP}} = 7.1$ Hz, $^3J_{\text{CP}} = 5.6$ Hz, CH_3), 26.5 (m, CH_2), 27.1 (m, CH_2), 27.8 (m, CH_2), 28.1 (m, CH_2), 28.8 (m, CH_2), 32.5 (m, CH_2), 33.2 (2C, m, CH), 35.4 (2C, m, CH),

122.6 (1C, q, $^1J_{CF_3} = 321.1$ Hz, CF₃), 125.6 (1C, s, C2), 131.9 (1C, dd, $^2J_{CP} = 46.1$ Hz, $^3J_{CP} = 9.2$ Hz, C4), 138.6 (1C, dd, $^3J_{CP} = 11.9$ Hz, $^4J_{CP} = 2.2$, C3), 152.0 (1C, d, $^3J_{CP} = 3.2$ Hz, C1), 155.3 (1C, dd, $^1J_{CP} = 19.1$ Hz, $^2J_{CP} = 2.9$ Hz, C5); **¹⁹F NMR (CD₃CN, 300 K, in ppm):** $\delta = -79.3$ (3F, s); **³¹P NMR (CD₃CN, 300 K, in ppm):** AMX spin system: $\delta(P_A) = -46.2$ (1P), $\delta(P_M) = -12.9$ (1P), $\delta(P_X) = 34.2$ (1P); $^1J(P_AP_M) = -290.3$ Hz, $^1J(P_AP_X) = -281.0$ Hz, $^2J(P_MP_X) = 58.5$ Hz; **elemental analysis:** calcd. for C₃₁H₅₁F₃NO₃P₃S: C: 55.76, H: 7.70, N: 2.10, S: 4.80; found: C: 55.83, H: 7.83, N: 2.16, S: 4.96.

12.3.13. Preparation of 58[OTf]₂

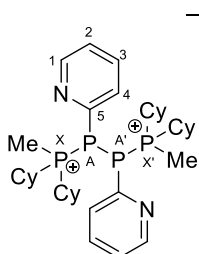


To **48** (250 mg, 0.496 mmol) an excess of MeOTf (407 mg, 2.482 mmol) is added. After stirring for 16 h all volatiles are removed *in vacuo*. Recrystallization from MeCN/Et₂O and subsequent removal of all volatiles *in vacuo* yields the product as colorless crystals.

Yield: 401 mg (97%); **m.p.:** 161 °C dec.; **Raman (100 mW, 298 K, in cm⁻¹):** $\nu = 3068$ (34), 3009 (21), 2940 (100), 2910 (76), 2864 (96), 1614 (23), 1562 (31), 1449 (40), 1356 (27), 1328 (23), 1301 (28), 1278 (33), 1250 (24), 1222 (27), 1180 (24), 1083 (21), 1044 (28), 1030 (56), 992 (27), 849 (24), 816 (29), 757 (27), 702 (24), 574 (21), 520 (19), 444 (20), 431 (20), 348 (19), 313 (17), 212 (21), 136 (19); **IR (ATR, 298 K, in cm⁻¹):** $\nu = 3010$ (vw), 2935 (w), 2861 (w), 1571 (vw), 1561 (vw), 1447 (w), 1424 (vw), 1308 (w), 1260 (vs), 1246 (vs), 1223 (m), 1152 (vs), 1085 (vw), 1029 (vs), 1005 (w), 991 (w), 923 (w), 909 (w), 923 (w), 909 (w), 893 (w), 884 (w), 869 (m), 850 (w), 816 (vw), 774 (w), 757 (w), 701 (vw), 636 (vs), 573 (m), 517 (s), 466 (w), 443 (vw), 432 (vw), 407 (vw); **¹H NMR (CD₃CN, 300 K, in ppm):** $\delta = 0.86$ -0.96 (2H, m, CH₂), 0.98-1.14 (4H, m, CH₂), 1.20-1.31 (2H, m, CH₂), 1.34-1.43 (4H, m, CH₂), 1.47-1.55 (4H, m, CH₂), 1.57-1.62 (2H, m, CH₂), 1.62-1.69 (4H, m, CH₂), 1.71-1.82 (10H, m, CH₂), 1.90-2.06 (4H, m, CH₂), 2.07-2.15 (4H, m, CH₂), 2.30-2.37 (2H, m, CH), 2.39-2.42 (6H, m, CH₃), 2.57-2.67 (2H, m, CH), 7.75-7.79 (1H, m, C2-H), 8.06-8.11 (1H, m, C3-H), 8.23-8.27 (1H, m, C4-H), 8.93-8.95 (1H, m, C1-H); **¹³C{¹H} NMR (CD₃CN, 300 K, in ppm):** $\delta = 6.23$ (2C, m, CH₃), 25.9 (m, CH₂), 26.0 (m, CH₂), 27.4 (m, CH₂), 27.6 (m, CH₂), 27.9 (m, CH₂), 28.2 (m, CH₂), 28.4 (m, CH₂), 29.1 (m, CH₂), 29.3 (m, CH₂), 37.0 (2C, m, CH), 38.0 (2C, m, CH), 122.5 (1C, q, $^1J_{CF_3} = 321.2$ Hz, CF₃), 129.7 (1C, bs, C2), 137.6 (1C, dd, $^2J_{CP} = 54.5$ Hz, $^3J_{CP} = 5.7$ Hz, C4), 141.1 (1C, d, $^3J_{CP} = 15.5$ Hz, C3), 145.9 (1C, dd, $^1J_{CP} = 10.7$ Hz, $^2J_{CP} = 4.3$ Hz, C5), 154.9 (1C, d, $^3J_{CP} = 4.3$ Hz, C1); **¹⁹F NMR (CD₃CN, 300 K, in ppm):** $\delta = -79.2$ (3F, s); **³¹P NMR (CD₃CN, 300 K, in ppm):** AX₂ spin system: $\delta(P_A) = -67.9$ (1P), $\delta(P_X) = 44.0$ (2P); $^1J(P_AP_X) = -315.4$ Hz; **elemental**

analysis: calcd. for $C_{33}H_{54}F_6NO_6P_3S_2$: C: 47.65, H: 6.54, N: 1.68, S: 7.71; found: C: 47.13, H: 6.28, N: 1.69, S: 8.23.

12.3.14. Preparation of $59[OTf]_2$



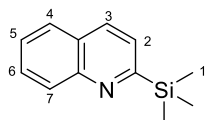
To $58[OTf]_2$ (500 mg, 0.60 mmol) in MeCN (3 ml) pentaphospholane **52** (66 mg, 0.12 mmol) is added. After stirring for 24 h the solvent is evaporated *in vacuo*. The residue is washed with PhF (3 x 4 ml) and recrystallized from MeCN/Et₂O to yield the product as colorless crystals after filtration and evaporation of

all volatiles *in vacuo*.

Yield: 287 mg (51%); **m.p.:** 181 °C dec.; **Raman (100 mW, 298 K, in cm^{-1}):** $\nu = 3063$ (43), 2982 (24), 2946 (89), 2915 (75), 2895 (57), 2856 (75), 1620 (21), 1573 (53), 1562 (35), 1522 (19), 1451 (52), 1350 (25), 1334 (25), 1308 (58), 1299 (39), 1283 (39), 1255 (21), 1223 (22), 1209 (25), 1185 (19), 1176 (20), 1120 (27), 1093 (20), 1080 (27), 1048 (61), 1032 (100), 991 (66), 851 (25), 821 (42), 770 (25), 753 (39), 724 (20), 706 (39), 625 (25), 572 (29), 530 (25), 518 (26), 500 (48), 479 (31), 436 (27), 426 (43), 410 (35), 356 (38), 347 (44); **IR (ATR, 298 K, in cm^{-1}):** $\nu = 3063$ (vw), 2981 (vw), 2936 (w), 2858 (w), 1572 (w), 1558 (vw), 1449 (w), 1426 (vw), 1351 (vw), 1307 (vw), 1299 (w), 1268 (s), 1253 (vs), 1222 (m), 1184 (vw), 1176 (w), 1139 (s), 1079 (vw), 1030 (vs), 1007 (w), 989 (w), 930 (w), 918 (w), 906 (m), 886 (w), 869 (vw), 849 (vw), 820 (vw), 776 (m), 752 (w), 703 (vw), 635 (vs), 571 (w), 516 (s), 492 (w), 466 (w), 441 (vw), 427 (vw), 405 (vw); **1H NMR (CD_2Cl_2 , 300 K, in ppm):** $\delta = 0.94$ -1.14 (4H, m, CH₂), 1.17-1.24 (4H, m, CH₂), 1.31-1.44 (6H, m, CH₂), 1.54-1.75 (12H, m, CH₂), 1.80-1.88 (6H, m, CH₂), 2.00-2.08 (4H, m, CH₂), 2.09-2.23 (4H, m, CH₂), 2.23-2.32 (2H, m, CH), 2.40-2.44 (6H, m, CH₃), 2.81-2.89 (2H, m, CH), 7.28-7.32 (1H, m, C2-H), 7.82-7.87 (1H, m, C3-H), 7.97-7.99 (1H, m, C1-H), 8.20-8.24 (1H, m, C4-H); **$^{13}C\{^1H\}$ NMR (CD_2Cl_2 , 300 K, in ppm):** $\delta = 4.5$ (2C, m, CH₃), 25.6 (m, CH₂), 25.9 (m, CH₂), 26.8 (m, CH₂), 27.1 (m, CH₂), 27.9 (m, CH₂), 28.1 (m, CH₂), 28.5 (m, CH₂), 28.7 (m, CH₂), 35.2 (2C, m, CH), 35.7 (2C, m, CH), 121.6 (1C, q, $^1J_{CF_3} = 322.2$ Hz, CF₃), 126.3 (1C, s, C2), 135.9 (1C, m, C4), 138.6 (1C, m, C3), 150.3 (1C, m, C5), 151.3 (1C, bs, C1); **^{19}F NMR (CD_2Cl_2 , 300 K, in ppm):** $\delta = -79.2$ (3F, s); **^{31}P NMR (CD_2Cl_2 , 300 K, in ppm):** AA'XX' spin system: $\delta(P_A) = -55.1$ (2P), $\delta(P_X) = 40.7$ (2P); $^1J(P_AP_{A'}) = -298.7$ Hz, $^1J(P_AP_X) = -287.0$ Hz, $^2J(P_AP_{X'}) = 58.6$ Hz, $^3J(P_XP_{X'}) = 38.9$ Hz; **elemental analysis:** calcd. for $C_{38}H_{58}F_6N_2O_6P_4S_2$: C: 48.51, H: 6.21, N: 2.98, S: 6.81; found: C: 48.50, H: 5.83, N: 3.13, S: 6.99.

12.4. Syntheses and Characterization Data regarding Compounds in Chapter 5

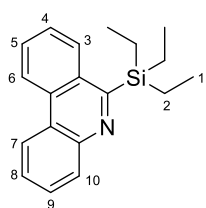
12.4.1. Preparation of 2-(Trimethylsilyl)quinoline



Synthesized according to a modified literature procedure.¹⁵² A Solution of *n*-butyllithium in hexanes (100 ml, 250 mmol) is cooled to 0 °C. To this dimethylaminoethanol (12.5 ml, 125 mmol) in *n*-hexane (80 ml) is added dropwise while keeping the temperature at 0 °C. Then the mixture is cooled to -100 °C and a solution of quinoline (3.7 ml, 31.25 mmol) in *n*-hexane (50 ml) is added dropwise. The so obtained crimson solution is stirred for 30 min at -100 °C before adding a solution of trimethylsilylchloride (20 ml, 156.3 mmol) in Et₂O (80 ml) dropwise. The reaction mixture is allowed to rise to room temperature and is carefully diluted with water (250 ml). The aqueous phase is extracted with pentane three times. The combined organic layers are dried over MgSO₄ and concentrated *in vacuo* after filtration. The obtained yellow oil is distilled (T = 49 °C; p = 8 x 10⁻³ mbar) to obtain the product as a pale-yellow oil. The spectral data are in accordance with the ones reported in the literature.¹⁵²

Yield: 1.717 g (27 %); **¹H NMR (CDCl₃, 300 K, [ppm]):** δ = 0.44 (9H, s, C1–H), 7.48-7.53 (1H, m, C5–H), 7.60-7.62 (1H, m, C2–H), 7.67-7.72 (1H, m, C6–H), 7.75-7.78 (1H, m, C4–H), 8.03-8.05 (1H, m, C3–H), 8.18-8.21 (1H, m, C7–H). **²⁹Si{¹H} NMR (CDCl₃, 300 K, [ppm]):** δ = -5.0 (1Si, s).

12.4.2. Preparation of 6-(Triethylsilyl)phenanthridine

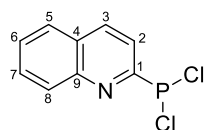


Synthesized according to a modified literature procedure.¹⁵³ A Suspension of 2-isocyano-1,1'-biphenyl (2.00 g, 11.16 mmol), triethylsilane (8.9 ml, 55.80 mmol), *tert*-butyl hydroperoxide (10.7 ml, 78.12 mmol, 70% in water), *p*-benzoquinone (362 mg, 3.348 mmol) and caesium carbonate (10.91 g, 33.48 mmol) in propionitrile is refluxed for 16 h under nitrogen. The reaction mixture is then filtrated through a pad of silica gel and concentrated *in vacuo* to yield the crude product as an orange-red oil. After column chromatography (100 % petrol ether 40/60; R_f = 0.7) and subsequent evaporation of all volatiles the product is obtained as a pale-yellow oil. The spectral data are in accordance with the ones reported in the literature.¹⁵³

Yield: 784 mg (24 %); **¹H NMR (CDCl₃, 300 K, [ppm]):** δ = 1.04-1.10 (9H, m, C1–H), 1.13-1.18 (6H, m, C2–H), 7.63-7.75 (3H, m), 7.78-7.83 (1H, m), 8.23-8.27 (1H, m), 8.29-

8.34 (1H, m), 8.56-8.59 (1H, m), 8.64-8.68 (1H, m). $^{29}\text{Si}\{^1\text{H}\}$ NMR (CDCl_3 , 300 K, [ppm]): $\delta = 2.9$ (1Si, s).

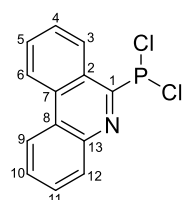
12.4.3. Preparation of 65



2-(Trimethylsilyl)quinoline (1.717 g, 8.528 mmol) and PCl_3 (2.2 ml, 25.58 mmol) are placed in a Schlenk flask and heated under reflux for 48 h. After evaporation of all volatiles, the residue is recrystallized from $\text{CH}_2\text{Cl}_2/n$ -pentane to afford the product as a red, crystalline solid.

Yield: 760 mg (39 %); **m.p.:** 135 °C; **Raman:** Due to fluorescence a suitable Raman spectra could not be obtained; **IR (ATR, 298 K, in cm^{-1}):** $\nu = 3070$ (vw), 2957 (vw), 2899 (vw), 2318 (w), 2001 (w), 1639 (vw), 1593 (w), 1491 (w), 1418 (w), 1385 (w), 1325 (w), 1298 (w), 1250 (w), 1239 (w), 1223 (w), 1151 (vw), 1137 (w), 1015 (w), 948 (w), 870 (vs), 859 (vs), 835 (vs), 825 (vs), 763 (vs), 711 (w), 640 (m), 617 (w), 590 (vw), 524 (w), 475 (s), 442 (w); **^1H NMR (CD_2Cl_2 , 300 K, in ppm):** $\delta = 7.66$ -7.70 (1H, m, C6-H), 7.80-7.84 (1H, m, C7-H), 7.89-7.92 (1H, m, C5-H), 8.14-8.17 (1H, m, C8-H), 8.18-8.20 (1H, m, C2-H), 8.35-8.38 (1H, m, C3-H); **$^{13}\text{C}\{^1\text{H}\}$ NMR (CD_2Cl_2 , 300 K, in ppm):** $\delta = 120.5$ (1C, d, $^2J_{\text{CP}} = 10.9$ Hz, C2), 128.5 (1C, s, C5), 129.0 (1C, s, C4), 129.3 (1C, s, C6), 130.3 (1C, s, C8), 131.2 (1C, s, C7), 138.2 (1C, s, C3), 147.6 (1C, d, $^3J_{\text{CP}} = 22.8$ Hz, C9), 164.4 (1C, d, $^1J_{\text{CP}} = 30.0$ Hz, C1); **^{31}P NMR (CD_2Cl_2 , 300 K, in ppm):** $\delta = 136.0$ (1P, s); **elemental analysis:** calcd. for $\text{C}_9\text{H}_6\text{NPCl}_2$: C: 46.99, H: 2.63, N: 6.09; found: C: 47.49, H: 2.50, N 6.04.

12.4.4. Preparation of 66

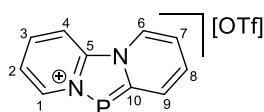


6-(Triethylsilyl)phenanthridine (784 mg, 2.671 mmol) and PCl_3 (0.7 ml, 8.014 mmol) are placed in a Schlenk flask and heated under reflux for 48 h. After evaporation of all volatiles the residue is sublimated ($T = 140$ °C, $p = 8 \times 10^{-3}$ mbar) to yield the product as colorless crystals.

Yield: 532 mg (71 %); **m.p.:** 191 °C; **Raman (80 mW, 250 scans, 298 K, in cm^{-1}):** $\nu = 3099$ (17), 3088 (42), 3077 (58), 3065 (100), 3036 (50), 3017 (21), 1614 (17), 1608 (29), 1578 (21), 1571 (25), 1443 (17), 1436 (25), 1406 (38), 1399 (38), 1357 (83), 1351 (92), 1344 (21), 1294 (13), 1287 (8), 1243 (13), 1236 (13), 1048 (8), 1038 (13), 751 (13), 715 (38), 707 (8), 481 (67), 473 (33), 420 (67), 413 (13), 255 (38), 237 (25), 162 (75), 129 (33); **IR (ATR, 298 K, in cm^{-1}):** $\nu = 3064$ (w), 3036 (w), 2955 (w), 2922 (w), 2853 (w), 1609 (w), 1573 (w), 1553 (w), 1518 (w), 1482 (w), 1455 (m), 1438 (m), 1417 (w), 1401 (w), 1346 (m), 1283 (w), 1202 (w), 1157 (w), 1136 (w), 1032 (w), 1004 (w), 979 (w), 951 (w), 872 (w), 757 (vs), 721 (s), 709 (m), 609 (m), 550 (m), 463 (vs), 433 (s), 416 (s); **^1H NMR (CD_2Cl_2 , 300 K, in**

ppm): $\delta = 7.78-7.84$ (3H, m, C6/C11/C12-H), $7.92-7.96$ (1H, m, C5-H), $8.25-8.27$ (1H, m, C10-H), $8.60-8.63$ (1H, m, C9-H), $8.71-8.74$ (1H, m, C4-H), $8.96-8.99$ (1H, m, C3-H); **$^{13}\text{C}\{^1\text{H}\}$ NMR (CD_2Cl_2 , 300 K, in ppm):** $\delta = 122.9$ (1C, s, C9), 123.6 (1C, s, C4), 125.2 (1C, d, $^2J_{\text{CP}} = 12.7$ Hz, C2), 125.6 (1C, s, C8), 127.5 (1C, d, $^3J_{\text{CP}} = 9.6$ Hz, C3), 128.2 (1C, s, C6), 129.9 (1C, s, C11), 130.1 (1C, s, C12), 131.5 (1C, s, C10), 132.0 (1C, s, C5), 133.7 (1C, s, C7), 143.1 (1C, d, $^3J_{\text{CP}} = 23.9$ Hz, C13), 163.0 (1C, d, $^1J_{\text{CP}} = 44.9$ Hz, C1); **^{31}P NMR (CD_2Cl_2 , 300 K, in ppm):** $\delta = 143.6$ (1P, s); **elemental analysis:** calcd. for $\text{C}_{13}\text{H}_8\text{NPCl}_2$: C: 55.75, H: 2.88, N: 5.00; found: C: 56.34, H: 2.87, N 5.03.

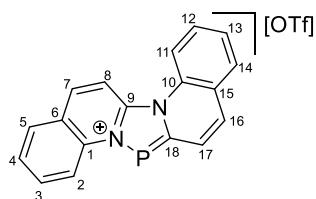
12.4.5. Preparation of **61**[OTf]



Dichlorophosphane **40** (3.908 g, 21.714 mmol) is dissolved in *o*- $\text{C}_6\text{H}_4\text{Cl}_2$ (20 ml). To this solution is added Me_3SiOTf (3.90 ml, 21.714 mmol) while stirring. The reaction mixture is stirred at 110°C for 16 h to obtain a bright yellow precipitate. After cooling to r.t. Et_2O (10 ml) is added to the reaction mixture for further precipitation of the product, which is then filtered off, washed with Et_2O (3 x 10 ml) and dried *in vacuo* to afford the product as a bright yellow crystalline solid.

Yield: 3.650 g (86 %); **m.p.:** $177-180^\circ\text{C}$; **Raman (75 mW, 128 scans, 298 K, in cm^{-1}):** $\nu = 3115(4)$, $3089(7)$, $1620(28)$, $1552(19)$, $1522(19)$, $1477(16)$, $1460(35)$, $1336(13)$, $1309(100)$, $1280(9)$, $1254(13)$, $1125(5)$, $1078(27)$, $1058(12)$, $1031(13)$, $1017(7)$, $988(18)$, $776(8)$, $755(6)$, $723(14)$, $694(15)$, $519(6)$, $500(35)$, $424(26)$, $402(10)$, $349(5)$, $315(5)$, $260(5)$, $234(13)$; **IR (ATR, 298 K, in cm^{-1}):** $\nu = 3117(\text{w})$, $3038(\text{vw})$, $1624(\text{w})$, $1550(\text{vw})$, $1520(\text{w})$, $1476(\text{w})$, $1457(\text{w})$, $1444(\text{w})$, $1352(\text{vw})$, $1308(\text{vw})$, $1278(\text{w})$, $1266(\text{m})$, $1252(\text{m})$, $1223(\text{m})$, $1156(\text{m})$, $1137(\text{m})$, $1096(\text{w})$, $1076(\text{w})$, $1056(\text{w})$, $1030(\text{m})$, $986(\text{w})$, $787(\text{w})$, $747(\text{m})$, $731(\text{w})$, $692(\text{w})$, $635(\text{m})$, $622(\text{m})$; **^1H NMR (CD_3CN , 300 K, in ppm):** $\delta = 7.28-7.32$ (1H, m, C7-H), $7.45-7.49$ (1H, m, C9-H), $7.66-7.70$ (1H, m, C4-H), $8.18-8.23$ (1H, m, C3-H), $8.27-8.30$ (1H, m, C8-H), $8.66-8.68$ (1H, m, C2-H), $9.06-9.08$ (1H, m, C6-H), $9.16-9.19$ (1H, m, C1-H); **$^{13}\text{C}\{^1\text{H}\}$ NMR (CD_3CN , 300 K, in ppm):** $\delta = 115.7$ (1C, d, $^3J_{\text{CP}} = 5.0$ Hz, C2), 118.4 (1C, s, C7), 121.6 (1C, d, $^3J_{\text{CP}} = 6.5$ Hz, C4), 122.8 (1C, q, $^1J_{\text{CF}} = 320.2$ Hz, CF_3), 124.8 (1C, d, $^3J_{\text{CP}} = 17.3$ Hz, C8), 129.3 (1C, d, $^2J_{\text{CP}} = 20.4$ Hz, C9), 129.5 (1C, bs, C6), 137.0 (1C, d, $^4J_{\text{CP}} = 1.7$ Hz, C3), 138.5 (1C, d, $^2J_{\text{CP}} = 19.3$ Hz, C1), 167.7 (1C, d, $^1J_{\text{CP}} = 59.1$ Hz, C10); **^{19}F NMR (CD_3CN , 300 K, in ppm):** $\delta = -79.2$ (3F, s); **^{31}P NMR (CD_3CN , 300 K, in ppm):** $\delta = 152.9$ (1P, *pseudo t*, $^1J_{\text{PN}} = 42.8$ Hz); **elemental analysis:** calcd. for $\text{C}_{11}\text{H}_8\text{F}_3\text{N}_2\text{O}_3\text{PS}$: C: 39.30, H: 2.40, N: 8.33, S: 9.54; found: C: 38.85, H: 2.14, N: 8.10, S: 8.94.

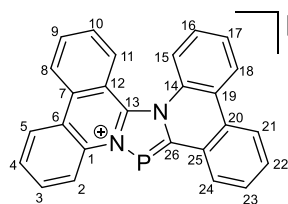
12.4.6. Preparation of **62**[OTf]



Dichlorophosphane **65** (200 mg, 0.869 mmol) is dissolved in *o*-C₆H₄Cl₂ (5 ml). To this solution is added Me₃SiOTf (0.16 ml, 0.869 mmol) while stirring. The reaction mixture is stirred at 110 °C for 16 h. To the reaction mixture is added *n*-pentane (10 ml) to precipitate the crude product, which is filtered off, washed with *n*-pentane (2 x 5 ml) and dried *in vacuo*. The crude product is recrystallized from MeCN/Et₂O to afford the product as an orange solid.

Yield: 94 mg (50 %); **m.p.:** 171 °C; **Raman (80 mW, 250 scans, 298 K, in cm⁻¹):** $\nu = 1609$ (56), 1554 (63), 1516 (49), 1449 (88), 1429 (50), 1376 (60), 1355 (92), 1324 (96), 1283 (56), 1232 (58), 1191 (69), 1159 (62), 1113 (65), 1052 (63), 861 (74), 474 (86), 398 (87), 375 (100), 340 (92), 312 (90), 283 (92), 224 (91), 174 (90), 151 (93); **IR (ATR, 298 K, in cm⁻¹):** $\nu = 3057$ (w), 1606 (m), 1562 (m), 1515 (w), 1446 (w), 1427 (w), 1386 (w), 1372 (w), 1352 (w), 1256 (vs), 1220 (s), 1140 (vs), 1026 (vs), 875 (m), 805 (s), 778 (s), 754 (s), 738 (m), 633 (vs), 571 (s), 539 (m), 514 (vs), 492 (s), 471 (m), 406 (m); **¹H NMR (CD₃CN, 300 K, in ppm):** $\delta = 7.75$ -7.78 (1H, m, C8-H), 7.79-7.83 (1H, m, C12-H), 7.89-7.92 (1H, m, C2-H), 7.94-7.96 (1H, m, C11-H), 8.05-8.10 (2H, m, C3/C4-H), 8.12-8.15 (1H, m, C16-H), 8.29-8.31 (1H, m, C14-H), 8.63-8.68 (2H, m, C7/17-H), 8.70-8.72 (1H, m, C13-H), 8.91-8.94 (1H, m, C5-H); **¹³C{¹H} NMR (CD₃CN, 300 K, in ppm):** $\delta = 115.8$ (1C, d, ⁴J_{CP} = 4.6 Hz, C5), 120.3 (1C, d, ²J_{CP} = 24.4 Hz, C17), 120.4 (1C, s, C13), 121.2 (1C, d, ³J_{CP} = 20.0 Hz, C16), 122.4 (1C, q, ¹J_{CF} = 320.8 Hz, CF₃), 125.5 (1C, d, ⁴J_{CP} = 2.7 Hz, C15), 128.2 (1C, d, ³J_{CP} = 2.7 Hz, C10), 130.1 (1C, s, C8), 130.3 (1C, s, C12), 131.0 (1C, s, C11), 131.1 (1C, d, ³J_{CP} = 2.7 Hz, C2), 131.6 (1C, d, ⁵J_{CP} = 2.2 Hz, C4), 131.9 (1C, s, C14), 134.6 (1C, d, ⁴J_{CP} = 3.3 Hz, C3), 135.6 (1C, s, C6), 138.6 (1C, d, ²J_{CP} = 9.6 Hz, C1), 139.4 (1C, d, ⁴J_{CP} = 1.5 Hz, C7), 147.8 (1C, d, ²J_{CP} = 4.4 Hz, C9), 168.3 (1C, d, ¹J_{CP} = 50.0 Hz, C18); **¹⁹F NMR (CD₃CN, 300 K, in ppm):** $\delta = -79.3$ (3F, s); **³¹P NMR (CD₃CN, 300 K, in ppm):** $\delta = 140.8$ (1P, s); **elemental analysis:** calcd. for C₁₉H₁₂F₃N₂O₃PS: C: 52.30, H: 2.77, N: 6.42, S: 7.35; found: C: 51.75, H: 2.81, N: 6.47, S: 7.97.

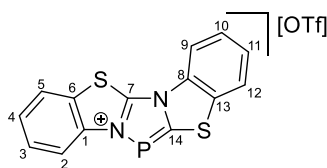
12.4.7. Preparation of **63**[OTf]



Dichlorophosphane **66** (400 mg, 1.428 mmol) is suspended in *o*-C₆H₄Cl₂ (6 ml). To this suspension is added Me₃SiOTf (0.26 ml, 1.428 mmol) while stirring. The reaction mixture is stirred at 110 °C for 16 h. To this suspension is added Et₂O (5 ml) to precipitate more product, which is filtered off, washed with Et₂O (2 x 5 ml) and dried *in vacuo* to obtain the product as a yellow solid.

Yield: 304 mg (79 %); **m.p.:** 317-318 °C; **Raman (80 mW, 500 scans, 298 K, in cm⁻¹):** $\nu = 1606$ (81), 1589 (33), 1560 (30), 1513 (30), 1495 (37), 1468 (22), 1458 (22), 1438 (63), 1421 (59), 1403 (100), 1362 (59), 1352 (56), 1342 (52), 1333 (56), 1280 (48), 1227 (22), 1173 (26), 1160 (22), 1093 (15), 1053 (41), 1034 (22), 1010 (15), 896 (19), 757 (22), 666 (26), 409 (30), 299 (19), 152 (22), 127 (30); **IR (ATR, 298 K, in cm⁻¹):** $\nu = 3064$ (w), 1603 (w), 1561 (w), 1492 (m), 1464 (w), 1456 (w), 1439 (w), 1419 (m), 1401 (w), 1262 (vs), 1223 (s), 1171 (m), 1142 (s), 1049 (w), 1029 (vs), 960 (w), 873 (w), 815 (w), 784 (w), 754 (vs), 720 (s), 706 (m), 689 (m), 666 (w), 634 (vs), 611 (m), 601 (m), 593 (m), 571 (m), 515 (s), 485 (w), 467 (w), 448 (w), 429 (m); **¹H NMR (CD₃CN, 300 K, [ppm]):** $\delta = 7.49$ -7.53 (1H, m, C17-H), 7.65-7.69 (1H, m, C8-H), 7.74-7.81 (2H, m, C3/C11-H), 7.89-7.93 (1H, m, C24-H), 7.95-8.03 (2H, m, C5/C21-H), 8.04-8.07 (1H, m, C22-H), 8.07-8.11 (1H, m, C9-H), 8.40-8.43 (2H, m, C10/C16-H), 8.55-8.59 (3H, m, C2/C15/18-H), 8.81-8.84 (1H, m, C4-H), 8.85-8.87 (1H, m, C23-H); **¹³C{¹H} NMR (CD₃CN, 300 K, [ppm]):** $\delta = 120.7$ (1C, d, ³J_{CP} = 25.7 Hz, C2), 120.7 (1C, d, ³J_{CP} = 3.7 Hz, C12), 122.6 (1C, q, ¹J_{CF} = 320.4 Hz, CF₃), 123.3 (1C, d, C22), 124.4 (1C, d, ³J_{CP} = 3.0 Hz, C6), 125.1 (1C, s, C18), 125.8 (1C, s, C8), 126.3 (1C, s, C23), 126.7 (1C, d, ³J_{CP} = 11.5 Hz, C20), 127.0 (1C, s, C14), 127.1 (1C, s, C15), 127.3 (1C, s, C10), 127.7 (1C, s, C16), 128.1 (1C, d, ²J_{CP} = 11.6 Hz, C25), 129.3 (1C, s, C8), 129.5 (1C, s, C17), 131.2 (1C, s, C11), 131.2 (1C, s, C5), 131.6 (1C, s, C3), 133.0 (1C, d, ⁴J_{CP} = 2.5 Hz, C21), 133.8 (1C, s, C7), 134.2 (1C, d, ⁴J_{CP} = 1.8 Hz, C19), 134.8 (1C, d, ³J_{CP} = 4.3 Hz, C24), 135.1 (1C, d, ²J_{CP} = 9.7 Hz, C1), 136.0 (1C, s, C9), 149.1 (1C, d, ²J_{CP} = 4.1 Hz, C13), 173.3 (1C, d, ¹J_{CP} = 49.3 Hz, C26); **¹⁹F NMR (CD₃CN, 300 K, in ppm):** $\delta = -79.3$ (3F, s); **³¹P NMR (CD₃CN, 300 K, in ppm):** $\delta = 146.3$ (1P); **elemental analysis:** calcd. for C₂₇H₁₆F₃N₂O₃PS: C: 60.45, H: 3.01, N: 5.22, S: 5.98; found: C: 59.87, H: 3.06, N: 5.14, S: 6.24.

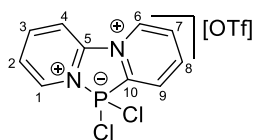
12.4.8. Preparation of **64**[OTf]



Dichlorophosphane **42** (300 mg, 1.271 mmol) is dissolved in *o*-C₆H₄Cl₂ (5 ml). To this solution is added Me₃SiOTf (0.23 ml, 1.271 mmol) while stirring. The reaction mixture is stirred at 110 °C for 16 h. The so obtained suspension is filtered. The residue is washed with Et₂O (2 x 5 ml) and dried *in vacuo* to obtain the product as an off-white solid.

Yield: 218 mg (76 %); **m.p.:** 230 °C; **Raman (80 mW, 250 scans, 298 K, [cm⁻¹]):** ν = 3081 (22), 3063 (22), 1599 (22), 1581 (39), 1502 (26), 1465 (48), 1384 (52), 1370 (13), 1338 (100), 1309 (43), 1286 (17), 1270 (17), 1238 (13), 1189 (26), 1180 (17), 1142 (43), 1134 (39), 1030 (39), 756 (13), 699 (13), 659 (26), 594 (13), 512 (17), 444 (26), 429 (17), 389 (17), 375 (48), 351 (13), 314 (26), 290 (13), 240 (17), 232 (13), 164 (22), 152 (13); **IR (ATR, 298 K, [cm⁻¹]):** ν = 3088 (w), 3060 (w), 1497 (m), 1456 (w), 1381 (w), 1281 (s), 1247 (vs), 1221 (vs), 1162 (s), 1146 (s), 1128 (s), 1068 (w), 1028 (vs), 980 (m), 946 (w), 931 (w), 910 (w), 794 (m), 759 (vs), 741 (vs), 712 (m), 695 (w), 631 (vs), 592 (w), 572 (m), 513 (s), 495 (m), 443 (w), 425 (s); **¹H NMR (CD₃CN, 300 K, [ppm]):** δ = 7.72-7.75 (1H, m, C9-H), 7.77-7.81 (2H, m, C5/10-H), 7.82-7.86 (1H, m, C3-H), 8.05-8.07 (1H, m, C12-H), 8.08-8.10 (1H, m, C11-H), 8.23-8.25 (1H, m, C2-H), 8.29-8.31 (1H, m, C4-H); **¹³C{¹H} NMR (CD₃CN, 300 K, [ppm]):** δ = 116.1 (1C, s, C11), 117.8 (1C, d, ³J_{CP} = 6.0 Hz, C2), 122.5 (1C, q, ¹J_{CF} = 322.2 Hz, CF₃), 125.7 (1C, s, C12), 126.9 (1C, s, C9), 129.3 (1C, s, C10), 130.0 (1C, s, C9), 130.1 (1C, s, C5), 130.4 (1C, s, C6), 130.5 (1C, s, C3), 134.3 (1C, d, ³J_{CP} = 2.3 Hz, C8), 134.8 (1C, d, ³J_{CP} = 2.2 Hz, C13), 137.6 (1C, d, ²J_{CP} = 7.2 Hz, C1), 149.7 (1C, bs, C7), 178.8 (1C, d, ¹J_{CP} = 92.7 Hz, C14); **¹⁹F NMR (CD₃CN, 300 K, [ppm]):** δ = -79.2 (3F, s); **³¹P NMR (CD₃CN, 300 K, [ppm]):** δ = 141.7 (1P, s); **elemental analysis:** calcd. for C₁₃H₈F₃N₂O₃PS₃: C: 40.18, H: 1.80, N: 6.25, S: 21.45; found: C: 39.92, H: 1.56, N: 6.21, S: 21.62.

12.4.9. Preparation of **61**^{Cl2}[OTf]

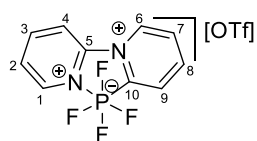


To a solution of diazaphospholium triflate **61**[OTf] (3.000 g, 8.923 mmol) in MeCN SO₂Cl₂ (0.72 ml, 8.923 mmol) is added dropwise at -40 °C while stirring. After 5 min of stirring all volatiles are evaporated *in vacuo*. MeCN (10 ml) is added to the residue and the resulting suspension is filtered. To the orange filtrate Et₂O is added until a voluminous orange precipitate appears.

This precipitate is filtered off, washed with Et₂O (3 x 5 ml) and dried *in vacuo* to yield the product as a bright orange powder.

Yield: 2.705 g (74%); **m.p.:** 168 °C (dec.); **Raman (100 mW, 298 K, in cm⁻¹):** $\nu = 3104$ (15), 3078 (22), 1620 (63), 1602 (69), 1579 (85), 1477 (70), 1456 (64), 1308 (75), 1298 (85), 1268 (86), 1174 (65), 1079 (73), 1062 (100), 1029 (82), 1018 (68), 769 (63), 759 (65), 501 (65), 471 (66), 423 (65), 406 (63), 385 (64), 348 (66), 313 (65), 280 (66), 262 (65), 221 (68); **IR (ATR, 298 K, in cm⁻¹):** $\nu = 3123$ (w), 3079 (w), 3032 (vw), 1617 (m), 1603 (w), 1577 (vw), 1486 (w), 1477 (w), 1440 (w), 1329 (vw), 1295 (w), 1269 (s), 1248 (vs), 1222 (s), 1163 (vs), 1114 (m), 1083 (w), 1062 (w), 1027 (vs), 1017 (vs), 909 (vw), 893 (vw), 788 (vs), 768 (m), 735 (w), 715 (vw), 693 (vw), 638 (vs), 575 (m), 516 (s), 505 (vs), 465 (s), 431 (w), 410 (m); **¹H NMR (CD₃CN, 300 K, in ppm):** $\delta = 7.98$ -8.01 (1H, m, C2-H), 8.40-8.44 (1H, m, C7-H), 8.51-8.56 (2H, m, C1/C3-H), 8.87-8.91 (2H, m, C4/C6-H), 9.53-9.56 (1H, m, C9-H), 9.70-9.71 (1H, m, C8-H); **¹³C{¹H} NMR (CD₃CN, 300 K, in ppm):** $\delta = 117.4$ (1C, d, ⁴J_{CP} = 2.6 Hz, C3), 122.4 (1C, q, ¹J_{CF} = 319.8 Hz, CF₃), 129.8 (1C, d, ³J_{CP} = 3.4 Hz, C2), 131.0 (1C, s, C7), 135.2 (1C, ²J_{CP} = 6.1 Hz, C9), 143.4 (1C, d, ³J_{CP} = 3.6 Hz, C8), 144.7 (1C, d, ³J_{CP} = 2.5 Hz, C4), 146.0 (1C, d, ²J_{CP} = 4.3 Hz, C1), 148.0 (1C, d, ²J_{CP} = 4.7 Hz, C5), 158.4 (1C, d, ¹J_{CP} = 97.2 Hz, C10); **¹⁹F NMR (CD₃CN, 300 K, in ppm):** $\delta = -79.3$ (3F, s); **³¹P NMR (CD₃CN, 300 K, in ppm):** $\delta = 56.6$ (1P, s); **elemental analysis:** calcd. for C₁₁H₈Cl₂F₃N₂O₃PS: C: 32.45, H: 1.98, N: 6.88, S: 7.87; found: C: 32.51, H: 1.90, N: 6.90, S: 8.04.

12.4.10. Preparation of **6I^{F4}[OTf]**

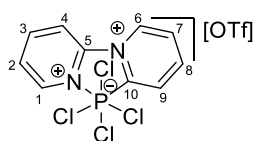


To a solution of diazaphospholium triflate salt **6I[OTf]** (300 mg, 0.892 mmol) in MeCN a solution of XeF₂ (317 mg, 1.874 mmol) in MeCN is added dropwise at -30 °C while stirring. The reaction mixture is allowed to reach r.t.. After that all volatiles are evaporated *in vacuo* to yield the product as a beige colored solid.

Yield: quant.; **m.p.:** 269 °C (dec.); **Raman (100 mW, 298 K, in cm⁻¹):** $\nu = 3108$ (17), 1637 (41), 1617 (70), 1581 (81), 1493 (55), 1450 (36), 1335 (39), 1307 (100), 1276 (43), 1263 (43), 1228 (32), 1166 (40), 1132 (40), 1109 (37), 1079 (31), 1052 (60), 1031 (56), 774 (32), 762 (35), 704 (41), 662 (27), 637 (28), 625 (31), 577 (29), 414 (27), 370 (30), 349 (35), 315 (37), 292 (30), 264 (27), 171 (37); **IR (ATR, 298 K, in cm⁻¹):** $\nu = 3136$ (vw), 3105 (vw), 3087 (vw), 3048 (vw), 1635 (w), 1616 (w), 1580 (w), 1491 (w), 1450 (w), 1334 (vw), 1306 (vw), 1252 (vs), 1227 (m), 1160 (vs), 1131 (w), 1108 (w), 1083 (w), 1071 (vw), 1051 (w), 1029 (vs), 978 (vw), 855 (m), 832 (vs), 806 (vs), 776 (vs), 740 (m), 702 (vw), 662 (vw), 635

(vs), 625 (s); **¹H NMR (CD₃CN, 300 K, in ppm):** δ = 8.25-8.29 (1H, m, C1-H), 8.38-8.41 (1H, m, C7-H), 8.48-8.52 (1H, m, C9-H), 8.87-8.91 (2H, m, C2/C4-H), 8.92-8.98 (1H, m, C8-H), 9.18-9.21 (1H, m, C3-H), 9.74-9.77 (1H, m, C6-H); **¹³C{¹H} NMR (CD₃CN, 300 K, in ppm):** δ = 117.9 (1C, dd, ³J_{CP} = 3.7 Hz, ⁴J_{CF} = 1.4 Hz, C2), 122.4 (1C, q, ¹J_{CF} = 320.5 Hz, CF₃), 128.2 (1C, ddt, ²J_{CP} = 11.7 Hz, ³J_{CF} = 3.7 Hz, ³J_{CF} = 1.6 Hz, C9), 130.5 (1C, d, ⁴J_{CP} = 2.0 Hz, C7), 131.1 (1C, dd, ²J_{CP} = 2.3 Hz, ³J_{CF} = 1.0 Hz, C1), 140.0 (1C, d, ³J_{CP} = 9.2 Hz, C6), 142.1 (1C, d, ²J_{CP} = 14.7 Hz, C5), 144.7 (1C, d, ⁴J_{CP} = 14.3 Hz, C3), 150.9 (1C, bs, C4), 151.7 (1C, m, C10), 154.1 (1C, d, ³J_{CP} = 11.4 Hz, C8); **¹⁹F NMR (CD₃CN, 300 K, in ppm):** ABM₂ spin system: δ = -83.8 (1F, ddt, ¹J_{FP} = 838.0 Hz, ²J_{Feq.Feq.} = 65.4 Hz, ²J_{Feq.Fax.} = 46.1 Hz, F_{eq.}), -79.3 (3F, s, CF₃), -74.8 (1F, ddt, ¹J_{FP} = 805.7 Hz, ²J_{Feq.Feq.} = 65.4 Hz, ²J_{Feq.Fax.} = 52.4 Hz, F_{eq.}), -55.6 (2F, ddd, ¹J_{FP} = 811.8 Hz, ²J_{Fax.Feq.} = 52.4 Hz, ²J_{Fax.Feq.} = 46.1 Hz, F_{ax.}); **³¹P NMR (CD₃CN, 300 K, in ppm):** δ = -138.7 (1P, dtd, ¹J_{PFeq.} = 838.0 Hz, ¹J_{PFax.} = 811.8 Hz, ¹J_{PFeq.} = 805.7 Hz); **elemental analysis:** calcd. for C₁₁H₈F₇N₂O₃PS x 0.25 MeCN: C: 32.69, H: 2.09, N: 7.46, S: 7.59; found: C: 32.84, H: 1.90, N: 7.39, S: 7.83.

12.4.11. Preparation of **61**^{Cl⁴}[OTf]



To a solution of diazaphospholium triflate salt **61**[OTf] (1.000 g, 2.974 mmol) in MeCN SO₂Cl₂ (0.48 ml, 5.948 mmol) is added dropwise at -40 °C while stirring. The reaction mixture is allowed to

reach room temperature. After that, all volatiles are evaporated *in vacuo* to yield the product as an off-white solid.

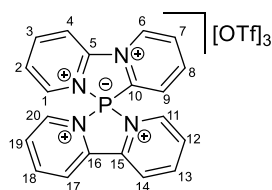
Yield: quant.; **m.p.:** 176 °C (dec.); **Raman (100 mW, 298 K, in cm⁻¹):** ν = 3113 (16), 3100 (21), 3085 (18), 1625 (31), 1606 (45), 1575 (72), 1482 (27), 1439 (14), 1328 (41), 1299 (52), 1275 (26), 1224 (12), 1170 (19), 1150 (16), 1128 (19), 1093 (36), 1079 (22), 1062 (34), 1037 (31), 1028 (52), 770 (20), 758 (19), 705 (11), 655 (10), 634 (11), 573 (11), 501 (12), 457 (11), 405 (18), 351 (100), 313 (21), 299 (29), 284 (34), 241 (16), 213 (42), 161 (13), 134 (25); **IR (ATR, 298 K, in cm⁻¹):** ν = 3128 (vs), 3100 (vs), 3076 (vs), 3037 (vs), 1624 (vs), 1606 (vs), 1573 (vs), 1483 (vs), 1440 (vs), 1327 (vs), 1271 (vs), 1252 (vs), 1222 (vs), 1156 (vs), 1127 (vs), 1092 (vs), 1079 (vs), 1064 (vs), 1027 (vs), 968 (vs), 771 (vs), 758 (vs), 731 (vs), 704 (vs), 655 (vs), 633 (vs), 573 (vs), 517 (vs), 499 (vs), 456 (vs), 438 (vs), 412 (vs); **¹H NMR (CD₃CN, 300 K, in ppm):** δ = 8.37-8.43 (2H, m, C2/C7-H), 8.88-8.98 (2H, m, C4/C6-H), 9.04-9.10 (1H, m, C1-H), 9.20-9.26 (1H, m, C9-H), 9.63-9.67 (1H, m, C3-H), 10.40-10.45 (1H, m, C8-H); **¹³C{¹H} NMR (CD₃CN, 300 K, in ppm):** δ = 118.9 (1C, s, C6), 122.6 (1C, q, ¹J_{CF} = 320.8 Hz, CF₃), 123.9 (1C, d, ²J_{CP} = 17.5 Hz, C9), 130.3 (1C, d,

$^4J_{CP} = 2.8$ Hz, C7), 131.5 (1C, d, $^3J_{CP} = 2.2$ Hz, C2), 138.9 (1C, d, $^4J_{CP} = 5.5$ Hz, C3), 142.5 (1C, bs, C8), 151.0 (1C, d, $^5J_{CP} = 1.0$ Hz, C4), 156.0 (1C, d, $^2J_{CP} = 14.0$ Hz, C1), 160.0 (1C, s, C10), 162.0 (1C, s, C5); ^{19}F NMR (CD_3CN , 300 K, in ppm): $\delta = -79.3$ (3F, s); ^{31}P NMR (CD_3CN , 300 K, in ppm): $\delta = -208.9$ (1P, s); **elemental analysis**: calcd. for $\text{C}_{11}\text{H}_8\text{Cl}_4\text{F}_3\text{N}_2\text{O}_3\text{PS}$: C: 27.64, H: 1.69, N: 5.86, S: 6.71; found: C: 27.89, H: 1.66, N: 5.79, S: 6.86.

12.4.12. Preparation of **69**[OTf]₃

Starting from diazaphospholium triflate 61[OTf]. To a solution of **61**[OTf] (300 mg, 0.892 mmol) in MeCN a solution of XeF_2 (152 mg, 0.892 mmol) in MeCN is added dropwise at -40 °C while stirring. After stirring for 30 min at -40 °C a solution of 2-2' bipyridine (139 mg, 0.892 mmol) in MeCN is added dropwise. Subsequent addition of Me_3SiOTf (0.32 ml, 1.784 mmol) leads to a yellowish precipitate. The supernatant is filtered off by means of a cannula and the precipitate is washed with Et_2O (3 x 3 ml). After that, all volatiles are removed *in vacuo*, to yield the product as a yellow powder (**yield: 324mg, 46%**).

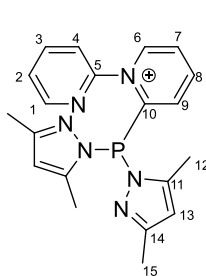
Starting from 61^{Cl2}[OTf]. To a suspension of **61**^{Cl2}[OTf] (407 mg, 1 mmol) in CH_2Cl_2 , 2-2' bipyridine (156 mg, 1 mmol) and Me_3SiOTf (0.362 ml, 2 mmol) are added in that order. Stirring for 2 h the suspension changes its color from orange to yellow. Subsequent filtration, washing with CH_2Cl_2 (3 x 2 ml) and evaporation of all volatiles *in vacuo* yields the product quantitatively. Crystals suitable for X-ray analysis grow from concentrated MeCN solutions upon slow diffusion of Et_2O at -30 °C.



M.p.: 281 °C (dec.); **Raman (100 mW, 298 K, in cm^{-1}):** $\nu = 3105$ (16), 3076 (25), 2943 (15), 2251 (11), 1618 (100), 1606 (29), 1574 (49), 1566 (51), 1510 (53), 1481 (22), 1436 (11), 1340 (45), 1303 (36), 1276 (27), 1228 (11), 1176 (11), 1143 (11), 1114 (15), 1098 (15), 1060 (35), 1039 (98), 1013 (20), 770 (27), 756 (22), 647 (9), 573 (13), 518 (13), 403 (15), 372 (13), 348 (15), 313 (13), 288 (9); **IR (ATR, 298 K, in cm^{-1}):** $\nu = 3104$ (vw), 3071 (vw), 3033 (vw), 2251 (vw), 1620 (w), 1574 (vw), 1509 (vw), 1489 (vw), 1474 (w), 1455 (w), 1445 (w), 1330 (vw), 1244 (vs), 1225 (s), 1143 (s), 1099 (w), 1080 (w), 1029 (vs), 1012 (s), 891 (vw), 769 (m), 757 (w), 740 (vw), 720 (w), 710 (w), 680 (vw), 658 (w), 636 (vs), 573 (m), 536 (vw), 516 (vs), 461 (w), 451 (w), 426 (m), 407 (m); **^1H NMR (CD_3CN , 300 K, in ppm):** $\delta = 7.88$ -7.93 (1H, m, C12-H), 8.09-8.15 (1H, m, C19-H), 8.34-8.37 (2H, m, C4-H), 8.38-8.44 (1H, m, C14-H), 8.68-8.73 (1H, m, C17-H), 8.87-8.94 (4H, m, C2/C3/C7/C9-H), 9.02-9.16 (3H, m, C11/C13/C18-H), 9.26-9.29 (1H, m, C1-H), 9.33-9.39 (1H, m, C20-H), 9.97-10.01 (1H, m, C6-H); **$^{13}\text{C}\{^1\text{H}\}$ NMR (CD_3CN , 300 K, in ppm):**

$\delta = 119.3$ (1C, d, $^2J_{CP} = 5.4$ Hz, C9), 122.1 (3C, q, $^1J_{CF} = 320.2$ Hz, CF₃), 126.9 (1C, s, C13), 128.0 (1C, s, C18), 131.8 (1C, s, C19), 132.0 (1C, s, C4), 132.8 (2C, s, C8/C14), 134.8 (1C, d, $^2J_{CP} = 4.6$ Hz, C12), 144.5 (1C, s, C20), 144.6 (1C, s, C6), 146.7 (1C, d, $^2J_{CP} = 9.5$ Hz, C1), 147.1 (2C, s, C15/C16), 147.2 (1C, bs, C5), 148.0 (1C, d, $^1J_{CP} = 22.0$ Hz, C10), 149.0 (1C, bs, C11), 149.2 (1C, s, C2), 149.8 (1C, s, C7), 151.0 (1C, s, C3), 151.9 (1C, s, C17); **^{19}F NMR (CD₃CN, 300 K, in ppm):** $\delta = -79.3$ (3F, s); **^{31}P NMR (CD₃CN, 300 K, in ppm):** $\delta = 20.5$ (1P, s); **elemental analysis:** calcd. for C₂₃H₁₆F₉N₄O₉PS₃ x 1 MeCN: C: 36.11, H: 2.30, N: 8.42, S: 11.57; found: C: 35.82, H: 2.34, N: 8.75, S: 11.42.

12.4.13. Preparation of **70a**[OTf]

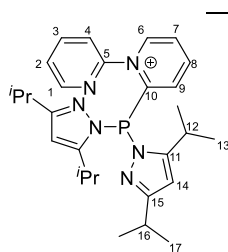


To a suspension of **61**^{Cl₂}[OTf] (100 mg, 0.246 mmol) in Et₂O **5a** (87 mg, 0.518 mmol) is added. After stirring for 16 h the suspension is filtered. The residue is recrystallized from CH₂Cl₂/Et₂O to yield the product as a light-yellow powder after evaporation of all volatiles *in vacuo*.

Yield: 118 mg (91%); **m.p.:** 151 °C (dec.); **Raman (100 mW, 298 K, in cm⁻¹):** $\nu = 3141$ (12), 3094 (20), 3069 (26), 2975 (23), 2930 (34), 1606 (63), 1574 (70), 1473 (60), 1461 (55), 1438 (60), 1308 (51), 1295 (55), 1277 (50), 1245 (100), 1166 (49), 1143 (50), 1092 (50), 1068 (76), 1030 (74), 1006 (59), 768 (48), 756 (52), 626 (50), 589 (55), 574 (49), 535 (50), 498 (50), 425 (48), 405 (51), 348 (55), 338 (51), 313 (52), 277 (49), 234 (50), 208 (57), 172 (51); **IR (ATR, 298 K, in cm⁻¹):** $\nu = 3125$ (vw), 3101 (vw), 3069 (vw), 1606 (w), 1567 (m), 1487 (w), 1472 (w), 1442 (w), 1410 (w), 1381 (vw), 1318 (w), 1292 (m), 1268 (vs), 1256 (vs), 1243 (s), 1222 (m), 1162 (vs), 1139 (m), 1121 (s), 1104 (w), 1061 (vw), 1024 (vs), 1005 (m), 965 (m), 830 (w), 804 (w), 790 (w), 775 (s), 765 (m), 747 (w), 722 (vw), 694 (vw), 634 (vs), 591 (vw), 573 (m), 547 (w), 534 (s), 515 (vs), 489 (vs), 449 (w), 426 (s), 418 (m); **^1H NMR (CD₂Cl₂, 300 K, in ppm):** $\delta = 2.08$ (6H, s, C15-H), 2.34 (6H, s, C12-H), 5.84 (2H, s, C13-H), 7.51-7.57 (2H, m, C7/C9-H), 7.88-7.90 (1H, m, C3-H), 8.04-8.08 (1H, m, C1-H), 8.32-8.36 (1H, m, C2-H), 8.46-8.48 (1H, m, C4-H), 8.55-8.60 (1H, m, C8-H), 9.49-9.53 (1H, m, C6-H); **$^{13}\text{C}\{^1\text{H}\}$ NMR (CD₂Cl₂, 300 K, in ppm):** $\delta = 12.5$ (2C, d, $^3J_{CP} = 16.0$ Hz, C12), 14.0 (2C, s, C15), 109.8 (2C, s, C13), 119.5 (1C, s, C3), 121.5 (1C, q, $^1J_{CF} = 320.4$ Hz, CF₃), 127.3 (1C, s, C2), 129.4 (1C, s, C7), 134.1 (1C, d, $^2J_{CP} = 9.2$ Hz, C9), 141.8 (1C, s, C1), 146.4 (1C, s, C8), 147.7 (1C, s, C4), 147.8 (1C, s, C6), 148.8 (1C, d, $^2J_{CP} = 26.0$ Hz, C11), 153.1 (1C, s, C5), 156.1 (1C, s, C14), 156.4 (1C, d, $^1J_{CP} = 25.5$, C10); **^{19}F NMR (CD₂Cl₂, 300 K, in ppm):** $\delta = -78.9$ (3F, s); **^{31}P NMR (CD₂Cl₂, 300 K, in ppm):** $\delta = 38.6$

(1P, s); **elemental analysis**: calcd. for C₂₁H₂₂F₃N₆O₃PS x 0.15 CH₂Cl₂: C: 47.11, H: 4.17, N: 15.59, S: 5.95; found: C: 47.07, H: 4.07, N: 15.47, S: 5.95.

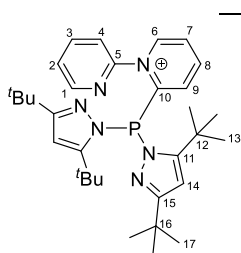
12.4.14. Preparation of **70b**[OTf]



To a suspension of **61**^{Cl₂}[OTf] (100 mg, 0.246 mmol) in Et₂O **5b** (116 mg, 0.518 mmol) is added. After stirring for 16 h the suspension is filtered. The residue is recrystallized from CH₂Cl₂/Et₂O to yield the product as a light-yellow powder after evaporation of all volatiles *in vacuo*.

Yield: 144 mg (92%); **m.p.**: 141 °C (dec.); **Raman (100 mW, 298 K, in cm⁻¹)**: $\nu = 3111$ (5), 3081 (7), 3062 (25), 3028 (6), 2968 (40), 2923 (29), 2868 (34), 2711 (5), 1591 (13), 1554 (29), 1474 (17), 1450 (52), 1410 (100), 1382 (8), 1368 (7), 1314 (18), 1274 (35), 1237 (53), 1162 (5), 1126 (22), 1109 (10), 1049 (7), 1002 (31), 989 (10), 959 (6), 878 (19), 853 (9), 707 (18), 670 (5), 504 (18), 443 (5), 377 (7), 214 (8), 174 (15), 124 (33); **IR (ATR, 298 K, in cm⁻¹)**: $\nu = 3125$ (vw), 3090 (vw), 2966 (w), 2933 (vw), 2871 (vw), 1602 (w), 1557 (w), 1487 (w), 1470 (w), 1439 (w), 1384 (vw), 1365 (w), 1294 (w), 1262 (vs), 1225 (m), 1158 (s), 1110 (w), 1068 (w), 1031 (vs), 999 (w), 985 (m), 800 (w), 781 (m), 756 (vw), 746 (vw), 722 (vw), 701 (vw), 638 (vs), 623 (w), 587 (vw), 573 (m), 517 (vs), 493 (m), 435 (w), 416 (w); **¹H NMR (CD₂Cl₂, 300 K, in ppm)**: $\delta = 1.06$ -1.12 (24H, m, C13/C17-H), 2.77 (2H, sept., ³J_{HH} = 6.87 Hz, C16-H), 3.18-3.25 (2H, m, C12-H), 5.94 (2H, s, C14-H), 7.33-7.36 (1H, m, C9-H), 7.49-7.53 (1H, m, C2-H), 7.95-7.98 (1H, m, C4-H), 8.02-8.06 (1H, m, C3-H), 8.37-8.40 (2H, m, C1/C7-H), 8.50-8.54 (1H, m, C8-H), 9.64-9.66 (1H, m, C6-H); **¹³C{¹H} NMR (CD₂Cl₂, 300 K, in ppm)**: $\delta = 22.5$ (4C, d, ⁴J_{CP} = 26.4 Hz, C13), 23.5 (4C, d, ⁴J_{CP} = 17.4 Hz, C17), 26.9 (2C, d, ³J_{CP} = 13.9 Hz, C12), 28.6 (2C, s, C16), 103.2 (2C, s, C14), 119.4 (1C, s, C4), 121.5 (1C, q, ¹J_{CF} = 320.9 Hz, CF₃), 127.1 (1C, s, C2), 129.5 (1C, s, C7), 133.4 (1C, d, ²J_{CP} = 8.9 Hz, C9), 141.9 (1C, s, C3), 146.3 (1C, s, C8), 147.6 (1C, s, C1), 147.7 (1C, d, ³J_{CP} = 2.8 Hz, C6), 153.1 (1C, d, ³J_{CP} = 4.5 Hz, C5), 157.1 (1C, d, ¹J_{CP} = 36.0 Hz, C10), 159.7 (2C, d, ²J_{CP} = 18.8 Hz, C11), 165.4 (2C, d, ³J_{CP} = 4.4, C15); **¹⁹F NMR (CD₂Cl₂, 300 K, in ppm)**: $\delta = -78.9$ (3F, s); **³¹P NMR (CD₂Cl₂, 300 K, in ppm)**: $\delta = 41.6$ (1P, s); **elemental analysis**: calcd. for C₂₉H₃₈F₃N₆O₃PS x 0.25 CH₂Cl₂: C: 53.24, H: 5.88, N: 12.73 S: 4.86; found: C: 53.58, H: 5.61, N: 12.65, S: 4.86.

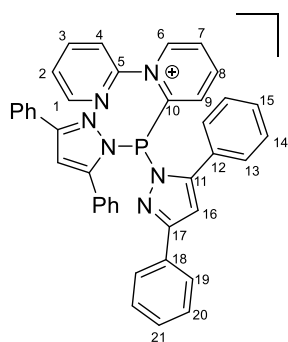
12.4.15. Preparation of 70c[OTf]



To a suspension of **61**^{Cl2}[OTf] (100 mg, 0.264 mmol) in Et₂O **5c** (155 mg, 0.614 mmol) is added. After stirring for five days the suspension is filtered. The residue is washed with Et₂O (3 x 2 ml). Evaporating all volatiles *in vacuo* yields the product as a light-yellow powder.

Yield: 157 mg (92%); **m.p.:** 174 °C (dec.); **Raman (100 mW, 298 K, in cm⁻¹):** ν = 3140 (24), 3098 (36), 3086 (40), 3068 (52), 2971 (100), 2927 (96), 2910 (92), 2877 (60), 2715 (36), 1911 (36), 1877 (36), 1798 (36), 1759 (36), 1742 (36), 1717 (36), 1704 (36), 1674 (36), 1606 (48), 1569 (48), 1487 (40), 1450 (52), 1309 (36), 1263 (44), 1236 (48), 1202 (40), 1149 (32), 1099 (32), 1068 (44), 1056 (40), 1029 (48), 997 (36), 930 (32), 822 (40), 563 (32); **IR (ATR, 298 K, in cm⁻¹):** ν = 3127 (vw), 3087 (vw), 2960 (w), 2871 (vw), 1600 (vw), 1547 (vw), 1487 (w), 1466 (w), 1438 (w), 1407 (vw), 1364 (w), 1295 (vw), 1265 (vs), 1237 (m), 1225 (m), 1200 (w), 1185 (w), 1153 (vs), 1125 (m), 1107 (m), 1031 (vs), 1015 (w), 997 (w), 986 (w), 977 (w), 804 (w), 787 (m), 766 (vw), 757 (vw), 727 (vw), 694 (vw), 651 (w), 637 (vs), 581 (w), 574 (w), 554 (w), 517 (vs), 503 (m), 487 (m), 443 (w), 423 (w); **¹H NMR (CD₃CN, 300 K, in ppm):** δ = 1.08 (18H, s, C17-H), 1.26 (18H, s, C13-H), 6.10 (2H, d, ⁴J_{HP} = 2.40 Hz, C14-H), 7.26-7.29 (1H, m, C9-H), 7.53-7.56 (1H, m, C4-H), 7.65-7.69 (1H, m, C2-H), 8.05-8.10 (1H, m, C3-H), 8.16-8.20 (1H, m, C7-H), 8.54-8.60 (1H, m, C8-H), 8.60-8.63 (1H, m, C1-H), 9.01-9.04 (1H, m, C6-H); **¹³C{¹H} NMR (CD₃CN, 300 K, in ppm):** δ = 30.5 (6C, s, C17), 31.7 (6C, d, ⁴J_{CP} = 8.8 Hz, C13), 33.2 (2C, s, C16), 33.4 (2C, s, C12), 105.5 (2C, d, ³J_{CP} = 3.1 Hz, C14), 121.3 (1C, ⁴J_{CP} = 2.1 Hz, C4), 122.6 (1C, q, ¹J_{CF} = 319.6 Hz, CF₃), 128.6 (1C, s, C2), 129.4 (1C, s, C7), 134.2 (1C, ²J_{CP} = 5.6 Hz, C9), 142.6 (1C, s, C3), 147.1 (1C, d, ³J_{CP} = 2.3 Hz, C6), 147.6 (1C, s, C8), 150.7 (1C, s, C1), 154.1 (1C, s, C5), 159.4 (1C, d, ¹J_{CP} = 31.6, C10), 162.2 (2C, d, ²J_{CP} = 15.9, C11), 166.9 (2C, s, C15); **¹⁹F NMR (CD₃CN, 300 K, in ppm):** δ = -79.3 (3F, s); **³¹P NMR (CD₃CN, 300 K, in ppm):** δ = 61.4 (1P, s); **elemental analysis:** calcd. for C₁₁H₈Cl₂F₃N₂O₃PS: C: 57.05, H: 6.67, N: 12.10, S: 4.61; found: C: 56.66, H: 6.46, N: 11.86, S: 5.06.

12.4.16. Preparation of 70d[OTf]

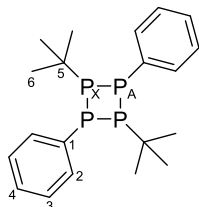


To a suspension of **61**^{Cl₂}[OTf] (110 mg, 0.270 mmol) in Et₂O a solution of **5d** (158 mg, 0.540 mmol) in Et₂O is added. After stirring for 16 h the suspension is filtered. The residue is washed with Et₂O (3 x 2 ml). Evaporating all volatiles *in vacuo* yields the product as a light-yellow powder.

Yield: 205 mg (98%); **m.p.:** 172 °C (dec.); **Raman (100 mW, 298 K, in cm⁻¹):** ν = 3071 (16), 1604 (100), 1576 (37), 1548 (32), 1515 (53), 1477 (26), 1430 (68), 1397 (32), 1297 (26), 1250 (42), 1224 (26), 1182 (26), 1160 (26), 1141 (26), 1094 (32), 1067 (42), 1031 (37), 1002 (58), 984 (32), 953 (42), 769 (26), 698 (26), 618 (32), 544 (32), 279 (32), 249 (32), 200 (32); **IR (ATR, 298 K, in cm⁻¹):** ν = 3123 (vw), 3108 (vw), 3070 (vw), 3032 (vw), 1610 (vw), 1576 (vw), 1548 (vw), 1484 (w), 1459 (vw), 1442 (vw), 1434 (vw), 1398 (vw), 1318 (vw), 1283 (m), 1276 (m), 1250 (m), 1242 (m), 1224 (w), 1171 (w), 1149 (w), 1131 (w), 1110 (w), 1074 (w), 1056 (vw), 1027 (m), 1010 (w), 980 (vw), 951 (vw), 929 (vw), 902 (vw), 847 (vw), 811 (vw), 802 (vw), 771 (m), 760 (s), 726 (vw), 716 (w), 697 (m), 686 (m), 668 (vw), 636 (m), 579 (w), 543 (w), 515 (m), 482 (w), 469 (m); **¹H NMR (CD₃CN, 300 K, in ppm):** δ = 6.86 (2H, d, ⁴J_{HP} = 2.93 Hz, C16-H), 7.22-7.26 (4H, m, C13-H), 7.35-7.46 (12H, m, C14/C15/C20/C21-H), 7.53-7.56 (1H, m, C2-H), 7.66-7.70 (4H, m, C19-H), 7.90-7.94 (1H, m, C4-H), 7.99-8.03 (1H, m, C3-H), 8.13-8.15 (1H, m, C1-H), 8.30-8.33 (1H, m, C9-H), 8.33-8.37 (1H, m, C7-H), 8.70-8.75 (1H, m, C8-H), 9.34-9.37 (1H, m, C6-H); **¹³C{¹H} NMR (CD₃CN, 300 K, in ppm):** δ = 107.8 (2C, s, C16), 119.4 (1C, C4), 122.6 (1C, q, ¹J_{CF} = 320.8 Hz, CF₃), 127.4 (4C, s, C19), 128.5 (1C, s, C2), 130.2 (10C, 2s, C14/C20/C21), 130.3 (1C, s, C7), 130.6 (4C, d, ⁴J_{CP} = 4.5 Hz, C13), 130.7 (2C, s, C12), 133.2 (2C, s, C18), 136.0 (1C d, ²J_{CP} = 7.7 Hz, C9), 143.0 (1C, s, C3), 147.3 (1C, s, C6), 148.2 (1C, s, C1), 148.6 (1C, s, C8), 152.9 (1C, d, ³J_{CP} = 3.4 Hz, C5), 155.8 (1C, d, ¹J_{CP} = 33.1, C10), 154.8 (2C, d, ²J_{CP} = 15.9, C11), 158.0 (2C, s, C17); **¹⁹F NMR (CD₃CN, 300 K, in ppm):** δ = -79.3 (3F, s); **³¹P NMR (CD₃CN, 300 K, in ppm):** δ = 44.1 (1P, s); **elemental analysis:** calcd. for C₄₁H₃₀F₃N₆O₃PS: C: 61.74, H: 3.85, N: 10.45, S: 3.99; found: C: 62.00, H: 3.57, N: 10.70, S: 4.02.

12.5. Syntheses and Characterization Data regarding Compounds in Chapter 6

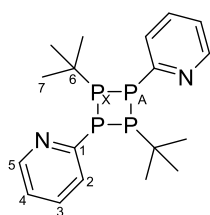
12.5.1. Preparation of 71



To a solution of *t*BuPH₂ (700 mg, 7.77 mmol, 1.00 ml) in 10 ml of MeCN phenyldipyrazolyolphosphane **73a** (2.213 g, 7.77 mmol) in 10 ml of MeCN is added at -45 °C. The reaction mixture is stored at -30 °C for 16 h to give a colorless suspension. All volatiles of this suspension are evaporated *in vacuo* to give a colorless residue. After sublimation of 3,5-dimethylpyrazole from the residue (80 °C; 6 x 10⁻³ mbar) compound **71** is obtained quantitatively in a purity of >95%. Analytically pure **71** is obtained by washing the crude product with cold MeCN (-30 °C; 3 x 2 ml) and subsequent evaporation of all volatiles *in vacuo*.

Yield: 1.113 g (69%); **m.p.:** 96 °C; **Raman (100 mW, 298 K, in cm⁻¹):** $\nu = 3058$ (32), 3046 (36), 2962 (25), 2944 (24), 2930 (25), 2915 (31), 2889 (39), 2854 (25), 1582 (61), 1455 (19), 1443 (14), 1283 (5), 1272 (8), 1199 (8), 1180 (18), 1157 (14), 1085 (20), 1064 (9), 1026 (33), 1014 (6), 999 (100), 936 (14), 806 (18), 691 (8), 618 (11), 575 (18), 486 (23), 471 (44), 241 (17), 207 (32), 178 (45), 167 (38), 130 (74); **IR (ATR, 298 K, in cm⁻¹):** $\nu = 3059$ (w), 2943 (m), 2929 (m), 2887 (w), 2852 (m), 1580 (w), 1520 (w), 1469 (m), 1455 (m), 1433 (m), 1400 (w), 1387 (w), 1359 (s), 1323 (w), 1300 (w), 1282 (m), 1168 (s), 1155 (s), 1099 (w), 1081 (w), 1064 (m), 1024 (s), 998 (m), 934 (m), 911 (w), 805 (m), 742 (vs), 691 (vs), 610 (m), 573 (m), 541 (m), 508 (s), 480 (m), 440 (m), 428 (m), 406 (m); **¹H NMR (CD₂Cl₂, 300 K, in ppm):** $\delta = 1.28$ -1.31 (18H, m, C6-H), 7.28-7.31 (2H, m, C4-H), 7.33-7.37 (4H, m, C3-H), 7.72-7.76 (4H, m, C2-H); **¹³C{¹H} NMR (CD₂Cl₂, 300 K, in ppm):** $\delta = 28.4$ -28.6 (6C, m, C6), 31.5-31.9 (2C, m, C5), 128.7 (2C, m, C4), 128.9 (4C, m, C3), 133.8-134.1 (4C, m, C2), 140.3-141.2 (2C, m, C1); **³¹P NMR (CD₂Cl₂, 300 K, in ppm):** A₂X₂ spin system: $\delta(P_A) = -88.4$ (2P), $\delta(P_X) = -15.5$ (2P); **¹J(P_AP_X) = -130 Hz; elemental analysis:** calcd. for C₂₀H₂₈P₄: C: 61.23, H: 7.19; found: C: 60.80, H: 7.23.

12.5.2. Preparation of 72

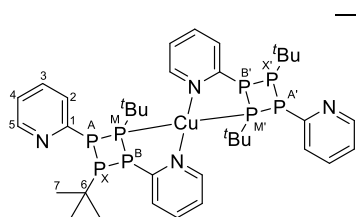


To a solution of *t*BuPH₂ (700 mg, 7.77 mmol, 1.00 ml) in 10 ml of MeCN Pyridyldipyrazolyolphosphane **41a** (2.326 g, 7.77 mmol) in 20 ml of MeCN is added at -45 °C. The reaction mixture is stored at -30 °C for 16 h to give a colorless suspension. All volatiles of this suspension are evaporated *in vacuo* to give a colorless residue. After sublimation of 3,5-dimethylpyrazole from the residue (80 °C; 6 x 10⁻³ mbar) compound **72** is obtained quantitatively in a purity

of >95%. Analytically pure **72** is obtained by washing the crude product with cold MeCN (-30 °C; 3 x 2 ml) and subsequent evaporation of all volatiles *in vacuo*.

Yield: 860 mg (53%); **m.p.:** 173 °C; **Raman (100 mW, 298 K, in cm⁻¹):** $\nu = 3134$ (5), 3119 (9), 3060 (23), 3039 (63), 2950 (66), 2927 (53), 2918 (54), 2890 (90), 2855 (53), 2769 (8), 2704 (10), 1571 (74), 1559 (34), 1458 (29), 1440 (21), 1419 (15), 1389 (6), 1276 (10), 1201 (12), 1174 (15), 1158 (16), 1127 (25), 1084 (7), 1048 (58), 987 (100), 936 (17), 807 (31), 714 (15), 619 (12), 579 (30), 500 (28), 479 (24), 468 (41), 424 (10), 397 (14), 384 (11), 247 (16), 204 (42), 174 (28), 164 (37), 124 (49); **IR (ATR, 298 K, in cm⁻¹):** $\nu = 3036$ (w), 2943 (m), 2927 (m), 2888 (m), 2853 (m), 2709 (w), 1569 (vs), 1556 (s), 1470 (m), 1447 (vs), 1416 (vs), 1388 (m), 1360 (vs), 1268 (m), 1227 (m), 1202 (m), 1167 (s), 1149 (s), 1082 (m), 1046 (m), 1008 (m), 986 (m), 934 (w), 887 (w), 804 (m), 768 (s), 757 (vs), 740 (s), 712 (m), 639 (w), 618 (s), 574 (m), 554 (w), 517 (m), 500 (s), 467 (m), 407 (m); **¹H NMR (CD₂Cl₂, 300 K, in ppm):** $\delta = 1.36$ -1.40 (18H, m, C7-H), 7.06-7.10 (2H, m, C4-H), 7.53-7.58 (2H, m, C3-H), 7.72-7.76 (2H, m, C2-H), 8.53-8.57 (2H, m, C5-H); **¹³C{¹H} NMR (CD₂Cl₂, 300 K, in ppm):** $\delta = 28.4$ -28.7 (6C, m, C7), 30.9-31.8 (2C, m, C6), 121.9 (2C, s, C4), 127.5-127.8 (2C, m, C2), 135.8 (2C, m, C3), 150.3-150.4 (2C, m, C5), 167.4-167.8 (2C, m, C1); **³¹P NMR (CD₂Cl₂, 300 K, in ppm):** A₂X₂ spin system: $\delta(P_A) = -81.9$ (2P), $\delta(P_X) = -18.8$ (2P); $^1J(P_AP_X) = -131$ Hz; **elemental analysis:** calcd. for C₁₈H₂₆N₂P₄: C: 54.83, H: 6.65, N: 7.10; found: C: 54.60, H: 6.59, N: 7.21.

12.5.3. Preparation of [(**72**)₂Cu][OTf]



To a solution of Tetraphosphetane **72** (50 mg, 0.13 mmol) in 1 ml of CH₂Cl₂ [Cu(MeCN)₄][OTf] (24 mg, 0.065 mmol) dissolved in 0.5 ml CH₂Cl₂ is added. The reaction mixture is stirred for 1 h at room temperature. Vapor diffusion of *n*-pentane into this solution at -30 °C yields yellow crystals of [(**72**)₂Cu][OTf]. These are isolated by decantation, washing with *n*-pentane (3 x 1 ml) and evaporation of all volatiles *in vacuo*.

Yield: 56 mg (89%); **m.p.:** 273 (dec.) °C; **Raman (100 mW, 298 K, in cm⁻¹):** $\nu = 3120$ (15), 3066 (43), 3048 (49), 2992 (23), 2957 (71), 2934 (78), 2919 (69), 2893 (100), 2857 (59), 2775 (11), 2711 (16), 1579 (30), 1572 (39), 1558 (35), 1456 (26), 1445 (25), 1421 (14), 1393 (8), 1275 (9), 1224 (9), 1199 (13), 1158 (15), 1120 (21), 1090 (13), 1052 (25), 1043 (23), 1030 (20), 1006 (51), 986 (33), 935 (9), 805 (21), 755 (9), 714 (13), 702 (9), 588 (19), 513 (43), 498 (16), 487 (10), 471 (26), 447 (14), 398 (11), 364 (8); **IR (ATR, 298 K, in cm⁻¹):** $\nu = 3066$ (w), 3035 (w), 2984 (w), 2950 (w), 2931 (w), 2892 (w), 2857 (w), 1577 (m),

1572 (m), 1557 (w), 1455 (s), 1449 (m), 1419 (m), 1390 (w), 1362 (m), 1260 (vs), 1223 (m), 1148 (vs), 1090 (w), 1051 (w), 1042 (w), 1028 (vs), 1004 (m), 985 (m), 912 (w), 883 (w), 804 (w), 784 (m), 768 (m), 758 (vs), 738 (s), 715 (w), 700 (m), 636 (vs), 618 (m); **¹H NMR (CD₂Cl₂, 300 K, in ppm):** δ = 1.57 (36H, d, ¹J_{HP} = 15.1 Hz, C7–H), 6.68-6.72 (4H, m, C4–H), 7.38-7.45 (4H, m, C3–H), 7.52-7.56 (4H, m, C2–H), 7.98-8.02 (4H, m, C5–H); **¹³C{¹H} NMR (CD₂Cl₂, 300 K, in ppm):** δ = 27.3 (12C, dt, ¹J_{CP} = 11.1 Hz, ²J_{CP} = 5.7 Hz, C7), 32.2-32.7 (4C, m, C6), 121.1 (1C, q, ¹J_{CF} = 321.1 Hz, CF₃), 122.6 (4C, br, C4), 127.0-127.6 (4C, m, C2), 136.3 (4C, br, C3), 150.7-151.2 (4C, m, C5), 162.0-162.6 (4C, m, C1); **¹⁹F NMR (CD₂Cl₂, 300 K, in ppm):** δ = -78.9 (3F, s); **³¹P NMR (CD₂Cl₂, 190 K, in ppm):** AA'BB'MM'XX' spin system δ(P) = δ(P_A) = -81.4 ppm, δ(P_B) = -68.9 ppm, δ(P_M) = -45.1 ppm, δ(P_X) = -15.4 ppm; **elemental analysis:** calcd. for C₃₇H₅₂CuF₃N₄O₃P₈S x 0.75 CH₂Cl₂: C: 42.58, H: 5.06, N: 5.26, S: 3.01; found: C: 42.66, H: 4.93, N: 5.30, S: 3.17.

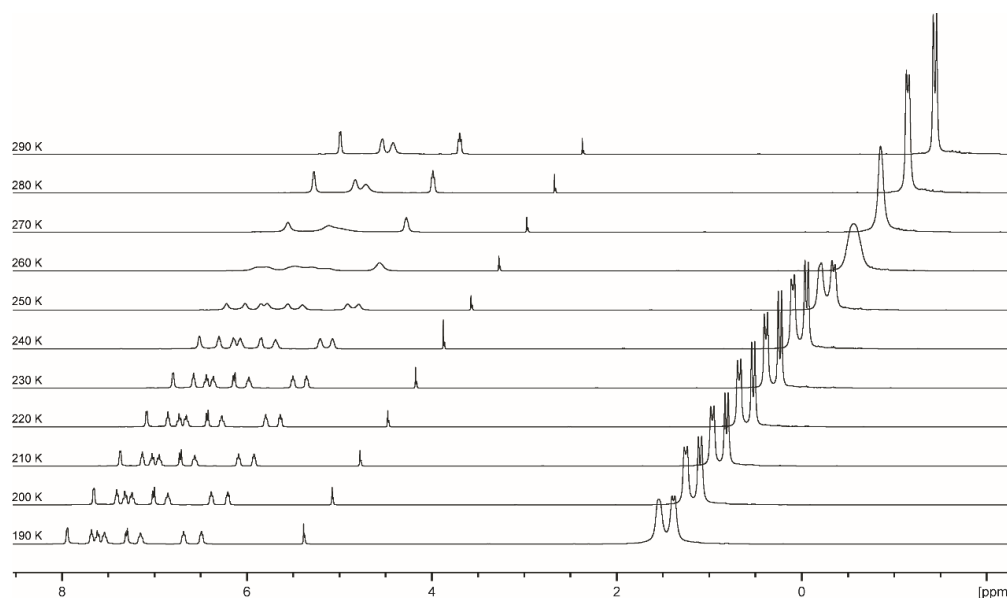


Figure 57. ¹H spectra of [(72)₂Cu][OTf] in CD₂Cl₂ from 190-290 K.

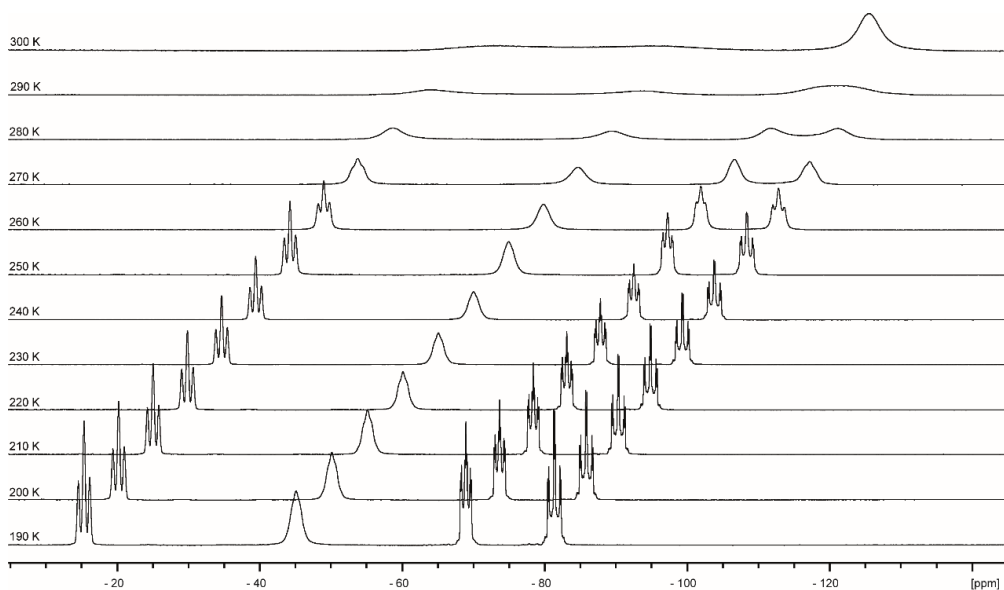
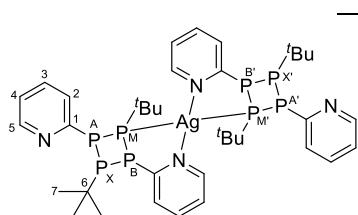


Figure 58. ^{31}P spectra of $[(72)_2\text{Cu}][\text{OTf}]$ in CD_2Cl_2 from 190-290 K.

12.5.4. Preparation of $[(72)_2\text{Ag}][\text{OTf}]$



To a solution of tetraphosphetane **72** (79 mg, 0.2 mmol) in 1 ml of CH_2Cl_2 $\text{Ag}[\text{OTf}]$ (26 mg, 0.1 mmol) dissolved in 0.5 ml CH_2Cl_2 is added. The reaction mixture is stirred for 1 h at room temperature. Vapor diffusion of *n*-pentane into this solution at $-30\text{ }^\circ\text{C}$ yields colorless crystals of $[(72)_2\text{Ag}][\text{OTf}]$. These are isolated by decantation, washing with *n*-pentane (3 x 1 ml) and evaporation of all volatiles *in vacuo*. Crystals suitable for X-ray analysis are obtained by recrystallization from $\text{MeCN}/\text{Et}_2\text{O}$ at $-30\text{ }^\circ\text{C}$.

Yield: 79 mg (76%); **m.p.:** $247\text{ }^\circ\text{C}$ (dec.); **Raman (100 mW, 298 K, in cm^{-1}):** $\nu = 3119$ (13), 3061 (43), 3042 (34), 2955 (74), 2933 (75), 2919 (62), 2894 (100), 2857 (62), 2775 (13), 2711 (21), 1572 (75), 1559 (47), 1458 (38), 1443 (34), 1422 (19), 1392 (13), 1364 (9), 1274 (13), 1225 (15), 1201 (19), 1171 (26), 1129 (26), 1114 (28), 1087 (21), 1046 (72), 1032 (40), 1014 (13), 998 (72), 985 (62), 936 (19), 805 (42), 768 (9), 755 (19), 740 (9), 712 (23), 629 (13), 618 (13), 594 (30), 576 (28), 515 (55), 497 (40), 489 (26), 471 (57), 446 (28); **IR (ATR, 298 K, in cm^{-1}):** $\nu = 3066$ (w), 3037 (vw), 2950 (w), 2930 (w), 2891 (w), 2856 (w), 1572 (m), 1558 (w), 1458 (m), 1448 (m), 1418 (m), 1391 (w), 1362 (w), 1262 (vs), 1223 (m), 1150 (s), 1088 (w), 1045 (w), 1029 (vs), 997 (m), 985 (w), 883 (vw), 804 (w), 783 (m), 759 (vs), 739 (m), 713 (w), 701 (w), 637 (vs), 628 (s); **^1H NMR (CD_2Cl_2 , 300 K, in ppm):** $\delta = 1.43\text{-}1.48$ (36H, m, C7-H), 6.82-6.87 (4H, m, C4-H), 7.47-7.54 (4H, m, C3-H), 7.61-7.67 (4H, m, C2-H), 7.98-8.02 (4H, m, C5-H); **$^{13}\text{C}\{^1\text{H}\}$ NMR (CD_2Cl_2 , 300 K, in ppm):**

$\delta = 27.4\text{-}27.6$ (12C, m, C7), $32.1\text{-}32.4$ (4C, m, C6), 121.1 (1C, q, $^1J_{CF} = 321.2$ Hz), 123.0 (4C, s, C4), $128.0\text{-}128.9$ (4C, m, C2), 136.4 (4C, *pseudo-t.* $J_{CP} = 4.4$ Hz, C3), 151.3 (4C, br, C5), $161.2\text{-}161.7$ (4C, m, C1); ^{19}F NMR (CD_2Cl_2 , 300 K, in ppm): $\delta = -78.9$ (3F, s); ^{31}P NMR (CD_2Cl_2 , 190 K, in ppm): AA'BB'MM'XX' spin system: $\delta(\text{P}_A) = -87.6$ ppm, $\delta(\text{P}_B) = -82.4$ ppm, $\delta(\text{P}_M) = -32.5$ ppm, $\delta(\text{P}_X) = -12.4$ ppm; **elemental analysis**: calcd. for $\text{C}_{37}\text{H}_{52}\text{AgF}_3\text{N}_4\text{O}_3\text{P}_8\text{S} \times 1.0 \text{ CH}_2\text{Cl}_2$: C: 40.37, H: 4.81, N: 4.96, S: 2.84; found: C: 40.32, H: 4.53, N: 5.10, S: 3.20.

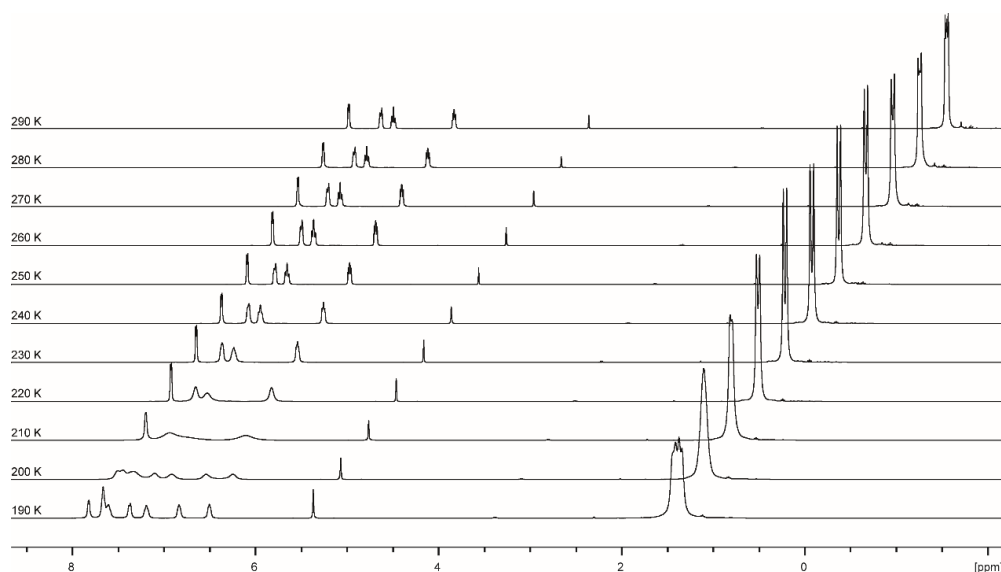


Figure 59. ^1H spectra of $[(72)_2\text{Ag}][\text{OTf}]$ in CD_2Cl_2 from 190-290 K.

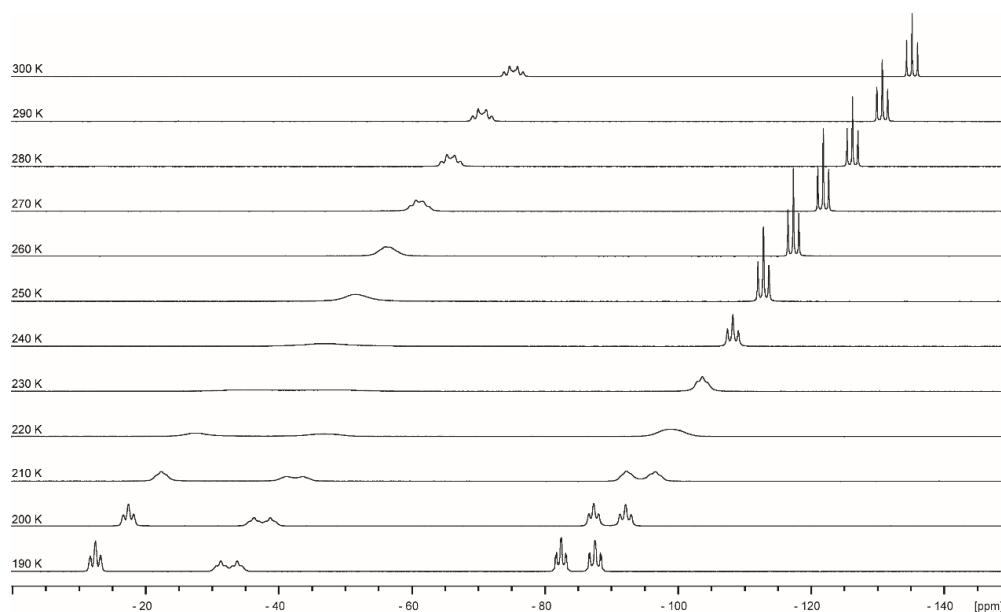
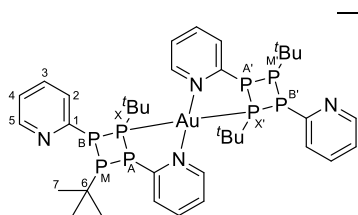


Figure 60. ^{31}P spectra of $[(72)_2\text{Ag}][\text{OTf}]$ in CD_2Cl_2 from 190-290 K.

12.5.5. Preparation of $[(72)_2Au][OTf]$



To a solution of tetraphosphetane **72** (87 mg, 0.22 mmol) in 1 ml of CH_2Cl_2 (tbt)AuCl (35 mg, 0.11 mmol) dissolved in 0.5 ml CH_2Cl_2 is added, followed by the addition of Me_3SiOTf (20 μ l, 0.11 mmol). The reaction

mixture is stirred for 1 h at room temperature. Vapor diffusion of *n*-pentane into this solution at $-30\text{ }^\circ\text{C}$ yields colorless crystals of $[(72)_2Au][OTf]$. These are isolated by decantation, washing with *n*-pentane (3 x 1 ml) and evaporation of all volatiles *in vacuo*.

Yield: 93 mg (74%); **m.p.:** 217 (dec.) $^\circ\text{C}$; **Raman (100 mW, 298 K, in cm^{-1}):** $\nu = 3120$ (19), 3062 (46), 3040 (41), 2957 (80), 2934 (74), 2919 (70), 2894 (100), 2857 (64), 2775 (26), 2711 (31), 1570 (80), 1559 (69), 1458 (58), 1443 (52), 1423 (36), 1275 (34), 1200 (36), 1172 (43), 1113 (49), 1086 (39), 1044 (98), 1031 (57), 991 (82), 986 (86), 936 (32), 805 (52), 755 (34), 713 (39), 702 (33), 624 (30), 598 (43), 576 (45), 537 (63), 496 (47), 486 (37), 473 (61), 445 (42), 436 (39), 391 (43), 364 (34), 347 (35), 313 (42); **IR (ATR, 298 K, in cm^{-1}):** $\nu = 3063$ (w), 3037 (w), 2953 (w), 2930 (w), 2891 (w), 2856 (w), 1569 (m), 1458 (m), 1445 (m), 1419 (m), 1391 (w), 1362 (m), 1262 (vs), 1223 (m), 1149 (vs), 1086 (w), 1042 (w), 1029 (vs), 988 (m), 937 (w), 883 (w), 804 (w), 782 (m), 759 (vs), 738 (s), 714 (w), 700 (w), 637 (vs), 623 (s); **1H NMR (CD_2Cl_2 , 300 K, in ppm):** $\delta = 1.35$ -1.40 (36H, m, C7-H), 6.94-6.98 (4H, m, C4-H), 7.45-7.50 (4H, m, C3-H), 7.55-7.59 (4H, m, C2-H), 8.23-8.25 (4H, m, C5-H); **$^{13}C\{^1H\}$ NMR (CD_2Cl_2 , 300 K, in ppm):** $\delta = 27.9$ -28.3 (12C, m, C7), 33.6-35.8 (4C, m, C6), 121.7 (1C, q, $^1J_{CF} = 320.1$ Hz), 123.7 (4C, s, C4), 128.3-129.1 (4C, m, C2), 136.8 (4C, *pseudo-t*, $J_{CP} = 3.2$ Hz, C3), 151.5 (4C, br, C5), 161.3-161.7 (4C, m, C1); **^{19}F NMR (CD_2Cl_2 , 300 K, in ppm):** $\delta = -78.8$ (3F, s); **^{31}P NMR (CD_2Cl_2 , 190 K, in ppm):** AA'BB'MM'XX' spin system $\delta(P_A) = -77.3$, $\delta(P_B) = -73.0$, $\delta(P_M) = -17.5$, $\delta(P_X) = 19.2$; $^4J(P_A P_{A'}) = -0.01$ Hz, $^2J(P_A P_B) = 3.95$ Hz, $^4J(P_A P_{B'}) = 20.96$ Hz, $^1J(P_A P_M) = -135.52$ Hz, $^5J(P_A P_{M'}) = -2.35$ Hz, $^1J(P_A P_X) = 165.95$ Hz, $^4J(P_A P_{X'}) = -0.92$ Hz, $^4J(P_A \cdot P_B) = 26.27$ Hz, $^2J(P_A \cdot P_{B'}) = -4.31$ Hz, $^5J(P_A \cdot P_M) = 2.64$ Hz, $^1J(P_A \cdot P_{M'}) = -134.40$ Hz, $^4J(P_A \cdot P_X) = 0.87$ Hz, $^1J(P_A \cdot P_{X'}) = 167.77$ Hz, $^4J(P_B P_{B'}) = -1.19$ Hz, $^1J(P_B P_M) = -121.33$ Hz, $^5J(P_B P_{M'}) = 0.18$ Hz, $^1J(P_B P_X) = 153.18$ Hz, $^3J(P_B P_{X'}) = -5.67$ Hz, $^5J(P_B \cdot P_M) = -0.03$ Hz, $^1J(P_B \cdot P_{M'}) = -121.46$ Hz, $^3J(P_B \cdot P_X) = 5.18$ Hz, $^1J(P_B \cdot P_{X'}) = 142.87$ Hz, $^6J(P_M P_{M'}) = 4.55$ Hz, $^2J(P_A P_X) = 7.50$ Hz, $^4J(P_M P_{X'}) = -20.44$ Hz, $^4J(P_M \cdot P_X) = -25.96$ Hz, $^2J(P_M \cdot P_{X'}) = -0.55$ Hz, $^2J(P_X P_{X'}) = 250.91$ Hz; **elemental analysis:** calcd. for $C_{37}H_{52}AuF_3N_4O_3P_8S \times 1.0 CH_2Cl_2$: C: 37.42, H: 4.46, N: 4.59, S: 2.63; found: C: 37.51, H: 4.50, N: 4.50, S: 2.74.

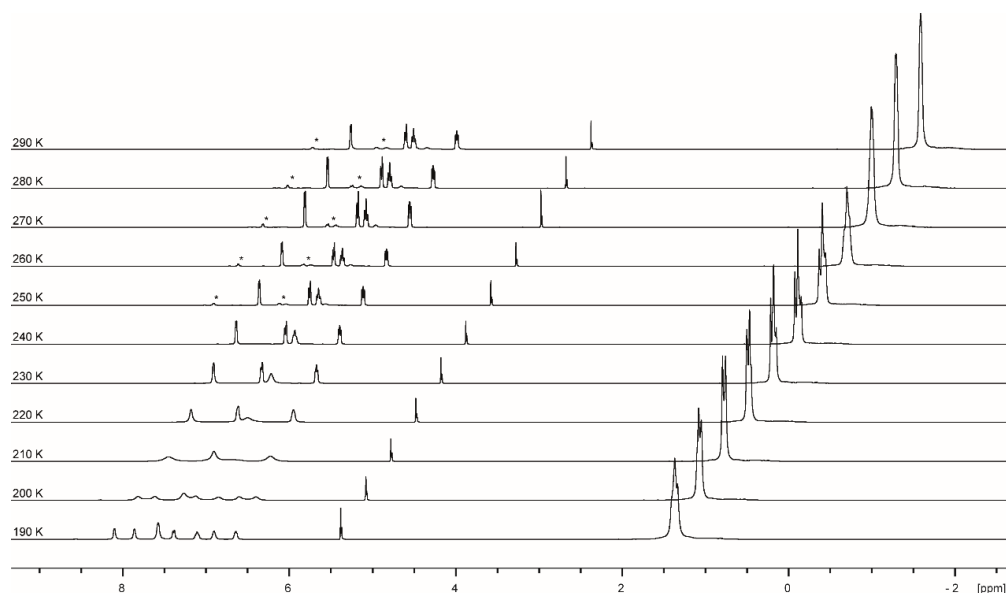


Figure 61. ^1H spectra of $[(72)_2\text{Au}][\text{OTf}]$ in CD_2Cl_2 from 190-290 K; asterisks indicate small amounts of impurities.

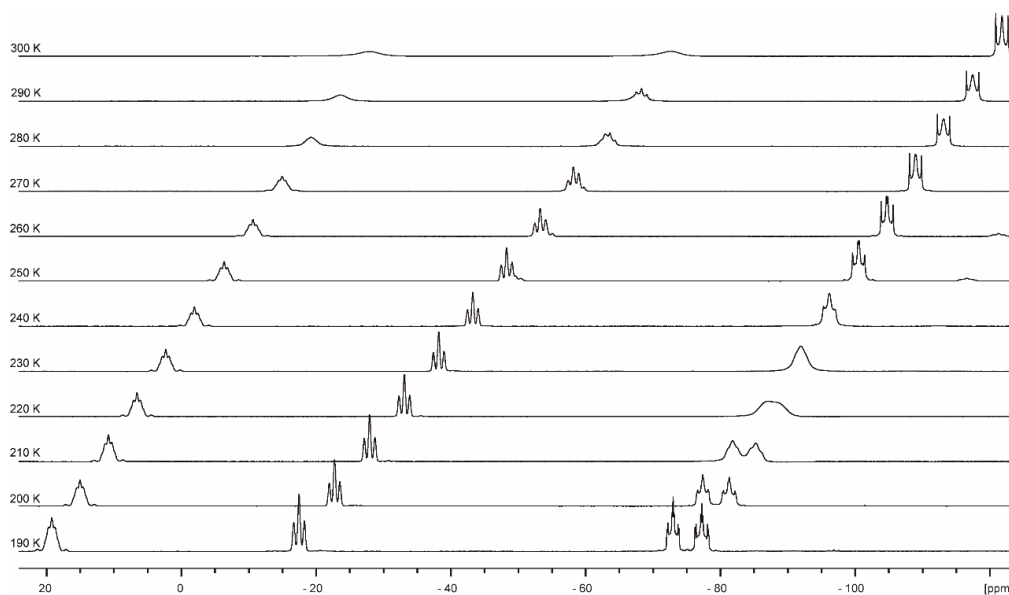
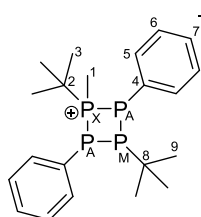


Figure 62. ^{31}P spectra of $[(72)_2\text{Cu}][\text{OTf}]$ in CD_2Cl_2 from 190-290 K.

12.5.6. Preparation of $74[\text{OTf}]$

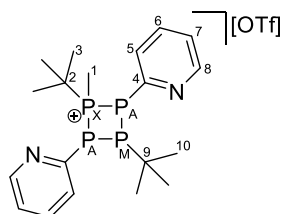


To tetrakis(phenyl)phosphorane **71** (100 mg, 0.25 mmol) in 2 ml Et_2O MeOTf (41 mg, 0.25 mmol) is added yielding a colorless suspension. After stirring for 16 h at r.t. the suspension is filtered and the residue is washed with Et_2O (2 x 2 ml). Subsequent recrystallization of the residue from MeCN/ Et_2O yields crystals of $74[\text{OTf}]$ which are isolated.

Yield: 124 mg (87%); **m.p.:** 185 °C; **Raman (100 mW, 298 K, in cm^{-1}):** $\nu = 3057$ (46), 2958 (53), 2911 (60), 2896 (52), 1581 (79), 1461 (20), 1440 (19), 1394 (11), 1275 (11), 1224

(14), 1165 (22), 1083 (31), 1025 (60), 1000 (100), 944 (14), 804 (26), 753 (22), 694 (14), 610 (16), 574 (27), 475 (43), 454 (19), 426 (17), 398 (17), 375 (19), 346 (21), 310 (23), 293 (20), 233 (35), 208 (27), 177 (40); **IR (ATR, 298 K, in cm^{-1}):** $\nu = 3059$ (w), 2943 (m), 2929 (m), 2887 (w), 2852 (m), 1580 (w), 1520 (w), 1469 (m), 1455 (m), 1433 (m), 1400 (w), 1387 (w), 1359 (s), 1323 (w), 1300 (w), 1282 (m), 1168 (s), 1155 (s), 1099 (w), 1081 (w), 1064 (m), 1024 (s), 998 (m), 934 (m), 911 (w), 805 (m), 742 (vs), 691 (vs), 610 (m), 573 (m), 541 (m), 508 (s), 480 (m), 440 (m), 428 (m), 406 (m); **^1H NMR (CD_2Cl_2 , 300 K, in ppm):** $\delta = 1.26$ (3H, d, $^2J_{\text{HP}} = 12.11$ Hz, C1–H), 1.40 (9H, s, C3–H), 1.42–1.44 (9H, m, C9–H), 7.60–7.64 (6H, m, C6/C7–H), 7.80–7.85 (4H, m, C5–H); **$^{13}\text{C}\{^1\text{H}\}$ NMR (CD_2Cl_2 , 300 K, in ppm):** $\delta = 3.2$ –3.4 (1C, m, C1), 24.5 (3C, m, C3), 28.6 (3C, dt, $^2J_{\text{CP}} = 15.4$ Hz, $^3J_{\text{CP}} = 5.6$ Hz, C9), 32.6–33.2 (1C, m, C8), 35.8–36.1 (1C, m, C2), 121.5 (1C, q, $^1J_{\text{CF}_3} = 320.3$ Hz, CF_3), 123.7–124.2 (2C, m, C4), 131.0–131.1 (4C, m, C6), 132.6–132.7 (2C, m, C7), 135.5–135.8 (4C, m, C5); **^{19}F NMR (CD_2Cl_2 , 300 K, in ppm):** $\delta = -79.5$ (3F, s); **^{31}P NMR (CD_2Cl_2 , 300 K, in ppm):** A_2MX spin system: $\delta(\text{P}_\text{A}) = -81.2$ (2P), $\delta(\text{P}_\text{M}) = -39.8$ (1P), $\delta(\text{P}_\text{X}) = 22.0$ (1P); $^1J(\text{P}_\text{A}\text{P}_\text{X}) = -248$ Hz, $^1J(\text{P}_\text{A}\text{P}_\text{M}) = -127$ Hz, $^2J(\text{P}_\text{M}\text{P}_\text{X}) = 23$ Hz; **elemental analysis:** calcd. for $\text{C}_{22}\text{H}_{31}\text{F}_3\text{O}_3\text{P}_4\text{S}$: C: 47.49, H: 5.62, S: 5.76; found: C: 47.28, H: 5.39, S: 6.16.

12.5.7. Preparation of **75**[OTf]

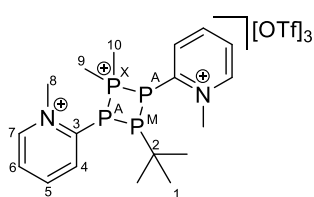


To tetraphosphatane **72** (360 mg, 0.91 mmol) in 3 ml of Et_2O MeOTf (150 mg, 0.91 mmol) is added yielding a colorless suspension. After stirring for 16 h at r.t. the suspension is filtered and the residue is washed with Et_2O (2 x 2 ml). Subsequent recrystallization of the residue from $\text{MeCN}/\text{Et}_2\text{O}$ yields crystals of **75**[OTf] which are isolated.

Yield: 466 mg (91%); **m.p.:** 121 °C; **Raman (100 mW, 298 K, in cm^{-1}):** $\nu = 3122$ (15), 3056 (43), 2964 (57), 2942 (70), 2904 (100), 2783 (9), 1570 (72), 1560 (48), 1464 (26), 1442 (22), 1276 (15), 1223 (15), 1175 (17), 1113 (20), 1044 (61), 1031 (61), 987 (93), 938 (11), 804 (28), 753 (24), 715 (13), 617 (15), 608 (15), 574 (26), 498 (17), 476 (37), 422 (13), 397 (15), 368 (15), 347 (15), 312 (20), 223 (20), 198 (41); **IR (ATR, 298 K, in cm^{-1}):** $\nu = 3036$ (w), 2943 (m), 2927 (m), 2888 (m), 2853 (m), 2709 (w), 1569 (vs), 1556 (s), 1470 (m), 1447 (vs), 1416 (vs), 1388 (m), 1360 (vs), 1268 (m), 1227 (m), 1202 (m), 1167 (s), 1149 (s), 1082 (m), 1046 (m), 1008 (m), 986 (m), 934 (w), 887 (w), 804 (m), 768 (s), 757 (vs), 740 (s), 712 (m), 639 (w), 618 (s), 574 (m), 554 (w), 517 (m), 500 (s), 467 (m), 407 (m); **^1H NMR (CD_3CN , 300 K, in ppm):** $\delta = 1.44$ (3H, d, $^2J_{\text{HP}} = 12.95$ Hz, C1–H), 1.47–1.50 (9H, m, C10–H), 1.51–1.54 (9H, m, C3–H), 7.39–7.42 (2H, m, C7–H), 7.84–7.91 (4H, m, C5/C6–H), 8.66–8.68 (2H, m, C8–H); **$^{13}\text{C}\{^1\text{H}\}$ NMR (CD_3CN , 300 K, in ppm):** $\delta = 5.6$ –5.8 (1C, m, C1),

25.0-25.1 (3C, m, C3), 28.9 (3C, dt, $^2J_{CP} = 15.4$ Hz, $^3J_{CP} = 5.7$ Hz, C10), 32.7-33.2 (1C, m, C9), 36.2-36.6 (1C, m, C2), 122.6 (1C, q, $^1J_{CF_3} = 321.1$ Hz, CF₃), 125.7 (2C, d, $^4J_{CP} = 1.8$ Hz, C7), 130.5-130.7 (2C, m, C5), 139.1 (2C, m, C6), 152.4-152.5 (2C, m, C8), 155.2-155.6 (2C, m, C4); **¹⁹F NMR (CD₃CN, 300 K, in ppm):** $\delta = -79.3$ (3F, s); **³¹P NMR (CD₃CN, 300 K, in ppm):** A₂MX spin system: $\delta(P_A) = -70.5$ (2P), $\delta(P_M) = -24.9$ (1P), $\delta(P_X) = 24.2$ (1P); $^1J(P_AP_X) = -225$ Hz, $^1J(P_AP_M) = -132$ Hz, $^2J(P_MP_X) = 15$ Hz; **elemental analysis:** calcd. for C₂₀H₂₉F₃N₂O₃P₄S: C: 43.02, H: 5.23, N: 5.02, S: 5.74; found: C: 42.56, H: 4.89, N: 5.04, S: 5.96.

12.5.8. Preparation of 78[OTf]₃

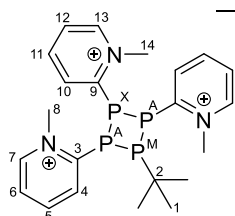


To tetraphosphetane **72** (100 mg, 0.25 mmol) MeOTf (600 μ l, 5.5 mmol) is added. After stirring this mixture for 4 h at 80 °C a red solution is obtained. Upon adding Et₂O (2 ml) a colorless precipitate forms which is filtered off and washed with Et₂O (2 x 2 ml) and CH₂Cl₂ (1 x 2 ml). Subsequent evaporation of all volatiles *in vacuo* yields the product as a colorless solid.

Yield: 195 mg (91%); **m.p.:** 212 °C; **Raman (100 mW, 298 K, in cm⁻¹):** $\nu = 3093$ (22), 3037 (11), 2963 (52), 2943 (29), 2906 (67), 2864 (18), 1606 (59), 1575 (29), 1491 (19), 1467 (20), 1443 (19), 1400 (15), 1315 (19), 1278 (25), 1227 (25), 1186 (27), 1156 (25), 1091 (22), 1062 (67), 1033 (100), 799 (34), 758 (47), 721 (15), 711 (16), 692 (19), 574 (41), 563 (35), 519 (14), 489 (29), 448 (38), 433 (31), 409 (16), 393 (19), 375 (18), 349 (39), 315 (32), 274 (21), 225 (34), 176 (32); **IR (ATR, 298 K, in cm⁻¹):** $\nu = 3082$ (vs), 2986 (vs), 2905 (vs), 1606 (vs), 1575 (vs), 1490 (vs), 1467 (vs), 1445 (vs), 1403 (vs), 1371 (vs), 1248 (vs), 1224 (vs), 1149 (vs), 1090 (vs), 1064 (vs), 1027 (vs), 961 (vs), 912 (vs), 865 (vs), 781 (vs), 758 (vs), 720 (vs), 692 (vs), 635 (vs), 573 (vs), 516 (vs), 499 (vs), 436 (vs), 409 (vs); **¹H NMR (CD₃NO₂, 300 K, in ppm):** $\delta = 1.48$ (9H, d, $^2J_{HP} = 16.64$ Hz, C1-H), 2.26 (3H, d, $^2J_{HP} = 13.67$ Hz, C9/C10-H), 2.83 (3H, dt, $^2J_{HP} = 14.31$ Hz, $^3J_{HP} = 7.10$ Hz, C9/C10-H), 4.80 (6H, s, C8-H), 8.27-8.31 (2H, m, C6-H), 8.78-8.83 (2H, m, C5-H), 9.07-9.10 (2H, m, C7-H), 9.10-9.14 (2H, m, C4-H); **¹³C{¹H} NMR (CD₃NO₂, 300 K, in ppm):** $\delta = 10.2$ (1C, d, $^1J_{CP} = 21.2$ Hz, C9/C10), 17.8 (1C, dtd, $^1J_{CP} = 31.3$ Hz, $^2J_{CP} = 13.5$ Hz, $^3J_{CP} = 3.3$ Hz, C9/C10), 28.9 (3C, dt, $^2J_{CP} = 15.0$ Hz, $^3J_{CP} = 5.0$ Hz, C1), 35.8-36.4 (1C, m, C2), 51.4 (2C, *pseudo-t*, $J_{CP} = 11.7$ Hz, C8), 122.6 (3C, q, $^1J_{CF_3} = 320.0$ Hz, CF₃), 131.6 (2C, s, C6), 139.9 (2C, dd, $^2J_{CP} = 22.2$ Hz, $^3J_{CP} = 4.1$ Hz, C4), 147.2 (2C, s, C5), 148.6 (2C, m, C3), 152.7 (2C, s, C7); **¹⁹F NMR (CD₃NO₂, 300 K, in ppm):** $\delta = -79.6$ (9F, s); **³¹P NMR (CD₃NO₂, 300 K, in**

ppm): A₂MX spin system: $\delta(\text{P}_A) = -73.5$ (2P), $\delta(\text{P}_M) = -12.0$ (1P), $\delta(\text{P}_X) = 19.9$ (1P); $^1J(\text{P}_A\text{P}_X) = -228$ Hz, $^1J(\text{P}_A\text{P}_M) = -118$ Hz, $^2J(\text{P}_M\text{P}_X) = 31$ Hz; **elemental analysis:** calcd. for C₂₁H₂₉F₉N₂O₉P₄S₃: C: 29.87, H: 3.46, N: 3.32, S: 11.39; found: C: 30.31, H: 3.70, N: 3.12, S: 11.57.

12.5.9. Preparation of **82**[OTf]₃



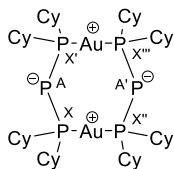
To tetraphosphetanium triflate **78**[OTf]₃ (109 mg, 0.129 mmol) in 1 ml of MeCN Me₂PPMe₂ (15.8 mg, 0.129 mmol) in 0.2 ml of MeCN is added. The deep red reaction mixture is stirred at r.t. for 4 h. Upon addition of CH₂Cl₂ *via* vapor diffusion at -30 °C colorless crystals of tetraphosphetane **82**[OTf]₃ are obtained over the course of 36 h. The mother liquor is decanted of and the crystals are washed with CH₂Cl₂ and are subsequently dried *in vacuo* to yield tetraphosphetane **82**[OTf]₃.

Yield: 26 mg (45%); **m.p.:** 275 °C (dec.); **Raman (100 mW, 298 K, in cm⁻¹):** $\nu = 3091$ (22), 2965 (30), 2935 (20), 2897 (24), 2861 (10), 2721 (5), 1610 (47), 1571 (31), 1496 (18), 1442 (17), 1276 (19), 1228 (22), 1181 (46), 1156 (33), 1095 (34), 1068 (80), 1032 (100), 798 (42), 758 (41), 692 (26), 576 (36), 564 (43), 498 (72), 443 (34), 428 (33), 399 (24), 350 (39), 316 (35), 279 (23), 242 (24), 206 (23), 171 (60); **IR (ATR, 298 K, in cm⁻¹):** $\nu = 3126$ (vw), 3089 (vw), 3043 (vw), 2956 (vw), 1608 (vw), 1570 (vw), 1495 (w), 1444 (vw), 1367 (vw), 1313 (vw), 1274 (s), 1245 (vs), 1224 (s), 1176 (m), 1150 (s), 1026 (vs), 896 (vw), 798 (vw), 775 (m), 756 (w), 718 (w), 691 (vw), 635 (vs), 572 (m), 516 (s), 456 (w), 431 (m); **¹H NMR (CD₃CN, 300 K, in ppm):** $\delta = 1.41$ (9H, d, $^2J_{\text{HP}} = 15.26$ Hz, C1–H), 4.36 (3H, d, $^4J_{\text{HP}} = 3.23$ Hz, C14–H), 4.43 (6H, bs, C8–H), 8.01–8.07 (3H, m, C6/C12–H), 8.56–8.62 (3H, m, C5/C11–H), 8.64–8.68 (1H, m, C10–H), 8.69–8.73 (1H, m, C13–H), 8.75–8.78 (2H, m, C7–H), 8.83–8.87 (2H, m, C4–H); **¹³C{¹H} NMR (CD₃CN, 300 K, in ppm):** $\delta = 29.1$ (3C, dt, $^2J_{\text{CP}} = 14.7$ Hz, $^3J_{\text{CP}} = 5.2$ Hz, C1), 34.8–35.0 (1C, m, C2), 50.2 (2C, bs, C8), 50.4 (1C, d, $^3J_{\text{CP}} = 11.9$ Hz, C14), 122.1 (3C, q, $^1J_{\text{CF}_3} = 322.2$ Hz, CF₃), 129.6 (2C, s, C6), 129.8 (1C, s, C12), 138.8–139.2 (1C, m, C10), 139.2–139.6 (2C, m, C4), 145.7 (2C, s, C5), 145.9 (1C, s, C11), 149.9 (1C, s, C13), 149.6 (2C, m, C7), 158.3–158.8 (1C, m, C9), 159.7–160.1 (2C, m, C3); **¹⁹F NMR (CD₃CN, 300 K, in ppm):** $\delta = -79.3$ (9F, s); **³¹P NMR (CD₃CN, 300 K, in ppm):** A₂MX spin system: $\delta(\text{P}_A) = -68.3$ (2P), $\delta(\text{P}_M) = -51.1$ (1P), $\delta(\text{P}_X) = 2.7$ (1P); $^1J(\text{P}_A\text{P}_X) = -123$ Hz, $^1J(\text{P}_A\text{P}_M) = -100$ Hz, $^2J(\text{P}_M\text{P}_X) = 91$ Hz; **elemental analysis:** calcd. for C₂₅H₃₀F₉N₃O₉P₄S₃: C: 33.09, H: 3.33, N: 4.63, S: 10.60; found: C: 32.78, H: 3.27, N: 4.61, S: 10.52.

12.6. Syntheses and Characterization Data regarding Compounds in

Chapter 7

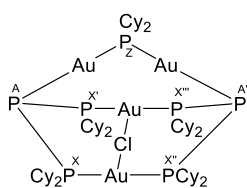
12.6.1. Preparation of **84**



To *iso*-tetraphosphane **8** (1245 mg, 2.00 mmol) and (tbt)AuCl (641 mg, 2.00 mmol) THF (20 ml) is added. The mixture is stirred for 15 minutes to form an orange solution. After that all volatiles are evaporated *in vacuo*. The residue is washed with *n*-pentane (3 x 10 ml) and subsequently dried *in vacuo* to yield the product as a beige powder.

Yield: 1108mg (89%); **m.p.:** 199 °C (dec.); **Raman (100 mW, 50 scans, 298 K, in cm⁻¹):** $\nu = 2934$ (90), 2885 (46), 2862 (94), 2847 (100), 1462 (20), 1443 (47), 1329 (22), 1291 (28), 1267 (34), 1190 (27), 1169 (15), 1105 (14), 1077 (14), 1042 (24), 1026 (41), 999 (18), 851 (22), 818 (35), 733 (33), 549 (18), 516 (14), 441 (22), 422 (19), 335 (16), 257 (34), 236 (29), 198 (38), 170 (43); **IR (ATR, 298 K, in cm⁻¹):** $\nu = 2915$ (vs), 2845 (vs), 1443 (s), 1336 (m), 1291 (w), 1262 (w), 1189 (w), 1175 (m), 1168 (m), 1104 (w), 1074 (w), 1048 (w), 1026 (w), 1001 (m), 918 (w), 884 (m), 848 (m), 816 (w), 727 (m); **¹H NMR (THF-d₈, 300 K, in ppm):** $\delta = 1.16$ -1.26 (8H, m, CH₂), 1.27-1.37 (8H, m, CH₂), 1.50-1.60 (8H, m, CH₂), 1.67-1.72 (8H, m, CH₂), 1.73-1.79 (8H, m, CH₂), 1.80-1.86 (16H, m, CH₂), 1.90-1.98 (8H, m, CH), 2.00-2.06 (8H, m, CH₂), 2.13-2.20 (8H, m, CH₂); **¹³C{¹H} NMR (THF-d₈, 300 K, in ppm):** $\delta = 27.6$ (8C, s, CH₂), 28.1-28.3 (16C, m, CH₂), 30.4-30.5 (8C, m, CH₂), 32.2 (8C, m, CH₂), 39.4-39.8 (8C, m, CH); **³¹P NMR (THF-d₈, 300 K, in ppm):** AA'XX'X''X''' spin system: $\delta(\text{P}_A) = -172.0$ (1P), $\delta(\text{P}_{A'}) = -172.0$ (1P), $\delta(\text{P}_X) = 49.0$ (1P), $\delta(\text{P}_{X'}) = 49.0$ (1P), $\delta(\text{P}_{X''}) = 49.0$ (1P), $\delta(\text{P}_{X'''}) = 49.0$ (1P), $\delta(\text{P}_{X''''}) = 49.0$ (1P); $^4J(\text{P}_A\text{P}_{A'}) = -1.66$ Hz, $^1J(\text{P}_A\text{P}_X) = -406.15$ Hz, $^1J(\text{P}_A\text{P}_{X'}) = -417.84$ Hz, $^3J(\text{P}_A\text{P}_{X''}) = 8.37$ Hz, $^4J(\text{P}_A\text{P}_{X''''}) = -4.66$ Hz, $^3J(\text{P}_{A'}\text{P}_X) = 9.64$ Hz, $^3J(\text{P}_{A'}\text{P}_{X'}) = -8.50$ Hz, $^1J(\text{P}_{A'}\text{P}_{X''}) = -405.61$ Hz, $^1J(\text{P}_{A'}\text{P}_{X''''}) = -416.90$ Hz, $^2J(\text{P}_X\text{P}_{X'}) = 41.89$ Hz, $^2J(\text{P}_X\text{P}_{X''}) = 18.18$ Hz, $^4J(\text{P}_X\text{P}_{X''''}) = 252.48$ Hz, $^4J(\text{P}_{X'}\text{P}_{X''''}) = 256.88$ Hz, $^2J(\text{P}_{X'}\text{P}_{X''''}) = 20.48$ Hz, $^3J(\text{P}_{X''}\text{P}_{X''''}) = 41.79$ Hz; **elemental analysis:** calcd. for C₄₈H₈₈Au₂P₆: C: 46.31, H: 7.12; found: C: 46.21, H: 6.89.

12.6.2. Preparation of **86**



To *iso*-tetraphosphane **8** (622 mg, 1.00 mmol) and Cy₄P₂ (197 mg, 0.5 mmol) in THF (10 ml) (tbt)AuCl (641 mg, 2.00 mmol) is added. The mixture is stirred for 30 minutes. After that all volatiles are evaporated *in vacuo*. The residue is washed with *n*-pentane (3 x 10 ml) and subsequently dried *in vacuo* to yield the product as a beige powder.

Yield: 901 mg (96%); **m.p.:** 178 °C (dec.); **Raman (100 mW, 128 scans, 298 K, in cm⁻¹):** $\nu = 2932$ (100), 2893 (43), 2852 (71), 2657 (17), 1460 (9), 1444 (20), 1345 (9), 1334 (9), 1327 (9), 1294 (11), 1265 (11), 1196 (8), 1175 (7), 1047 (8), 1028 (14), 1000 (8), 850 (9), 817 (11), 740 (8), 710 (9), 542 (5), 516 (6), 440 (5), 401 (5), 313 (6), 287 (7), 175 (9), 152 (9), 130 (5); **IR (ATR, 298 K, in cm⁻¹):** $\nu = 2918$ (vs), 2845 (s), 1444 (s), 1335 (w), 1291 (m), 1264 (m), 1221 (w), 1194 (w), 1174 (m), 1120 (m), 1070 (w), 1043 (w), 1026 (w), 998 (m), 914 (w), 888 (m), 849 (m), 815 (w), 740 (w), 708 (w); **¹H NMR (THF-d₈, 300 K, in ppm):** $\delta = 1.17$ -1.41 (32H, m, CH/CH₂), 1.47-1.60 (4H, m, CH/CH₂), 1.64-1.75 (32H, m, CH/CH₂), 1.80-1.91 (18H, m, CH/CH₂), 2.11-2.24 (12H, m, CH/CH₂), 2.24-2.34 (6H, m, CH/CH₂), 2.69-2.78 (3H, m, CH/CH₂), 2.82-2.97 (3H, m, CH/CH₂); **¹³C{¹H} NMR (THF-d₈, 300 K, in ppm):** $\delta = 27.2$ -27.3 (m, CH/CH₂), 27.8 (s, CH/CH₂), 28.5-28.6 (m, CH/CH₂), 28.6 (s, CH/CH₂), 28.7 (s, CH/CH₂), 28.8-30.0 (m, CH/CH₂), 29.3 (bs, CH/CH₂), 29.7-29.8 (m, CH/CH₂), 33.5 (s, CH/CH₂), 33.7 (s, CH/CH₂), 33.8 (s, CH/CH₂), 35.1-35.2 (m, CH/CH₂), 37.2 (s, CH/CH₂), 39.3 (s, CH/CH₂), 39.4 (s, CH/CH₂), 39.5-39.8 (m, CH/CH₂), 44.4-44.5 (m, CH/CH₂); **³¹P NMR (THF-d₈, 300 K, in ppm):** AA'XX'X''X'''Z spin system: $\delta(P_A) = -113.0$ (1P), $\delta(P_{A'}) = -113.0$ (1P), $\delta(P_X) = 36.4$ (1P), $\delta(P_{X'}) = 36.4$ (1P), $\delta(P_{X''}) = 36.4$ (1P), $\delta(P_{X'''}) = 36.4$ (1P), $\delta(P_Z) = 65.1$ (1P); $^4J(P_A P_{A'}) = -1.84$ Hz, $^1J(P_A P_X) = -257.00$ Hz, $^1J(P_A P_{X'}) = -260.92$ Hz, $^3J(P_A P_{X''}) = 0.14$ Hz, $^3J(P_A P_{X'''}) = -2.59$ Hz, $^2J(P_A P_Z) = 71.69$ Hz, $^3J(P_{A'} P_X) = -2.08$ Hz, $^3J(P_{A'} P_{X'}) = 2.87$ Hz, $^1J(P_{A'} P_{X''}) = -264.17$ Hz, $^1J(P_{A'} P_{X'''}) = -256.32$ Hz, $^2J(P_{A'} P_Z) = 71.66$ Hz, $^2J(P_X P_{X'}) = 32.44$ Hz, $^2J(P_X P_{X''}) = 6.26$ Hz, $^4J(P_X P_{X'''}) = 293.91$ Hz, $^3J(P_X P_Z) = 6.38$ Hz, $^4J(P_{X'} P_{X''}) = 292.09$ Hz, $^2J(P_{X'} P_{X'''}) = -3.39$ Hz, $^3J(P_{X'} P_Z) = 7.07$ Hz, $^3J(P_{X''} P_{X'''}) = 32.97$ Hz, $^3J(P_{X''} P_Z) = 6.63$ Hz, $^3J(P_{X'''} P_Z) = 7.20$ Hz; **elemental analysis:** calcd. for C₆₀H₁₁₀Au₄ClP₇ x 0.85 THF: C: 39.40, H: 6.09; found: C: 39.47, H: 5.99.

12.6.3. Degradation reaction of **86**

A solution of **86** (100 mg, 0.05 mmol) is stirred in PhMe at 100 °C for 24 h, giving an orange-red-colored reaction mixture. Slow vapor addition of *n*-hexane to the reaction mixture gives X-ray quality crystals of **87** next to copious amounts of amorphous material, thus hampering isolation of analytically pure **87**. The ³¹P{¹H} NMR spectrum is depicted in Figure 42.

³¹P NMR (C₆D₆-capillary, 300 K, in ppm): AUVWXYZ spin system (**87**): $\delta(P_A) = -101.1$, $\delta(P_U) = 64.4$, $\delta(P_V) = 66.1$, $\delta(P_W) = \delta(P_X) = \delta(P_Y) = \delta(P_Z) = 70.0$ -81.0 ppm; $\delta(P) = 46.3$ ppm ((C₂P–Au)_n), $\delta(P) = 54.2$ ppm ((C₂P–Au)₆); $\delta(P) = 127.3$ ppm (C₂PCl).

12.7. Syntheses and Characterization Data regarding Compounds in Chapter 8

12.7.1. Reaction of 48 with (PhCN)₂PtCl₂

To triphosphane **48** (50 mg, 0.1 mmol) in CH₂Cl₂ (1 ml) (PhCN)₂PtCl₂ (47 mg, 0.1 mmol) in CH₂Cl₂ (1 ml) is added. The initially yellow-colored solution turns to dark green over the course of 16 h. The ³¹P{¹H} NMR spectrum is depicted in Figure 44.

³¹P NMR (C₆D₆-capillary, 300 K, in ppm): AX₂ spin system (**48**): δ(P_A) = -57.3, δ(P_X) = -7.7, ¹J(P_AP_X) = -251.3 Hz; AA'MM' spin system (**88**): δ(P_A) = -33.2, δ(P_M) = 32.4 ppm; A₂M spin system (**48**PtCl₂): δ(P_A) = -32.5, δ(P_M) = 5.2 ppm; ¹J_{AM} = 168 Hz; δ(P) = 118.5 ppm (“Cy₂P(Cl)Pt”).

To a suspension of (PhCN)₂PtCl₂ (25 mg, 0.053 mmol) in PhMe (1 ml) a solution of **48** (27 mg, 0.053 mmol) in PhMe (1 ml) is added. The suspension turns into a clear, lightly yellow-colored solution after 16 h. Cooling this solution to -30 °C gives crystals of **48**PtCl₂*PhMe in X-ray quality.

12.7.2. Reaction of 48 with (PhCN)₂PtCl₂ and 52 at ambient temperature

Triphosphane **48** (50 mg, 0.10 mmol), (PhCN)₂PtCl₂ (47 mg, 0.10 mmol) and **52** (11 mg, 0.02 mmol) are stirred in PhF (2 ml) for 16 h, giving a dark yellow-colored solution. The ³¹P{¹H} NMR spectrum is depicted in Figure 63.

³¹P NMR (C₆D₆-capillary, 300 K, in ppm): AX₂ spin system (**48**): δ(P_A) = -57.3, δ(P_X) = -7.7, ¹J(P_AP_X) = -251.3 Hz; AA'MM' spin system (**88**): δ(P_A) = -33.2, δ(P_M) = 32.4 ppm; A₂M spin system (**48**PtCl₂): δ(P_A) = -32.5, δ(P_M) = 5.2 ppm; ¹J_{AM} = 168 Hz; δ(P) = 118.5 ppm (“Cy₂P(Cl)Pt”); δ(P) = 127.5 ppm (Cy₂PCL).

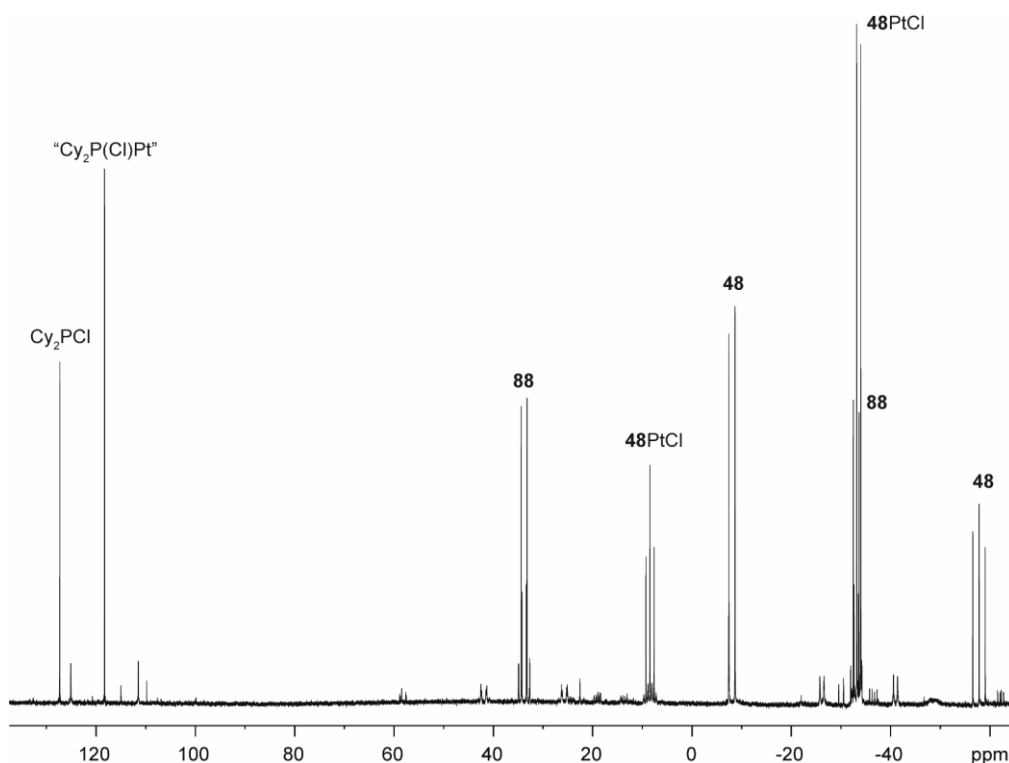


Figure 63. $^{31}\text{P}\{^1\text{H}\}$ NMR spectrum of a mixture of **48**, $(\text{PhCN})_2\text{PtCl}_2$ and $1/5$ eq. of **52** in PhF after 16 h at ambient temperature.

12.7.3. Reaction of **48** with $(\text{PhCN})_2\text{PtCl}_2$ and **52** at elevated temperature

Triphospane **48** (27 mg, 0.05 mmol), $(\text{PhCN})_2\text{PtCl}_2$ (25 mg, 0.05 mmol) and **52** (6 mg, 0.01 mmol) are stirred in PhF (2 ml) for 14 h at 100 °C, giving a dark green-colored solution. Upon addition of *n*-pentane (2 ml) a voluminous, green precipitate appears, which is filtered off, washed with *n*-pentane (2 x 1 ml) and Et_2O (2 x 1 ml) and dried *in vacuo*. This crude product is recrystallized by slow vapor addition of Et_2O to a CH_2Cl_2 solution giving a few crystals of **88***3 CH_2Cl_2 next to copious amounts of a green-colored oil, which was not further investigated. The $^{31}\text{P}\{^1\text{H}\}$ NMR spectrum is depicted in Figure 45.

^{31}P NMR (C_6D_6 -capillary, 300 K, in ppm): AA'MM' spin system (**88**): $\delta(\text{P}_A) = -33.2$, $\delta(\text{P}_M) = 32.4$ ppm; $\delta(\text{P}) = 127.5$ ppm ($\text{Cy}_2\text{P-Cl}$).

12.7.4. Reaction of **48** with $(\text{PhCN})_2\text{PdCl}_2$

To triphospane **48** (50 mg, 0.1 mmol) in CH_2Cl_2 (1 ml) $(\text{PhCN})_2\text{PdCl}_2$ (38 mg, 0.1 mmol) in CH_2Cl_2 (1 ml) is added to form a clear, orange-colored solution. Slow vapor addition of *n*-pentane gives crystal of **48PdCl}_2***3 CH_2Cl_2 after 2 days. Crystals of **89***3 CH_2Cl_2 * $1/2$ *n*-pentane grew after three weeks in the same vial.

12.7.5. Reaction of **48** with $(PhCN)_2PdCl_2$ and **52** at ambient temperature

Triphosphane **48** (53 mg, 0.1 mmol), $(PhCN)_2PdCl_2$ (40 mg, 0.1 mmol) and **52** (11 mg, 0.02 mmol) are stirred in PhF (2 ml) for 16 h at ambient temperature, giving an orange-colored solution. The $^{31}P\{^1H\}$ NMR spectrum is depicted in Figure 48.

^{31}P NMR (C_6D_6 -capillary, 300 K, in ppm): A_2M spin system (**48** $PdCl_2$): $\delta(P_A) = -25.8$, $\delta(P_M) = -12.8$ ppm, $^1J_{AM} = 179$ Hz; $AA'MM'$ spin system (**89**): $\delta(P_A) = -23.9$, $\delta(P_M) = 54.2$ ppm; $\delta(P) = 127.3$ ppm (Cy_2PCL).

12.7.6. Reaction of **48** with $(PhCN)_2PdCl_2$ and **52** at elevated temperature

Triphosphane **48** (66 mg, 0.13 mmol), $(PhCN)_2PdCl_2$ (50 mg, 0.13 mmol) and **52** (14 mg, 0.026 mmol) are stirred in PhF (2 ml) for 3 h at 100 °C, giving a dark red-colored solution. Addition of *n*-pentane gives a fine, orange-colored precipitate, which is filtered off, washed with *n*-pentane (3 x 1 ml) and dried *in vacuo*. Recrystallization from a 1,2- $C_6H_4F_2$ solution by slow vapor addition of *n*-hexane yields few crystals of **90*** $^{3/2}$ 1,2- $C_6H_4F_2$ * $^{1/2}$ *n*-hexane next to crystals of **89**. The $^{31}P\{^1H\}$ NMR spectrum is depicted in Figure 49.

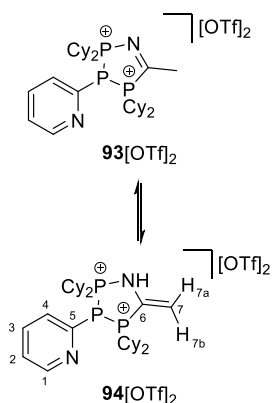
^{31}P NMR (C_6D_6 -capillary, 300 K, in ppm): $ACMNPQ$ spin system (**90**): $\delta(P_A) = -35.4$, $\delta(P_C) = -10.7$, $\delta(P_M) = 47.4$, $\delta(P_N) = 49.3$, $\delta(P_P) = 64.9$, $\delta(P_Q) = 78.5$ ppm; $AA'MM'$ spin system (**89**): $\delta(P_A) = -23.8$, $\delta(P_M) = 54.2$ ppm; $\delta(P) = 21.3$ ppm (Cy_4P_2); $\delta(P) = 127.3$ ppm (Cy_2PCL).

12.7.7. Reaction of **72** with $(PhCN)_2PdCl_2$

Tetraphosphetane **72** (41 mg, 0.1 mmol) and $(PhCN)_2PdCl_2$ (40 mg, 0.1 mmol) are stirred in CH_2Cl_2 , giving a red-colored solution. Addition of Et_2O gives a voluminous, orange-colored precipitate, which is filtered off, washed with Et_2O (3 x 1 ml) and dried *in vacuo*. Recrystallization from a MeCN solution by slow vapor addition of Et_2O yields few crystals of **91***MeCN next to an orange-colored oil, which was not further investigated.

12.8. Syntheses and Characterization Data regarding Compounds in Chapter 9

12.8.1. Preparation of a tautomeric mixture of **93**[OTf]₂ and **94**[OTf]₂



To a solution of triphosphane **48** (252 mg, 0.5 mmol) in 2 ml of MeCN [Ph₃As][OTf]₂ (302 mg, 0.5 mmol) is added while stirring. The initially colorless suspension turns yellow and forms a red-colored solution after 1 h of stirring at ambient temperature. Addition of Et₂O (5 ml) gives a light-yellow precipitate, which is filtered off and washed with Et₂O (3 x 2 ml). Evaporation of all volatiles *in vacuo* yields the product as a light-yellow powder. The product is obtained as a mixture of the tautomers **93**[OTf]₂ (imine form) and **94**[OTf]₂

(enamine form). In a CD₃CN solution the enamine form **94**[OTf]₂ is observed as the major tautomer (85% by integration in the ³¹P NMR spectrum). Thus, resonances in the ¹H and ¹³C NMR spectra are only assignable to **94**[OTf]₂. The ³¹P NMR data allows assignment to **93**²⁺ and **94**²⁺.

Yield: 364 mg (86%); **¹H NMR (CD₃CN, 300 K, in ppm):** δ = 1.15-1.51 (16H, m, CH₂), 1.51-1.69 (8H, m, CH₂), 1.69-1.98 (10H, m, CH₂), 1.98-2.18 (6H, m, CH₂), 2.98-3.11 (3H, m, CH), 3.16-3.27 (1H, m, CH), 5.51 (1H, dd, ⁴J_{HH} = 11.43 Hz, ²J_{HH} = 4.14 Hz, H-7a), 6.17 (1H, dd, ³J_{HP} = 34.04 Hz, ²J_{HH} = 4.14 Hz, H-7b), 7.66-7.70 (1H, m, C2-H), 8.00-8.05 (1H, m, C3-H), 8.19-8.24 (1H, m, C4-H), 8.53 (1H, dd, ²J_{HP} = 23.36 Hz, ⁴J_{HH} = 11.43 Hz, N-H), 8.84-8.86 (1H, m C1-H); **¹³C{¹H} NMR (CD₃CN, 300 K, in ppm):** δ = 26.0 (m, CH₂), 26.8 (m, CH₂), 26.9 (m, CH₂), 27.1 (m, CH₂), 27.2 (m, CH₂), 27.4 (m, CH₂), 27.5 (m, CH₂), 27.7 (m, CH₂), 27.8 (m, CH₂), 34.0 (1C, ddd, ¹J_{CP} = 29.3 Hz, ²J_{CP} = 15.2 Hz, ³J_{CP} = 2.3 Hz, CH), 36.3 (1C, dd, ¹J_{CP} = 15.8 Hz, ²J_{CP} = 1.4 Hz, CH), 37.3 (1C, ddd, ¹J_{CP} = 34.7 Hz, ²J_{CP} = 12.5 Hz, ³J_{CP} = 1.4 Hz, CH), 40.7 (1C, dd, ¹J_{CP} = 24.7 Hz, ²J_{CP} = 2.9 Hz, CH), 117.3 (1C, m, C7), 122.5 (2C, q, ¹J_{CF3} = 321.2 Hz, CF₃), 129.2 (1C, s, C2), 129.5 (1C, d, ¹J_{CP} = 63.9 Hz, C6), 137.7 (1C, ddd, ²J_{CP} = 57.1 Hz, ³J_{CP} = 5.8 Hz, ³J_{CP} = 5.7 Hz, C4), 140.4 (1C, d, ³J_{CP} = 15.3 Hz, C3), 144.9 (1C, ddd, ¹J_{CP} = 19.4 Hz, ²J_{CP} = 5.2 Hz, ²J_{CP} = 4.7 Hz, C5), 163.6 (1C, d, ³J_{CP} = 5.9 Hz); **¹⁹F NMR (CD₃CN, 300 K, in ppm):** δ = -79.3 (3F, s); **³¹P NMR (CD₃CN, 300 K, in ppm):** AXZ spin system (**94**²⁺): δ(P_A) = -84.3 ppm, δ(P_X) = 44.1 ppm, δ(P_Z) = 77.4 ppm; ¹J(P_AP_X) = ¹J(P_AP_Z) = -295 Hz, ²J(P_XP_Z) = 7 Hz); AXZ spin system (**93**²⁺): δ(P_A) = -95.2 ppm, δ(P_X) = 96.2 ppm, δ(P_Z) = 119.2 ppm; ¹J(P_AP_X) = -350 Hz, ¹J(P_AP_Z) = -330 Hz, ²J(P_XP_Z) = 32 Hz.

12.8.2. Deprotonation of a tautomeric mixture of 93[OTf]₂ and 94[OTf]₂ with NaO^tBu

To a tautomeric mixture of **93**[OTf]₂ and **94**[OTf]₂ (42 mg, 0.5 mmol) in CH₂Cl₂ (1 ml) NaO^tBu (5 mg, 0.5 mmol) is added giving a orange-colored solution. The ³¹P{¹H} NMR spectrum is depicted in figure 55.

³¹P NMR (C₆D₆-capillary, 300 K, in ppm): AXZ spin system (**95**⁺): δ(P_A) = -84.0 ppm, δ(P_X) = 68.9 ppm, δ(P_Y) = 72.3 ppm; ¹J(P_AP_X) = -306 Hz, ¹J(P_AP_Y) = -265 Hz, ²J(P_XP_Y) = 44 Hz.

12.8.3. Deprotonation of a tautomeric mixture of 93[OTf]₂ and 94[OTf]₂ with NaH

To a tautomeric mixture of **93**[OTf]₂ and **94**[OTf]₂ (176 mg, 0.21 mmol) in Et₂O (3 ml) solid NaH is added. After stirring for 16 h at ambient temperature all volatiles are evaporated *in vacuo*. The residue is dissolved in PhF and filtered. Slow vapor addition of *n*-pentane to the filtrate at -30 °C gives crystals of **96**[OTf] in X-ray quality. The ³¹P{¹H} NMR spectrum of the reaction mixture is depicted in figure 55.

³¹P NMR (C₆D₆-capillary, 300 K, in ppm): AXZ spin system (**96**⁺): δ(P_A) = -46.2 ppm, δ(P_M) = 8.9 ppm, δ(P_X) = 86.0 ppm; ¹J(P_AP_X) = -306 Hz, ³J(P_AP_M) = 10 Hz, ³J(P_MP_Y) = 10 Hz.

13. Crystallographic Details

Table 10. Crystallographic data and details of the structure refinements of **41a**, **41b** and **41c**.

	41a	41b	41c
formula	C ₁₅ H ₁₈ N ₅ P	C ₂₃ H ₃₄ N ₅ P	C ₂₇ H ₄₂ N ₅ P
Mr in g mol ⁻¹	299.31	411.52	476.62
color, habit	Clear colorless, block	Colorless, block	Colorless, block
crystal system	Triclinic	Triclinic	Orthorhombic
space group	P-1	P-1	P2 ₁ 2 ₁ 2 ₁
a in Å	8.4080(3)	9.46068(16)	13.12839(14)
b in Å	8.7414(2)	10.82752(18)	14.61308(14)
c in Å	24.3551(7)	12.98312(18)	14.66829(16)
α in °	89.776(2)	106.2183(13)	90
β in °	85.729(3)	94.1178(12)	90
γ in °	61.439(3)	113.5005(16)	90
V in Å ³	1566.81(9)	1145.47(3)	2814.05(5)
Z	4	2	4
T in K	100.01(10)	100.01(10)	100.01(10)
crystal size in mm ³	0.623 x 0.575 x 0.278	0.186 x 0.171 x 0.132	0.351 x 0.196 x 0.167
ρ _c in g cm ⁻³	1.269	1.193	1.104
F(000)	632.0	444.0	1016.0
diffractometer	Super Nova	Super Nova	Super Nova
λ _{XKα} in Å	X = Cu 1.54184	X = Cu 1.54184	X = Cu 1.54184
θ _{min} in °	7.284	7.25	8.541
θ _{max} in °	153.212	153.226	153.21
index range	-10 ≤ h ≤ 10 -10 ≤ k ≤ 10 -30 ≤ l ≤ 29	-11 ≤ h ≤ 11 -13 ≤ k ≤ 13 -11 ≤ l ≤ 16	-16 ≤ h ≤ 15 -12 ≤ k ≤ 18 -15 ≤ l ≤ 18
μ in mm ⁻¹	1.559	1.193	1.023
abs. correction	Gaussian	Gaussian	Gaussian
reflections collected	14923	10831	15438
reflections unique	6482	4729	5859
R _{int}	0.0200	0.0231	0.0199
reflections obs. [F > 2σ(F)]	6309	4423	5813
residual density in e Å ⁻³	0.31, -0.42	0.38, -0.40	0.19, -0.24
parameters	523	270	341
GOOF	1.054	1.031	1.014
R ₁ [I > 2σ(I)]	0.0325	0.0357	0.0273
wR2 (all data)	0.0859	0.0918	0.0726
CCDC	1950469	-	-

Table 11. Crystallographic data and details of the structure refinements of **41d**, **41e** and **41f**.

	41d	41e	41f
formula	C ₃₅ H ₂₆ N ₅ P	C ₁₃ H ₈ F ₆ N ₅ P	C ₁₅ H ₁₂ F ₆ N ₅ P
M _r in g mol ⁻¹	547.58	379.21	407.27
color, habit	Clear colorless, block	Clear colorless, block	Clear colorless, block
crystal system	Triclinic	Monoclinic	Monoclinic
space group	P-1	C2/c	P2 ₁ /c
a in Å	9.5823(3)	22.824(3)	9.43191(9)
b in Å	10.5764(4)	5.9836(6)	22.65308(17)
c in Å	14.0230(5)	24.269(3)	8.31139(7)
α in °	84.512(3)	90	90
β in °	76.246(3)	113.859(14)	104.6093(9)
γ in °	79.321(3)	90	90
V in Å ³	1354.53(8)	3031.2(6)	1718.41(3)
Z	2	8	4
T in K	100.0(4)	100.01(10)	100.0
crystal size in mm ³	0.147 x 0.115 x 0.078	0.097 x 0.063 x 0.026	0.429 x 0.235 x 0.169
ρ _c in g cm ⁻³	1.343	1.662	1.574
F(000)	572.0	1520.0	824.0
diffractometer	Super Nova	Super Nova	Super Nova
λ _{XKα} in Å	X = Cu 1.54184	X = Cu 1.54184	X = Cu 1.54184
θ _{min} in °	6.498	7.966	7.806
θ _{max} in °	153.38	152.91	153.226
index range	-12 ≤ h ≤ 11 -13 ≤ k ≤ 13 -15 ≤ l ≤ 17	-26 ≤ h ≤ 28 -7 ≤ k ≤ 7 -30 ≤ l ≤ 30	-11 ≤ h ≤ 11 -27 ≤ k ≤ 28 -10 ≤ l ≤ 10
μ in mm ⁻¹	1.168	2.351	2.116
abs. correction	Gaussian	Gaussian	Gaussian
reflections collected	12878	7354	22517
reflections unique	5619	3126	3605
R _{int}	0.0252	0.0377	0.0206
reflections obs. [F > 2σ(F)]	5175	2595	3504
residual density in e Å ⁻³	0.41, -0.39	0.47, -0.45	0.28, -0.29
parameters	370	226	320
GOOF	1.031	1.042	1.038
R ₁ [I > 2σ(I)]	0.0356	0.0534	0.0280
wR ₂ (all data)	0.0925	0.1502	0.0713
CCDC	-	-	-

Table 12. Crystallographic data and details of the structure refinements of **43a**, **43b***CH₂Cl₂ and **43d**.

	43a	43b *CH ₂ Cl ₂	43d
formula	C ₁₇ H ₁₈ N ₅ PS	C ₂₆ H ₃₆ N ₅ Cl ₂ PS	C ₃₇ H ₂₆ N ₅ PS
M _r in g mol ⁻¹	355.39	552.32	603.66
color, habit	colorless, block	Clear colorless, irregular	colorless, block
crystal system	Monoclinic	Orthorhombic	Triclinic
space group	P2 ₁ /m	Pmn2 ₁	P-1
a in Å	7.03718(11)	13.5782(2)	11.16832(18)
b in Å	13.3782(2)	10.05519(15)	12.2836(2)
c in Å	8.85308(16)	10.21819(16)	24.26706(18)
α in °	90	90	87.2749(9)
β in °	98.7503(16)	90	82.1736(10)
γ in °	90	90	65.4642(16)
V in Å ³	823.77(2)	1395.10(4)	3000.15(8)
Z	2	2	4
T in K	100.00(10)	99.97(11)	100.0(2)
crystal size in mm ³	0.123 x 0.074 x 0.023	0.204 x 0.182 x 0.074	0.165 x 0.125 x 0.064
ρ _c in g cm ⁻³	1.433	1.315	1.336
F(000)	372.0	584.0	1256.0
diffractometer	Super Nova	Super Nova	Super Nova
λ _{XKα} in Å	X = Cu 1.54184	X = Cu 1.54184	X = Cu 1.54184
θ _{min} in °	10.11	8.794	7.354
θ _{max} in °	152.746	136.29	153.254
index range	-8 ≤ h ≤ 8 -14 ≤ k ≤ 16 -9 ≤ l ≤ 11	-16 ≤ h ≤ 15 -10 ≤ k ≤ 12 -11 ≤ l ≤ 12	-13 ≤ h ≤ 13 -15 ≤ k ≤ 15 -30 ≤ l ≤ 25
μ in mm ⁻¹	2.733	3.520	1.741
abs. correction	Gaussian	Gaussian	Multi-scan
reflections collected	3923	11974	32293
reflections unique	1774	2531	12463
R _{int}	0.0201	0.0325	0.0193
reflections obs. [F > 2σ(F)]	1676	2528	11807
residual density in e Å ⁻³	0.47, -0.32	0.36, -0.53	0.35, -0.33
parameters	126	183	793
GOOF	1.111	1.221	1.016
R ₁ [I > 2σ(I)]	0.0284	0.0515	0.0311
wR ₂ (all data)	0.0748	0.1272	0.0805
CCDC	1950473	-	-

Table 13. Crystallographic data and details of the structure refinements of **43e**, **43f** and **44**.

	43e	43f	44
formula	C ₁₅ H ₈ F ₆ N ₅ PS	C ₁₇ H ₁₂ F ₆ N ₅ PS	C ₁₁ H ₁₉ Cl ₂ N ₂ P
M _r in g mol ⁻¹	435.29	463.35	281.15
color, habit	colorless, plate	colorless, block	Colorless, needles
crystal system	Monoclinic	Monoclinic	Orthorhombic
space group	P2 ₁ /c	P2 ₁ /n	Pca2 ₁
a in Å	10.05493(2)	6.87272(8)	18.2868(3)
b in Å	16.1596(2)	13.65367(15)	5.85565(9)
c in Å	10.74083(18)	20.6837(3)	13.82911(18)
α in °	90	90	90
β in °	103.1222(17)	99.4243(12)	90
γ in °	90	90	90
V in Å ³	1699.64(5)	1914.72(4)	1480.84(4)
Z	4	4	4
T in K	100.01(10)	100.00(10)	101(1)
crystal size in mm ³	0.311 x 0.144 x 0.019	0.184 x 0.082 x 0.055	0.382 x 0.056 x 0.043
ρ _c in g cm ⁻³	1.701	1.607	1.261
F(000)	872.0	936.0	592.0
diffractometer	Super Nova	Super Nova	Super Nova
λ _{XKα} in Å	X = Cu 1.54184	X = Cu 1.54184	X = Cu 1.54184
θ _{min} in °	9.03	7.792	9.674
θ _{max} in °	152.672	153.222	153.246
index range	-12 ≤ h ≤ 12 -16 ≤ k ≤ 20 -13 ≤ l ≤ 13	-8 ≤ h ≤ 8 -17 ≤ k ≤ 14 -25 ≤ l ≤ 25	-22 ≤ h ≤ 22 -5 ≤ k ≤ 7 -17 ≤ l ≤ 14
μ in mm ⁻¹	3.308	2.975	4.783
abs. correction	Multi-scan	Gaussian	Gaussian
reflections collected	8993	9471	8607
reflections unique	3534	3956	2751
R _{int}	0.0284	0.0189	0.0244
reflections obs. [F > 2σ(F)]	3239	3781	2714
residual density in e Å ⁻³	1.10, -0.81	0.35, -0.40	0.24, -0.31
parameters	253	301	151
GOOF	1.039	1.044	1.052
R ₁ [I > 2σ(I)]	0.0524	0.0315	0.0267
wR ₂ (all data)	0.1424	0.0824	0.0698
CCDC	-	-	-

Table 14. Crystallographic data and details of the structure refinements of **45**, **46** and **47**.

	45	46	47
formula	C ₂₂ H ₃₈ ClN ₄ P	C ₁₀ H ₁₁ ClN ₃ P	C ₁₂ H ₁₁ ClN ₃ PS
M _r in g mol ⁻¹	424.98	239.64	295.72
color, habit	Clear colorless, block	Clear colorless, block	Clear colorless, block
crystal system	Monoclinic	Triclinic	Triclinic
space group	P2 ₁ /n	P-1	P-1
a in Å	10.33914(7)	7.9469(8)	6.4220(4)
b in Å	16.91847(13)	8.5872(9)	7.7832(4)
c in Å	13.96335(10)	8.6205(7)	14.1341(6)
α in °	90	89.430(8)	99.979(4)
β in °	93.5163(6)	74.167(8)	94.001(4)
γ in °	90	81.021(9)	110.048(5)
V in Å ³	2437.91(3)	558.69(9)	647.22(6)
Z	4	2	2
T in K	99.98(14)	100.01(10)	100.01(10)
crystal size in mm ³	0.17 x 0.158 x 0.047	0.289 x 0.24 x 0.163	0.191 x 0.151 x 0.078
ρ _c in g cm ⁻³	1.158	1.424	1.517
F(000)	920.0	248.0	304.0
diffractometer	Super Nova	Super Nova	Super Nova
λ _{XKα} in Å	X = Cu 1.54184	X = Cu 1.54184	X = Cu 1.54184
θ _{min} in °	8.22	10.436	6.412
θ _{max} in °	153.446	153.44	152.722
index range	-12 ≤ h ≤ 12 -21 ≤ k ≤ 19 -17 ≤ l ≤ 12	-9 ≤ h ≤ 9 -6 ≤ k ≤ 10 -10 ≤ l ≤ 9	-8 ≤ h ≤ 8 -9 ≤ k ≤ 9 -16 ≤ l ≤ 17
μ in mm ⁻¹	2.103	4.133	5.159
abs. correction	Multi-scan	Gaussian	Gaussian
reflections collected	24428	4416	6419
reflections unique	5100	2297	2674
R _{int}	0.0204	0.0139	0.0224
reflections obs. [F > 2σ(F)]	4964	2258	2455
residual density in e Å ⁻³	0.52, -0.34	0.26, -0.47	0.33, -0.30
parameters	265	139	165
GOOF	1.050	1.077	1.059
R ₁ [I > 2σ(I)]	0.0289	0.0287	0.0281
wR ₂ (all data)	0.0763	0.0759	0.0749
CCDC	-	-	-

Table 15. Crystallographic data and details of the structure refinements of **48**, **49** and **50**.

	48	49	50
formula	C ₂₇ H ₄₈ NP ₃	C ₃₁ H ₄₈ NP ₃ S	C ₂₁ H ₄₀ NP ₃
M _r in g mol ⁻¹	503.59	559.67	399.45
color, habit	Colorless, needle	Yellow, plate	Clear, colorless, block
crystal system	Monoclinic	Triclinic	Triclinic
space group	P2 ₁ /c	P-1	P-1
a in Å	11.06652(11)	16.0052(2)	7.9088(3)
b in Å	23.6010(3)	17.2802(2)	11.2925(4)
c in Å	10.85205(11)	23.3958(3)	14.4882(6)
α in °	90	104.8628(12)	73.202(3)
β in °	99.7411(10)	100.6013(12)	86.167(3)
γ in °	90	90.2605(12)	72.923(3)
V in Å ³	2793.48(5)	6138.29(16)	1183.90(8)
Z	4	8	2
T in K	100.01(10)	100.00(10)	100.01(10)
crystal size in mm ³	0.292 x 0.065 x 0.05	0.136 x 0.08 x 0.039	0.397 x 0.18 x 0.081
ρ _c in g cm ⁻³	1.197	1.211	1.121
F(000)	1096.0	2416.0	436.0
diffractometer	Super Nova	Super Nova	Super Nova
λ _{XKα} in Å	X = Cu 1.54184	X = Cu 1.54184	X = Cu 1.54184
θ _{min} in °	7.492	3.982	6.374
θ _{max} in °	152.996	153.556	153.842
index range	-13 ≤ h ≤ 7 -29 ≤ k ≤ 29 -13 ≤ l ≤ 13	-19 ≤ h ≤ 20 -17 ≤ k ≤ 21 -29 ≤ l ≤ 29	-9 ≤ h ≤ 9 -14 ≤ k ≤ 13 -17 ≤ l ≤ 18
μ in mm ⁻¹	2.069	2.555	2.319
abs. correction	Gaussian	Multi-scan	Gaussian
reflections collected	14711	72032	14550
reflections unique	5806	25591	4930
R _{int}	0.0243	0.0333	0.0125
reflections obs. [F > 2σ(F)]	5416	21917	4861
residual density in e Å ⁻³	0.33, -0.26	0.47, -0.55	0.35, -0.26
parameters	490	1380	238
GOOF	1.039	1.012	1.057
R ₁ [I > 2σ(I)]	0.0277	0.0336	0.0265
wR ₂ (all data)	0.0688	0.0858	0.0692
CCDC	1950471	1950484	1950474

Table 16. Crystallographic data and details of the structure refinements of **51**, [(48Cu)₂][OTf]₂*MeCN and [(48Ag)₂][OTf]₂*MeCN.

	51	[(48Cu) ₂][OTf] ₂ *MeCN	[(48Ag) ₂][OTf] ₂ *MeCN
formula	C ₁₉ H ₁₈ NP ₃	C ₆₄ H ₁₀₄ Cl ₈ Cu ₂ F ₆ N ₂ O ₆ P ₆ S ₂	C ₆₄ H ₁₀₂ Ag ₂ F ₆ N ₄ O ₆ P ₆ S ₂
M _r in g mol ⁻¹	353.25	1772.11	1603.17
color, habit	Clear, colorless, block	Clear colorless, plate	Colorless, block
crystal system	Orthorhombic	Triclinic	Monoclinic
space group	Pna2 ₁	P-1	P2 ₁ /c
a in Å	26.5691(4)	12.3686(3)	12.1473(3)
b in Å	10.80809(17)	13.7415(3)	15.0565(4)
c in Å	5.99320(10)	13.9572(3)	20.4248(7)
α in °	90	113.879(2)	90
β in °	90	109.229(2)	102.677(3)
γ in °	90	93.1122(18)	90
V in Å ³	1721.01(5)	1999.20(9)	3644.55(18)
Z	4	1	2
T in K	100.01(10)	100.01(10)	99.97(13)
crystal size in mm ³	0.408 x 0.301 x 0.115	0.307 x 0.194 x 0.047	0.095 x 0.035 x 0.022
ρ _c in g cm ⁻³	1.363	1.472	1.461
F(000)	736.0	920.0	1664.0
diffractometer	Super Nova	Super Nova	Super Nova
λ _{XKα} in Å	X = Cu 1.54184	X = Cu 1.54184	X = Cu 1.54184
θ _{min} in °	6.654	7.208	7.358
θ _{max} in °	154.09	153.02	144.254
index range	-33 ≤ h ≤ 32 -13 ≤ k ≤ 13 -7 ≤ l ≤ 7	-13 ≤ h ≤ 15 -17 ≤ k ≤ 16 -14 ≤ l ≤ 17	-14 ≤ h ≤ 14 -10 ≤ k ≤ 10 -25 ≤ l ≤ 25
μ in mm ⁻¹	3.145	5.255	6.637
abs. correction	Gaussian	Gaussian	Gaussian
reflections collected	20567	19879	23315
reflections unique	3535	8310	7033
R _{int}	0.0280	0.0231	0.0464
reflections obs. [F > 2σ(F)]	3531	7795	6108
residual density in e Å ⁻³	0.84, -0.39	0.88, -0.82	1.33, -0.88
parameters	209	470	407
GOOF	1.116	1.063	1.026
R ₁ [I > 2σ(I)]	0.0479	0.0323	0.0393
wR ₂ (all data)	0.1291	0.0835	0.1065
CCDC	1950481	1950472	1950476

Table 17. Crystallographic data and details of the structure refinements of [(48Au)₂][OTf]₂, [(48)₂Cu][OTf]^{*}*n*-C₅H₁₂ and (48CuBr)₂*THF**n*-C₅H₁₂.

	[(48Au) ₂][OTf] ₂	[(48) ₂ Cu][OTf] [*] <i>n</i> -C ₅ H ₁₂	(48CuBr) ₂ *THF* <i>n</i> -C ₅ H ₁₂
formula	C ₆₀ H ₉₆ Au ₂ F ₆ N ₂ O ₆ P ₆ S ₂	C ₆₄ H ₁₀₈ CuF ₃ N ₂ O ₃ P ₆ S	C _{65.92} H _{113.69} Br ₂ Cu ₂ N ₂ O _{0.82} P ₆
M _r in g mol ⁻¹	1699.26	1191.94	1420.29
color, habit	Clear colorless, irregular	Clear colorless, block	Clear colorless, block
crystal system	Monoclinic	Monoclinic	Triclinic
space group	C2/c	P2 ₁ /n	P-1
a in Å	21.8614(6)	10.16325(10)	10.85215(11)
b in Å	16.4069(4)	25.8990(2)	17.65905(19)
c in Å	26.8718(6)	26.5556(3)	19.63512(16)
α in °	90	90	102.4758(8)
β in °	115.147(3)	99.3487(10)	101.6435(8)
γ in °	90	90	98.8895(9)
V in Å ³	8724.8(4)	6897.07(12)	3520.31(5)
Z	4	4	2
T in K	100.00(11)	100.01(10)	100.01(10)
crystal size in mm ³	0.318 x 0.27 x 0.192	0.36 x 0.208 x 0.144	0.221 x 0.067 x 0.042
ρ _c in g cm ⁻³	1.294	1.244	1.340
F(000)	3408.0	2768.0	1496.0
diffractometer	Super Nova	Super Nova	Super Nova
λ _{XKα} in Å	X = Cu 1.54184	X = Cu 1.54184	X = Cu 1.54184
θ _{min} in °	6.956	6.746	4.752
θ _{max} in °	153.546	153.264	153.292
index range	-26 ≤ h ≤ 26 -16 ≤ k ≤ 20 -29 ≤ l ≤ 33	-12 ≤ h ≤ 12 -32 ≤ k ≤ 32 -33 ≤ l ≤ 31	-13 ≤ h ≤ 8 -22 ≤ k ≤ 22 -24 ≤ l ≤ 24
μ in mm ⁻¹	8.144	2.453	3.660
abs. correction	Gaussian	Gaussian	Gaussian
reflections collected	23941	41516	38405
reflections unique	9046	14152	14673
R _{int}	0.0240	0.0247	0.0289
reflections obs. [F > 2σ(F)]	8619	13572	13137
residual density in e Å ⁻³	1.41, -2.51	0.89, -0.58	0.90, -0.59
parameters	379	843	814
GOOF	1.104	1.12	1.025
R ₁ [I > 2σ(I)]	0.0353	0.0529	0.0353
wR ₂ (all data)	0.0926	0.1311	0.0970
CCDC	1950485	1950479	1950470

Table 18. Crystallographic data and details of the structure refinements of **52**, **56***0.5 CH₂Cl₂ and **57**[OTf].

	52	56 *0.5 CH ₂ Cl ₂	57 [OTf]
formula	C ₂₅ H ₂₀ N ₅ P ₅	C _{35.5} H ₂₁ ClN ₅ P ₅ S ₅	C ₃₁ H ₅₁ F ₃ NO ₃ P ₃ S
M _r in g mol ⁻¹	545.31	868.17	667.69
color, habit	Colorless, block	Colorless, block	Yellow, block
crystal system	Monoclinic	Triclinic	Triclinic
space group	P2 ₁ /n	P-1	P-1
a in Å	8.88106(6)	10.2485(3)	10.9026(4)
b in Å	19.32439(15)	12.3713(3)	12.5147(3)
c in Å	14.68865(11)	15.6969(4)	14.0376(4)
α in °	90	112.462(2)	74.779(3)
β in °	92.3033(7)	90.355(2)	67.319(3)
γ in °	90	99.439(2)	84.620(2)
V in Å ³	2518.84(3)	1809.09(8)	1705.17(10)
Z	4	2	2
T in K	100.01(10)	100.00(10)	100.00(10)
crystal size in mm ³	0.265 x 0.202 x 0.101	0.135 x 0.081 x 0.052	0.192 x 0.118 x 0.054
ρ _c in g cm ⁻³	1.438	1.594	1.300
F(000)	1120.0	882.0	712.0
diffractometer	Super Nova	Super Nova	Super Nova
λ _{XKα} in Å	X = Cu 1.54184	X = Cu 1.54184	X = Cu 1.54184
θ _{min} in °	7.564	6.11	7.042
θ _{max} in °	153.066	153.416	153.3
index range	-11 ≤ h ≤ 11 -22 ≤ k ≤ 24 -18 ≤ l ≤ 18	-12 ≤ h ≤ 10 -15 ≤ k ≤ 15 -19 ≤ l ≤ 19	-13 ≤ h ≤ 13 -15 ≤ k ≤ 15 -15 ≤ l ≤ 17
μ in mm ⁻¹	3.577	6.032	2.581
abs. correction	Gaussian	Multi-scan	Gaussian
reflections collected	14356	22889	16998
reflections unique	5232	7537	7087
R _{int}	0.0206	0.0229	0.0252
reflections obs. [F > 2σ(F)]	5073	7164	6566
residual density in e Å ⁻³	0.30, -0.27	0.89, -0.48	0.75, -0.47
parameters	396	478	380
GOOF	1.038	1.025	1.018
R ₁ [I > 2σ(I)]	0.0258	0.0333	0.0365
wR ₂ (all data)	0.0677	0.0884	0.1003
CCDC	1950478	1950477	1950475

Table 19. Crystallographic data and details of the structure refinements of **58**[OTf]₂, **59**[OTf]₂ and **60**[OTf].

	58 [OTf] ₂	59 [OTf] ₂	60 [OTf]
formula	C ₃₃ H ₅₄ F ₆ NO ₆ P ₃ S ₂	C ₃₈ H ₅₈ F ₆ N ₂ O ₆ P ₄ S ₂	C ₂₇ H ₅₀ F ₃ O ₃ P ₃ N
M _r in g mol ⁻¹	831.80	940.86	604.64
color, habit	Colorless, block	Clear colorless, needle	Clear yellow, block
crystal system	Monoclinic	Triclinic	Triclinic
space group	P2 ₁ /n	P-1	P-1
a in Å	13.83650(10)	9.5582(7)	12.4338(41)
b in Å	21.99929(12)	9.6936(8)	12.5077(3)
c in Å	13.99782(10)	11.8527(8)	13.0479(4)
α in °	90	87.895(6)	114.387(3)
β in °	109.4646(8)	80.107(6)	96.369(2)
γ in °	90	86.923(6)	116.073(3)
V in Å ³	4017.32(5)	1079.88(14)	1550.40(9)
Z	4	1	2
T in K	99.97(12)	100.01(10)	100.01(10)
crystal size in mm ³	0.22 x 0.115 x 0.065	0.229 x 0.048 x 0.036	0.226 x 0.105 x 0.092
ρ _c in g cm ⁻³	1.375	1.447	1.295
F(000)	1752.0	494.0	648.0
diffractometer	Super Nova	Super Nova	Super Nova
λ _{XKα} in Å	X = Cu 1.54184	X = Cu 1.54184	X = Cu 1.54184
θ _{min} in °	7.782	7.574	7.966
θ _{max} in °	153.374	136.62	153.428
index range	-14 ≤ h ≤ 17 -27 ≤ k ≤ 23 -17 ≤ l ≤ 17	-11 ≤ h ≤ 11 -11 ≤ k ≤ 11 -14 ≤ l ≤ 14	-15 ≤ h ≤ 15 -14 ≤ k ≤ 15 -16 ≤ l ≤ 14
μ in mm ⁻¹	2.944	3.155	2.770
abs. correction	Gaussian	Analytical	Gaussian
reflections collected	44324	7302	15021
reflections unique	8432	7302	6454
R _{int}	0.0272	0.0953	0.0248
reflections obs. [F > 2σ(F)]	8188	5821	5907
residual density in e Å ⁻³	0.57, -0.47	1.39, -0.42	0.43, -0.40
parameters	462	328	336
GOOF	1.027	0.998	1.035
R ₁ [I > 2σ(I)]	0.0313	0.0700	0.0281
wR ₂ (all data)	0.0838	0.1893	0.0729
CCDC	1950482	1950486	1950483

Table 20. Crystallographic data and details of the structure refinements of **65**, **42** and **66**.

	65	42	66
formula	C ₉ H ₆ Cl ₂ NP	C ₇ H ₄ Cl ₂ NPS	C ₁₃ H ₈ Cl ₂ NP
M _r in g mol ⁻¹	230.02	236.04	280.07
color, habit	red, block	colorless, block	colorless, block
crystal system	Monoclinic	Triclinic	Monoclinic
space group	P2 ₁ /n	P-1	P2 ₁ /c
a in Å	12.4333(5)	6.71538(17)	8.62852(12)
b in Å	5.84986(19)	6.98592(18)	13.86704(18)
c in Å	14.1072(5)	10.6276(2)	9.96682(12)
α in °	90	91.2912(19)	90
β in °	109.657(4)	107.150(2)	93.9632(12)
γ in °	90	108.239(2)	90
V in Å ³	966.27(6)	448.83(2)	1189.70(3)
Z	4	2	4
T in K	100.01(10)	100.01(10)	100.0(2)
crystal size in mm ³	0.255 x 0.169 x 0.139	0.204 x 0.111 x 0.058	0.252 x 0.134 x 0.054
ρ _c in g cm ⁻³	1.581	1.747	1.564
F(000)	464.0	236.0	568.0
diffractometer	Super Nova	Super Nova	Super Nova
λ _{XKα} in Å	X = Cu 1.54184	X = Cu 1.54184	X = Cu 1.54184
θ _{min} in °	8.216	8.778	10.276
θ _{max} in °	153.616	153.11	152.568
index range	-13 ≤ h ≤ 15 -7 ≤ k ≤ 6 -17 ≤ l ≤ 16	-7 ≤ h ≤ 8 -8 ≤ k ≤ 8 -13 ≤ l ≤ 12	-10 ≤ h ≤ 10 -17 ≤ k ≤ 16 -12 ≤ l ≤ 10
μ in mm ⁻¹	7.181	9.863	5.953
abs. correction	Gaussian	Multi Scan	Gaussian
reflections collected	4303	3556	6081
reflections unique	2004	1850	2471
R _{int}	0.0407	0.0156	0.0157
reflections obs. [F > 2σ(F)]	1915	1796	2374
residual density in e Å ⁻³	1.04, -0.87	0.25, -0.40	0.30, -0.26
parameters	118	125	186
GOOF	1.086	1.074	1.040
R ₁ [I > 2σ(I)]	0.0625	0.0223	0.0625
wR ₂ (all data)	0.1596	0.0612	0.1596
CCDC	1986655	1986657	19866556

Table 21. Crystallographic data and details of the structure refinements of **61**[OTf], **62**[OTf]*MeCN and **63**[OTf].

	61 [OTf]	62 [OTf]*MeCN	63 [OTf]
formula	C ₁₁ H ₈ F ₃ N ₂ O ₃ PS	C ₂₁ H ₁₅ F ₃ N ₃ O ₃ PS	C ₂₇ H ₁₆ F ₃ N ₂ O ₃ PS
M _r in g mol ⁻¹	336.22	477.39	536.45
color, habit	yellow, parallelepiped	yellow, block	orange, block
crystal system	triclinic	Triclinic	Monoclinic
space group	P-1	P-1	Cc
a in Å	7.2241(5)	7.0876(3)	17.5520(2)
b in Å	9.0577(7)	12.8437(4)	8.75829(9)
c in Å	10.9162(8)	13.035(4)	16.02248(19)
α in °	95.055(3)	116.376(3)	90
β in °	99.126(3)	101.678(3)	113.4693(14)
γ in °	109.450(3)	96.308(3)	90
V in Å ³	657.34(8)	1013.70(7)	2259.30(5)
Z	2	2	4
T in K	100.0	99.99(10)	99.99(17)
crystal size in mm ³	0.19 x 0.12 x 0.06	0.239 x 0.194 x 0.107	0.454 x 0.3 x 0.073
ρ _c in g cm ⁻³	1.699	1.564	1.577
F(000)	340.0	488.0	1096.0
diffractometer	Bruker APEX II	Super Nova	Super Nova
λ _{XKα} in Å	X = Mo 0.71073	X = Cu 1.54184	X = Cu 01.54184
θ _{min} in °	3.822	7.89	10.99
θ _{max} in °	60.246	153.316	153.212
index range	-10 ≤ h ≤ 10 -10 ≤ k ≤ 12 -15 ≤ l ≤ 13	-8 ≤ h ≤ 8 -16 ≤ k ≤ 15 -15 ≤ l ≤ 16	-21 ≤ h ≤ 22 -10 ≤ k ≤ 10 -17 ≤ l ≤ 20
μ in mm ⁻¹	0.415	2.698	2.486
abs. correction	multi-scan	Gaussian	Gaussian
reflections collected	8822	9124	8418
reflections unique	3836	4208	3760
R _{int}	0.0175	0.0264	0.0178
reflections obs. [F > 2σ(F)]	3277	3959	3750
residual density in e Å ⁻³	0.59, -0.30	0.33, -0.43	0.86, -0.38
parameters	190	349	335
GOOF	1.044	1.035	1.092
R ₁ [I > 2σ(I)]	0.0340	0.0413	0.0400
wR ₂ (all data)	0.0915	0.1148	0.1092
CCDC	1950480	1986660	1986667

Table 22. Crystallographic data and details of the structure refinements of **64**[OTf]*MeCN, **61**^{Cl₂}[OTf] and **61**^{F₄}[OTf].

	64 [OTf]*MeCN	61 ^{Cl₂} [OTf]	61 ^{F₄} [OTf]
formula	C ₁₇ H ₁₁ F ₃ N ₃ O ₃ PS ₃	C ₁₁ H ₈ Cl ₂ F ₃ N ₂ O ₃ PS ₃	C ₁₁ H ₈ F ₇ N ₂ O ₃ PS
M _r in g mol ⁻¹	489.44	407.14	412.22
color, habit	colorless, block	orange, plate	Clear, colorless, block
crystal system	Triclinic	Monoclinic	Monoclinic
space group	P-1	P2 ₁ /n	Pn
a in Å	8.9698(2)	12.7884(5)	8.73091(8)
b in Å	9.62662(19)	5.86021(18)	7.86576(5)
c in Å	11.58620(18)	21.1423(9)	11.09899(9)
α in °	93.2154(14)	90	90
β in °	102.3339(17)	107.479(4)	110.5932(10)
γ in °	90.6727(19)	90	90
V in Å ³	975.54(4)	1511.30(11)	713.521(10)
Z	2	4	2
T in K	100.01(10)	100.0(4)	100.0
crystal size in mm ³	0.16 x 0.061 x 0.039	0.175 x 0.134 x 0.01	0.15 x 0.12 x 0.12
ρ _c in g cm ⁻³	1.666	1.789	1.919
F(000)	496.0	816.0	412.0
diffractometer	Super Nova	Super Nova	Super Nova
λ _{XKα} in Å	X = Cu 1.54184	X = Cu 1.54184	X = Cu 1.54184
θ _{min} in °	7.824	7.248	11.174
θ _{max} in °	153.082	153.056	153.032
index range	-11 ≤ h ≤ 10 -12 ≤ k ≤ 12 -14 ≤ l ≤ 10	-16 ≤ h ≤ 16 -7 ≤ k ≤ 5 -26 ≤ l ≤ 26	-10 ≤ h ≤ 10 -9 ≤ k ≤ 9 -13 ≤ l ≤ 13
μ in mm ⁻¹	4.767	6.637	4.089
abs. correction	Gaussian	Gaussian	Multi-Scan
reflections collected	8995	14505	11042
reflections unique	4048	3323	2814
R _{int}	0.0252	0.0330	0.0108
reflections obs. [F > 2σ(F)]	3807	3283	2814
residual density in e Å ⁻³	0.60, -0.55	0.30, -0.90	0.28, -0.33
parameters	315	209	226
GOOF	1.042	1.129	1.085
R ₁ [I > 2σ(I)]	0.0383	0.0354	0.0230
wR ₂ (all data)	0.1051	0.1052	0.0634
CCDC	1986666	1986665	1986664

Table 23. Crystallographic data and details of the structure refinements of **61**^{C14}[OTf], **69**[OTf]₃*2MeCN, **70a**[OTf]

	61 ^{C14} [OTf]	69 [OTf] ₃ *2MeCN	70a [OTf]
formula	C ₁₁ H ₈ Cl ₄ F ₃ N ₂ O ₃ PS	C ₂₇ H _{21.13} F ₉ N ₆ O ₉ PS ₃	C ₂₁ H ₂₂ F ₃ N ₆ O ₃ PS
M _r in g mol ⁻¹	478.02	871.78	526.47
color, habit	colorless, block	Clear yellow, block	Clear yellow, block
crystal system	Monoclinic	Monoclinic	monoclinic
space group	Pn	I2/a	P2 ₁ /c
a in Å	9.33396(12)	30.8800(3)	13.34132(11)
b in Å	8.28139(10)	7.96591(7)	11.57043(8)
c in Å	11.25557(14)	29.4064(3)	16.78264(15)
α in °	90	90	90
β in °	109.4015(14)	110.0904(10)	112.3951(10)
γ in °	90	90	90
V in Å ³	820.629(19)	6793.46(11)	2395.26(4)
Z	2	8	4
T in K	100.01(10)	100.00(10)	100.01(10)
crystal size in mm ³	0.188 x 0.115 x 0.059	0.327 x 0.176 x 0.097	0.224 x 0.2 x 0.076
ρ _c in g cm ⁻³	1.935	1.705	1.460
F(000)	476.0	3529.0	1088.0
diffractometer	Super Nova	Super Nova	Super Nova
λ _{XKα} in Å	X = Cu 1.54184	X = Cu 1.54184	X = Cu 1.54184
θ _{min} in °	10.682	7.164	7.166
θ _{max} in °	153.146	153.368	153.178
index range	-11 ≤ h ≤ 11 -9 ≤ k ≤ 10 -14 ≤ l ≤ 14	-33 ≤ h ≤ 38 -9 ≤ k ≤ 9 -37 ≤ l ≤ 36	-9 ≤ h ≤ 16 -14 ≤ k ≤ 14 -21 ≤ l ≤ 20
μ in mm ⁻¹	9.153	3.472	2.371
abs. correction	Gaussian	Gaussian	Multi-scan
reflections collected	14816	18509	12926
reflections unique	3415	7053	4986
R _{int}	0.0229	0.0186	0.0140
reflections obs. [F > 2σ(F)]	3415	6831	4836
residual density in e Å ⁻³	0.24, -0.40	1.09, -0.74	0.24, -0.0754
parameters	227	713	441
GOOF	1.092	1.043	1.020
R ₁ [I > 2σ(I)]	0.0246	0.0697	0.0285
wR ₂ (all data)	0.0587	0.1857	0.0754
CCDC	1986658	1986659	1986662

Table 24. Crystallographic data and details of the structure refinements of **70b**[OTf]*Et₂O, **70c**[OTf]*Et₂O and **70d**[OTf].

	70b [OTf]*Et ₂ O	70c [OTf]*Et ₂ O	70d [OTf]
formula	C ₃₁ H ₄₃ F ₃ N ₆ O _{3.5} PS	C ₃₇ H ₅₆ F ₃ N ₆ O ₄ PS	C ₄₁ H ₃₀ F ₃ N ₆ O ₃ PS
M _r in g mol ⁻¹	675.74	768.90	774.74
color, habit	colorless, plate	colorless, block	Clear colorless, needle
crystal system	Triclinic	Monoclinic	Orthorhombic
space group	P-1	P2 ₁ /c	Pbca
a in Å	13.8270(2)	17.32700(13)	8.79642(10)
b in Å	13.9544(3)	12.54811(10)	19.3254(2)
c in Å	20.1132(3)	19.52034(14)	42.2670(6)
α in °	73.762(2)	90	90
β in °	72.1020(10)	99.5180(7)	90
γ in °	78.218(2)	90	90
V in Å ³	3515.84(11)	4185.70(5)	7185.17(15)
Z	4	4	8
T in K	100.01(10)	100.01(10)	99.99(8)
crystal size in mm ³	0.4 x 0.235 x 0.105	0.268 x 0.169 x 0.1	0.549 x 0.065 x 0.036
ρ _c in g cm ⁻³	1.277	1.220	1.432
F(000)	1428.0	1640.0	3200.0
diffractometer	Super Nova	Super Nova	Super Nova
λ _{XKα} in Å	X = Cu 1.54184	X = Cu 1.54184	X = Cu 1.54184
θ _{min} in °	6.654	5.172	8.368
θ _{max} in °	153.386	153.376	153.168
index range	-17 ≤ h ≤ 17 -17 ≤ k ≤ 17 -25 ≤ l ≤ 25	-21 ≤ h ≤ 20 -14 ≤ k ≤ 15 -22 ≤ l ≤ 24	-7 ≤ h ≤ 11 -17 ≤ k ≤ 24 -52 ≤ l ≤ 52
μ in mm ⁻¹	1.736	1.525	1.781
abs. correction	Analytical	Gaussian	Gaussian
reflections collected	25162	24645	27926
reflections unique	12373	8707	7476
R _{int}	?	0.0218	0.0366
reflections obs. [F > 2σ(F)]	11364	8017	6892
residual density in e Å ⁻³	1.62, -0.58	0.67, -0.39	0.38, -0.50
parameters	858	483	616
GOOF	1.024	1.053	1.110
R ₁ [I > 2σ(I)]	0.0609	0.0407	0.0451
wR ₂ (all data)	0.1638	0.1148	0.01131
CCDC	1986668	1986663	1986661

Table 25. Crystallographic data and details of the structure refinements of **71**, **72** and [(**72**)₂Cu][OTf]*CH₂Cl₂

	71	72	[(72) ₂ Cu][OTf]*CH ₂ Cl ₂
formula	C ₂₀ H ₂₈ P ₄	C ₁₈ H ₂₆ N ₂ P ₄	C ₃₈ H ₅₄ Cl ₂ CuF ₃ N ₄ O ₃ P ₈ S
M _r in g mol ⁻¹	392.30	394.29	1086.11
color, habit	Colorless, block	Clear, colorless, block	Clear yellow, block
crystal system	Triclinic	Triclinic	Triclinic
space group	P-1	P-1	P-1
a in Å	9.1061(3)	8.32598(17)	14.9813(3)
b in Å	10.8015(4)	10.35329(18)	16.6700(3)
c in Å	11.0270(4)	13.62138(17)	22.63748(19)
α in °	75.983(3)	107.2865(13)	72.9307(11)
β in °	89.224(3)	90.3167(14)	82.9453(11)
γ in °	85.882(3)	109.4435(17)	67.1309(17)
V in Å ³	1049.40(7)	1050.07(3)	4979.38(15)
Z	2	2	4
T in K	100.01(10)	100.01(10)	100.01(10)
crystal size in mm ³	0.204 x 0.109 x 0.08	0.166 × 0.116 × 0.077	0.264 x 0.142 x 0.064
ρ _c in g cm ⁻³	1.242	1.247	1.449
F(000)	416.0	416.0	240.0
diffractometer	Super Nova	Super Nova	Super Nova
λ _{XKα} in Å	X = Cu 1.54184	X = Cu 1.54184	X = Cu 1.54184
θ _{min} in °	8.266	6.842	5.974
θ _{max} in °	153.07	153.072	153.786
index range	-11 ≤ h ≤ 11 -9 ≤ k ≤ 13 -13 ≤ l ≤ 13	-10 ≤ h ≤ 10 -12 ≤ k ≤ 12 -16 ≤ l ≤ 17	-16 ≤ h ≤ 18 -21 ≤ k ≤ 20 -28 ≤ l ≤ 26
μ in mm ⁻¹	3.304	3.333	4.861
abs. correction	Multi-Scan	Gaussian	Gaussian
reflections collected	9775	9375	50722
reflections unique	4351	4346	20368
R _{int}	0.0185	0.0196	0.0416
reflections obs. [F > 2σ(F)]	4156	4141	18310
residual density in e Å ⁻³	0.30, -0.27	0.35, -0.30	1.05, -0.86
parameters	223	240	1105
GOOF	1.026	1.033	1.044
R ₁ [I > 2σ(I)]	0.0244	0.0293	0.0416
wR ₂ (all data)	0.0645	0.0789	0.1191
CCDC	1990335	1990345	1990336

Table 26. Crystallographic data and details of the structure refinements of [(72)₂Ag][OTf]*MeCN, [(72)₂Au][OTf]*CH₂Cl₂ and 74[OTf].

	[(72) ₂ Ag][OTf]*MeCN	[(72) ₂ Au][OTf]*CH ₂ Cl ₂	74[OTf]
formula	C ₃₉ H ₅₅ AgF ₃ N ₅ O ₃ P ₈ S	C ₃₈ H ₅₄ AuCl ₂ F ₃ N ₄ O ₃ P ₈ S	C ₂₂ H ₃₁ F ₃ O ₃ P ₄ S
M _r in g mol ⁻¹	1086.57	1219.54	556.41
color, habit	Clear colorless, block	Clear colorless, block	Clear, colorless, block
crystal system	Triclinic	Triclinic	Orthorhombic
space group	P-1	P-1	P2 ₁ 2 ₁ 2 ₁
a in Å	12.6802(3)	14.8924(2)	10.94462(9)
b in Å	14.2616(4)	16.7756(2)	14.08128(12)
c in Å	16.8114(4)	22.8908(4)	17.64605(14)
α in °	65.300(3)	73.4752(13)	90
β in °	89.294(2)	83.6786(13)	90
γ in °	67.278(3)	67.3194(13)	90
V in Å ³	2507.03(13)	5058.59(14)	2719.51(4)
Z	2	4	4
T in K	100.0(3)	100.01(10)	100.01(10)
crystal size in mm ³	0.257 x 0.156 x 0.138	0.178 x 0.087 x 0.041	0.259 x 0.169 x 0.092
ρ _c in g cm ⁻³	1.439	1.601	1.359
F(000)	1116.0	2440.0	1160.0
diffractometer	Super Nova	Super Nova	Super Nova
λ _{XKα} in Å	X = Cu 1.54184	X = Cu 1.54184	X = Cu 1.54184
θ _{min} in °	5.88	5.92	8.032
θ _{max} in °	153.426	153.442	153.262
index range	-15 ≤ h ≤ 15 -16 ≤ k ≤ 17 -21 ≤ l ≤ 20	-17 ≤ h ≤ 18 -20 ≤ k ≤ 21 -28 ≤ l ≤ 28	-7 ≤ h ≤ 13 -16 ≤ k ≤ 17 -22 ≤ l ≤ 18
μ in mm ⁻¹	6.464	9.642	3.662
abs. correction	Gaussian	Gaussian	Gaussian
reflections collected	25869	72942	15014
reflections unique	10409	21100	5654
R _{int}	0.0206	0.0214	0.0197
reflections obs. [F > 2σ(F)]	10196	20520	5186
residual density in e Å ⁻³	1.50, -1.31	1.28, -1.78	0.17, -0.24
parameters	568	1105	305
GOOF	1.024	1.038	1.043
R ₁ [I > 2σ(I)]	0.0265	0.0234	0.0190
wR ₂ (all data)	0.0670	0.0584	0.0481
CCDC	1990340	1990341	1990339

Table 27. Crystallographic data and details of the structure refinements of **75**[OTf], **76**[OTf]₂ and **77**[OTf]₃*2 MeNO₂.

	75 [OTf]	76 [OTf] ₂	77 [OTf] ₃ *2 MeNO ₂
formula	C ₂₀ H ₂₉ F ₃ N ₂ O ₃ P ₄ S	C ₂₂ H ₃₂ F ₆ N ₂ O ₆ P ₄ S ₂	C ₂₆ H ₄₁ F ₉ N ₄ O ₁₃ P ₄ S ₃
M _r in g mol ⁻¹	558.39	722.49	1008.69
color, habit	Clear, colorless, block	Colorless, block	Clear, colorless, block
crystal system	Monoclinic	Orthorhombic	Triclinic
space group	P2 ₁ /c	Pccn	P-1
a in Å	13.97178(9)	11.21381(12)	13.3125(3)
b in Å	15.50651(11)	19.60180(19)	13.4806(3)
c in Å	24.38356(18)	13.59001(18)	13.9690(4)
α in °	90	90	61.919(2)
β in °	94.7277(6)	90	84.582(2)
γ in °	90	90	71.999(2)
V in Å ³	5264.81(6)	2987.23(6)	2099.62(10)
Z	8	4	2
T in K	100.01(10)	99.9(5)	100.00(10)
crystal size in mm ³	0.192 × 0.099 × 0.084	0.216 × 0.076 × 0.053	0.221 × 0.198 × 0.078
ρ _c in g cm ⁻³	1.409	1.606	1.595
F(000)	2320.0	1488.0	1036.0
diffractometer	Super Nova	Super Nova	Super Nova
λ _{XKα} in Å	X = Cu 1.54184	X = Cu 1.54184	X = Cu 1.54184
θ _{min} in °	6.348	9.022	6.994
θ _{max} in °	153.41	153.29	153.582
index range	-17 ≤ h ≤ 17 -19 ≤ k ≤ 17 -27 ≤ l ≤ 30	-14 ≤ h ≤ 13 -15 ≤ k ≤ 24 -17 ≤ l ≤ 16	-14 ≤ h ≤ 16 -17 ≤ k ≤ 16 -17 ≤ l ≤ 17
μ in mm ⁻¹	3.808	4.367	3.993
abs. correction	Gaussian	Gaussian	Gaussian
reflections collected	50820	14708	23898
reflections unique	11024	3118	8722
R _{int}	0.0229	0.0213	0.0158
reflections obs. [F > 2σ(F)]	10434	2536	8518
residual density in e Å ⁻³	0.86, -0.48	0.61, -0.55	0.43, -0.57
parameters	628	194	543
GOOF	1.032	1.064	1.030
R ₁ [I > 2σ(I)]	0.0343	0.0330	0.0288
wR ₂ (all data)	0.0895	0.0889	0.0766
CCDC	1990337	1990344	1990342

Table 28. Crystallographic data and details of the structure refinements of **78**[OTf]₃*MeNO₂, **82**[OTf]₃ and **84**.

	78 [OTf] ₃ *MeNO ₂	82 [OTf] ₃	84
formula	C ₂₂ H ₃₂ F ₉ N ₃ O ₁₁ P ₄ S ₃	C ₂₅ H ₃₀ F ₉ N ₃ O ₉ P ₄ S ₃	C ₄₈ H ₈₈ Au ₂ P ₆
M _r in g mol ⁻¹	905.56	907.58	1244.93
color, habit	Clear colorless, block	Clear yellow, block	Clear colorless, block
crystal system	Triclinic	Monoclinic	Triclinic
space group	P-1	P2 ₁ /c	P-1
a in Å	13.1277(3)	11.97360(10)	10.9267(2)
b in Å	13.5583(3)	12.42100(10)	15.7924(2)
c in Å	22.2736(4)	24.8508(2)	16.2263(3)
α in °	98.981(2)	90	85.4103(13)
β in °	97.504(2)	94.1930(10)	79.3391(16)
γ in °	104.540(2)	90	70.9080(15)
V in Å ³	3730.20(14)	3686.02(5)	2599.73(8)
Z	4	4	2
T in K	100.00(10)	100.00(10)	100.01(10)
crystal size in mm ³	0.593 × 0.316 × 0.186	0.347 × 0.233 × 0.169	0.22 x 0.18 x 0.104
ρ _c in g cm ⁻³	1.612	1.635	1.590
F(000)	1848.0	1848.0	1248.0
diffractometer	Super Nova	Super Nova	Super Nova
λ _{XKα} in Å	X = Cu 1.54184	X = Cu 1.54184	X = Cu 1.54184
θ _{min} in °	6.87	7.134	4.37
θ _{max} in °	153.692	153.822	52.744
index range	-16 ≤ h ≤ 14 -15 ≤ k ≤ 16 -25 ≤ l ≤ 27	-15 ≤ h ≤ 14 -12 ≤ k ≤ 15 -31 ≤ l ≤ 31	-13 ≤ h ≤ 13 -19 ≤ k ≤ 19 -20 ≤ l ≤ 20
μ in mm ⁻¹	4.372	4.388	5.852
abs. correction	Gaussian	Gaussian	Gaussian
reflections collected	41107	39477	27513
reflections unique	15525	7710	10635
R _{int}	0.0415	0.0369	0.0412
reflections obs. [F > 2σ(F)]	14705	6974	9435
residual density in e Å ⁻³	0.65, -0.91	0.40, -0.38	4.44, -2.82
parameters	1171	690	505
GOOF	1.149	1.047	1.045
R ₁ [I > 2σ(I)]	0.0741	0.0362	0.0381
wR ₂ (all data)	0.1533	0.0968	0.1026
CCDC	1990338	1990343	-

Table 29. Crystallographic data and details of the structure refinements of **86***2 THF, **87****n*-C₆H₁₄ and **48**PtCl₂*PhMe.

	86 *2 THF	87 * <i>n</i> -C ₆ H ₁₄	48 PtCl ₂ *PhMe
formula	C ₆₈ H ₁₂₆ Au ₄ ClO ₂ P ₇	C ₇₈ H ₁₄₆ Au ₆ ClP ₇	C ₃₆ H ₅₆ Cl ₂ NP ₃ Pt
M _r in g mol ⁻¹	2015.79	2517.98	861.71
color, habit	Clear colorless, block	Clear colorless, block	Clear yellow, block
crystal system	Triclinic	Monoclinic	Monoclinic
space group	P-1	P2 ₁ /n	P2 ₁ /c
a in Å	14.42900(10)	12.04330(10)	12.62090(10)
b in Å	14.71530(10)	29.7708(2)	14.61390(10)
c in Å	18.4887(2)	24.0692(2)	19.86860(10)
α in °	84.5490(10)	90	90
β in °	74.6830(10)	91.9930(10)	90.2400(10)
γ in °	79.1890(10)	90	90
V in Å ³	3714.73(6)	8624.52(12)	3664.54(4)
Z	2	4	4
T in K	100.01(10)	100.01(10)	99.97(15)
crystal size in mm ³	0.152 x 0.146 x 0.067	0.271 x 0.044 x 0.033	0.155 × 0.105 × 0.076
ρ _c in g cm ⁻³	1.802	1.939	1.562
F(000)	1976.0	4840.0	1744.0
diffractometer	Super Nova	Super Nova	Super Nova
λ _{XKα} in Å	X = Cu 1.54184	X = Cu 1.54184	X = Cu 1.54184
θ _{min} in °	4.962	4.722	7.004
θ _{max} in °	153.546	144.252	154.312
index range	-18 ≤ h ≤ 18 -18 ≤ k ≤ 18 -23 ≤ l ≤ 23	-14 ≤ h ≤ 14 -36 ≤ k ≤ 26 -29 ≤ l ≤ 29	-12 ≤ h ≤ 15 -18 ≤ k ≤ 17 -25 ≤ l ≤ 24
μ in mm ⁻¹	16.572	20.495	9.929
abs. correction	Gaussian	Gaussian	Gaussian
reflections collected	18603	46616	38756
reflections unique	18603	16970	7675
R _{int}	0.0310	0.0311	0.0331
reflections obs. [F > 2σ(F)]	18557	16514	7416
residual density in e Å ⁻³	1.56, -1.55	1.33, -2.10	0.96, -1.25
parameters	757	831	389
GOOF	1.113	1.074	1.058
R ₁ [I > 2σ(I)]	0.0310	0.0308	0.0232
wR ₂ (all data)	0.1157	0.0811	0.0603
CCDC	-	-	-

Table 30. Crystallographic data and details of the structure refinements of **88***3 CH₂Cl₂, **48PdCl₂***3 CH₂Cl₂ and **89***3 CH₂Cl₂*^{1/2} *n*-C₅H₁₂.

	88 *3 CH ₂ Cl ₂	48PdCl₂ *3 CH ₂ Cl ₂	89 *3 CH ₂ Cl ₂ * ^{1/2} <i>n</i> -C ₅ H ₁₂
formula	C ₃₆ H ₅₆ Cl ₆ N ₂ P ₄ Pt	C _{61.5} H ₁₀₃ Cl ₁₁ N ₂ P ₆ Pd ₂	C _{38.5} H ₆₁ Cl ₆ N ₂ P ₄ Pd
M _r in g mol ⁻¹	1048.49	1659.02	994.87
color, habit	Clear yellow, block	Clear colorless, needle	Yellow, plate
crystal system	Monoclinic	Monoclinic	Monoclinic
space group	P2 ₁ /n	P2 ₁ /n	P2 ₁ /n
a in Å	15.59596(17)	20.06282(11)	16.0145(2)
b in Å	18.00133(16)	18.55034(9)	17.7540(2)
c in Å	17.41022(16)	20.98058(10)	17.1678(2)
α in °	90	90	90
β in °	103.7603(10)	102.6738(5)	103.8760(10)
γ in °	90	90	90
V in Å ³	4747.60(8)	7618.14(7)	4738.72(10)
Z	4	4	4
T in K	100.01(10)	104(6)	100.01(10)
crystal size in mm ³	0.192 × 0.122 × 0.097	0.383 × 0.084 × 0.061	0.17 × 0.108 × 0.054
ρ _c in g cm ⁻³	1.467	1.446	1.394
F(000)	2104.0	3420.0	2056.0
diffractometer	Super Nova	Super Nova	Super Nova
λ _{XKα} in Å	X = Cu 1.54184	X = Cu 1.54184	X = Cu 1.54184
θ _{min} in °	6.846	5.52	6.782
θ _{max} in °	153.386	153.506	136.502
index range	-19 ≤ h ≤ 18 -21 ≤ k ≤ 22 -18 ≤ l ≤ 21	-24 ≤ h ≤ 25 -23 ≤ k ≤ 22 -26 ≤ l ≤ 24	-19 ≤ h ≤ 19 -21 ≤ k ≤ 18 -19 ≤ l ≤ 20
μ in mm ⁻¹	10.109	8.835	7.766
abs. correction	Multi-Scan	Gaussian	Gaussian
reflections collected	28189	64218	49238
reflections unique	9887	15925	8680
R _{int}	0.0255	0.0321	0.0436
reflections obs. [F > 2σ(F)]	9685	15332	8017
residual density in e Å ⁻³	0.68, -0.87	1.44, -2.00	1.80, -1.54
parameters	486	841	505
GOOF	1.064	1.087	1.064
R ₁ [I > 2σ(I)]	0.0255	0.0475	0.0551
wR ₂ (all data)	0.0638	0.1245	0.1605
CCDC	-	-	-

Table 31. Crystallographic data and details of the structure refinements of **90***^{3/2} *o*-C₆H₄F₂ *^{1/2} *n*-C₆H₁₄, **91***MeCN and **93**[OTf]₂*2 MeCN.

	90 * ^{3/2} <i>o</i> -C ₆ H ₄ F ₂ * ^{1/2} <i>n</i> -C ₆ H ₁₄	91 *MeCN	93 [OTf] ₂ *2 MeCN
formula	C ₁₁₂ H ₁₄₄ Cl ₄ F ₆ N ₈ P ₁₂ Pd ₄	C ₂₀ H ₂₉ Cl ₄ N ₃ P ₄ Pd ₂	C ₃₇ H ₅₇ F ₆ N ₄ O ₆ P ₃ S ₂
M _r in g mol ⁻¹	2655.38	789.94	924.89
color, habit	Clear yellow, block	Clear brown, plate	Clear colorless, needle
crystal system	Triclinic	Monoclinic	triclinic
space group	P-1	P ₂ /n	P-1
a in Å	15.67394(15)	12.73769(19)	9.65639(17)
b in Å	18.2686(2)	13.66343(19)	12.3961(2)
c in Å	21.3739(2)	16.9399(2)	19.6766(3)
α in °	84.0590(9)	90	75.3991(14)
β in °	78.9522(8)	100.6013(14)	78.8391(14)
γ in °	87.4801(9)	90	79.7637(14)
V in Å ³	5972.72(11)	2897.91(7)	2215.44(7)
Z	2	4	2
T in K	100.01(10)	100.01(10)	100.00(10)
crystal size in mm ³	0.116 × 0.11 × 0.045	0.102 × 0.051 × 0.012	0.34 × 0.085 × 0.052
ρ _c in g cm ⁻³	1.477	1.811	1.386
F(000)	2716.0	1560.0	972.0
diffractometer	Super Nova	Super Nova	Super Nova
λ _{XKα} in Å	X = Cu 1.54184	X = Cu 1.54184	X = Cu 1.54184
θ _{min} in °	4.864	8.016	4.698
θ _{max} in °	153.376	152.956	153.644
index range	-19 ≤ h ≤ 19 -22 ≤ k ≤ 22 -24 ≤ l ≤ 26	-15 ≤ h ≤ 15 -17 ≤ k ≤ 13 -21 ≤ l ≤ 14	-12 ≤ h ≤ 11 -15 ≤ k ≤ 15 -23 ≤ l ≤ 24
μ in mm ⁻¹	7.596	15.627	2.749
abs. correction	Gaussian	Gaussian	Gaussian
reflections collected	66823	16225	22904
reflections unique	24759	6014	9214
R _{int}	0.0482	0.0443	0.0277
reflections obs. [F > 2σ(F)]	22808	5116	8463
residual density in e Å ⁻³	1.66, -1.59	1.97, -0.78	0.44, -0.43
parameters	1526	305	526
GOOF	1.024	1.0073	1.038
R ₁ [I > 2σ(I)]	0.0552	0.0440	0.0332
wR ₂ (all data)	0.1594	0.145	0.0859
CCDC	-	-	-

Table 32. Crystallographic data and details of the structure refinements of **96***C₆H₅F.

96 *C ₆ H ₅ F	
formula	C ₃₈ H ₅₅ F ₄ N ₂ O ₃ P ₃ S
M _r in g mol ⁻¹	788.81
color, habit	Clear colorless, block
crystal system	Monoclinic
space group	Cc
a in Å	13.51580(8)
b in Å	16.17008(8)
c in Å	18.73266(11)
α in °	90
β in °	101.5007(6)
γ in °	90
V in Å ³	4011.85(4)
Z	4
T in K	100.01(10)
crystal size in mm ³	0.247 × 0.178 × 0.103
ρ _c in g cm ⁻³	1.306
F(000)	1672.0
diffractometer	Super Nova
λ _{XKα} in Å	X = Cu 1.54184
θ _{min} in °	8.63
θ _{max} in °	153.53
index range	-16 ≤ h ≤ 17 -18 ≤ k ≤ 20 -21 ≤ l ≤ 23
μ in mm ⁻¹	2.324
abs. correction	Gaussian
reflections collected	19781
reflections unique	7065
R _{int}	0.0246
reflections obs. [F > 2σ(F)]	7017
residual density in e Å ⁻³	1.20, -0.53
parameters	497
GOOF	1.049
R ₁ [I > 2σ(I)]	0.0337
wR ₂ (all data)	0.0933
CCDC	-

17. Abbreviations

Å	Ångström (= 10^{-10} m)
ATR	attenuated total reflexion
BTz	2-benzo[<i>d</i>]thiazolyl
d	day(s) or doublet (in NMR spectra)
dec.	decomposes
DFT	density functional theory
eq.	equivalent(s)
h	hour
HSAB	hard and soft (Lewis) acids and bases (Pearsons' concept)
Hz	Hertz (= s^{-1})
m	multiplet (in NMR spectra)
MEP	molecular electrostatic potential
m.p.	melting point
NHC	<i>N</i> -heterocyclic carbene
NICS	nucleus-independent chemical shift
NMR	nuclear magnetic resonance
OTf	triflate (= trifluoromethanesulfonate)
PAH	polycyclic aromatic hydrocarbons
ppm	parts per million
Py	2-pyridyl
pyr	3,5-dimethylpyrazolyl
q.	quartet (in NMR spectra)
quant.	quantitative(ly)
quint.	quintet (in NMR spectra)
r.t.	room temperature
s	singlet (in NMR spectra)
sept.	septet (in NMR spectra)
t	triplet (in NMR spectra)
THF	tetrahydrofuran
tht	tetrahydrothiophene
X _{ax.}	axial (indicating position of X)
X _{eq.}	equatorial (indicating position of X)

18. References

- [1] See the reviews on “Main Group Chemistry”: a) G. Bertrand, *Chem. Rev.* **2010**, *110*, 3851; b) *New J. Chem.* **2010**, *34*, 1510.
- [2] K. B. Dillon, F. Mathey, J. F. Nixon in *Phosphorus: The Carbon Copy: From Organophosphorus to Phospha-organic Chemistry*, Wiley, Chichester, **1998**.
- [3] Y. R. Luo in *Comprehensive Handbook of Chemical Bond Energies*, CRC Press, Boca Raton, **2007**.
- [4] a) M. Baudler, K. Glinka, *Chem. Rev.* **1993**, *93*, 1623; b) S. Gómez-Ruiz, E. Hey-Hawkins, *Coord. Chem. Rev.* **2011**, *255*, 1360; c) M. Donath, F. Hennersdorf, J. J. Weigand, *Chem. Soc. Rev.* **2016**, *45*, 1145.
- [5] S. Greenberg, D. W. Stephan, *Chem. Soc. Rev.* **2008**, *37*, 1482.
- [6] S. Molitor, C. Mahler, V. H. Gessner, *New J. Chem.* **2016**, *40*, 6467.
- [7] S. J. Geier, D. W. Stephan, *Chem. Comm.* **2008**, 2779.
- [8] L. Wu, S. S. Chitnis, H. Jiao, V. T. Annibale, I. Manners, *J. Am. Chem. Soc.* **2017**, *139*, 16780.
- [9] V. T. Annibale, T. G. Ostapowicz, S. Westhues, T. C. Wambach, M. D. Fryzuk, *Dalton Trans.* **2016**, *45*, 16011.
- [10] S. S. Chitnis, H. A. Sparkes, V. T. Annibale, N. E. Pridmore, A. M. Oliver, I. Manners, *Angew. Chem. Int. Ed.* **2017**, *56*, 9536.
- [11] K.-O. Feldmann, J. J. Weigand, *J. Am. Chem. Soc.* **2012**, *134*, 15443.
- [12] a) K. Hirano, M. Miura, *Tetrahedron Lett.* **2017**, *58*, 4317; b) I. Hajdók, F. Lissner, M. Nieger, S. Strobel, D. Gudat, *Organometallics* **2009**, *28*, 1644.
- [13] Y. Sato, S.-i. Kawaguchi, A. Nomoto, A. Ogawa, *Angew. Chem. Int. Ed.* **2016**, *55*, 9700.
- [14] a) M. Baudler, *Angew. Chem. Int. Ed.* **1982**, *21*, 492; M. Baudler, *Angew. Chem. Int. Ed.* **1987**, *26*, 419; M. Baudler, W. Driehsen, S. Klautke, *Z. anorg. Allg. Chem.* **1979**, *459*, 48; M. Baudler, M. Michels, J. Hahn, M. Pieroth, *Angew. Chem. Int. Ed.* **1985**, *24*, 504; b) H. Cowley, *Chem. Rev.* **1965**, *65*, 617; c) K. Issleib, W. Seidel, *Chem. Ber.* **1959**, *92*, 2681; d) G. Fritz, *Comments Inorg. Chem.* **1982**, *6*, 329; e) G. Fritz, *Advances Inorg. Chem.* **1987**, 171; f) I. Kovacs, H. Krautscheid, E. Matern, G. Fritz, *Z. anorg. allg. Chem.* **1994**, *620*, 1369.
- [15] a) J. J. Weigand, A. Decken, N. Burfrod, *Acta Cryst.* **2008**, *C64*, 64; b) J. Bresien, K. Faust, C. Hering-Junghans, J. Rothe, A. Schulz, A. Villinger, *Dalton Trans.* **2016**, *45*, 1998; c) S. Borucki, Z. Kelemen, M. Maurer, C. Bruhn, L. Nyulászi, R. Pietschnig,

- Chem. Eur. J.* **2017**, *23*, 10438; d) A. D. Gorman, J. A. Cross, R. A. Doyle, T. R. Leonard, P. G. Pringle, H. A. Sparks, *Eur. J. Inorg. Chem.* **2019**, 1633.
- [16] a) M. Baudler, B. Makowka, *Angew. Chem. Int. Ed.* **1984**, *12*, 987; b) M. Baudler, B. Makowka, *Z. anorg. allg. Chem.* **1985**, *528*, 7; c) M. Baudler, L. de Riese-Meyer, *Z. Naturforsch.* **1986**, *41b*, 399; d) S. Burck, K. Götz, M. Kaupp, M. Nieger, J. Weber, J. S. auf der Günne, D. Gudat, *J. Am. Chem. Soc.* **2009**, *131*, 10763.
- [17] a) I. Haiduc in *The Chemistry of Inorganic Ring Systems*, Wiley-Interscience, London, **1970**; b) G. M. Kosolapoff, L. Maier in *Organic Phosphorus Compounds*, Wiley-Interscience, New York, **1972**; c) M. Baudler, J. Hellmann, P. Bachmann, K.-F. Tebbe, R. Fröhlich, M. Fehér, *Angew. Chem. Int. Ed.* **1981**, *20*, 406; d) E. Niecke, R. Rüger, B. Krebs, *Angew. Chem. Int. Ed.* **1982**, *21*, 544.
- [18] a) R. J. Less, R. L. Melen, V. Naseri, D. S. Wright, *Chem. Comm.* **2009**, 4929; b) R. J. Less, R. L. Melen, D. S. Wright, *RSC Adv.* **2012**, *2*, 2191; c) R. Dobrovetsky, K. Takeuchi, D. W. Stephan, *Chem. Comm.* **2015**, *51*, 2396; d) H. Schneider, D. Schmidt, U. Radius, *Chem. Comm.* **2015**, *51*, 10138; e) K. Schwedtmann, R. Schoemaker, F. Hennersdorf, A. Bauzá, A. Frontera, R. Weiss, J. J. Weigand, *Dalton Trans.* **2016**, *45*, 11384; f) S. Molitor, J. Becker, V. H. Gessner, *J. Am. Chem. Soc.* **2014**, *136*, 15517; g) L. Wu, V. T. Annibale, H. Jiao, A. Brookfield, D. Collison, I. Manners, *Nat. Commun.* **2019**, *10*, 2786.
- [19] a) R. Waterman, *Acc. Chem. Res.* **2019**, *52*, 2361; b) R. Waterman, *Curr. Org. Chem.* **2008**, *12*, 1322; c) N. Etkin, M. C. Fermin, D. W. Stephan, *J. Am. Chem. Soc.* **1997**, *119*, 2954; d) V. P. W. Böhm, M. Brookhart, *Angew. Chem. Int. Ed.* **2001**, *40*, 4694.
- [20] a) A. B. Burg, *J. Am. Chem. Soc.* **1961**, *83*, 2226; b) L. Maier, *Helv. Chim. Acta* **1966**, *49*, 1119; c) K. Jurkschat, C. Mugge, A. Tzschach, W. Uhlig, A. Zschunke, *Tetrahedron Lett.* **1982**, *23*, 1345; d) K. Rauzy, M. R. Mazières, P. Page, M. Sanchez, J. Bellan, *Tetrahedron Lett.* **1990**, *31*, 4463.
- [21] a) K.-O. Feldmann, S. Schulz, F. Klotter, J. J. Weigand, *ChemSusChem* **2011**, *4* 1805; b) K.-O. Feldmann, R. Fröhlich, J. J. Weigand, *Chem. Comm.* **2012**, *48*, 4296; c) K.-O. Feldmann, J. J. Weigand, *Angew. Chem. Int. Ed.* **2012**, *51*, 7545; d) K.-O. Feldmann, J. J. Weigand, *J. Am. Chem. Soc.* **2012**, *134*, 15443; e) R. Schoemaker, K. Schwedtmann, A. Franconetti, A. Frontera, F. Hennersdorf, J. J. Weigand, *Chem. Sci.* **2019**, *10*, 11054; f) C. Taube, K. Schwedtmann, M. Noikham, E. Somsook, F. Hennersdorf, R. Wolf, J. J. Weigand, *Angew. Chem. Int. Ed.* **2019**, *58*, 2.

- [22] a) S. Fisher, L. K. Peterson, J. F. Nixon, *Can. J. Chem.* **1974**, *52*, 3981; b) S. Fisher, J. Hoyano, L. K. Peterson, *Can. J. Chem.* **1976**, *54*, 2710.
- [23] a) C. G. J. Tazelaar, E. Nicolas, T. van Dijk, D. L. J. Broere, M. Cardol, M. Lutz, D. Gudat, J. C. Slootweg, K. Lammertsman, *Dalton Trans.* **2016**, *45*, 2237; b) R. Panzer, C. Guhrenz, D. Haubold, R. Hübner, N. Gaponik, A. Eychmüller, J. J. Weigand, *Angew. Chem. Int. Ed.* **2017**, *56*, 14737.
- [24] a) A. Michaelis, *Justus Liebigs Ann. Chem.* **1903**, *326*, 1293; b) R. Burgada, G. Martin, G. Mavel, *Bull. Soc. Chim. Fr.* **1963**, 2154; c) G. Mavel in *Progress in NMR Spectroscopy, Vol. 1* (Ed.: J. W. Emsley, J. Feeney, L. H. Sutcliffe), Pergamon, Oxford, **1966**.
- [25] G. Ewart, D. S. Payne, A. L. Porte, A. P. Lane, *J. Chem. Soc.* **1962**, 3984.
- [26] A. K. Bartholomew, L. M. Guard, N. Hazari, E. D. Luzik Jr., *Aust. J. Chem.* **2013**, *66*, 1455.
- [27] For recent reviews on the coordination chemistry of azolyl-substituted phosphanes see:
a) A. Thakur, D. Mandal, *Coord. Chem. Rev.* **2016**, *329*, 16; b) C. G. J. Tazelaar, J. C. Slootweg, K. Lammertsma, *Coord. Chem. Rev.* **2018**, *356*, 115.
- [28] a) S. Trofimenko, *Polyhedron* **2004**, *23*, 197; b) S. Trofimenko, *Chem. Rev.* **1993**, *93*, 943.
- [29] M. Scheer, St. Gremler, E. Herrmann, M. Dargatz, H.-D. Schädler, *Z. anorg. Allg. Chem.* **1993**, *619*, 1047.
- [30] a) M. Baudler, K. Hammerström, *Z. Naturforschg.* **1965**, *20b*, 810; b) A. H. Cowley, R. P. Pinnel, *Inorg. Chem.* **1966**, 1459; c) L. R. Smith, J. L. Mills, *J. Am. Chem. Soc.* **1976**, *98*, 3852; d) K. Schwedtmann, J. Haberstroh, S. Roediger, A. Bauzá, A. Frontera, F. Hennersdorf, J. J. Weigand, *Chem. Sci.* **2019**, *10*, 6868.
- [31] a) A. H. Cowley, D. S. Dierdorf, *J. Am. Chem. Soc.* **1969**, *91*, 6609; b) R. K. Harris, E. M. Norval, M. Fild, *J. Chem. Soc., Dalton Trans.* **1979**, 826; c) A. B. Burg, *Inorg. Chem.* **1981**, *20*, 3731; d) L. R. Avens, R. A. Wolcott, L. V. Cribbs, J. L. Mills, *Inorg. Chem.* **1989**, *28*, 200; e) L. R. Avens, L. V. Cribbs, J. L. Mills, *Inorg. Chem.* **1989**, *28*, 205; f) L. R. Avens, L. V. Cribbs, J. L. Mills, *Inorg. Chem.* **1989**, *28*, 211.
- [32] K.-O. Feldmann, J. J. Weigand, *Angew. Chem. Int. Ed.* **2012**, *51*, 7545.
- [33] K.-O. Feldmann, J. J. Weigand, *J. Am. Chem. Soc.* **2012**, *134*, 15443.
- [34] a) D. Schomburg, G. Bettermann, L. Ernst, R. Schmutzler, *Angew. Chem.* **1985**, *11*, 971; b) L. Ernst, P. G. Jones, P. Look-Herber, R. Schmutzler, *Chem. Ber.* **1990**, *123*, 35.

- [35] a) N. Burford, C. A. Dyker, A. Decken, *Angew. Chem. Int. Ed.* **2005**, *44*, 2364; b) N. Burford, C. A. Dyker, M. Lumsden, A. Decken, *Angew. Chem. Int. Ed.* **2005**, *44*, 6196; c) S. D. Riegel, N. Burford, M. D. Lumsden, A. Decken, *Chem. Commun.* **2007**, 4668; d) D. A. Dyker, N. Burford, G. Menard, M. D. Lumsden, A. Decken, *Inorg. Chem.* **2007**, *46*, 4277; e) J. J. Weigand, S. D. Riegel, N. Burford, A. Decken, *J. Am. Chem. Soc.* **2007**, *129*, 7969; f) C. A. Dyker, S. D. Riegel, N. Burford, M. D. Lumsden, A. Decken, *J. Am. Chem. Soc.* **2007**, *129*, 7464.
- [36] S. S. Chitnis, M. Whalen, N. Burford, *J. Am. Chem. Soc.* **2014**, *136*, 12489.
- [37] A. P. M. Robertson, C. A. Dyker, P. A. Gray, B. O. Patrick, A. Decken, N. Burford, *J. Am. Chem. Soc.* **2014**, *136*, 1491.
- [38] S. S. Chitnis, R. A. Musgrave, H. A. Sparkes, N. E. Pridmore, V. T. Annibale, I. Manners, *Inorg. Chem.* **2017**, *56*, 4521.
- [39] S. S. Chitnis, H. A. Sparkes, V. T. Annibale, N. E. Pridmore, A. M. Oliver, I. Manners, *Angew. Chem.* **2017**, *129*, 9664.
- [40] M. H. Holthausen, D. Knackstedt, N. Burford, J. J. Weigand, *Aust. J. Chem.* **2013**, *66*, 1155.
- [41] R. Schoemaker, *TU Dresden*, Master's Thesis, **2015**.
- [42] For an alternative, previously reported synthesis of PyPCl_2 see: X. Chen, H. Zhu, T. Wang, C. Li, L. Yan, M. Jiang, J. Liu, X. Sun, Z. Jiang and Y. Ding, *J. Mol. Catal. A: Chem.* **2016**, *414*, 37.
- [43] For an alternative, previously reported synthesis of BTzPCl_2 **35** see: I. V. Komarov, A. V. Strizhak, M. Y. Kornilov, E. Zraudnitskiy, A. A. Tolmachev, *Synth. Commun.* **2000**, *30*, 243.
- [44] F. R. Keene, *Acta. Cryst.* **1988**, *C44*, 757.
- [45] T. Stey, M. Pfeiffer, J. Henn, S. K. Pandey, D. Stalke, *Chem. Eur. J.* **2007**, *13*, 3636.
- [46] R. E. Cobblestick, F. W. B. Bernstein, *Acta. Crystallogr.* **1975**, *B31*, 2731.
- [47] *Handbook of Chemistry and Physics*, 56th edition, ed. R. C. Weast, CRC Press, Cleveland, Ohio, **1975**, F-214.
- [48] a) T. A. van der Knaap, T. C. Kleebach, F. Visser, F. Bickelhaupt, P. Ros, E. J. Baerends, C. H. Stam, M. Konijn, *Tetrahedron* **1984**, *40*, 765; b) L. A. van der Veen, P. C. J. Kamer, P. W. N. M. van Leeuwen, *Organometallics* **1999**, *18*, 4765; c) J. J. M. de Pater, C. E. P. Maljaars, E. de Wolf, M. Lutz, A. L. Spek, B.-J. Deelman, C. J. Elsevier, G. van Koten, *Organometallics* **2005**, *24*, 5299; d) S. Warsink, E. J. Derrah,

- C. A. Boon, Y. Cabon, J. J. M. de Pater, M. Lutz, R. J. M. Klein Gebbink, B.-J. Deelman, *Chem. Eur. J.* **2015**, *21*, 1765.
- [49] J. J. Daly, *J. Chem. Soc. A* **1966**, *0*, 1020.
- [50] a) S. Gomez-Ruiz, E. Hey-Hawkins, *Coord. Chem. Rev.* **2011**, *255*, 1360; b) *Phosphorus Chemistry: Catalysis and Material Science Applications*, ed. M. Peruzzini, L. Gonsalvi, Springer, Volume 37, **2011**.
- [51] a) J. W. Dube, C. L. B. Macdonald, P. Ragogna, *Angew. Chem. Int. Ed.* **2012**, *51*, 13026; b) J. W. Dube, C. L. B. Macdonald, B. D. Ellis, Paul Ragogna, *Inorg. Chem.* **2013**, *52*, 11438.
- [52] a) M. Scheer, C. Kuntz, M. Stubenhofer, M. Zabel, A. Y. Timoshkin, *Angew. Chem., Int. Ed.* **2010**, *49*, 188; b) M. Baacke, S. Morton, G. Johannsen, N. Weferling, O. Stelzer, *Chem. Ber.* **1980**, *113*, 1328; c) W. S. Sheldrick, S. Morton, O. Stelzer, Z. *Anorg. Allg. Chem.* **1981**, *475*, 232; d) M. Scheer, S. Gremler, E. Herrmann, P. G. Jones, *J. Organomet. Chem.* **1991**, *414*, 337.
- [53] D. R. Armstrong, N. Feeder, A. D. Hopkins, M. J. Mays, D. Moncrieff, J. A. Wood, A. D. Woods, D. S. Wright, *Chem. Comm.* **2000**, 2483.
- [54] C. E. Averre, M. P. Coles, I. R. Crossley, I. J. Day, *Dalton Trans.* **2012**, *41*, 278.
- [55] For a review on argentophilic interactions see: H. Schmidbaur, A. Schier, *Angew. Chem., Int. Ed.* **2015**, *54*, 746; for aurophilic interactions see: H. Schmidbaur, A. Schier, *Chem. Soc. Rev.* **2012**, *41*, 370.
- [56] A. Bondi, *J. Phys. Chem.* **1964**, *68*, 441.
- [57] a) C.-M. Che, Z. Mao, V. M. Miskowski, M.-C. Tse, C.-K. Chan, K.-K. Cheung, D. L. Phillips, K.-H. Leung, *Angew. Chem., Int. Ed.* **2000**, *39*, 4084; C.-M. Che, M.-C. Tse, M. C. W. Chan, K.-K. Cheung, D. L. Phillips, K.-H. Leung, *J. Am. Chem. Soc.* **2000**, *122*, 2464; C.-M. Che, W.-F. Wu, K.-C. Chan, K.-K. Cheung, *Chem. Eur. J.* **2001**, *7*, 4656.
- [58] a) M. Henary, J. L. Wootton, S. I. Khan, J. I. Zink, *Inorg. Chem.* **1997**, *36*, 796; P. Aslanidis, P. J. Cox, S. Divanidis, A. C. Tsipis, *Inorg. Chem.* **2002**, *41*, 6875.
- [59] a) H. Friebolin in *Ein- und Zweidimensionale NMR-Spektroskopie*, Wiley VCH, Weinheim, **2006**; b) H. Fujii, M. Tomura, T. Kurahashi, M. Kujime, *Inorg. Chem.* **2007**, *46*, 541.
- [60] a) J. P. Albrand, D. Gagnaire, J. B. Robert, *J. Am. Chem. Soc.* **1973**, *95*, 6498; b) J. P. Albrand, J. B. Robert, *J. Chem. Soc. Chem. Comm.* **1974**, 644; c) L. R. Smith, J. L. Mills, *J. Chem. Soc. Chem. Comm.* **1974**, *20*, 808.

- [61] K.-O. Feldmann, *WWU Münster*, PhD Thesis, **2012**.
- [62] P. A. Gray, Y.-Y. Carpenter, N. Burford, R. McDonald, *Dalton Trans.* **2016**, *45*, 2124.
- [63] N. Burford, T. S. Cameron, P. J. Ragogna, *J. Am. Chem. Soc.* **2001**, *123*, 7947.
- [64] a) C. A. Dyker, N. Burford, M. D. Lumsden, A. Decken, *J. Am. Chem. Soc.* **2006**, *128*, 9632; b) Y.-Y. Carpenter, C. A. Dyker, N. Burford, M. D. Lumsden, A. Decken, *J. Am. Chem. Soc.* **2008**, *130*, 15732.
- [65] a) A. J. Arduengo III, H. V. R. Dias, J. C. Calabrese, *Chem. Lett.* **1997**, 143; b) A. J. Arduengo III, J. C. Calabrese, A. H. Cowley, H. V. R. Dias, J. R. Goerlich, W. J. Marshall, B. Riegel, *Inorg. Chem.* **1997**, *36*, 2151; c) J. H. Barnard, P. A. Brown, K. L. Shuford, C. D. Martin, *Angew. Chem. Int. Ed.* **2015**, *54*, 12083.
- [66] A. Schmidpeter, S. Lochschmidt, W. S. Sheldrick, *Angew. Chem.* **1985**, *97*, 214.
- [67] a) B. D. Ellis, M. Carlesimo, C. L. B. Macdonald, *Chem. Commun.* **2003**, 1946; b) B. D. Ellis, C. L. B. Macdonald, *Inorg. Chem.* **2006**, *45*, 6864; c) E. L. Norton, K. L. S. Szekely, J. W. Dube, P. G. Bomben, C. L. B. Macdonald, *Inorg. Chem.* **2008**, *47*, 1196.
- [68] M. Regitz, O. J. Scheerer in *Multiple Bonds and Low Coordination in Phosphorus Chemistry*, Georg Thieme Verlag Thieme Medical Publishers, New York, **1990**.
- [69] H. R. Allcock in *Phosphorus-Nitrogen Compounds*, Academic Press, New York, **1972**.
- [70] E. Payet, A. Auffrant, X. F. Le Goff, P. Le Floch, *J. Organomet. Chem.* **2010**, *695*, 1499.
- [71] a) E. Rüba, K. Mereiter, R. Schmid, V. N. Sapunov, K. Kirchner, H. Schottenberger, M. J. Calhorda, L. F. Veiros, *Chem. Eur. J.* **2002**, *8*, 3948; b) C. Coletti, L. Gonsalvi, A. Guerriero, L. Marvelli, M. Peruzzini, G. Reginato, N. Rem, *Organometallics* **2010**, *29*, 5982.
- [72] a) M. D. Watson, A. Fechtenkotter, K. Müllen, *Chem. Rev.* **2001**, *101*, 1267; b) J. S. Wu, W. Pisula, K. Müllen, *Chem. Rev.* **2007**, *107*, 718; c) L. Schmidt-Mende, A. Fechtenkotter, K. Müllen, E. Moons, R. H. Friend, J. D. MacKenzie, *Science* **2001**, *293*, 1119; d) W. Pisula, X. Feng, K. Müllen, *Chem. Mater.* **2011**, *21*, 3295; e) Z. Zeng, X. Shi, C. Chi, J. T. Lopez-Navarette, J. Casado, J. Wu, *Chem. Soc. Rev.* **2015**, *44*, 6578; f) T. J. J. Müller, U. H. F. Bunz in *Functional Organic Materials: Syntheses, Strategies and Applications*, Wiley-VCH, Weinheim, **2007**.
- [73] a) W. Pisula, X. Feng, K. Müllen, *Chem. Mater.* **2011**, *22*, 3634; b) X. Yan, L.-S. Li, *J. Mater. Chem.* **2011**, *21*, 3295.
- [74] M. Stępień, E. Gońka, M. Żyła, N. Sprutta, *Chem. Rev.* **2017**, *117*, 3479.

- [75] a) T. Hatakeyama, S. Hashimoto, S. Seki, M. Nakamura, *J. Am. Chem. Soc.* **2011**, *133*, 18614; b) Z. Zhou, A. Wakamiya, T. Kushida, S. Yamaguchi, *J. Am. Chem. Soc.* **2012**, *134*, 4529.
- [76] a) S. M. Draper, D. J. Gregg, R. Mathadil, *J. Am. Chem. Soc.* **2002**, *124*, 3486; b) S. M. Draper, D. J. Gregg, E. R. Schofield, W. R. Browne, M. Duati, J. G. Vos, P. Passaniti, *J. Am. Chem. Soc.* **2004**, *126*, 8694; c) D. Q. Wu, W. Pisula, V. Enkelmann, X. Feng, K. Müllen, *J. Am. Chem. Soc.* **2009**, *131*, 9620; d) N. K. S. Davis, A. L. Thompson, H. L. Anderson, *J. Am. Chem. Soc.* **2011**, *133*, 30; e) Y. Fogel, M. Kastler, Z. Wang, D. Andrienko, G. J. Bodwell, K. Müllen, *J. Am. Chem. Soc.* **2007**, *129*, 11743; f) D. Wu, W. Pisula, V. Enkelmann, X. Feng, K. Müllen, *J. Am. Chem. Soc.* **2009**, *131*, 9620; g) D. Q. Wu, X. Feng, M. Takase, M. C. Haberecht, K. Müllen, *Tetrahedron* **2008**, *64*, 11379; h) D. J. Gregg, C. M. Fitchett, S. M. Draper, *Chem. Commun.* **2006**, 3090.
- [77] D. Wu, W. Pisula, M. C. Haberecht, X. Feng, K. Müllen, *Org. Lett.* **2009**, *11*, 5686.
- [78] a) C. J. Martin, B. Gil, S. D. Perera, S. M. Draper, *Chem. Commun.* **2011**, *47*, 3616; b) X. Feng, J. Wu, M. Ai, W. Pisula, L. Zhi, J. P. Rabe, K. Müllen, *Angew. Chem., Int. Ed.* **2007**, *46*, 3033; c) A. A. Gorodetsky, C.-Y. Chiu, T. Schiros, M. Palma, M. Cox, Z. Jia, W. Sattler, I. Kymissis, M. Steigerwald, C. Nuckolls, *Angew. Chem., Int. Ed.* **2010**, *49*, 7909; d) R. Benshafrut, M. Rabinovitz, R. E. Hoffman, N. Ben-Mergui, K. Müllen, V. S. Iyer, *Eur. J. Org. Chem.* **1999**, 37.
- [79] a) C. Fave, T. Y. Cho, M. Hissler, C. W. Chen, T. Y. Luh, C. C. Wu, R. Réau, *J. Am. Chem. Soc.* **2003**, *125*, 9254; b) H. C. Su, O. Fadhel, C. J. Yang, T. Y. Cho, C. Fave, M. Hissler, C. C. Wu, R. Réau, *J. Am. Chem. Soc.* **2006**, *128*, 983; c) J. Crassous, R. Réau, *Dalton Trans.* **2008**, *48*, 6865; d) Y. Matano, H. Imahori, *Org. Biomol. Chem.* **2009**, *7*, 1258; e) A. Bruch, A. Fukazawa, E. Yamaguchi, S. Yamaguchi, A. Studer, *Angew. Chem., Int. Ed.* **2011**, *50*, 12094; f) Y. Ren, T. Baumgartner, *J. Am. Chem. Soc.* **2011**, *133*, 1328; g) Y. Ren, T. Baumgartner, *Dalton Trans.* **2012**, *41*, 7792; h) P.-A. Bouit, A. Escande, R. Szücs, D. Szieberth, C. Lescop, L. Nyulászi, M. Hissler, R. Réau, *J. Am. Chem. Soc.* **2012**, *134*, 6524; i) H. Chen, W. Delaunay, J. Li, Z. Wang, P. A. Bouit, D. Tondelier, B. Geffroy, F. Mathey, Z. Duan, R. Réau, M. Hissler, *Org. Lett.* **2013**, *15*, 330; j) J. C.-H. Chan, W. H. Lam, H.-L. Wong, W.-T. Wong, V. W.-W. Yam, *Angew. Chem., Int. Ed.* **2013**, *52*, 11504; k) M. Stolar, T. Baumgartner, *Chem. Asian J.* **2014**, *9*, 1212; l) M. Takahashi, K. Nakano, K. Nozaki, *J. Org. Chem.* **2015**,

- 80, 3790; m) P. Hibner-Kulicka, J. A. Joule, J. Skalik, P. Bałczewski, *RSC Adv.* **2017**, 7, 9194.
- [80] a) M. Hissler, P. W. Dyer, R. Réau, *Coord. Chem. Rev.* **2003**, 244, 1; b) T. Baumgartner, R. Réau, *Chem. Rev.* **2006**, 106, 4681; c) B. Nohra, S. Graule, C. Lescop, R. Réau, *J. Am. Chem. Soc.* **2006**, 128, 3520; d) S. Graule, M. Rudolph, N. Vanthuyne, J. Autschbach, C. Roussel, J. Crassous, R. Réau, *J. Am. Chem. Soc.* **2009**, 131, 3183; e) Z. Benkő, L. Nyulászi, *Top. Heterocycl. Chem.* **2009**, 19, 27; f) Y. Matano, A. Saito, T. Fukushima, Y. Tokudome, F. Suzuki, D. Sakamaki, H. Kaji, A. Ito, K. Tanaka, H. Imahori, *Angew. Chem., Int. Ed.* **2011**, 50, 8016; g) A. Bruch, A. Fukazawa, E. Yamaguchi, S. Yamaguchi, A. Studer, *Angew. Chem., Int. Ed.* **2011**, 50, 12094; h) Y. Ren, W. H. Kan, M. A. Henderson, P. G. Bomben, C. P. Berlinguette, V. Thangadurai, T. Baumgartner, *J. Am. Chem. Soc.* **2011**, 133, 17014; i) H. Chen, W. Delaunay, L. Yu, D. Joly, Z. Wang, J. Li, Z. Wang, C. Lescop, D. Tondelier, B. Geffroy, Z. Duan, M. Hissler, F. Mathey, R. Réau, *Angew. Chem., Int. Ed.* **2012**, 51, 214; j) P.-A. Bouit, A. Escande, R. Szűcs, D. Szieberth, C. Lescop, L. Nyulászi, M. Hissler, R. Réau, *J. Am. Chem. Soc.* **2012**, 134, 6524.
- [81] a) O. Fadhel, M. Gras, N. Lemaitre, V. Deborde, M. Hissler, B. Geffroy, R. Réau, *Adv. Mater.* **2009**, 21, 1261; b) D. Joly, D. Tondelier, V. Deborde, B. Geffroy, M. Hissler, R. Réau, *New J. Chem.* **2010**, 34, 1603; c) D. Joly, D. Tondelier, V. Deborde, W. Delaunay, A. Thomas, K. Bhanuprakash, B. Geffroy, M. Hissler, R. Réau, *Adv. Funct. Mater.* **2012**, 22, 567; d) K. Baba, M. Tobisu, N. Chatani, *Angew. Chem., Int. Ed.* **2013**, 52, 11892; *Angew. Chem.* **2013**, 125, 12108; e) A. Oukhrib, L. Bonnafoux, A. Panossian, A. Waifang, D. H. Nguyen, M. Urrutigoity, F. Colobert, M. Gouygou, F. R. Leroux, *Tetrahedron* **2014**, 70, 1431; f) Y. Zhou, Z. Gan, B. Su, J. Li, Z. Duan, F. Mathey, *Org. Lett.* **2015**, 17, 5722.
- [82] a) K. M. Pietrusiewicz, M. Kuźnikowski, *Phosphorus, Sulfur/Silicon Relat. Elem.* **1993**, 77, 57; b) D. Fabbri, S. Gladiali, O. De Lucchi, *Synth. Commun.* **1994**, 24, 1271; c) S. M. Reid, R. C. Boyle, J. T. Mague, M. J. Fink, *J. Am. Chem. Soc.* **2003**, 125, 7816; d) M. Widhalm, C. Aichinger, K. Mereiter, *Tetrahedron Lett.* **2009**, 50, 2425; e) T. Agou, M. D. Hossain, T. Kawashima, K. Kamada, K. Ohta, *Chem. Commun.* **2009**, 6762; f) A. Fukazawa, H. Yamada, Y. Sasaki, S. Akiyama, S. Yamaguchi, *Chem. Asian J.* **2010**, 5, 466; g) A. Muller, C. W. Holzapfel, *Acta Crystallogr., Sect. E: Struct. Rep. Online* **2013**, 69, o20; h) A. Fukazawa, H. Yamada, S. Yamaguchi, *Angew. Chem., Int. Ed.* **2008**, 47, 5582; *Angew. Chem.* **2008**, 120, 5664; i) A.

- Fukazawa, E. Yamaguchi, E. Ito, H. Yamada, J. Wang, S. Irle, S. Yamaguchi, *Organometallics* **2011**, *30*, 3870; j) S. Arndt, M. M. Hansmann, F. Rominger, M. Rudolph, A. S. K. Hashmi, *Chem. Eur. J.* **2017**, *23*, 5429; k) Q. Ge, J. Zong, B. Li, B. Wang, *Org. Lett.* **2017**, *19*, 6670.
- [83] a) T. Imamoto, M. Matsuo, T. Nonomura, K. Kishikawa, M. Yanagawa, *Heteroatom Chem.* **1993**, *4*, 475; b) V. Diemer, A. Berthelot, J. Bayardon, S. Jugé, F. R. Leroux, F. Colobert, *J. Org. Chem.* **2012**, *77*, 6117; c) K. V. Rajendran, D. G. Gilheany, *Chem. Commun.* **2012**, *48*, 817; d) K. Fourmy, S. Mallet-Ladeira, O. Dechy-Cabaret, M. Gouygou, *Organometallics* **2013**, *32*, 1571; e) X. Wei, X. Lu, X. Zhao, Z. Duan, F. Mathey, *Angew. Chem. Int. Ed.* **2015**, *54*, 1583.
- [84] L. Nyulászi, *Tetrahedron* **2000**, *56*, 79.
- [85] a) K. Karaghiosoff, C. Cleve, A. Schmidpeter, *Phosphorus and Sulfur* **1986**, *28*, 289; b) K. Karaghiosoff, A. Schmidpeter, *Phosphorus and Sulfur* **1988**, *36*, 217; c) I. A. Litvinov, K. Karaghiosoff, A. Schmidpeter, E. Y. Zabolina, E. N. Dianova, *Heteroatom Chem.* **1991**, *2*, 369; d) R. K. Bansal, N. Gupta, K. Karaghiosoff, *Z. Naturforsch.* **1992**, *47b*, 373; e) R. K. Bansal, R. Mahnot, D. C. Sharma, K. Karaghiosoff, *Synthesis* **1992**, 267; f) R. K. Bansal, K. Karaghiosoff, A. Schmidpeter, *Tetrahedron* **1994**, *50*, 7675; g) K. Karaghiosoff, R. Mahnot, C. Cleve, N. Gandhi, R. K. Bansal, A. Schmidpeter, *Chem. Ber.* **1995**, *128*, 581; h) N. Gupta in *Top. Heterocycl. Chem., Vol 21*. (Vol. Ed.: R. K. Bansal), Springer-Verlag, Berlin Heidelberg, **2010**, 175.
- [86] a) T. Baumgartner, *Acc. Chem. Res.* **2014**, *47*, 1613; b) T. Hatakeyama, S. Hashimoto, M. Nakamura, *Org. Lett.* **2011**, *13*, 2130; c) P.-A. Bouit, A. Escande, R. Szűcs, D. Szieberth, C. Lescop, L. Nyulászi, M. Hissler, R. Réau, *J. Am. Chem. Soc.* **2012**, *134*, 6524; d) M. Stolar, J. Borau-Garcia, M. Toonen, T. Baumgartner, *J. Am. Chem. Soc.* **2015**, *137*, 3366.
- [87] a) P. Metrangolo, F. Meyer, T. Pilati, G. Resnati, G. Terraneo, *Angew. Chem. Int. Ed.* **2008**, *47*, 6114; b) A. Bauzá, J. T. Mooibkoek, A. Frontera, *ChemPhysChem* **2015**, *16*, 2496.
- [88] a) G. Müller, J. Brand, S. B. Z. Jetter, *Z. Naturforsch. B* **2001**, *56*, 1163; b) K. Schwedtmann, M. H. Holthausen, K.-O. Feldmann, J. J. Weigand, *Angew. Chem. Int. Ed.* **2013**, *52*, 14204.
- [89] P. Kilian, A. M. Slawin, A. L. Fuller, P. Wawrzyniak, *Inorg. Chem.* **2009**, *48*, 2500.
- [90] K. B. Dillon, *Chem. Rev.* **1994**, *94*, 1441.
- [91] T. Q. Nguyen, F. Qu, X. Huang, A. F. Janzen, *Can. J. Chem.* **1992**, *70*, 2089.

- [92] K. B. Dillon, R. N. Reeve, T. C. Waddington, *J.C.S. Dalton* **1977**, *23*, 2382.
- [93] C. Kaes, A. Katz, M. W. Hosseini, *Chem. Rev.* **2000**, *100*, 3553.
- [94] S. Kobayashi, M. Sugiura, H. Kitagawa, W. W. L. Lam, *Chem. Rev.* **2002**, *102*, 2227.
- [95] I. Tsuneo, Y. Koide, S. Hiyama, *Chem. Lett.* **1990**, *19*, 1445.
- [96] R. Corbo, T. P. Bell, B. D. Stringer, C. F. Hogan, D. J. D. Wilson, P. J. Barnard, J. L. Dutton, *J. Am. Chem. Soc.* **2014**, *136*, 12415.
- [97] M. Donath, M. Bodensteiner, J. J. Weigand, *Chem. Eur. J.* **2014**, *20*, 1730.
- [98] C. D. Martin, C. M. Le, P. J. Ragogna, *J. Am. Chem. Soc.* **2009**, *131*, 15126.
- [99] J. Beckmann, J. Bolsinger, A. Duthie, P. Finke, E. Lork, C. Lütke, O. Mallow, S. Mebs, *Inorg. Chem.* **2012**, *51*, 12395.
- [100] P. A. Rupar, V. N. Staroverov, K. M. Baines, *Science* **2008**, *322*, 1360
- [101] S. S. Chitnis, A. P. M. Robertson, N. Burford, J. J. Weigand, R. Fischer, *Chem. Sci.* **2015**, *6*, 2559.
- [102] S. S. Chitnis, A. P. M. Robertson, N. Burford, B. O. Patrick, R. McDonald, M. J. Ferguson, *Chem. Sci.* **2015**, *6*, 6545.
- [103] *Handbook of Chemistry and Physics*, 65th edition, ed. R. C. Weast, CRC Press, Boca Raton, Florida, **1975**.
- [104] a) W. Mahler, A. B. Burg, *J. Am. Chem. Soc.* **1957**, *79*, 251; b) P. R. Bloomfield, K. Parvin, *Chem. Ind.-Lond.* **1959**, *90*, 148; c) F. Pass, H. Schindlbauer, *Monatsh. Chem.* **1959**, *90*, 148; d) W. A. Henderson, M. Epstein, F. S. Seichter, *J. Am. Chem. Soc.* **1963**, *85*, 2462; e) R. B. King, N. D. Sadani, *J. Org. Chem.* **1985**, *50*, 1719; f) M. Baudler, D. Grenz, U. Arndt, H. Budzikiewicz, M. Fehér, *Chem. Ber.* **1988**, *121*, 1707.
- [105] a) H. Matschiner, H. Tannerberg, *Z. Chem.* **1980**, *20*, 218; b) H. P. Stritt, H. P. Latscha, *Z. Anorg. Allg. Chem.* **1986**, *542*, 167.
- [106] G. He, O. Shynkaruk, M. W. Lui, E. Rivard, *Chem. Rev.* **2014**, *114*, 7815.
- [107] M. Baudler, K. Glinka, A. H. Cowley, M. Pakulski, *Inorganic Syntheses, Volume 11* *25*, Inorganic Syntheses, Inc. **1989**.
- [108] a) I. S. Yoshifuji, N. Inamoto, K. Hirotsu, T. Higuchi, *J. Am. Chem. Soc.* **1981**, *103*, 4587; b) R. C. Smith, E. Urzenius, K.-C. Lam, A. L. Rheingold, J. D. Protasiewicz, *Inorg. Chem.* **2002**, *41*, 5296.
- [109] a) G. Fritz, H. Fleischer, *Z. Anorg. Allg. Chem.* **1989**, *570*, 67; b) R. Appel, D. Gudat, E. Niecke, M. Nieger, C. Porz, H. Westermann, *Z. Naturforsch.* **1991**, *46b*, 865; c) A. Beil, R. J. Gilliard Jr., H. Grützmacher, *Dalton Trans.* **2016**, *45*, 2044.

- [110] a) J. Bresien, C. Hering, A. Schulz, A. Villinger, *Chem. Eur. J.* **2014**, *20*, 12607; b) J. Bresien, L. Eickhoff, A. Schulz, T. Suhrbier, A. Villinger, *Chem. Eur. J.* **2019**, *25*, 1.
- [111] a) M. Baudler, G. Reuschenbach, *Z. Anorg. Allg. Chem.* **1980**, *464*, 9; b) G. Fritz, J. Härer, *Z. Anorg. Allg. Chem.* **1983**, *504*, 23.
- [112] T. L. Breen, D. W. Stephan, *Organometallics* **1997**, *16*, 365.
- [113] J. J. Weigand, N. Burford, R. J. Davidson, T. S. Cameron, P. Sellheim, *J. Am. Chem. Soc.* **2009**, *131*, 17943.
- [114] a) H. G. Ang, J. S. Shannon, B. O. West, *Chem. Commun.* **1965**, 10; b) A. Forster, C. S. Cundy, M. Green, F. G. A. Stone, *Inorg. Nucl. Chem. Letters* **1966**, *2*, 233; c) C. S. Cundy, M. Green, F. G. A. Stone, A. Taunton-Rigby, *J. Chem. Soc (A)* **1968**, 1776; d) N. H. Tran Huy, Y. Inubushi, L. Ricard, F. Mathey, *Organometallics* **2011**, *30*, 1734.
- [115] G. Horvat, T. Portada, V. Stilinović, V. Tomišić, *Acta. Cryst. E* **2007**, *63*, m1734.
- [116] R. G. Pearson, *Inorg. Chim. Acta* **1995**, *240*, 93 and references therein.
- [117] Keith R. Dixon in *Multinuclear NMR* (Ed. Joan Mason), Plenum Press, New York, **1987**, 369.
- [118] a) S. I. Hommeltoft, O. Ekelund, J. Zavilla, *Ind. Eng. Chem. Res.* **1997**, *36*, 3491; b) T. T. Dang, F. Boeck, L. Hintermann, *J. Org. Chem.* **2011**, *76*, 9353.
- [119] N. Weferling, *Z. anorg. allg. Chem.* **1987**, *548*, 55.
- [120] A. B. Burg, *Inorg. Chem.* **1985**, *24*, 3342.
- [121] R. Ramage, B. Atrash, D. Hopton, M. J. Parrott, *J. Chem. Soc. Perkin Trans. I*, **1985**, 1217.
- [122] R. Appel, R. Milker, *Chem. Ber.*, **1975**, *108*, 1783.
- [123] W. Wolfsberger, *J. Organomet. Chem.*, **1986**, *317*, 167.
- [124] Holleman-Wiberg, *Lehrbuch der anorganischen Chemie, Vol. 102*, Walter DeGruyter, **2007**.
- [125] S. Ahrland, K. Dreisch, B. Norén, A. Oskarsson, *Materials Chemistry and Physics* **1993**, *35*, 281-289.
- [126] D. M. Stefanescu, H. F. Yuen, D. S. Glueck, J. A. Golen, L. N. Zakharov, C. D. Incarvito, A. L. Rheingold, *Inorg. Chem.*, **2003**, *42*, 8891.
- [127] I. G. Phillips, R. G. Ball, R. G. Cavell, *Inorg. Chem.*, **1992**, *31*, 1633.
- [128] S. Gómez-Ruiz, A. Schisler, P. Lönnecke, E. Hey-Hawkins, *Chem. Eur. J.*, **2007**, *13*, 7974.
- [129] D. E. Berry, K. A. Beveridge, G. W. Bushnell, K. R. Dixon, *Can. J. Chem.*, **1985**, *63*, 2949.

- [130] H.-K. Fun, S. Chantrapromma, Y.-C. Liu, Z.-F. Chen, H. Liang, *Acta Cryst.* **2006**, *E62*, m1252.
- [131] Q. Liu, L. Thorne, I. Kozin, D. Song, C. Seward, M. D'Iorio, Y. Tao, S. Wang, *J. Chem. Soc., Dalton Trans.*, **2002**, 3234.
- [132] M. A. Fox, J. K. Whitesell in *Organische Chemie*, Spektrum Akademischer Verlag, Heidelberg, **1995**.
- [133] H. Goldwhite in *Introduction to Phosphorus Chemistry*, Cambridge University Press, Cambridge, **1981**.
- [134] A. Dewanji, C. Mück-Lichtenfeld, K. Bergander, C. G. Daniliuc, A. Studer, *Chem. Eur. J.*, **2015**, *21*, 12295.
- [135] H. Chikashita, K. Itoh, *Heterocycles*, **1985**, *23*, 295.
- [136] K. Issleib, H. Weichmann., *Chem. Ber.*, **1968**, *101*, 2197.
- [137] G. Becker, O. Mundt, M. Rössler, E. Schneider, *Z. anorg. allg. Chem.*, **1978**, *443*, 42.
- [138] B. A. Pindzola, J. Jin, D. L. Gin, *J. Am. Chem. Soc.*, **2003**, *125*, 2940.
- [139] CrysAlisPRO, Oxford Diffraction /Agilent Technologies UK Ltd, Yarnton, England.
- [140] Bruker (2007). SMART. Bruker AXS Inc., Madison, Wisconsin, USA.
- [141] Bruker (2001). SADABS. Bruker AXS Inc., Madison, Wisconsin, USA.
- [142] O. V. Dolomanov, L. J. Bourhis, R. J. Gildea, J. A. K. Howard, H. Puschmann, *J. Appl. Cryst.*, **2009**, *42*, 339.
- [143] G. Sheldrick, *Acta Cryst.* **2008**, *64*, 112.
- [144] G. Sheldrick, *Acta Cryst. C* **2015**, *71*, 3.
- [145] R. Ahlrichs, M. Bär, M. Hacer, H. Horn, C. Kömel, *Chem. Phys. Lett.*, **1989**, *162*, 165.
- [146] A. Klamt, G. Schüürmann, *J. Chem. Soc. Perkin Trans. 2*, **1993**, *2*, 799.
- [147] S. Grimme, J. Antony, S. Ehrlich, H. Krieg, *J. Chem. Phys.*, **2010**, *132*, 154104.
- [148] P. von Ragué Schleyer, C. Maerker, A. Dransfeld, H. Jiao, N. J. R. van Eikema Hommes, *J. Am. Chem. Soc.*, **1996**, *118*, 6317.
- [149] Gaussian 09, Revision A.02, M. J. Frisch, G. W. Trucks, H. B. Schlegel, G. E. Scuseria, M. A. Robb, J. R. Cheeseman, G. Scalmani, V. Barone, G. A. Petersson, H. Nakatsuji, X. Li, M. Caricato, A. Marenich, J. Bloino, B. G. Janesko, R. Gomperts, B. Mennucci, H. P. Hratchian, J. V. Ortiz, A. F. Izmaylov, J. L. Sonnenberg, D. Williams-Young, F. Ding, F. Lipparini, F. Egidi, J. Goings, B. Peng, A. Petrone, T. Henderson, D. Ranasinghe, V. G. Zakrzewski, J. Gao, N. Rega, G. Zheng, W. Liang, M. Hada, M. Ehara, K. Toyota, R. Fukuda, J. Hasegawa, M. Ishida, T. Nakajima, Y. Honda, O. Kitao, H. Nakai, T. Vreven, K. Throssell, J. A. Montgomery, Jr., J. E. Peralta, F.

Ogliaro, M. Bearpark, J. J. Heyd, E. Brothers, K. N. Kudin, V. N. Staroverov, T. Keith, R. Kobayashi, J. Normand, K. Raghavachari, A. Rendell, J. C. Burant, S. S. Iyengar, J. Tomasi, M. Cossi, J. M. Millam, M. Klene, C. Adamo, R. Cammi, J. W. Ochterski, R. L. Martin, K. Morokuma, O. Farkas, J. B. Foresman, and D. J. Fox, Gaussian, Inc., Wallingford CT, **2016**.

[150] A. Klampt, *WIREs Comput. Mol. Sci.*, **2011**, *1*, 699-709. www.wavefunction.com

[151] a) N. T. T. Chau, M. Meyer, S. Komagawa, F. Chevallier, Y. Fort, M. Uchiyama, F. Mongin, P. C. Gros, *Chem. Eur. J.*, **2010**, *16*, 12425; b) J. Verbeek, L. Brandsma, J. *Org. Chem.*, **1984**, *49*, 3857.

[152] a) P. Gros, Y. Fort, P. Caubere, *J. Chem. Soc., Perkin Trans. 1*, **1997**, 3597; b) E. Lukevics, E. Liepins, I. Segal, M. Fleisher, *Journal of Organometallic Chemistry*, **1991**, *406*, 283.

[153] L. Wang, H. Zhu, S. Guo, J. Cheng, J.-T. Yu, *Chem. Commun.*, **2014**, *50*, 10864.

19. Acknowledgement

I owe my deepest gratitude to my supervisor Prof. Jan J. Weigand for his comprehensive support and advice. I am very thankful that he gave me the opportunity to work on this intriguing chemistry.

As a part of the brewery team I furthermore like to thank him and Prof. Dr. Thomas Henle as well as my brewing colleagues. Starting with a 20 l batch just for fun, I'm still amazed to see our beer in supermarkets nowadays.

Many thanks go out to our collaboration partner Antonio Franconetti, Antonio Bauzá and Prof. Dr. Antonio Frontera who performed all theoretical investigations in this work. Moreover I would like to thank Prof. Jan J. Weigand, Dr. Felix Hennersdorf, Jannis Fidelius and Johannes Steup for X-ray analysis. I further like to thank all my colleagues past and present and especially Dr. Kai Schwedtmann for his general support. He and others became good friends and not only made lab work even more enjoyable but especially the after work part of life. To one of them I even became a lab wife, yet he left and washed ashore the coast of Miami, where he became a convertible driving hotshot.

Darüber hinaus möchte ich meinen Freunden aus Emlichheim und Umgebung danken, die ich seit Jahren an meiner Seite schätze.

Zu guter Letzt gilt mein Dank meiner Familie, besonders meinen Eltern Jürgen und Judith, meinem Bruder Nico und meiner Freundin Sina, die immer für mich da sind.

20. Publications and Conference Contributions

20.1. Peer Reviewed Publications

3) R. Schoemaker, P. Kossatz, K. Schwedtmann, F. Hennersdorf, J. J. Weigand “*Coordination Chemistry and Methylation of Mixed-substituted Tetraphosphetanes (RP-P^tBu)₂ (R = Ph, Py)*”, *Chem. Eur. J.* **2020**, *accepted*.

2) R. Schoemaker, K. Schwedtmann, F. Hennersdorf, A. Bauzá, A. Frontera, J. J. Weigand “*Toward N,P-Doped π -Extended PAHs – A One-Pot Synthesis to Diannulated 1,4,2-Diazaphospholium Triflate Salts*”, *J. Org. Chem.* **2020**, DOI: 10.1021/acs.joc.0c00577.

1) R. Schoemaker, K. Schwedtmann, A. Franconetti, A. Frontera, F. Hennersdorf, J. J. Weigand “*Controlled Scrambling Reactions to Polyphosphanes via Bond Metathesis Reactions*”, *Chem. Sci.* **2019**, *10*, 11054.

20.2. Oral presentations

2) “New synthetic approaches to novel acyclic- and cyclo-polyphosphanes”
R. Schoemaker, F. Hennersdorf, D. Harting, J. J. Weigand; *15th European Workshop on Phosphorus Chemistry*, Uppsala, Sweden, **2018**.

1) “Synthesis and Reactivity of a Diannulated, Cationic Diazaphosphole”
R. Schoemaker, F. Hennersdorf, C. H. Sala, J. J. Weigand; *14. Mitteldeutsches Anorganiker-Nachwuchssymposium (MANS-14)*, Halle (Saale), Germany, **2016**.

20.3. Poster presentations

9) “Diazaphospholium salts for a bottom-up approach towards Phosphorus substituted Polycyclic Aromatic Hydrocarbons”
R. Schoemaker, F. Hennersdorf, C. H. Sala, J. J. Weigand; *GDCh-Wissenschaftsforum Chemie 2017*; Berlin, Germany.

8) “Diazaphospholium salts for a bottom-up approach towards Phosphorus substituted Polycyclic Aromatic Hydrocarbons”

R. Schoemaker, F. Hennersdorf, C. H. Sala, J. J. Weigand; *Anglo-German Inorganic Chemistry 2017*; Göttingen, Germany

7) “Phospholium triflates as building blocks for 2D graphene-type materials”

R. Schoemaker, F. Hennersdorf, C. H. Sala, J. J. Weigand; *14th European Workshop on Phosphorus Chemistry*, Cluj-Napoca, Romania, **2017**.

6) “Synthesis and chlorination reactions of a diannelated, cationic diazaphosphole”

R. Schoemaker, C. H. Sala, J. J. Weogand; *18. Wöhler Tagung*, Berlin, Germany, **2016**.

5) “Synthesis and reactivity of a diannelated, cationic diazaphosphole”

R. Schoemaker, J. J. Weigand; *21st International Conference on Phosphorus Chemistry*, Kazan, Russia, **2016**.

4) “Application of 2-(dichlorophosphanyl)pyridine in heterocycle synthesis”

R. Schoemaker, J. J. Weigand; *13th European Workshop on Phosphorus Chemistry*, Berlin, Germany, **2016**, awarded with the **Best Poster Award**.

3) “Deoxygenation of Aromatic Aldehydes Using SynPhos Reagents”

R. Schoemaker, J. J. Weigand; *GDCh Wissenschaftsforum Chemie*, Dresden, Germany, **2015**.

2) “Deoxygenation of Aromatic Aldehydes Using SynPhos Reagents” R. Schoemaker, J. J. Weigand; *12th European Workshop on Phosphorus Chemistry*, Kassel, Germany, **2015**.

1) “Synthesis of Cationic, Highly Lewis Acidic NHCs”

R. Schoemaker, K. Schwedtmann, J. J. Weigand; *17th Wöhlertagung*, Saarbrücken, Germany, **2014**.

Versicherung

Hiermit versichere ich, dass ich die vorliegende Arbeit ohne unzulässige Hilfe Dritter und ohne Benutzung anderer als der angegebenen Hilfsmittel angefertigt habe; die aus fremden Quellen direkt oder indirekt übernommenen Gedanken sind als solche kenntlich gemacht. Die Arbeit wurde bisher weder im Inland noch im Ausland in gleicher oder ähnlicher Form einer anderen Prüfungsbehörde vorgelegt.

Erklärung

Die vorliegende Dissertation wurde in der Zeit von 10/2015 bis 06/2020 in der Professur für Anorganische Molekülchemie der Technischen Universität Dresden unter der wissenschaftlichen Betreuung von Herrn Prof. Dr. rer. nat. habil. Jan. J. Weigand angefertigt.

Frühere Promotionsverfahren haben nicht stattgefunden.

Robin Schoemaker